Impact of pharmacological and environmental manipulations on neuronal structural plasticity and dynamics

Marta Pérez Rando

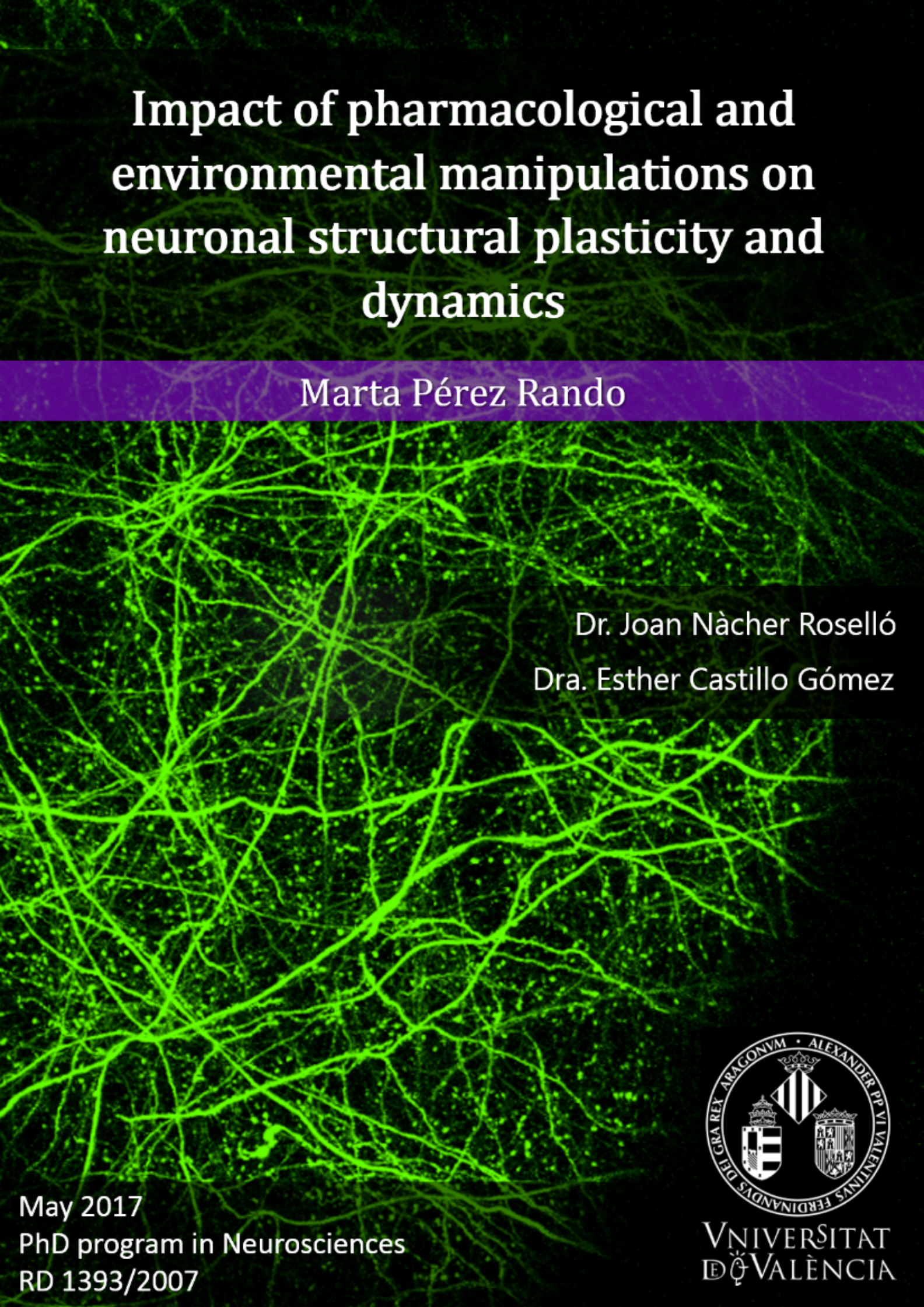

Dr. Joan Nàcher Roselló

Dra. Esther Castillo Gómez

May 2017
PhD program in Neurosciences
RD 1393/2007

VNIVERSITAT DE VALÈNCIA

VNIVERSITAT DE VALÈNCIA

PhD program in Neurosciences

RD 1393/2007

Impact of pharmacological and environmental manipulations on neuronal structural plasticity and dynamics

Marta Pérez Rando

May 2017

Dr. Joan Nàcher Roselló

Dra. Esther Castillo Gómez

VNIVERSITAT DE VALÈNCIA

Facultat de Ciències Biològiques

Departament de Biologia Cel·lular

Juan Nàcher Roselló, Associate Professor of Cell Biology and Esther Castillo Gómez, Postdoctoral Fellow, of the Department of Cell Biology, Functional Biology and Antropology at the Universitat de València,

Hereby certify That Ms. Marta Pérez Rando, MSc in Neuroscience at the University of València, has performed, under our supervision the work entitled:

"Impact of pharmacological and environmental manipulations on neuronal structural plasticity and dynamics"

to obtain the PhD in Neuroscience.

What we sign as required in Burjassot, on May the 25th, 2017

Juan Nàcher Roselló, PhD

Esther Castillo Gómez, PhD

Para la realización de esta tesis, la autora ha sido beneficiaria de una beca predoctoral de Formación de Profesorado Universitario concedida por el Ministerio de Educación, Cultura y Deporte (FPU12/03200) según la resolución del 25 de abril de 2012, de la Secretaría General de Universidades.

La vida es crecimiento, y cuanto más viajamos más verdad podemos comprender. Entender aquello que nos rodea es la mejor preparación para comprender las cosas que yacen más allá.

Hipatia de Alejandría

A mis padres

Content

AGRADECIMIENTOS

Para empezar, agradecer a mis directores que me hayan guiado en este trayecto. Mil gràcies a Joan per haver-me acollit al seu laboratori i per donar-me l'oportunitat d'emocionar-me amb la ciència i ajudar-me quan les coses no funcionaven com tots volguérem. També gràcies per totes eixes recomanacions de series i llibres, però això estic segura que no va a terminar! A Esther, mi codirectora, por apoyarme día a día y motivarme para terminar proyectos y empezar nuevos. Por forzarme a seguir adelante y a buscar una versión mejor de mi yo investigadora. Y cómo no, también por los ánimos constantes para enfrentarme a ese abismo de futuro.

Hablando de abismos (y de precipicios y de caminar con una venda en los ojos), a Ramón, quien hizo que la ciencia fuera divertida y quisiera quedarme a intentarlo. Y porque hemos pasado muchísimas cosas juntos y sé que, lejos o cerca, siempre puedo contar contigo (con preferencia de cerca). A ver qué superpoder consigo cuando pase todo esto.

Als meus companys de laboratori (+Héctor, una més). A Maria, perquè ha compartit tot aquest procés amb mi, l'hem liada milers de vegades juntes, però ens hem rigut moltíssim pel camí. I ja fa 11 anys des que vam començar la carrera (molt fort!). A Clara García, que m'imagine que estarà passant per açò ara mateix (+/- 1 dia), gràcies per ajudar-me i comprendre'm amb tot! A Héctor, que transmet serenitat i relativitza el mon. Per la seva ajuda incessant per tirar endavant tot l'infern del temps real (i el que calga!!!). A Yasmina, que ja ha passat l'equador, molta sort en el que queda, i per donar-me suport i riure's de tot. A Clara (en mode companya de laboratori), per ajudar-me amb qualsevol dificultat i alleugerar els problemes! A Simona, por invitarnos a probar los mejores capuchinos que hay en Valencia, ¡los que hace ella! Gracias también por su apoyo y su comprensión en el día a día. A los colaboradores, que van y vienen, pero siempre están llenos de ilusión, en especial a Esther Rodríguez, que tiene pinta de quedarse y sería una gran adquisición. Y a mis antiguas compañeras, ¡os echo de menos! A Laura, a quien echo de menos contarle cualquier tontería y que siempre ha sabido cómo hacerme sentir mejor, fue muy buena época cuando vivíamos al ladito. A Tere, que, aunque esté muy lejos, sé que

siempre va a entenderme. ¡Espero que volváis pronto! I a tots en conjunt, gràcies per compartir viatges i congressos i fer-los inoblidables. Per totes aquelles vegades que m'heu tret un somriure, i per fer que aquests X anys ($x \rightarrow \infty$) hagen sigut dels millors de la meva vida. Vos dessitge a tots un gran futur.

A todos los profesores que me han ayudado a entender mejor cualquier cosa, o a solucionar contratiempos, en el departamento. A Emilio por resolverme todas las dudas de docencia e institucionales (¡y por animarnos con sus cajas de galletas!). A José Miguel por todas las dudas conceptuales, por ser el manitas de la casa y por todos esos inventos que nos solucionan la vida. A Carlos, por todos sus consejos, y porque tiene siempre ánimos para repartir. ¡Entre los tres habéis hecho el doctorado muchísimo más fácil!

A mis padres, que creo que han vivido más todo este proceso que yo misma, y lo han hecho posible con su apoyo constante. Sin ellos no habría estudiado aquello que más quería, y estoy segura que no habría acabado metiéndome en ciencia y buscando un futuro de investigadora. ¡Así que muchísimas gracias! La tesis va para vosotros.

To Holtmaat lab too! For teaching me everything they could and always supporting me. They allowed me to go further and to reach a distant dream. Also for showing me how great Geneva and its beautiful surroundings are, and always giving me great advice.

A María, Marina y Alba. Perquè durant els últims anys, setmana a setmana, ens hem estat contant les misèries i alegries. Sempre juntes i endavant! A Joel por siempre escucharme y aguantar mis ralladas. A Paula por no desaparecer nunca. A Miguel, por ser una gran adquisición y entenderme tan bien.

I a Clara de nou, que encara que t'he anomenat abans per tot el suport que em dones al laboratori com a companya, mil gràcies més per tot el suport que m'has donat fora d'ell. Perquè açò també és en part teu, i la veritat que ho has patit. Per tota la teva empatia i per compartir aquest somni!

ABBREVIATIONS

5-HT	Serotonin
5-HTT	Serotonin transporter
ACC	Anterior cingulate cortex
AD	Alzheimer's disease
AMPA-Ka receptors	α-amino-3-hydroxy-5-methyl-4-isoxazolepropionic acid and kainate receptors
BDNF	Brain-derived neurotrophic factor
BLa	Basolateral nucleus of the amygdala
BM	Basomedial nucleus of the amygdala
CA	*Cornu Ammonis*
CA1	*Cornu Ammonis* 1 from the hippocampus
CA2	*Cornu Ammonis* 2 from the hippocampus
CA3	*Cornu Ammonis* 3 from the hippocampus
CA4	*Cornu Ammonis* 4 from the hippocampus
CB1-R	Cannabinoid receptor type 1
CCK	Cholecystokinin
Ce	Central nucleus of the amygdala
Cg1	Cingulate cortex 1
Cg2	Cingulate cortex 2
Cl^-	Chloride anion
CNS	Central nervous system
CPP	3-(2- carboxypiperazin-4-yl) propyl-1-phosphonic acid
DG	Dentate gyrus
DHF	7,8-dihydroxyflavone
E/I balance	Excitatory/Inhibitory balance
EGFP	Enhanced green fluorescent protein
EPB	*En passant boutons*; axonal buttons

EPSP	Excitatory postsynaptic potential
ErbB4	Neuregulin 1 receptor
GABA	γ-Aminobutyric acid
GAD	Glutamic acid decarboxylase
GAD6	Mixture of isoforms 65 and 67 of the glutamic acid decarboxylase
GAD65	65-kDa isoform of the glutamic acid decarboxylase
GAD67	67-kDa isoform of the glutamic acid decarboxylase
GIN mice	FVB-Tg(GadGFP)45704Swn/J; GFP-expressing inhibitory neuron mice
GluN1	Obligatory subunit of the NMDA receptors
HS interneurons	Hippocampo-septal interneurons
IL	Infralimbic region of the prefrontal cortex
IPSP	Inhibitory postsynaptic potential
K^+	Potassium cation
La	Lateral nucleus of the amygdala
lPFC	Lateral prefrontal cortex
LTP	Long term potentiation
MAO	Monoamine oxidase
MAPK	Mitogen-activated protein kinase cascade
Me	Medial nucleus of the amygdala
MK-801	Dizocilpine
mPFC	Medial prefrontal cortex
mTOR	Mammalian target of rapamycin
NCAM	Neural cell adhesion molecule
NMDA	N-methyl-D-aspartate
NMDAR	N-methyl-D-aspartate receptor
NOR	Novel object recognitin test
NPY	Neuropeptide Y
Nrg1	Neuregulin 1

OFC	Orbitofrontal cortex
O-LM interneurons	*Oriens - Lacunosum moleculare* interneurons
PCP	Phencyclidine
PFC	Prefrontal cortex
PI3K	Phosphatidylinositol 3-kinase cascade
PLC-γ	Phospholipase C-γ cascade
PNNs	Perineuronal nets
PNS	Peripheral nervous system
PrL	Prelimbic region of the prefrontal cortex
PSA	Polysialic acid
PSA-NCAM	Polysialylated form of the neural cell adhesion molecule
PV	Parvalbumin
S1	Primary somatosensory cortex
S2	Secondary somatosensory cortex
SOM	Somatostatin
SSRIs	Selective serotonin reuptake inhibitors
ST8SiaII	ST8 alpha-N-acetyl-neuraminide alpha-2,8-sialyltransferase 2
ST8SiaIV	ST8 alpha-N-acetyl-neuraminide alpha-2,8-sialyltransferase 4
SYN	Synaptophysin
Thy1-YFP mice	B6.Cg-Tg(Thy1-YFP)HJrs/J mice; Thy1-YFP-H mice
TrkB	Tropomyosin receptor kinase B
VGAT	Vesicular transporter of GABA
VGlut-1	Vesicular glutamate transporter 1
VGlut-2	Vesicular glutamate transporter 2
VGlut-3	Vesicular glutamate transporter 3
VIP	Vasoactive intestinal peptide
YFP	Yellow fluorescent protein

RESUMEN EN CASTELLANO

INTRODUCCIÓN

El sistema nervioso de vertebrados es uno de los más estudiados, aunque peor comprendidos, del organismo de mamíferos. Desde que Ramón y Cajal postuló su teoría celular de este sistema (Ramón y Cajal, 1909), la neurona se ha postulado como su unidad funcional. Sin embargo, durante las últimas décadas se ha revolucionado la visión que se tenía de éste. Una de las percepciones más asentadas era que, tras el desarrollo embrionario, el sistema nervioso se mantenía inmutable. Sin embargo, ahora sabemos que diferentes formas de plasticidad gobiernan su adaptación, que son necesarias para importantes procesos del día a día, tales como el aprendizaje y la memoria (Berlucchi and Buchtel, 2009; Smythies, 2002) y que se ven afectadas en diferentes trastornos neuropsiquiátricos (Baroncelli *et al*, 2011; Duman *et al*, 2000; Flores *et al*, 2016; Nacher *et al*, 2013; Shin and Liberzon, 2010). Estos cambios plásticos comprenden diferentes procesos, como alteraciones en la estructura de neuronas (plasticidad estructural), y pueden estar modulados por diferentes neurotransmisores, neurotrofinas o moléculas relacionadas con la plasticidad. En la siguiente tesis voy a centrarme en la plasticidad estructural de la neurona y su modulación en diferentes áreas cerebrales: la amígdala, el hipocampo, y dos regiones del neocórtex: las cortezas prefrontal y de barriles.

La **corteza prefrontal (CPF)** es una corteza de asociación, situada en la parte anterior del cerebro de mamíferos. Es responsable de procesos como la motivación, el autoconocimiento, el comportamiento social y la memoria de trabajo, entre otros (Fuster, 2015). Sin embargo, su mal funcionamiento está involucrado en varios trastornos neuropsiquiátricos, que incluyen la esquizofrenia, la depresión severa y los trastornos del espectro autista (Bicks *et al*, 2015). Por otra parte, la **corteza de barriles** es una subregión de la corteza somatosensorial primaria, que sólo está presente en algunas especies, principalmente roedores, y que recibe la información desde las vibrisas del animal a través del tálamo. El **hipocampo** ha sido ampliamente estudiado debido a su papel en la memoria a corto plazo, la consolidación de la memoria a largo plazo y la memoria espacial. Por

último, la **amígdala**, como el hipocampo, forma parte del sistema límbico. Entre sus funciones principales se encuentran el procesamiento de comportamientos aversivos y la motivación y procesamiento de estímulos ambientales gratificantes. Su mal funcionamiento también está relacionado con varios trastornos psiquiátricos, como la esquizofrenia (Aleman and Kahn, 2005) o trastornos relacionados con la ansiedad (Shin and Liberzon, 2010).

La neurona como objeto de estudio

En la siguiente tesis se han estudiado tanto neuronas piramidales como interneuronas. Las **neuronas piramidales** son glutamatérgicas y por lo tanto liberan el aminoácido glutamato, el neurotransmisor excitador más común en el encéfalo. Son principalmente neuronas de proyección y son el tipo celular más estudiado en el sistema nervioso central (Kandel *et al*, 2012).

Una de las principales características de las neuronas piramidales es la presencia de **espinas dendríticas** que son especializaciones membranosas de sus dendritas, cuya función es agrupar los receptores y compartimentar espacialmente la señal eléctrica (Lee *et al*, 2012). Por otro lado, los axones también muestran varicosidades membranosas, llamadas **botones axónicos**, que contienen y liberan las vesículas sinápticas. Debido a sus funciones como elementos postsinápticos y presinápticos, las espinas y botones son marcadores apropiados para la inervación y la enervación neuronal, y aumentos de estas estructuras se han correlacionado con los aumentos de la actividad neuronal (Becker *et al*, 2008; Engert and Bonhoeffer, 1999).

Las **interneuronas** son neuronas inhibidoras en el sistema nervioso central. Su nombre se debe a su papel intermedio en los circuitos neuronales, ya que proyectan localmente, y generalmente, son responsables del correcto funcionamiento de estos circuitos. Al contrario que las neuronas piramidales, las interneuronas forman parte de una población heterogénea con diversas características morfológicas, fisiológicas, neuroquímicas y sinápticas, lo que complica su estudio y comprensión. Como característica

unificadora, todas son GABAérgicas, lo que significa que sintetizan y secretan el **ácido γ-aminobutírico (GABA)**, el principal neurotransmisor inhibitorio del encéfalo. También pueden expresar diferentes receptores excitadores e inhibidores en sus dendritas o somas. En esta tesis doctoral, utilizaré la clasificación molecular de la terminología de Petilla (Ascoli *et al*, 2008) que define cinco tipos de interneuronas dependiendo de la expresión de diferentes proteínas quelantes de Ca^{2+} y neuropéptidos; estas son: parvalbúmina, somatostatina, neuropéptido Y, péptido intestinal vasoactivo y colecistoquinina. En adelante me centraré en las poblaciones de interneuronas que expresan parvalbúmina y somatostatina.

En primer lugar, las interneuronas que expresan **parvalbúmina** pueden subdividirse en 2 subtipos: células en cestos y células en candelabro. En esta tesis se han estudiado únicamente las células en cestos, que reciben su nombre de las cestas perisomáticas que forman alrededor de los somas de las neuronas piramidales. De hecho, esta inhibición perisomática permite que una única célula que expresa parvalbúmina inhiba simultáneamente muchas neuronas piramidales. Este fenómeno produce la sincronización de las células piramidales, importante para el correcto funcionamiento del sistema (Singer, 1999). Debido a eso, las células en cestos son uno de los tipos más estudiados de interneuronas del encéfalo. La otra población de interneuronas estudiado en esta tesis fue la que expresa el neuropéptido **somatostatina**. Estas interneuronas se encuentran en diferentes zonas del encéfalo, incluyendo el neocórtex (Markram *et al*, 2004), el hipocampo (Freund and Buzsáki, 1996) y la amígdala (Real *et al*, 2009). Su morfología es diversa, pero su función es muy específica: inhiben fuertemente la porción distal de dendritas de las neuronas piramidales y frecuentemente reciben inhibición recíproca de otras interneuronas (Urban-Ciecko and Barth, 2016). Son esenciales para la maduración de los circuitos corticales profundos (Tuncdemir *et al*, 2016) y juegan un papel importante en otras etapas del neurodesarrollo, en diferentes patologías y en la plasticidad neuronal (Liguz-Lecznar *et al*, 2016). Además, presentan espinas dendríticas, una característica poco común en las interneuronas (Gilabert-Juan *et al*, 2013b, 2017; Guirado *et al*, 2014).

Plasticidad estructural

Las neuronas piramidales y las interneuronas pueden cambiar su morfología en diferentes condiciones, incluyendo cambios en la longitud y complejidad de sus árboles dendríticos, y en la densidad o morfología de sus espinas dendríticas (Fu and Zuo, 2011) y botones axónicos (Colicos *et al*, 2001; Florence *et al*, 1998; Nikonenko *et al*, 2003). Estos cambios ocurren tanto en condiciones naturales (Afroz *et al*, 2016; Burke and Barnes, 2006; Woolley and McEwen, 1994) como patológicas (Flores *et al*, 2016; Glausier and Lewis, 2013; McEwen, 1999; Qiao *et al*, 2016a). Entre todos los tipos neuronales, las interneuronas que expresan somatostatina son especialmente interesantes, ya que presentan espinas dendríticas que cambian su número y morfología en animales sometidos a estrés crónico (Gilabert-Juan *et al*, 2011, 2013b, 2017) o tras la depleción de moléculas relacionadas con la plasticidad (Castillo-Gómez *et al*, 2016a; Guirado *et al*, 2014).

Por otra parte, en los últimos años han emergido nuevas técnicas que estudian espinas dendríticas o botones axónicos longitudinalmente *in vitro* o *in vivo*. Estos métodos nos proporcionan información sobre las dinámicas estructurales de la neurona de interés, y además son sensibles a cambios transitorios y homeostáticos que de otra manera no podrían ser detectados. Se han observado cambios en las dinámicas estructurales de neuronas piramidales durante el envejecimiento cerebral natural (Grillo *et al*, 2013; Mostany *et al*, 2013) y después de paradigmas de privación sensorial tanto en circuitos excitadores (Cane *et al*, 2014; Hofer *et al*, 2009; Holtmaat and Svoboda, 2009) como inhibidores (Chen *et al*, 2011b, 2011c, 2012; Chen and Nedivi, 2013; Keck *et al*, 2011; van Versendaal *et al*, 2012).

Estas formas de plasticidad son moduladas por diferentes sistemas de neurotransmisores, la expresión de moléculas específicas y neurotrofinas. Respecto al primer punto, en la presente tesis me centraré en la modulación por los sistemas de neurotransmisión glutamatérgica, GABAérgica y serotonérgica.

Modulación de la plasticidad por diferentes sistemas de neurotransmisión

Existen tres receptores principales de glutamato, el neurotransmisor excitador más común en el encéfalo. Éstos son los receptores del ácido α-amino-3-hidroxi-5-metil-4-isoxazolpropiónico (AMPA), kainato y N-metil-D-aspartato (NMDA). Los **receptores NMDA** se expresan ampliamente en neuronas piramidales y en interneuronas (Alvarez *et al*, 2007; Collingridge *et al*, 1983; Nyíri *et al*, 2003; Oren *et al*, 2009), y juegan un papel clave en varios eventos de desarrollo del sistema nervioso central, tales como la neurogénesis y migración neuronal (Komuro and Rakic, 1993). Estructuralmente, son heterotetrameros compuestos por dos subunidades GluN1 obligatorias junto con dos subtipos diferentes de las subunidades GluN2 y GluN3. Por lo tanto, la inmunolocalización de la subunidad GluN1 es una herramienta excelente para mostrar la expresión de estos receptores (Moreau and Kullmann, 2013; Paoletti *et al*, 2013; Sanz-Clemente *et al*, 2013; VanDongen, 2009).

La activación de los receptores NMDA produce varios cambios estructurales en neuronas piramidales, y este efecto se puede conseguir administrando agonistas de estos receptores, siendo uno de los más conocidos la molécula de NMDA. Por una parte, su activación puede producir muerte celular debido a una entrada excesiva de Ca^{2+} en la célula (Kristensen *et al*, 2001; Sakaguchi *et al*, 1997; Shimono *et al*, 2002). Sin embargo, la administración sub-letal de esta molécula causa alteraciones en la densidad de espinas dendríticas de neuronas piramidales en cultivos primarios del hipocampo (Halpain *et al*, 1998; Tian *et al*, 2007).

Del mismo modo, los antagonistas de los receptores NMDA también se han utilizado para mejorar nuestra comprensión sobre estos receptores. Uno de los más estudiados es el MK-801, cuya administración afecta a la correcta formación de axones y a la regulación de la sinaptogénesis en neuronas piramidales durante el desarrollo (Butler *et al*, 1998; Cline and Constantine-Paton, 1990; Shatz, 1990). Por contra, existen muy pocos estudios acerca de la presencia de receptores NMDA en interneuronas (Nyíri *et al*, 2003) o de cómo estas células inhibidoras alteran su estructura después de su activación o bloqueo.

En segundo lugar, como se ha explicado anteriormente, el **GABA** es el principal neurotransmisor inhibitorio del encéfalo, y es sintetizado y liberado por interneuronas. Existen varios receptores de GABA, que se expresan tanto en neuronas piramidales (Alger and Nicoll, 1982) como en interneuronas (Freund and Buzsáki, 1996). Al igual que ocurría con la manipulación de los receptores NMDA, la activación o inhibición de los receptores de GABA puede alterar la estructura de neuronas piramidales (Curto *et al*, 2016; Romero *et al*, 2013; Shimizu *et al*, 2015).

Por último, la **serotonina** (5-hidroxitriptamina: 5-HT) es una monoamina sintetizada y liberada en el sistema nervioso central por neuronas ubicadas en los núcleos de Raphe, que inervan el neocórtex, el hipocampo y la amígdala (Jacobs and Azmitia, 1992). El papel de la neurotransmisión serotoninérgica está relacionado con comportamientos de bienestar, mientras que su mal funcionamiento está relacionado con varios trastornos psiquiátricos, incluyendo depresión y ansiedad (Andrews *et al*, 2015). Existen diferentes receptores de 5-HT, autoreceptores y transportadores, estos últimos encargados de la recaptación de 5-HT hacia el elemento presináptico (Fuller and Wong, 1990). Este transportador es especialmente importante por ser una excelente diana farmacológica para los antidepresivos, ya que así se prolonga el tiempo de activación de los receptores de 5-HT (Andrews *et al*, 2015; Belmaker and Agam, 2008; Fava and Kendler, 2000; Jonnakuty and Gragnoli, 2008; Nestler *et al*, 2002). Entre este grupo de antidepresivos, la **fluoxetina** (Prozac, Lilly) es uno de los más utilizados en sociedades occidentales (Byatt *et al*, 2013; Iñiguez *et al*, 2014). Además, se piensa que el mecanismo de actuación de este antidepresivo puede estar promoviendo un rejuvenecimiento de la plasticidad neuronal, reabriendo periodos críticos del desarrollo de varias áreas cerebrales (Kobayashi *et al*, 2010; Vetencourt *et al*, 2008). Estudios previos de nuestro laboratorio ya han demostrado que el tratamiento crónico con fluoxetina produce un aumento de la densidad de espinas dendríticas de neuronas piramidales de la corteza somatosensorial (Guirado *et al*, 2009). Sin embargo, todavía no sabemos cómo este antidepresivo afecta la estructura de interneuronas.

Modulación de la plasticidad por neurotrofinas

Existen muchas neurotrofinas que influyen sobre el desarrollo del sistema nervioso central. Una de las más importantes es el factor neurotrófico derivado del cerebro (**BDNF** por sus siglas en inglés), que ejerce un papel central en el neurodesarrollo y la plasticidad neural (Horch and Katz, 2002; McAllister *et al*, 1997; Murphy *et al*, 1998; Tolwani *et al*, 2002). El BDNF también promueve la potenciación a largo plazo en los circuitos excitadores del neocórtex, hipocampo y amígdala (Escobar *et al*, 2003; Kang *et al*, 1997; Meis *et al*, 2012). En cuanto a la plasticidad estructural, esta neurotrofina provoca un aumento de la densidad de espinas de neuronas piramidales en cultivos organotípicos de hipocampo (Tyler and Pozzo-Miller, 2003), así como un aumento de la complejidad de su árbol dendrítico en la corteza visual en desarrollo (McAllister *et al*, 1995).

Todos estos efectos son desencadenados por la activación del receptor de BDNF, el receptor de tropomiosina quinasa B (**TrkB**). Este receptor está presente en varias poblaciones neuronales, incluyendo neuronas piramidales (Kokaia *et al*, 1993; Merlio *et al*, 1993) e interneuronas (Gorba and Wahle, 1999), y su mal funcionamiento parece jugar un papel clave en la etiología de ciertas enfermedades neuropsiquiátricas como la depresión severa, la esquizofrenia o las enfermedades de Alzheimer y Parkinson (Angelucci *et al*, 2005; Castrén and Rantamäki, 2010; Pandya *et al*, 2013; Yoshii and Constantine-Paton, 2010; Zuccato and Cattaneo, 2009). Un fármaco muy interesante para el estudio de la activación de TrkB es la 7,8-dihidroxiflavona (**DHF**), un compuesto que puede administrarse de forma oral y que cruza fácilmente la barrera hematoencefálica (Du and Hill, 2015). De hecho, su efectividad ha sido recientemente demostrada en varios modelos animales de algunas de estas enfermedades (Castello *et al*, 2014; Jang *et al*, 2010; Korkmaz *et al*, 2014; Zhang *et al*, 2014, 2015). En algunos casos se ha descrito una mejoría de la sintomatología asociada a alteraciones de la estructura de neuronas piramidales (Castello *et al*, 2014; Zhang *et al*, 2015). En modelos animales de envejecimiento, el DHF aumenta la densidad de espinas dendríticas en neuronas piramidales en la amígdala, hipocampo y CPF, consiguiéndose niveles equiparables a los de ratas más jóvenes (Zeng *et al*, 2012a). Sin embargo, todavía no sabemos cómo esta flavona puede alterar las dinámicas estructurales de estas neuronas en animales sanos.

Moléculas relacionadas con la plasticidad y plasticidad estructural

Existen dos moléculas o compuestos relacionados con la plasticidad de especial interés en esta tesis doctoral: la forma polisializada de la molécula de adhesión celular neural (**PSA-NCAM**), y las redes perineuronales (**PNNs**). La primera presenta propiedades antiadhesivas (Rutishauser, 1996), y se expresa ampliamente durante el neurodesarrollo (Doherty *et al*, 1990; Miller *et al*, 1994; Rutishauser, 1996; Zhang *et al*, 1992). En este periodo facilita la migración neuronal, la extensión de neuritas y el remodelado dendrítico y sináptico (Bonfanti 2006; Rutishauser 2008). Su expresión se restringe mucho durante la vida adulta, pero todavía puede encontrarse en diferentes poblaciones de interneuronas del neocórtex adulto (Varea *et al*, 2005), hipocampo (Gomez-Climent *et al*, 2011; Nacher *et al*, 2002a) y amígdala (Nacher *et al*, 2002b). La depleción de la PSA unida a la NCAM utilizando la enzima endoneuraminidasa-N (EndoN) altera la densidad de espinas dendríticas en neuronas piramidales y en interneuronas que expresan somatostatina (Castillo-Gómez *et al*, 2016a, 2016b; Guirado *et al*, 2014). Además, las dinámicas de estas espinas también se alteran tras la administración de EndoN en el hipocampo (Guirado *et al*, 2014).

Por otro lado, las PNNs son estructuras especializadas de la matriz extracelular que rodean a las neuronas y restringen su conectividad y plasticidad (Karetko and Skangiel-Kramska, 2009; De Luca and Papa, 2016; Wang and Fawcett, 2012). Aunque rodean muchos tipos celulares, preferentemente se encuentran alrededor de las interneuronas que expresan parvalbúmina (Nowicka *et al*, 2009; Ueno *et al*, 2016). Las PNNs regulan muchas formas de plasticidad (McRae and Porter, 2012); de hecho, se piensa que su aparición, que ocurre bien adentrado el desarrollo neural, es lo que pone fin al periodo crítico de plasticidad aumentada (Hensch and Bilimoria, 2012; Wang and Fawcett, 2012). Es especialmente interesante el descubrimiento de alteraciones en la proporción de neuronas que expresan parvalbúmina y que son rodeadas por PNNs en diferentes paradigmas. Concretamente, estas variaciones se han observado en esquizofrenia (Berretta *et al*, 2015; Bitanihirwe *et al*, 2016; Mauney *et al*, 2013) y tras la administración crónica con fluoxetina (Karpova *et al*, 2011), pero hipótesis recientes apuntan a que podrían subyacer a otras enfermedades psiquiátricas o trastornos mentales.

OBJETIVOS

El objetivo principal de esta tesis doctoral es el estudio del impacto de las manipulaciones farmacológicas y ambientales sobre la estructura y dinámica de las neuronas excitadoras e inhibidoras del encéfalo de ratón, en un intento por comprender mejor la plasticidad del sistema nervioso adulto, y las bases neurobiológicas de trastornos psiquiátricos. Para lograr este objetivo principal, derivamos los siguientes objetivos específicos:

1. Estudiar el papel que desempeñan los receptores NMDA en la plasticidad estructural y dinámica de las interneuronas somatostatina del hipocampo.

2. Desarrollar un nuevo modelo de esquizofrenia de ratón, basado en la combinación de estrés por aislamiento social post-destete y del bloqueo perinatal de los receptores NMDA, y reportar sus efectos sobre la corteza prefrontal medial y la amígdala.

3. Analizar si el tratamiento crónico con el antidepresivo fluoxetina afecta la plasticidad del hipocampo y de la corteza prefrontal medial.

4. Estudiar in vivo, utilizando ventanas craneales y microscopía de 2 fotones, los efectos de un tratamiento crónico con el agonista de TrkB 7,8-dihidroxiflavona sobre la dinámica de las neuronas piramidales en la corteza de barriles.

METODOLOGÍA Y RESULTADOS

Efecto de la modulación de los receptores NMDA sobre la plasticidad estructural de interneuronas que expresan somatostatina

Con el fin de entender cómo el bloqueo de los receptores NMDA afecta la densidad de espinas dendríticas y botones axónicos de las interneuronas que expresan somatostatina en el estrato *oriens* del hipocampo, hemos inyectado MK-801, un antagonista de estos receptores, en ratones transgénicos que expresan EGFP constitutivamente en estas células

(ratones GIN, Oliva et al., 2000). Veinticuatro horas tras la inyección, se realizó el test de comportamiento *hole-board* para obtener una lectura de los comportamientos relacionados con la ansiedad y memoria de trabajo.

En la presente tesis muestro que el bloqueo agudo de los receptores NMDA con una inyección de MK-801 no provoca variaciones en la densidad de espinas dendríticas en las interneuronas somatostatina del estrato *oriens* del hipocampo. Las discrepancias entre nuestros resultados y los obtenidos con neuronas piramidales en otros experimentos pueden deberse a las diferencias estructurales y fisiológicas entre estas células y las interneuronas (Acsády *et al*, 1998; Freund and Buzsáki, 1996; Gulyás *et al*, 1992) o, también, a las diferencias en dosis y duración entre tratamientos con MK-801. Sin embargo, los botones axónicos de estas interneuronas sí varían tras la inyección con este antagonista. Estos resultados concuerdan con experimentos realizados por otros laboratorios que muestran *sprouting* axónico en las colaterales de Schaffer tras un tratamiento de 3 días con MK-801 *in vitro* (McKinney *et al*, 1999b).

Además, hemos encontrado fuertes alteraciones en los comportamientos relacionados con la ansiedad en ratones tratados con MK-801, incluyendo aumentos en la actividad locomotora, los cuales concuerdan con estudios previos utilizando este antagonista (Kalinichev *et al*, 2008; Zuo *et al*, 2006). Por el contrario, no hemos encontrado ninguna alteración significativa respecto a la memoria de trabajo en animales tratados, también de acuerdo con resultados previos utilizando el test de *hole-board* e inyectando MK-801 (Haj-Mirzaian *et al*, 2015; Hirose *et al*, 2016).

Para poder comprender mejor los resultados obtenidos en espinas dendríticas y botones axónicos, hemos realizado experimentos adicionales con análisis en tiempo real, que permiten el estudio de las dinámicas estructurales de estas células. Para ello hemos preparado y analizado cultivos organotípicos entorrino-hipocampales de la misma cepa de ratones (ratones GIN, Oliva et al., 2000), y a continuación hemos tomado *stacks* con un microscopio confocal de las mismas dendritas en diferentes tiempos, realizando un estudio en tiempo real de estas estructuras antes y después de la administración del MK-801 y del agonista de los receptores NMDA, la molécula de NMDA. Realizando estos estudios hemos

encontrado que 4 horas después de la administración de MK-801, la tasa de aparición de espinas dendríticas disminuye en interneuronas somatostatina del estrato *oriens*. Estos resultados de disminución del área postsináptica concuerdan con la retracción del árbol dendrítico de interneuronas que se muestra en tiempo real tras la administración de otro antagonista de receptores NMDA, la ketamina (Vutskits *et al*, 2007). La administración de NMDA no produce ninguna alteración en un período tan corto. Sin embargo, 24 horas tras la administración del MK-801 y el NMDA, los cambios sí son complementarios: MK-801 produce una disminución en la tasa de aparición, mientras que el NMDA provoca un aumento en este parámetro. Además, la administración del NMDA también produce un aumento en la tasa de desaparición y una disminución en la tasa de estabilidad de espinas dendríticas, mientras que MK-801 no causa ningún efecto. Estas alteraciones causadas por la infusión de NMDA pueden deberse a la desestabilización que produce la activación de los receptores NMDA en el citoesqueleto de F-actina (Halpain *et al*, 1998) o la excitotoxicidad producida por la apertura de receptores de NMDA y la consecuente entrada de calcio en la célula (Kristensen *et al*, 2001; Mody and MacDonald, 1995; Shimono *et al*, 2002).

Además, también se ha analizado la densidad relativa de espinas dendríticas en ambos experimentos. En el experimento realizado con el antagonista MK-801, se observa una disminución significativa en este parámetro 24 horas después de la infusión del fármaco cuando se comparan con la línea base del grupo, y una tendencia hacia una disminución cuando se compara con el grupo de control. Estos resultados son probablemente consecuencia de las disminuciones en la tasa de aparición que ocurren también en este punto temporal. Sin embargo, cuando los cultivos se tratan con el agonista NMDA, no encontramos ningún cambio en la densidad relativa de espinas dendríticas a lo largo del experimento.

Con respecto a las tasas de estabilidad que mostramos en ambos experimentos, existe una discrepancia aparente cuando se comparan los ensayos *in vitro* e *in vivo*. De hecho, experimentos de otros laboratorios en tiempo real con ventanas craneales han demostrado que, en condiciones control, las espinas de interneuronas de la corteza visual tienen una estabilidad cercana al 98% (Keck *et al*, 2011). Sin embargo, la tasa de estabilidad de las interneuronas somatostatina del estrato *oriens* en ambos ensayos presenta un valor

aproximadamente del 70%. Estas discrepancias pueden ser debidas a la diferencia en la estabilidad de diferentes subpoblaciones de interneuronas, a la región y la edad estudiada, o, más probablemente, a una mayor estabilidad *in vivo* que en nuestros cultivos organotípicos.

Estudio de las alteraciones sobre el comportamiento, los circuitos excitadores e inhibidores y la plasticidad molecular, en un modelo de esquizofrenia de doble impacto

En la presente tesis, he realizado un estudio multidisciplinar de la esquizofrenia, que combina el análisis conductual, estructural y molecular utilizando un modelo de esta enfermedad en ratones. Éste combina dos modelos simples de la enfermedad, la inyección postnatal de MK-801 y el aislamiento social tras el destete, que juntos conforman un "modelo de doble impacto" con el que además ya hemos obtenido resultados satisfactorios en ratas (Gilabert-Juan *et al*, 2013a). Con este modelo hemos estudiado la plasticidad estructural de neuronas piramidales (fluorescentes en ratones Thy1-YFP, Feng et al., 2000) y de interneuronas que expresan somatostatina (fluorescentes en ratones GIN, Oliva et al., 2000) en la amígdala y la CPF medial (CPFm). Además, hemos estudiado los comportamientos relacionados con la ansiedad y la memoria de trabajo, y hemos examinado la expresión de moléculas relacionadas con la plasticidad y la neurotransmisión excitadora e inhibidora en estas áreas.

En primer lugar, los ratones fueron sometidos al test de *hole-board* antes de su sacrificio, con el fin de analizar los comportamientos relacionados con la ansiedad, la hiperactividad y las alteraciones de la memoria de trabajo. Los cambios en estos parámetros son bastante comunes en pacientes (Pallanti *et al*, 2013; Pallanti and Salerno, 2015; Van Snellenberg *et al*, 2016) y en modelos animales de esta enfermedad (Jones *et al*, 2011; Lett *et al*, 2014). En nuestro experimento, los ratones Thy1-YFP del grupo de "doble impacto" y todos los ratones GIN criados en aislamiento (modelo simple de aislamiento y modelo de doble impacto) muestran un aumento en comportamientos relacionados con la ansiedad, tales como el tiempo pasado en la periferia del aparato, la velocidad media o el número movimientos estereotipados que realizaron (rotaciones del cuerpo de 360º). Estos

resultados concuerdan con los observados en otros modelos de esquizofrenia basados en la hipofunción de los receptores NMDA (Belforte *et al*, 2010; Bubeníková-Valešová *et al*, 2008). Sin embargo, no hemos observado cambios significativos en la memoria de trabajo en ninguno de nuestros modelos. Estos resultados reflejan la controversia que existe hoy en día a cerca de este parámetro en esquizofrenia, en el que algunos estudios sí que han descrito alteraciones en la memoria de trabajo (Andersen and Pouzet, 2004; Nozari *et al*, 2015), mientras que otros no lo han conseguido (Bubeníková-Valešová *et al*, 2008; Rompala *et al*, 2013).

En este experimento también se ha estudiado si alguno de los modelos simples de esquizofrenia o el modelo de doble impacto, presentan alteraciones en la expresión de moléculas relacionadas con la plasticidad, y de la neurotransmisión excitadora e inhibidora. Hemos encontrado que tanto los ratones aislados, como los pertenecientes al modelo de doble impacto, presentan una expresión reducida de PSA-NCAM en la amígdala. Este hecho aparentemente contradice informes anteriores que describen aumentos en la expresión de PSA-NCAM en el núcleo basolateral de la amígdala después de experimentar diferentes factores de estrés durante la adolescencia (Tsoory *et al*, 2008). Nuestros resultados también contrastan con los descritos usando este mismo modelo de aislamiento después del destete en ratas (Gilabert-Juan *et al*, 2012a). Estas diferencias podrían deberse al uso de diferentes especies o al hecho de que el presente estudio ha medido la expresión de estas moléculas en todos los núcleos de la amígdala juntos, y no en sus diferentes subnúcleos. De hecho, disminuciones similares a las que nosotros presentamos se han observado en el núcleo central de la amígdala de ratones y ratas después de un paradigma de estrés crónico (Cordero *et al*, 2005; Gilabert-Juan *et al*, 2011). Las alteraciones en PSA-NCAM en la amígdala parecen estar directamente relacionadas con los circuitos inhibidores, ya que esta molécula se expresa en interneuronas en esta región (Nacher *et al*, 2002b, 2013), hecho que hace que nuestros descubrimientos sean especialmente importantes para entender cómo la esquizofrenia afecta a esta área.

Por otra parte, también hemos estudiado si los modelos de esquizofrenia producen algún cambio en la expresión de PNNs que rodean a las interneuronas que expresan parvalbúmina en la amígdala y la CPFm. Hemos encontrado una tendencia hacia la

disminución en la región infralímbica de esta última, que está de acuerdo con reducciones similares detectadas en esta área en pacientes esquizofrénicos (Mauney *et al*, 2013) o en un modelo de ratón de esta enfermedad (Paylor *et al*, 2016). Del mismo modo, nuestros resultados muestran una disminución en el número de interneuronas que expresan parvalbúmina en la CPF y en la amígdala de nuestro modelo doble, y que también concuerda con las reducciones observadas en pacientes humanos (Enwright *et al*, 2016), y que coincide con resultados previamente publicados en la CPF en el mismo modelo en ratas (Gilabert-Juan *et al*, 2013a).

También hemos observado un descenso del balance entre excitación e inhibición en la CPFm y en la amígdala de tanto el modelo simple de aislamiento social como el modelo doble. Este equilibrio también puede verse afectado por la expresión de otras moléculas relacionadas con la neurotransmisión excitadora e inhibidora, y que también se han relacionado con modelos animales y pacientes de esta enfermedad. Esto mismo ocurre con la expresión de BDNF, CB1-R, ST8SiaII y St8SiaIV, que se encuentra alterada en seres humanos y otros modelos animales de esquizofrenia, específicamente: un aumento en la expresión de BDNF (Sánchez-Huertas and Rico, 2011) y una disminución en la expresión de ST8SiaIV (Nacher *et al*, 2010) ambos en la CPF; mientras que en la amígdala aumenta la expresión de CB1-R (den Boon *et al*, 2014; Volk and Lewis, 2010).

Por último, también hemos estudiado si la estructura de neuronas piramidales e interneuronas de amígdala y CPFm varía en los modelos simples de esquizofrenia o en el modelo de doble impacto. En cuanto a las neuronas piramidales, sólo aquellas de la CPFm pudieron ser estudiadas debido a que en la amígdala de ratones Thy1-YFP, la YFP se expresa muy abundantemente, haciendo imposible distinguir neuronas individuales. En la CPF, un estudio anterior utilizando el método de Golgi ha demostrado que las neuronas piramidales reducen su arborización y la densidad de sus espinas dendríticas tras inducir un modelo simple de esquizofrenia (aislamiento tras el destete, Wang et al., 2012). Sin embargo, en nuestro experimento, no encontramos diferencias significativas en la densidad de espinas dendríticas en neuronas piramidales prefrontocorticales, ni en los modelos simples ni en el modelo doble, aunque en este último se observa una tendencia hacia una disminución. Estas discrepancias pueden deberse a diferencias entre especies (rata versus ratones) o a

variaciones metodológicas, ya que se utilizaron diferentes técnicas para marcar constitutivamente las neuronas (método de Golgi versus expresión constitutiva de moléculas fluorescentes). Por otro lado, también sería posible que el aumento del número de animales produjera resultados estadísticamente significativos.

Por otra parte, la estructura de las interneuronas que expresan somatostatina también se estudió tras la inducción de los modelos simples y el modelo doble de esquizofrenia. Las células Martinotti de la CPFm muestran una mayor densidad de espinas dendríticas en los modelos simples y en el doble. Ya que la mayoría de las sinapsis establecidas en las espinas dendríticas de estas interneuronas son excitadoras (Guirado *et al*, 2014), este aumento podría representar una ganancia de su superficie sináptica activa. Esto significaría un aumento en la excitación recibida por estas células, lo que finalmente puede conducir a aumentos en la neurotransmisión inhibitoria para compensar la sobreexcitación del sistema. Este resultado concuerda con la elevada neurotransmisión excitadora que se encuentra en esta región en pacientes esquizofrénicos (Starc *et al*, 2017; Sun *et al*, 2013) y en modelos animales de este trastorno (Li *et al*, 2015; Rotaru *et al*, 2011; Yizhar *et al*, 2011). Además, también hemos encontrado un aumento en la arborización dendrítica de interneuronas que expresan somatostatina en la amígdala.

Estudio de las alteraciones sobre la estructura de interneuronas, la neurotransmisión excitadora e inhibidora, y la plasticidad, tras un tratamiento crónico con fluoxetina

En la presente tesis, he tratado de comprender cómo un tratamiento crónico con fluoxetina altera la estructura y conectividad de las interneuronas que expresan somatostatina y la expresión de moléculas relacionadas con la plasticidad, en el hipocampo y en la CPFm. Para ello, hemos inyectado fluoxetina durante 14 días en ratones GIN, en los que una subpoblación de interneuronas que expresan somatostatina expresan constitutivamente la EGFP (Oliva *et al*, 2000). En el hipocampo, no hemos encontrado cambios en la densidad de espinas dendritas de interneuronas somatostatina, mientras que en la CPFm esta densidad aumenta en interneuronas Martinotti. Debido a que las células que expresan somatostatina reciben principalmente contactos excitadores en sus espinas

dendríticas (Guirado *et al*, 2014), este aumento en la densidad de espinas dendríticas puede producir un aumento de la excitación que reciben estas células, y por lo tanto, un aumento en la inhibición que estas células ejercen sobre las neuronas piramidales. Este incremento en la inhibición coincide con el aumento de la expresión de moléculas relacionadas con la neurotransmisión inhibidora en esta región, que también se ha observado en otros estudios tras un tratamiento crónico con fluoxetina (Guirado *et al*, 2012; Tiraboschi *et al*, 2013; Varea *et al*, 2007a).

Por otra parte, la expresión de PSA-NCAM en el hipocampo aumenta en animales tratados crónicamente con fluoxetina. Estos resultados concuerdan con estudios anteriores de nuestro laboratorio en ratas que demostraron aumentos similares en varias regiones cerebrales (Guirado *et al*, 2012; Varea *et al*, 2007a, 2007b). Además, en cultivos organotípicos de la CPFm, la depleción de PSA causa alteraciones en la densidad de espinas dendríticas en la misma subpoblación de interneuronas (Castillo-Gómez *et al*, 2016a), hecho que vincula la expresión de este azúcar con la estructura de estas células. Nuestros resultados también muestran que la proporción de interneuronas que expresan parvalbúmina rodeadas por PNNs está disminuida en el hipocampo y en la CPF de animales tratados con fluoxetina. Estos resultados coinciden con alteraciones similares en otras áreas cerebrales tras tratamientos con este fármaco (Karpova *et al*, 2011).

También hemos analizado cómo un tratamiento crónico con fluoxetina afecta a la densidad de puncta que expresa sinaptofisina, GAD6 (un marcador de sinapsis inhibidoras) y VGlut-1 en el neuropilo de la CPFm y del hipocampo. De esta forma, hemos encontrado un aumento en la expresión de moléculas relacionadas con la neurotransmisión inhibidora (sinaptofisina y GAD6) en el neuropilo del hipocampo, pero no hemos observado ningún efecto en la CPFm. Debido a que no hay cambios en la expresión del marcador sináptico excitador VGlut-1, estos resultados sugieren la formación neta de nuevas sinapsis inhibidoras. En conjunto, estos aumentos están en consonancia con un fuerte incremento de la expresión de PSA-NCAM, ya que en el hipocampo la expresión de esta molécula se asocia principalmente a interneuronas (Guirado *et al*, 2014; Nacher *et al*, 2002a).

Por último, hemos estudiado cómo el tratamiento crónico con fluoxetina afecta a la densidad del puncta perisomático alrededor de neuronas piramidales. Así, hemos encontrado una tendencia hacia una disminución de la densidad de puncta perisomático que expresa parvalbúmina y sinaptofisina en la CPFm, lo que sugiere una disminución en la densidad de estas sinapsis. Estos resultados concuerdan con estudios previos de nuestro laboratorio en los que la depleción de la PSA causa un aumento en el número de puncta inhibidor alrededor de neuronas piramidales (Castillo-Gómez *et al*, 2011, 2016a). También hemos analizado la inervación perisomática sobre la misma población de interneuronas en las que se ha estudiado la estructura (interneuronas Martinotti en la CPFm e interneuronas somatostina del estrato *oriens* en el hipocampo). En estas células, la densidad perisomática de puncta que expresa GAD6 se incrementa después del tratamiento crónico con fluoxetina en el hipocampo, pero no se han encontrado efectos en la CPFm.

Estudio en tiempo real de alteraciones sobre las dinámicas estructurales de neuronas piramidales neocorticales durante la activación crónica de TrkB con la 7,8-dihidroxiflavona

En la presente tesis describo diferentes alteraciones en las dinámicas estructurales de neuronas piramidales del neocórtex después de un tratamiento crónico de 12 días con el agonista de TrkB, el DHF. Como se ha explicado anteriormente, este tipo de análisis resulta extremadamente importante, ya que se ha sugerido que los cambios en estas dinámicas son la fuerza que promueve la adaptación de los circuitos neuronales a ambientes cambiantes (Bhatt *et al*, 2009; Caroni *et al*, 2012; Chen *et al*, 2012; Holtmaat and Svoboda, 2009; Keck *et al*, 2011; Knott and Holtmaat, 2008). Para poder realizar este estudio *in vivo*, he implantado ventanas craneales a ratones Thy1-YFP (Feng *et al*, 2000; Porrero *et al*, 2010) y he obtenido imágenes en tiempo real, con un microscopio de 2 fotones, de las mismas dendritas y axones. Además, he realizado un análisis conductual relacionado con el área cerebral neocortical de interés (corteza de barriles), con el fin de correlacionar las alteraciones estructurales y las funcionales.

En cuanto a las dinámicas de espinas dendríticas de neuronas piramidales, se observaron diferentes alteraciones: un aumento en la función de ganancia de espinas 4 días

después del inicio del tratamiento, y un retorno a los niveles basales al final de éste. Este aumento puede ser debido a la inducción de LTP que causa la activación de TrkB (Minichiello, 2009; Minichiello *et al*, 2002). Dado que esta forma de plasticidad sináptica produce la aparición de espinas dendríticas (Engert and Bonhoeffer, 1999), el aumento de la función de ganancia no es sorprendente. Por otra parte, la función de estabilidad de espinas dendríticas se reduce gradualmente durante todo el experimento en ambos grupos experimentales, aunque más notablemente en animales control. Esta tendencia parece obedecer a la pérdida de estabilidad natural publicada en la misma cepa de ratones al realizar imágenes en tiempo real (Grutzendler *et al*, 2002).

También he estudiado la dinámica de las espinas dendríticas estables (aquellas presentes al menos durante 4 días), parámetros que son especialmente relevantes porque aseguran la presencia de al menos una sinapsis (Holtmaat *et al*, 2006; Knott *et al*, 2006) y , por lo tanto, son los que influyen en la red. Curiosamente, la función de pérdida de espinas estables aumenta significativamente en el grupo control, mientras que el tratamiento de DHF parece que protege contra estos cambios deletéreos. Además, también se observó que las espinas que son estables a lo largo de todo el experimento aumentan su volumen sólo en el grupo de control. Ambos resultados sugieren que el manejo continuo de los animales tiene un efecto deletéreo en la red neural, lo que provoca una pérdida de conexiones estables. Sin embargo, las espinas que se mantienen estables aumentarían su volumen y, en consecuencia, su potenciación, con el fin de mantener sinápticamente el circuito (Matsuzaki *et al*, 2004). Sugerimos que el DHF, debido a sus propiedades neurotróficas, ejercería un efecto protector rápido contra las repercusiones perjudiciales causadas por la imagen en tiempo real. Este efecto ya se ha demostrado con el DHF, mostrando que protege contra la excitotoxicidad causada por glutamato (Chen *et al*, 2011a), la hipoxia neonatal y la isquemia (Uluc *et al*, 2013), o incluso la degeneración de neuronas dopaminérgicas en modelos animales de la enfermedad de Parkinson (Luo *et al*, 2016) o apoptosis inducida por estaurosporina (Jang *et al*, 2010).

Las dinámicas de los botones de paso axónicos (EPB), varicosidades membranosas que forman los elementos presinápticos localizados en el axón, también fueron estudiadas. Nuestro estudio muestra un incremento en la función de ganancia de EPB 8 días después

del inicio del tratamiento y un aumento en la función de ganancia de EPB que se estabilizarán, es decir, aquellos que estarán presentes durante al menos 4 días. También describimos un aumento en la función de pérdida de EPB que fueron estables (EPB que estuvieron presentes durante al menos 4 días y se perdieron después), y una disminución en la función de estabilidad, en animales tratados con DHF.

Por otro lado, también hemos tratado de entender si la activación de TrkB con el DHF afectaría el comportamiento dependiente de la corteza barriles. La entrada sensorial de las vibrisas en roedores es recibida por esta región de la corteza somatosensorial. Dado que estos animales utilizan estos bigotes para discriminar diferentes texturas (Arabzadeh *et al*, 2005; Brecht, 2007; Guić-Robles *et al*, 1989; von Heimendahl *et al*, 2007), hemos realizado un test comportamental de reconocimiento de objetos novedosos modificado (Leger *et al*, 2013), que sirve como correlato para las alteraciones en esta región. Hemos cambiado el protocolo acortando el período entre objetos familiares y nuevos (Burke *et al*, 2011, 2012), para distinguir adecuadamente entre el comportamiento de reconocimiento de objetos (dependiente de la corteza de barriles, Brecht, 2007; Kleinfeld et al., 2006), y la memoria a largo plazo (dependiente de otras áreas corticales, Simons and Spiers, 2003; Wiltgen et al., 2004). También hemos adaptado los objetos con diferentes texturas para ser detectados principalmente por vibrisas, y hemos usado dos conjuntos de objetos con diferente dificultad para ser reconocidos (fácil y difícil), para así estudiar si el DHF mejora la percepción sensorial depende de la corteza de barriles. Nuestros resultados demuestran que los ratones tratados con DHF presentan una ratio de discriminación de objetos novedosos inferior a la de los ratones tratados con solución salina, lo que significa que son capaces de discriminar mejor los objetos difíciles (emplean menos tiempo en explorarlos) después de ser tratados con DHF. Así, mostramos que esta flavona mejora el comportamiento de reconocimiento de objetos, probablemente alterando la dinámica estructural de las neuronas piramidales de la capa V de la corteza de barriles. Nuestros resultados son una adición necesaria al conocimiento cada vez mayor de cómo la activación de la señalización de TrkB altera la estructura de las neuronas piramidales en el neocórtex.

1. Las interneuronas que expresan somatostatina del hipocampo expresan receptores NMDA en sus somas y en sus espinas dendríticas.

2. El tratamiento agudo de ratones adultos con el antagonista de receptores NMDA, el MK-801, aumenta la locomoción y los comportamientos relacionados con la ansiedad.

3. El tratamiento agudo de ratones adultos con el MK-801 aumenta la densidad de botones de paso en interneuronas hipocampales que expresan somatostatina, mientras que la densidad de sus espinas dendríticas permanece inalterada.

4. El análisis en tiempo real de las espinas dendríticas de las interneuronas que expresan somatostatina en cultivos organotípicos del hipocampo revela una disminución rápida en su función de ganancia después de la administración del MK-801.

5. El análisis en tiempo real de las espinas dendríticas de interneuronas que expresan somatostatina en cultivos organotípicos del hipocampo muestra una disminución en su densidad relativa después de la administración del MK-801.

6. El análisis en tiempo real de las espinas dendríticas de interneuronas que expresan somatostatina en cultivos organotípicos del hipocampo revela aumentos en sus funciones de ganancia y 24 horas después de la administración del NMDA.

7. El modelo de esquizofrenia de doble impacto en ratón muestra un aumento de la locomoción y los comportamientos relacionados con la ansiedad.

8. Las interneuronas de la amígdala en el modelo de esquizofrenia de doble impacto tienen una mayor arborización dendrítica en comparación con los controles.

9. Los modelos simples de esquizofrenia y el modelo de doble impacto presentan una mayor densidad de espinas dendríticas en interneuronas de la corteza prefontal.

10. La expresión de los marcadores de la neurotransmisión excitadora se incrementa en la amígdala lateral y medial en el modelo de esquizofrenia de doble impacto.

11. La inyección perinatal del MK-801, un modelo simple de esquizofrenia, aumenta la expresión del marcador inhibidor VGAT, y del equilibrio excitación-inhibición, en las regiones infralimbica y prelimbica de la corteza prefrontal.

12. La inyección perinatal de MK-801 aumenta la densidad de interneuronas que expresan parvalbúmina rodeadas por redes perineuronales, en la región infralimbica de la corteza prefrontal.

13. El tratamiento crónico con fluoxetina aumenta la densidad de espinas dendríticas en interneuronas que expresan somatostatina de la corteza prefrontal.

14. El tratamiento crónico con fluoxetina disminuye la densidad de interneuronas que expresan parvalbúmina rodeadas por redes perineuronales, en la corteza prefrontal y en el hipocampo.

15. El tratamiento crónico con fluoxetina aumenta la expresión de PSA-NCAM y sinaptofisina en diferentes regiones del hipocampo.

16. El tratamiento crónico con fluoxetina aumenta la densidad de puncta perisomáticos inhibidores sobre interneuronas pero no en neuronas piramidales de la corteza prefrontal.

17. Las neuronas piramidales de la corteza de barriles expresan TrkB en sus somas, espinas dendríticas y botones axónicos.

18. El tratamiento crónico con 7,8-dihidroxiflavona aumenta la función de ganancia de los botones axónicos y de las espinas dendríticas en las neuronas piramidales del neocortex.

19. La función de pérdida de espinas dendríticas estables, y el volumen de espinas que son estables a lo largo de todo el proceso experimental, permanecen inalterados durante un tratamiento crónico con 7,8-dihidroxiflavona, mientras que se incrementan en animales control.

20. El tratamiento crónico con 7,8-dihidroxiflavona mejora la discriminación de objetos difíciles en el test comportamental de reconocimiento de objetos novedosos.

21. El tiempo de exploración de un objeto nuevo difícil está positivamente correlacionado con la tasa de recambio de espinas dendríticas y botones axónicos en animales tratados con 7,8-dihidroxiflavona, pero no en controles.

I. INTRODUCTION

The nervous system is a set of cells that, altogether, receive information from the body and generate a response accordingly. Although most of the animal species have one, in vertebrates its complexity increases to make it one of the most interesting systems in biology. Anatomically, it is composed by the central nervous system (CNS), which is the brain and the spinal cord, and the peripheral nervous system (PNS), composed by all afferent and efferent nerves that reach every part of the body. The cellular basis of these systems were proficiently exposed by Ramon y Cajal more than 2 centuries ago in his book "*Textura del sistema nervioso del hombre y de los vertebrados"* (Ramón y Cajal, 1909). Indeed, the CNS is composed by several types of specialized cells, being the neuron the one responsible for the generation and transmission of the action potential. Although the brain, and consequently the neuron, has been classically viewed as a static element, during the last century researchers dared to defy this belief. Now it is accepted that, not only the nervous system remodels under pathological circumstances, but also that this plasticity occurs under natural ones, including the adaptation to aversive experiences, learning or memory (Berlucchi and Buchtel, 2009; Smythies, 2002). In the current thesis, I will focus my studies on this neuronal plasticity, and on how different neuronal populations alter their structure under diverse pharmacological and environmental manipulations. To achieve this goal, I will study these phenomena in different areas of the mouse brain: The amygdala, the hippocampus and the prefrontal (PFC) and barrel cortices.

1. AREAS OF STUDY

1.1. Neocortex

The neocortex is the largest and evolutionarily the most recent part of the mammalian cerebral cortex, which is involved in higher functions such as sensory perception. It is also called *isocortex* because of its uniform cytoarchitectural configuration, consisting of 6 horizontal layers, defined by the presence of pyramidal neurons in some of them, whereas interneurons are scattered throughout the extension of the region. These layers run parallel to the cortical surface and are numbered from I -the outermost- to VI -the innermost (figure 1A):

- Layer I: Contains very few neuronal bodies, most of them from interneurons. It is mainly composed by horizontal dendrites and axons that emerge from pyramidal neurons in inner layers of the neocortex. These dendrites receive their input from thalamic and intracortical afferents (Herkenham, 1980; Shipp, 2007).
- Layer II: It is mainly composed by granular neurons (small excitatory neurons) and it is generally considered in combination with layer III (layer II/III) (Shipp, 2007; Spruston, 2008).
- Layer III: Also known as the *external pyramidal layer*, it is composed by medium-sized pyramidal neurons, which project mainly within their region or to other cortical areas (Shipp, 2007; Spruston, 2008).
- Layer IV: It also contains granular neurons. Interestingly, it is the layer where cortical columns can be observed in the barrel cortex (Woolsey and Van der Loos, 1970), and it is absent from the PFC (Fuster, 2015).
- Layer V: Also known as the *internal pyramidal layer*, it is the layer where the large-sized pyramidal neurons are located. These neurons are specially interesting since they project mainly outside their local region to other cortical areas or subcortical structures (Shipp, 2007; Spruston, 2008).
- Layer VI: contains few pyramidal neurons which are interconnected with thalamic neurons (Herkenham, 1980; Lam and Sherman, 2010; Shipp, 2007).

Although the neocortex is a continuum, it is functionally divided in different regions and subregions. In the present thesis I will focus in the barrel cortex and the PFC of mice.

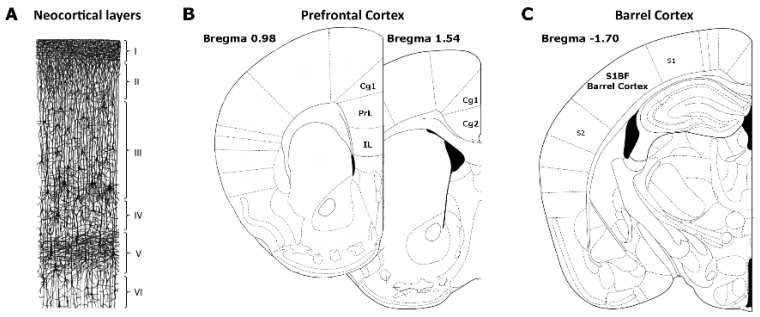

Figure 1: Neocortical regions of study. A) Necortical layers. B) Localization of the areas of interest from the PFC. C) Localization of the barrel cortex. Cg1: cingulate cortex 1. Cg2: cingulate cortex 2. PrL: prelimbic cortex. IL: infralimbic cortex. S1BF: primary somatosensory cortex, barrel field. S1: primary somatosensory cortex. S2: secondary somatosensory cortex. A adapted from (Ramón y Cajal, 1909). B & C modified from (Paxinos and Franklin, 2013).

1.1.1 Prefrontal cortex

The PFC is an association cortex, located in the anterior part of the mammalian brain. It is responsible for motivation, self-knowledge, social behaviour and working memory, among others (Fuster, 2015). Its malfunctioning is involved in several neuropsychiatric disorders, including schizophrenia, major depression and autism spectrum disorders (see section 4, Bicks *et al*, 2015). It comprises the medial (mPFC), the orbitofrontal (OFC) and the lateral (lPFC) prefrontal cortices, which present different cytoarchitectural and functional characteristics (Sul *et al*, 2010; Van De Werd *et al*, 2010; for reviews see Seamans *et al*, 2008; Uylings *et al*, 2003). In this thesis I will mainly focus on the mPFC, which, in rodents, can be subdivided into three areas with different anatomical and functional features: (1) the rostral portion of the anterior cingulate cortex (ACC), which in turn is divided into a dorsal (ACd or Cg1, in mice from bregma 2.34 to bregma -0.22) and a ventral (ACv or Cg2, in mice from bregma 1.42 to bregma -0.22) area; (2) the infralimbic cortex (IL, in mice from bregma 1.98 to bregma 1.34) and, (3) the prelimbic cortex (PrL, in mice from bregma 3.08 to bregma 1.54) (Paxinos and Franklin, 2013, figure 1B). The architectural order of cells and fibres in the rodent PFC basically conforms to the structural plan prevailing throughout the neocortical regions in mammals, but lacks the *internal granule cell layer* (layer IV; Fuster, 2015; Kandel *et al*, 2012).

1.1.2. Barrel cortex

The barrel cortex is a subregion of the primary somatosensory cortex (in mice from bregma 0.38 to bregma -1.94; Paxinos and Franklin 2013) that is only present in a few species, mostly rodents, and receives input from the animal whiskers via the thalamus (figure 1C). In this cortex, layer IV is organized into cylindrical columns of neurons (barrels), whose topographical distribution mirrors that of the whisker follicles (Woolsey *et al*, 1975). These features make the barrel cortex a very interesting region for functional studies: The study of this area has provided important insights into cortical processing and plasticity (Fox, 2008).

1.2. Hippocampus

The hippocampus is part of the mammalian archicortex, evolutionarily one of the oldest parts of the cerebral cortex. Being a region of the limbic system, it has been broadly studied due to its role in short-term memory, long-term memory consolidation and spatial memory. Its structure is beautifully conserved across the class *mammalia* (Clark and Squire, 2013). However, homologous regions, at least of some of its parts, are present in all vertebrates (Elliott *et al*, 2017; for a review see Striedter, 2016). Anatomically, it comprises a large portion of the cerebral cortex of rodents (in mice, from bregma -0.94 to bregma -4.16; Paxinos and Franklin 2013), and it is composed by the Ammon's horn (*Cornu Ammonis*, CA) and the dentate gyrus (DG). The former has four subdivisions: CA1, CA2, CA3 and CA4. The latter embraces CA4 and is one of the regions where adult neurogenesis occurs in the mammalian brain (Gonçalves *et al*, 2016; Gould, 2007). In addition, the Ammon's horn is generally divided in 6 *strata*: *Alveus, oriens, pyramidale, lucidum, radiatum* and *lacunosum moleculare;* whereas the DG comprises 3: The molecular, the granular, and the polymorphic cell layers (Amaral *et al*, 2007; Andersen *et al*, 2007; figure 2).

The basic circuitry of the hippocampus is called the trisynaptic circuit: The projection from the entorhinal cortex forms the first synapse onto the granular cells of the dentate gyrus via the perforant path. The second synapse is from the granule cells to the pyramidal neurons of CA3 via the mossy fiber pathway. Finally, the third synapse is from CA3 pyramidals to the pyramidal neurons of CA1 via the Schaffer collaterals (Ramón y Cajal, 1909). However, additional connections have been described in the hippocampus, such as a direct connection between the entorhinal cortex and the CA1 pyramidal neurons (Desmond *et al*, 1994; figure 2).

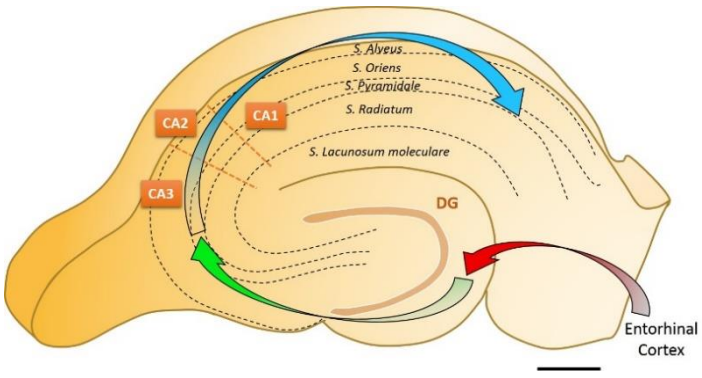

Figure 2: Drawing of the hippocampus highlighting the strata of study in CA1. Arrows schematically represent the trisynaptic circuit. Red arrow: perforant path, green arrow: mossy fibers, blue arrow: Schaffer collaterals. Scale bar: 1mm.

1.3. Amygdala

The amygdala is located medially in both hemispheres in mammals and, as the hippocampus, is part of the limbic system. It is not only responsible for fear behaviours, such as pavlovian fear-conditioning, but also for motivation and the processing of rewarding environmental stimuli (LaBar and Cabeza, 2006; Murray, 2007; Seymour and Dolan, 2008). Its malfunction is related to several psychiatric disorders, such as schizophrenia (see section 4.3; Aleman and Kahn, 2005) or anxiety-related disorders (see section 4.1; Shin and Liberzon, 2010). Anatomically, it is composed by several nuclei, generally encompassed in three greater interconnected groups: Basolateral, centromedial and cortical (Sah *et al*, 2003; figure 3).

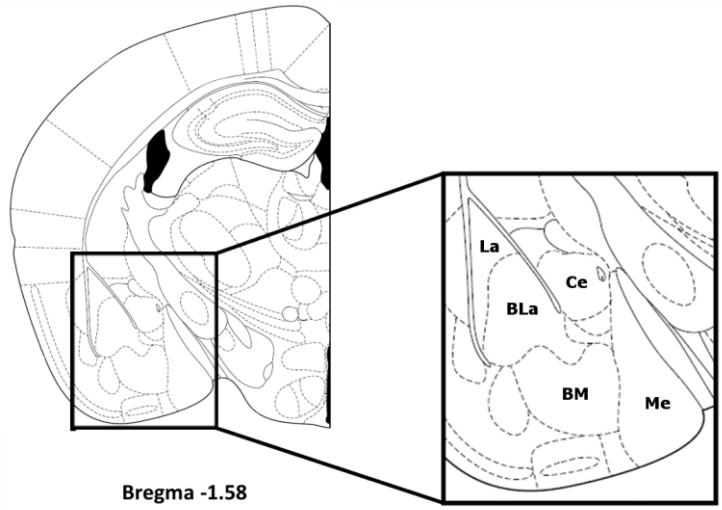

Figure 3: Amygdaloid regions of study. La: lateral nucleus. BLa: basolateral nucleus. BM: basomedial nucleus. Me: medial nucleus. Ce: central amygdala. Modified from Paxinos and Franklin, 2013.

1.4. Interconnections

Interestingly, some of the areas that have been described above interconnect with each other, complicating the understanding of their function. The PrL and IL areas of the PFC receive connections from the ventral hippocampus and the basolateral nucleus of the amygdala (Jay and Witter, 1991; Krettek and Price, 1977), and both mediate each other's input (Ishikawa and Nakamura, 2003). The hippocampal input is thought to mediate episodic memory processes (Preston and Eichenbaum, 2013) whereas the amygdaloid

input mediates fear conditioning behaviour (Garcia *et al*, 1999). The disruption of prefrontal innervation by those two areas is presumed to underlie the etiopathology of neuropsychiatric disorders such as schizophrenia (Thomases *et al*, 2014). In addition, the lateral and basal nuclei of the amygdala also directly innervate the hippocampus, and this structure back-forward innervate these nuclei; this connection mediates context-fear memory retrieval (Maren *et al*, 2013).

2. NEURONS IN THE CENTRAL NERVOUS SYSTEM

There are several neuronal classifications in Neuroscience, such as those based on neuronal morphology, the type of postsynaptic potentials they elicit in other cells or the neurotransmitter they release. Firstly, neurons present a huge variety of morphologies that range from rod-like to stellate shaped. Secondly, they can evoke postsynaptic potentials that can be either excitatory (EPSP, excitatory neurons) or inhibitory (IPSP, inhibitory neurons). Finally, the neurotransmitter they release is highly linked with the latter, being the L-Glutamate (glutamate henceforth, glutamatergic neurons) and the γ-Aminobutyric acid (GABA, GABAergic neurons), the most important excitatory and inhibitory (respectively) neurotransmitters in the CNS. In the current section I will focus on the excitatory pyramidal neurons and the inhibitory interneurons (figure 4).

2.1. Pyramidal neurons

Pyramidal neurons are glutamatergic and therefore release the amino-acid glutamate, the most common excitatory neurotransmitter in the brain, as their primary neurotransmitter. These cells have a strongly defined and consistent structure: A pyramidal-shaped soma (from which they receive their name), two separate dendritic trees (apical and basal) and a single axon (Van Aerde and Feldmeyer, 2015; Spruston, 2008). They are mainly projection neurons, and are the most studied cell type in the CNS (Kandel *et al*, 2012).

There are two types of dendrites in these cells, which branch profusely the further we are from the soma, and show different physiological proprieties. The **apical dendrite** is unique and emerges from the apex of the pyramid, whereas two or more **basal dendrites** emerge from the base of the soma. On the other hand, the **axon** arises from the base (Kandel *et al*, 2012). The dendrites, somata and initial segment of the axons contain different excitatory and inhibitory neurotransmitter receptors, although the latter is only innervated by a special type of interneuron (Kawaguchi and Kubota, 1997; Woodruff *et al*, 2010). The different types of inhibitory cells, as well as the neurotransmitter receptors, will be explained in detail hereafter.

One of the main characteristics of the pyramidal neurons is the presence of membranous specializations in the dendrites, very numerous in the apical dendrite and slightly less frequent in the basal dendrites. They are called **dendritic spines**, and they cluster the receptors and spatially compartmentalize the electrical signal (Hering and Sheng, 2001; Lee *et al*, 2012; Parajuli *et al*, 2017). On the other hand, the axons also display membranous thickenings, called **axonal *boutons***, which contain and release the synaptic vesicles (Kevenaar and Hoogenraad, 2015). Because of their roles as postsynaptic and presynaptic elements, spines and *boutons* have been found to be proper markers for neuronal input and output; therefore, increases in spine and axonal *bouton* density have been correlated to increases in neuronal activity (Becker *et al*, 2008; Engert and Bonhoeffer, 1999; figure 4).

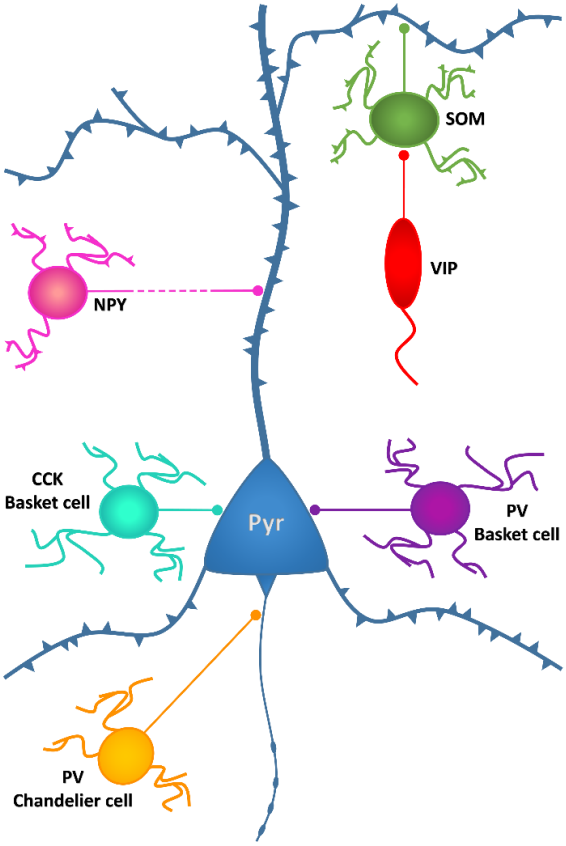

Figure 4: Scheme depicting the basic circuitry of the cerebral cortex, showing the pyramidal neurons and interneurons considered in this thesis. Pyr: pyramidal neuron. PV: parvalbumin-expressing interneurons, which can be basket or chandelier cells. CCK: cholecystokinin-expressing interneuron. NPY: neuropeptide Y-expressing interneuron. VIP: vasoactive intestinal peptide-expressing interneuron. SOM: somatostatin-expressing interneuron.

2.2. Interneurons

This type of cells is mainly inhibitory in the CNS. Their name is due to their intermediate role in the neural circuits, projecting locally, and generally are responsible for their correct functioning. However, contrary to pyramidal cells, interneurons are a heterogeneous population of neurons with diverse morphological, physiological, neurochemical and synaptic characteristics, which complicate their study and understanding. As a unifying characteristic, they are all GABAergic, which means they synthetize and secrete GABA, the main inhibitory neurotransmitter of the brain. They can also express different excitatory and inhibitory receptors in their dendrites or somata (see section 3.2.1). There are many classifications of interneurons following several criteria, which try to sort out different populations. In the present thesis, I will use the molecular classification of the Petilla terminology (Ascoli *et al*, 2008), which define five different types of interneurons depending on the expression of different calcium binding proteins and neuropeptides; these are: Parvalbumin (PV), somatostatin (SOM), neuropeptide Y (NPY), vasoactive intestinal peptide (VIP), and cholecystokinin (CCK) (figure 4).

2.2.1. Parvalbumin-expressing interneurons

These interneurons strongly express the calcium-binding protein parvalbumin (PV) throughout the cell. Morphologically, they can be subdivided into basket or chandelier cells. Basket cells are named after the perisomatic baskets they form around the somata of pyramidal neurons. In fact, this perisomatic inhibition allows for a single PV-expressing cell to inhibit simultaneously many pyramidal neurons. This phenomenon produces the firing synchrony of the pyramidal cells, important for the proper functioning of the system (Singer, 1999). Because of that, basket cells are one of the most studied types of interneurons of the brain. On the other hand, less is known about chandelier cells. They directly inhibit the excitatory output of the pyramidal neurons via axo-axonic synapses (see section 2.1; they innervate the initial segment of the axon of pyramidal cells), but they still pose a mystery to researchers in many ways (Woodruff *et al*, 2010).

2.2.2. Neuropeptide Y-expressing interneurons

Neuropeptide Y (NPY) is widely coexpressed with other proteins and neuropeptides throughout the cerebral cortex. However, only interneurons which express NPY, but not the neuropeptide SOM are considered to be in this group. They are present in the neocortex, hippocampus and amygdala (Real *et al*, 2009), as well as other brain regions (Allen *et al*, 1983; Markram *et al*, 2004). Their neuronal morphology and functionality is very diverse, which make this group of cells very heterogeneous. Among their main functions, they mediate long-range inhibition in the mPFC (Saffari *et al*, 2016).

2.2.3. Vasoactive intestinal peptide-expressing interneurons

These interneurons express the vasoactive intestinal peptide (VIP), another neuropeptide, but never PV or SOM. However, they can coexpress other proteins, constituting different subpopulations. They conform a very interesting interneuronal population due to their function: They inhibit other interneurons in the neocortex, such as SOM-expressing cells, producing a disinhibition of pyramidal neurons (Karnani *et al*, 2016; Pi *et al*, 2013). They are present in the neocortex (Markram *et al*, 2004), hippocampus (Freund and Buzsáki, 1996) and amygdala (Spampanato *et al*, 2011).

2.2.4. Cholecystokinin-expressing interneurons

This class of interneurons always expresses the neuropeptide Cholecystokinin (CCK), but not SOM or VIP. As the PV-expressing basket cells, they also innervate the somata of pyramidal neurons. However, they form smaller baskets and, therefore, allow a finer tuning of the network (Freund, 2003). They are also present in the neocortex (Markram *et al*, 2004), the hippocampus (Freund and Buzsáki, 1996) and the amygdala (Jasnow *et al*, 2009; Spampanato *et al*, 2011).

2.2.5. Somatostatin-expressing interneurons

They express the neuropeptide somatostatin (SOM), although sometimes they can coexpress other markers. They are widely present in the brain, including the neocortex (Markram *et al*, 2004), hippocampus (Freund and Buzsáki, 1996) and the amygdala (Real *et al*, 2009). Their morphology is diverse, but their functionality is very specific: They

strongly inhibit the distal dendrites of pyramidal cells (De Lima and Morrison, 1989; Wang *et al*, 2004), and frequently receive reciprocal inhibition from other interneurons, including SOM-expressing cells (Urban-Ciecko and Barth, 2016; Yavorska and Wehr, 2016). They are essential for the maturation of deep cortical circuits (Tuncdemir *et al*, 2016) and are important players in other stages of neurodevelopment, brain pathology and neuronal plasticity (Liguz-Lecznar *et al*, 2016). In addition, they display **dendritic spines**, a rare feature in interneurons (Gilabert-Juan *et al*, 2011, 2013b, 2017; Guirado *et al*, 2014). This thesis will focus specially on some subpopulations of SOM-expressing interneurons: The Martinotti cells in the neocortex, and the O-LM cells in the hippocampus.

2.2.5.1. Martinotti cells

They are found in layers II-IV of the neocortex, and their axons project to layer I to inhibit directly the apical dendrites of pyramidal cells. Because they can horizontally inhibit different neurons, they are also involved in cross-columnar inhibition (Wang *et al*, 2004). They also innervate the basal dendrites of pyramidal cells, their somata and even some PV-expressing interneurons, which produces a disinhibition of pyramidal cells and has massive functional ramifications (Pfeffer *et al*, 2013; Scheyltjens *et al*, 2016).

2.2.5.2. O-LM cells

The O-LM cells of the hippocampus are named after their microcircuitry: Their somata are located in the *stratum oriens*, where they branch and receive their inputs from pyramidal neurons of the *stratum pyramidale* (Blasco-Ibáñez and Freund, 1995), and reciprocally inhibit these cells and other interneurons, establishing these synapses in the *stratum lacunosum moleculare* (Müller and Remy, 2014). They are essential for the correct functioning of the hippocampus. In fact, they appear to mediate *theta* oscillations (Katona *et al*, 2014) and have been postulated to be essential for the establishment of spatial context-fear conditioning (Lovett-Barron *et al*, 2014; for a review see Müller and Remy, 2014).

3. PLASTICITY IN THE NERVOUS SYSTEM

3.1. Structural plasticity

Pyramidal neurons and interneurons can change their morphology under different conditions, involving changes in the length and complexity of dendritic arbors, and in the density or morphology of their dendritic spines (Fu and Zuo, 2011; Glausier and Lewis, 2013; Guirado *et al*, 2014; Lee *et al*, 2005) and axonal *boutons* (Colicos *et al*, 2001; Florence *et al*, 1998; Nikonenko *et al*, 2003). These structural alterations happen constantly in order to adapt to a changing environment, either in natural conditions, like ageing (Burke and Barnes, 2006), or disturbed ones. Regarding this, it is known that pyramidal neurons experience structural remodelling after chronic stress and in animal models of depression (see sections 4.1 and 4.2; McEwen, 1999; Qiao *et al*, 2016a), in neurodevelopmental disorders (see section 4.3; Flores *et al*, 2016; Glausier and Lewis, 2013), obesity (Dingess *et al*, 2017), and after different pharmacological manipulations (see section 3.2; Castillo-Gómez *et al*, 2016b; Guirado *et al*, 2009; Yang *et al*, 2015). On the other hand, studies on the effects on interneuron morphology are more scarce, even though these inhibitory neurons are at the base of the neural circuits (Kullmann, 2011; Roux and Buzsáki, 2015) and play an important role in CNS physiology (Nacher *et al*, 2013).

Dendritic spines were initially thought to be present only in pyramidal neurons, but different studies have shown that some interneuronal subpopulations also display these postsynaptic specializations, mainly SOM and NPY-expressing cells (see sections 2.2.2 and 2.2.5; Freund and Buzsáki, 1996; Scheuss and Bonhoeffer, 2014). Likewise, dendritic spines and axonal *boutons* have been found to be proper proxies for neuronal input and output; in fact, increases in their density have been correlated to increases in neuronal activity (Becker *et al*, 2008; Engert and Bonhoeffer, 1999). Therefore, the study of structural remodelling in interneurons has been gaining strength in the last decade. However, the structure of dendritic spines is slightly different than those found in pyramidal cells: They lack the spine apparatus, several synapses are established per spine (in contrast with the one or two found in pyramidal neuron spines) and they are usually less numerous (Acsády *et al*, 1998; Gulyás *et al*, 1992; Scheuss and Bonhoeffer, 2014). Among all the interneuronal types, dendrite-targeting cells, which express SOM, are of great interest because of their

role in the establishment of cortical circuits (Tuncdemir *et al*, 2016) and other neurodevelopmental processes (see section 2.2.5; Liguz-Lecznar *et al*, 2016). In addition, recent studies from our laboratory have demonstrated that they undergo dendritic remodelling after chronic stress (see sections 4.1 and 4.2; Gilabert-Juan *et al*, 2011, 2013b, 2017) or the depletion of plasticity related molecules (see section 3.2.3.1; Castillo-Gómez *et al*, 2016a; Guirado *et al*, 2014).

In order to study neuronal morphology, classic studies –such as those described in Cajal's *Textura del Sistema nervioso del hombre y los vertebrados* (Ramón y Cajal, 1909)- used Golgi's method (Golgi, 1873). However, in the last decade the emergence of transgenic mice has allowed the researcher to breed mice strains, in which particular neuronal populations express constitutively a fluorescent protein. These proteins, such as the enhanced green fluorescent protein (EGFP) or the yellow fluorescent protein (YFP), allow the use of fluorescence, confocal or 2-photon microscopy to follow the entire morphology of a neuron.

Excellent examples of these strains are the thy1-YFP-H, in which layer V cortical pyramidal neurons are densely labelled with YFP (Feng *et al*, 2000), and the GIN line (Oliva *et al*, 2000), in which a subpopulation of SOM-expressing interneurons of the neocortex, hippocampus and amygdala, express EGFP. In fact, these strains allow the longitudinal analysis of these neurons either after the chronic implantation of a cranial window upon the neocortex (Holtmaat *et al*, 2009; figure 5A), or in organotypic cultures of a given brain region (Stoppini *et al*, 1991; figure 5B).

It should be noted the importance of longitudinal analyses when studying neuronal morphology. In fact, these methods give us information on their structural dynamics, which are sensible to transient and homeostatic changes that otherwise would be undetected. Structurally, these changes in network configuration are represented by the addition of one spine on one site, compensated by the pruning on another (figure 5C). Changes in structural dynamics have been shown in pyramidal neurons after normal brain ageing (Grillo *et al*, 2013; Mostany *et al*, 2013) and after sensory deprivation (Cane *et al*, 2014; Hofer *et al*, 2009; Holtmaat and Svoboda, 2009). Importantly, similar changes have

been found in inhibitory circuits after sensory deprivation (Chen *et al*, 2011b, 2011c, 2012; Chen and Nedivi, 2013; Keck *et al*, 2011; van Versendaal *et al*, 2012).

Despite the enormous information that these studies provide, one limitation still persists: The position of the cranial window, which can only be used chronically, without brain damage, on studies of the neocortex (Holtmaat *et al*, 2009; Mostany and Portera-Cailliau, 2008; Xu *et al*, 2007). Another important area for this thesis is the hippocampus, which due to its central location in the brain, does not allow for the chronic implantation of a cranial window. This setback can be solved with the use of entorhino-hippocampal organotypic cultures (Stoppini *et al*, 1991), which allow us to follow elements from a hippocampal neuron throughout an entire experiment. Although they also present intrinsic limitations, these cultures have been broadly used as an *in vitro* model of the rodent hippocampus (Gähwiler *et al*, 1997; Humpel, 2015), allowing the study of structural changes in real-time (figure 5B).

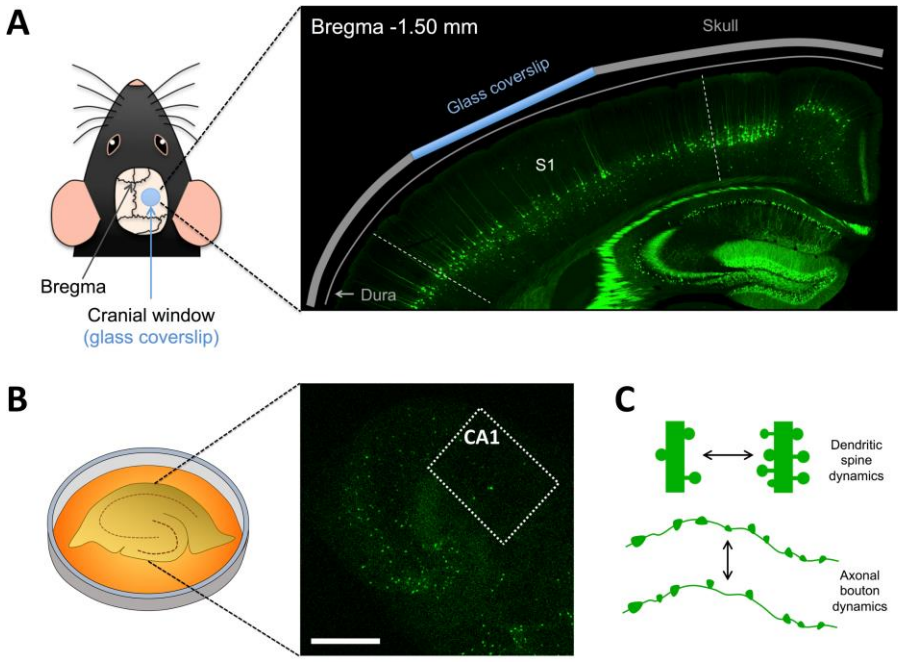

Figure 5: Methods of study and analysis of the structural dynamics. A) Schematics of a cranial window and a panoramic view of a Thy1-YFP mouse showing the primary somatosensory cortex. B) Schematics of a culture dish with an entorhino-hippocampal organotypic culture and a panoramic view of a representative slice from a GIN mouse. The CA1 region is squared. C) Scheme showing the longitudinal analysis of dendritic spines and axonal *boutons*. The scale bar is 600µm in A and 500µm in B.

3.2. Modulation of structural plasticity

3.2.1. Modulation by neurotransmitters

We can classify the modulation of structural plasticity on basis of the type of neurotransmitter receptors that are stimulated in our neuron of interest. In this thesis I will study the modulation by GABAergic, Glutamatergic and Serotonergic systems (figure 6).

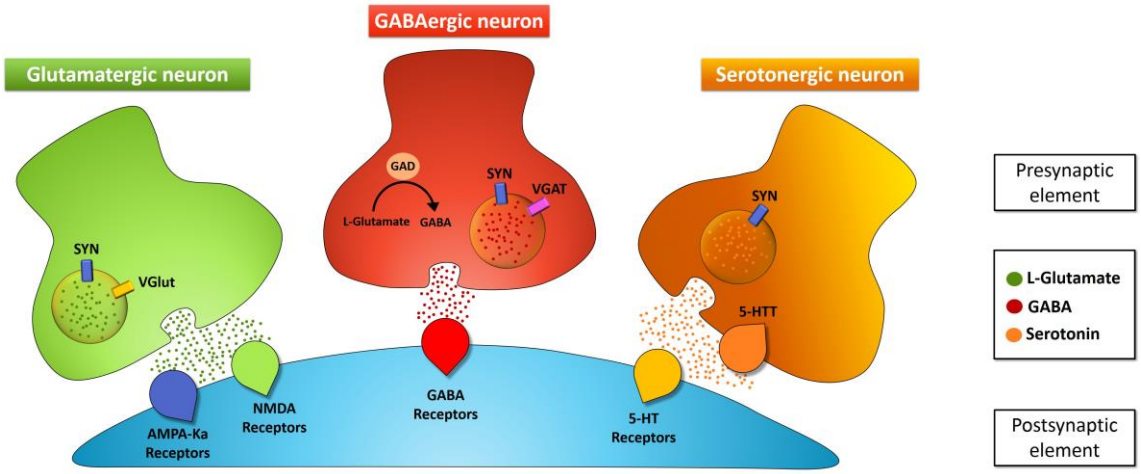

Figure 6: Scheme showing glutamatergic (green), GABAergic (red) and Serotonergic (orange) synapses. All the vesicular proteins and enzymes of interest for this thesis are shown in the diagram. GABA: gamma-aminobutyric acid. SYN: synaptophysin. VGlut: vesicular transporter of glutamate. GAD: glutamic acid decarboxylase. VGAT: vesicular transporter of GABA. AMPA-Ka Receptors: α-amino-3-hydroxy-5-methyl-4-isoxazolepropionic acid and kainate receptors. NMDA Receptors: N-methyl-D-aspartate receptors. GABA Receptors: gamma-aminobutyric acid receptors. 5-HT Receptors: receptors of serotonin. 5-HTT: serotonin transporter.

3.2.1.1. Glutamatergic neurotransmission

Glutamate is one of the most common amino acids of the organism and also the main excitatory neurotransmitter in the brain. It is synthetized mainly as a by-product of the Krebs cycle, fact that makes it easily available, although it can be also transported through the blood-brain barrier (Smith, 2000). Therefore, glutamatergic neurons account for those which release this neurotransmitter, being the main group the pyramidal neurons.

Once in the axon, glutamate is enclosed in synaptic vesicles, which are surrounded by synaptic proteins that will ensure the proper neurotransmitter release to the synaptic cleft.

One of these proteins, which has been studied profusely in this thesis, is **synaptophysin** (SYN). This protein is present in virtually all active synapses, including GABAergic and Serotonergic (Li *et al*, 2010a; Tarsa and Goda, 2002), trait that makes it an excellent marker for both excitatory and inhibitory connections. Another important protein employed in the studies constituting this thesis, is the **vesicular glutamate transporter** (VGlut), which is only present in glutamatergic vesicles. This protein specializes in the transport of the glutamate into the synaptic vesicles and stabilizes them at presynaptic terminals to ensure the release of the glutamate to the synaptic cleft (Siksou *et al*, 2013). In the CNS, we can find three isotypes of this transporter: VGlut-1, present in fibers projecting from other cortical areas; VGlut-2, present in fibers projecting from extracortical inputs; and VGlut-3, whose expression is broad but limited to a few glutamatergic fibers (Takamori, 2006). Because of their non-overlapping expression, these transporters are commonly used as markers of specific glutamatergic terminals (figure 6).

Once the glutamate is released to the synaptic cleft, it will be available to activate different glutamate receptors. There are three main glutamate receptors in the CNS: α-amino-3-hydroxy-5-methyl-4-isoxazolepropionic acid (AMPA), kainate and N-methyl-D-aspartate (NMDA) receptors.

AMPA and kainate receptors are homologous and exert similar functions. They are ionotropic, therefore they exert their function by being permeable to Na^+ and K^+, and are coexpressed with NMDA receptors (NMDARs) in glutamatergic synapses of the CNS (Kew and Kemp, 2005). In addition, they are present in both pyramidal neurons (Bettler and Mulle, 1995) and interneurons (Vissavajjhala *et al*, 1996; Wondolowski and Frerking, 2009) (figure 6). They are frequently bound by the same agonists and antagonists, fact that complicates their understanding by means of their modulation (Bettler and Mulle, 1995). However, in this thesis I will focus on the NMDARs.

3.2.1.1.1. NMDA receptors

N-methyl-D-aspartate receptors (NMDARs) are a subtype of glutamate receptors, which present ionotropic and metabotropic properties (Dore *et al*, 2016), and are expressed

widely in both pyramidal neurons and interneurons (Alvarez *et al*, 2007; Collingridge *et al*, 1983; Nyíri *et al*, 2003; Oren *et al*, 2009). They play a key role in several events of CNS development, such as neuronal birth and migration (Komuro and Rakic, 1993). Structurally, they are heterotetramers composed by two obligatory **GluN1** subunits together with two different subtypes of **GluN2** and **GluN3** subunits (Liu *et al*, 2004; Paoletti *et al*, 2013; Sanz-Clemente *et al*, 2013; figure 7A). Therefore, the immunolocalization of the GluN1 subunit is an excellent tool to report the expression of NMDARs. The other subunits, however, vary in their biophysical properties and are expressed differentially depending on the developmental stage or the neuron expressing them (Paoletti *et al*, 2013; Pérez-Otaño *et al*, 2016; Wyllie *et al*, 2013). For instance, in the hippocampus, there is a developmental switch from the subunit GluN2B to the subunit GluN2A during the second postnatal week (Barria and Malinow, 2002; Dumas, 2005; Paoletti *et al*, 2013; figure 7B).

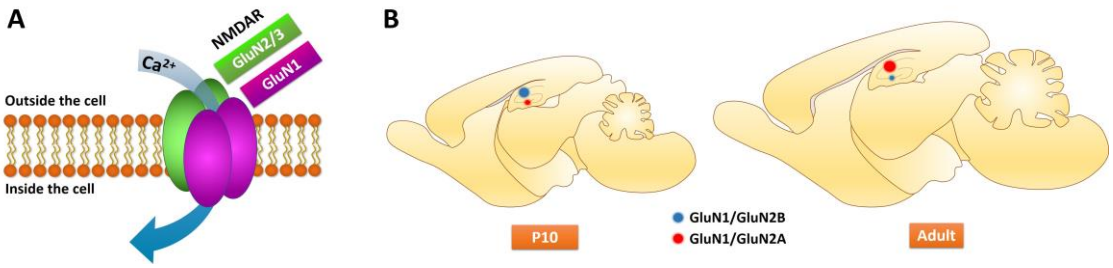

Figure 7: NMDA receptors and their composition. A) Schematic view of an NMDAR with the 4 GluN subunits: two obligatory GluN1 and two GluN2 or GluN3 subunits. B) Scheme of the subunit composition of NMDAR in the mouse hippocampus and its variation (GluN1/GluN2B) through postnatal development.

The use of agonists and antagonists of NMDARs is a common practice in order to understand how they modulate neural plasticity. In fact, these receptors are named after a strong agonist, the NMDA molecule. However, its administration also produces an increase in cell death in the CA1 of hippocampal organotypic cultures due to the Ca^{2+} excitotoxicity. This effect can be seen after an acute (Sakaguchi *et al*, 1997) or a chronic NMDA administration (Kristensen *et al*, 2001; Shimono *et al*, 2002). On the other hand, sub-lethal administrations of this molecule produce alterations in the spine density of pyramidal neurons of hippocampal primary cultures. In fact, short –albeit highly concentrated-

infusions of NMDA cause a marked decrease in this parameter in rats (Halpain *et al*, 1998), whereas a long mild infusion causes an increase in both the dendritic spine density, and the proportion of mushroom-shaped dendritic spines, in mice (Tian *et al*, 2007). However, there are no studies trying to understand how NMDAR activation affects the structure of interneurons, let alone the structural dynamics of these cells.

Likewise, antagonists of the NMDARs have also been used to understand the role of these receptors in different processes. One of the most studied antagonists is the MK-801, which has been shown to affect the targeting and pruning of axons and the regulation of synaptogenesis during development (Butler *et al*, 1998; Cline and Constantine-Paton, 1990; Shatz, 1990). Furthermore, MK-801 produces axonal sprouting in unlesioned hippocampal cultures (McKinney *et al*, 1999b). Regarding the density of dendritic spines, this antagonist does not produce effects on the dendritic spine density of pyramidal neurons, neither *in vivo* (Woolley and McEwen, 1994) nor *in vitro* (McKinney *et al*, 1999a). Nevertheless, this latter study showed the apparition of filopodia-like processes after chronic treatment with MK-801, resembling those in the developing hippocampus. In contrast with these studies about the expression and modulation of NMDARs on excitatory neurons, very few reports have focused on their presence in interneurons (Nyíri *et al*, 2003) or how these inhibitory cells alter their structure after NMDAR blockade. Particularly, in the PFC, treatment with MK-801 impairs the maturation of perisomatic inhibitory circuits formed by PV-expressing interneurons (Thomases *et al*, 2013). Interestingly, this antagonist elicited opposite changes in the prefrontocortical miniature excitatory postsynaptic currents when studying pyramidal neurons -an increase- and PV-expressing interneurons -a decrease- (Wang and Gao, 2012). However, only one study with ketamine, which is another NMDAR antagonist, has shown a diminution in the dendritic length of interneurons (Vutskits *et al*, 2007); there are no reports on how NMDAR blockade affects the structural dynamics of interneurons. Therefore, one of the aims of this thesis will be to study the effects of NMDAR activation and blockade in the structural dynamics of hippocampal interneurons.

3.2.1.2. GABAergic neurotransmission

The γ-amynobutyric acid (GABA) is the most common inhibitory neurotransmitter in the CNS and it is synthetized and released by interneurons. Its anabolism in the cell occurs through the activity of the **glutamic acid decarboxylase** (GAD), an enzyme which decarboxylases the glutamate to GABA releasing CO_2. There are two GAD isoforms in the CNS: **GAD67** and **GAD65**, the former being expressed throughout the cell and the latter only expressed in axonal terminals (Fish *et al*, 2011). This neurotransmitter is then encapsulated in synaptic vesicles, which also express **SYN** in their membrane (same as the glutamatergic synaptic vesicles) and the **vesicular GABA transporter** (VGAT). Like the VGlut transporters, the main function of VGAT consists in the facilitation of the storage of the neurotransmitter in the synaptic vesicles (Buddhala *et al*, 2009). Because all of these facts, both GAD67/GAD65 and VGAT are excellent markers for interneurons and inhibitory neurotransmission (figure 6; Erlander and Tobin, 1991; McIntire *et al*, 1997).

Once GABA is released to the synaptic cleft, it becomes available to activate the GABA receptors present in other cells, which can be pyramidal neurons (Alger and Nicoll, 1982) and interneurons (Freund and Buzsáki, 1996). There are three types of receptors: The $GABA_A$ and the $GABA_C$, which are ionotropic, and the $GABA_B$, which is metabotropic. Once activated, they open linked channels and hyperpolarize the neuron through the entry of Cl^- and the exit of K^+ (figure 6).

The activation of these receptors by GABA or other agonists can alter neuronal structure. In fact, GABA receptors have a binding site for benzodiazepines (Gavish and Snyder, 1980), and these drugs have been shown to decrease pyramidal spine density in the prefrontal cortex after a chronic treatment (Curto *et al*, 2016). These receptors also have a binding site for ethanol (Hunt, 1983), and its chronic administration alters the dendritic spine density of pyramidal neurons of the hippocampus (Romero *et al*, 2013). In addition, the activation of synaptic $GABA_A$ receptors produces an increase in the dendritic spine density of cultured neurons (Shimizu *et al*, 2015), whereas the appearance of extrasynaptic $GABA_A$ receptors during puberty is responsible for synaptic pruning in the hippocampus (Afroz *et al*, 2016), and their manipulation in this period results in an altered spine density of hippocampal pyramidal cells during adulthood (Afroz *et al*, 2017).

3.2.1.3. Excitatory-Inhibitory balance

In the last decade, the study of this balance (E/I balance) has gained strength with the increasing knowledge on the cellular basis of neurodevelopmental and neuropsychiatric disorders. During normal development, prior to the axonal pruning, excitatory contacts are more abundant in the brain. After a period of time, known as the critical period of heightened plasticity and, depending on the brain area (Hensch, 2005), this plasticity is restricted by the increased inhibition on the excitatory networks. Therefore, during normal development the balance would be displaced towards more excitation, whereas in the adult brain, this balance shows a stronger inhibitory factor (Baroncelli *et al*, 2011; Hensch, 2004; Hensch and Fagiolini, 2005). Moreover, recent studies have shown that some brain areas have a disrupted balance in neuropsychiatric disorders, including schizophrenia (Baroncelli *et al*, 2011; Curley and Lewis, 2012; Lewis *et al*, 2012; Morishita *et al*, 2015; Sun *et al*, 2013). This imbalance can be the consequence of an altered expression of several molecules implicated in the establishment and maintenance of inhibitory circuits, such as GAD65/67 (Akbarian 1995; Akbarian and Huang 2006; Straub et al. 2007; for a review see Mitchell et al. 2015), cannabinoid receptor 1 (CB1r) (Eggan et al. 2008; for a review see Volk and Lewis 2015) neuregulin 1 (Nrg1) and its receptor ErbB4 (Fazzari *et al*, 2010; Gilabert-Juan *et al*, 2013a) or brain-derived neurotrophic factor (BDNF, see section 3.2.2.1) (Weickert *et al*, 2003, 2005). Furthermore, an excellent method to obtain a readout of the E/I balance would be to compare the expression of proteins expressed in synaptic vesicles of excitatory and inhibitory synapses, such as VGlut, and VGAT, respectively (figure 6).

3.2.1.4. Serotonergic neurotransmission

Serotonin (5-Hydroxytryptamine: 5-HT) is a monoamine neurotransmitter synthetized and released in the CNS by neurons located in the Raphe nuclei, which innervate the neocortex, the hippocampus and the amygdala (Asan *et al*, 2013; Jacobs and Azmitia, 1992). The role of serotonergic neurotransmission has always been thought to be related to well-being behaviours, whereas the malfunction of the system relates to several psychiatric disorders, including depression and anxiety (Andrews *et al*, 2015). Its synthesis

consists in a rapid biochemical cascade which starts with L-tryptophan, and this, and the first by-product of the cascade, can cross easily the blood-brain barrier (Oldendorf, 1971; Yuwiler *et al*, 1977). Serotonin can be catabolized by monoamine oxidases (MAO), a classic target for some antidepressants. In the presynaptic zone, it is encapsulated in synaptic vesicles and released, where it becomes available to activate the different 5-HT receptors. Currently we know of 7 types –and 14 subtypes- of 5-HT receptors with plenty of different functions, which are expressed not only in the CNS but also in the gastrointestinal tract (Barnes and Sharp, 1999). These receptors are located extrasynaptically and have mainly modulatory roles. In addition, we find also auto-receptors and serotonin transporters (5-HTT or SERTs), responsible for the reuptake of serotonin to the presynaptic membrane (Fuller and Wong, 1990). I will focus on the 5-HTT, which is important for the development of this thesis (figure 6).

3.2.1.4.1. 5-HT transporter

This serotonin transporter (5-HTT) is located in the presynaptic membrane, and it is responsible for the reuptake of serotonin from the synaptic cleft. 5-HTTs are the prime target of the Selective Serotonin Reuptake Inhibitors (SSRIs), which nowadays are the most commonly prescribed antidepressants (figure 6; Isacsson *et al*, 2005; Lindsley, 2012). Particularly, **fluoxetine** (Prozac, Lilly) has been used in the occidental societies to treat anxiety and depression in all the stages of life (Byatt *et al*, 2013; Iñiguez *et al*, 2014). Despite the extensive use of these drugs, very little is known about their long-term effects on the function and structure of synaptic circuits. There are also studies suggesting that fluoxetine may act by recapitulating the structural plasticity that is normally seen during development. Therefore, it is thought that this antidepressant may act by promoting a "dematuration" in certain regions of the adult brain, such as the hippocampus (Kobayashi *et al*, 2010). Research in the visual cortex has, in fact, demonstrated that the plasticity induced by fluoxetine is similar to that observed during critical periods, when the activity-dependent neuronal wiring of this cortical region is established (Vetencourt *et al*, 2008). In addition, a chronic treatment with fluoxetine produces an increase of the spine density of pyramidal neurons in the somatosensory cortex (Guirado *et al*, 2009). However,

although this drug has been shown to alter GABAergic neurotransmission in the hippocampus (Mendez *et al*, 2012), there are no studies regarding its effect on the structure of interneurons. Therefore, one of the aims of this thesis will be to properly characterize the effect of a chronic treatment with fluoxetine on inhibitory circuits and the structure of SOM-expressing interneurons.

3.2.2. Plasticity modulation by neurotrophins

3.2.2.1. Brain-derived neurotrophic factor

BDNF was the second neurotrophin ever discovered (Barde *et al*, 1982), only preceded by the neural growth factor (Levi-Montalcini and Hamburger, 1951). Since then, multiple researchers have shown that it has an important role in neurodevelopment and neural plasticity. As a matter of fact, it promotes the survival and growth of neurons in the neocortex and the hippocampus (Horch and Katz, 2002; McAllister *et al*, 1997; Murphy *et al*, 1998; Tolwani *et al*, 2002). It also regulates the correct functional maturation of the neocortex, where, for example, blockade of BDNF signalling prevents the formation of ocular dominance columns in the visual cortex (Cabelli *et al*, 1997). BDNF has also important roles in the regulation of synaptic transmission: It appears to promote long term potentiation (LTP) in the excitatory circuits of the neocortex, hippocampus and amygdala (Escobar *et al*, 2003; Kang *et al*, 1997; Meis *et al*, 2012). Regarding structural plasticity, it is known that BDNF causes an increase in the spine density of CA1 pyramidal neurons in organotypic cultures (Tyler and Pozzo-Miller, 2003), as well as an increase in the complexity of the dendritic arbor of pyramidal neurons in the developing visual cortex (McAllister *et al*, 1995).

All these effects are triggered by the activation of the BDNF receptor, the tropomyosin receptor kinase B (TrkB, figure 8). This receptor is present in several neuronal populations, including pyramidal neurons and interneurons (Gonzalez *et al*, 2016; Gorba and Wahle, 1999). Once activated, TrkB undergoes autophosphorylation and binds to proteins responsible for the activation of several signalling cascades, including the PI3K-pathway. This pathway is in charge of activating mTOR-signalling (Gonzalez *et al*, 2016; Yoshii and Constantine-Paton, 2010), an integrative pathway for general processes such as protein

synthesis and cellular proliferation (Morita *et al*, 2015) or more specific processes in the CNS, like neural development, circuit formation or synaptic plasticity (Lipton and Sahin, 2014). Regarding the latter process, truncated TrkB has been shown to alter the growth of the dendritic arbor of pyramidal neurons in visual cortex organotypic cultures of ferrets (Yacoubian and Lo, 2000).

The activation or inhibition of this receptor has been broadly used to understand its role in different neural processes. Different antagonists of TrkB impair memory retrieval or learning in the hippocampus after an inhibitory avoidance paradigm (Blank *et al*, 2016) and decrease spine density in hippocampal pyramidal neurons of CA1 in a model of depression (Zhang *et al*, 2015). In this regard, cyclotraxin B, a potent inhibitor of TrkB that has recently been discovered (Cazorla *et al*, 2010), has already been used to prevent neuropathic pain (Constandil *et al*, 2012; Thibault *et al*, 2014).

Another interesting drug regarding BDNF signalling is **7,8-dihydroxyflavone** (DHF), a potent TrkB agonist. This drug is very promising for clinical applications, since it is orally active and can bypass the blood-brain barrier, a common problem for most compounds intended to reach the CNS (figure 8; Du and Hill, 2015). This drug appears to be therapeutically effective against several neurological diseases, such as Parkinson's disease (Jang *et al*, 2010), amyotrophic lateral sclerosis (Korkmaz *et al*, 2014) or Alzheimer's disease (AD; Castello *et al*, 2014; Zhang *et al*, 2014). There are evidences that this drug can alter the structure of pyramidal neurons in different paradigms. Regarding this, DHF affects the spine density of hippocampal pyramidal neurons in a rodent model of AD (Castello *et al*, 2014). This drug also augments the spine density of pyramidal neurons of the hippocampal CA3 and dentate gyrus in a model of depression in mice (Zhang *et al*, 2015). Interestingly, DHF has also been shown to increase the dendritic spine density of pyramidal neurons in the amygdala, hippocampus and prefrontal cortex of old rats, making it similar to that present in youngsters (Zeng *et al*, 2012a). However, to date there is no information on how DHF may be altering the structural dynamics of healthy animals, i.e. the study in real time of the addition or elimination of dendritic spines or axonal *boutons* in the same segment. Hence, one of the aims of this thesis will be the longitudinal study of

pyramidal neurons during a chronic treatment with DHF to understand how TrkB regulation through this drug affects structural dynamics.

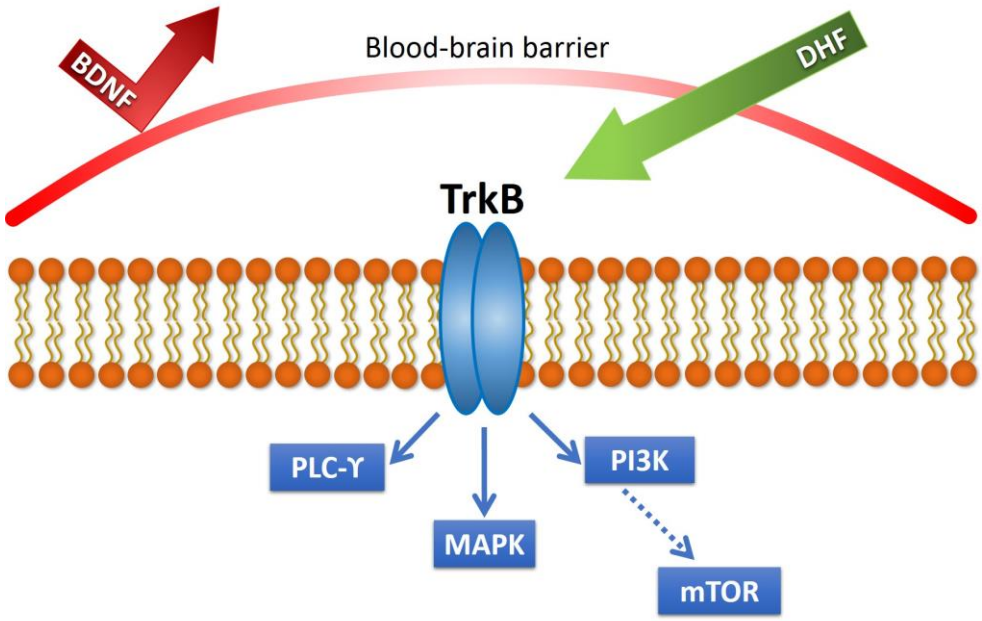

Figure 8: Molecular cascades dependent on TrkB activation and crossing of the blood-brain barrier by DHF. BDNF: brain-derived neurotrophic factor. TrkB: tropomyosin receptor kinase B. DHF: 7,8-dihydroxyflavone. PLC-γ: phospholipase C-γ cascade. MAPK: mitogen-activated protein kinase cascade. PI3K: phosphatidylinositol 3-kinase cascade. mTOR: mammalian target of rapamycin. Inspired by (Du and Hill, 2015).

3.2.3. Involvement of plasticity-related molecules on neuronal structural remodelling

3.2.3.1. PSA-NCAM

The polysialylated form of the neural cell adhesion molecule (PSA-NCAM) is widely expressed during neurodevelopment, when, because of its antiadhesive properties (Rutishauser, 1996), it is thought to facilitate neuronal migration, neurite extension, as well as dendritic and synaptic remodelling (figure 9A; Bonfanti 2006; Rutishauser 2008). Its expression becomes much more restricted during adult life, but PSA-NCAM is still expressed by different populations of interneurons in the adult neocortex (Varea *et al*, 2005), hippocampus (Gomez-Climent *et al*, 2011; Nacher *et al*, 2002a) and amygdala (Nacher *et al*, 2002b), including both PV and SOM-expressing interneurons (Gomez-Climent *et al*, 2011). Furthermore, different recent studies have shown that PSA-NCAM

expression is able to modulate the structural plasticity of these inhibitory neurons (Nacher *et al*, 2013).

Interestingly, PSA depletion from the NCAM using the enzyme Endoneuraminidase-N (EndoN) alters the spine density of pyramidal neurons and dendrite-targeting SOM-expressing interneurons. Specifically, the spine density of prefrontocortical pyramidal neurons is reduced after the treatment in adult animals (Castillo-Gómez *et al*, 2016b), whereas SOM-expressing interneurons from PFC-organotypic cultures only decrease their spine density in the distal dendritic segment after PSA depletion (Castillo-Gómez *et al*, 2016a). In the hippocampus, an interesting phenomenon has been described: The dendritic spine density of dendrite-targeting, SOM-expressing, interneurons increases two days after the intracranial injection of EndoN, but it is decreased seven days after the injection (Guirado *et al*, 2014), suggesting a compensatory response of the hippocampal microcircuitry. The dynamics of these spines have been also analysed in entorhino-hippocampal organotypic slices. In these cultures, the appearance rate of these spines is significantly increased 24 hours after the PSA depletion, as well as their relative density (Guirado *et al*, 2014). These effects of PSA on neuronal structure may be due to its antiadhesive properties, which facilitate neuronal and synaptic remodelling or the partial isolation of neuronal elements (figure 9A; see Nacher *et al*, 2012 for review). Furthermore, PSA depletion also increases the perisomatic GABAergic innervation on prefrontocortical pyramidal neurons (Castillo-Gómez *et al*, 2011). On the other hand, a chronic treatment with fluoxetine (see section 3.2.1.4.1) has been shown to cause an increase in the expression of PSA-NCAM in the hippocampus and a decrease in the amygdala (Varea *et al*, 2007b). Interestingly, this treatment causes an increase in the pyramidal spine density in the somatosensory cortex (Guirado *et al*, 2009), suggesting that changes in the inhibitory circuits expressing PSA-NCAM may underlie the structural changes seen in pyramidal neurons after fluoxetine treatment.

Furthermore, PSA-NCAM appears to be altered in some neuropsychiatric disorders, including schizophrenia. Interestingly, the genes of both NCAM and one of the polysialyltransferases (St8SiaII), which add PSA to NCAM (for a review see Hildebrandt *et al*, 2008) have been associated with this disease (Arai *et al*, 2006; Atz *et al*, 2007; McAuley

et al, 2012; Tao *et al*, 2007; see section 4.3). Moreover, alterations in the expression of NCAM and PSA-NCAM have been found in post-mortem studies in patients, including some on the amygdala (Varea *et al*, 2012) and the PFC (Gilabert-Juan *et al*, 2012b), as well as in the PFC of a double hit model developed in rats (Gilabert-Juan *et al*, 2013a).

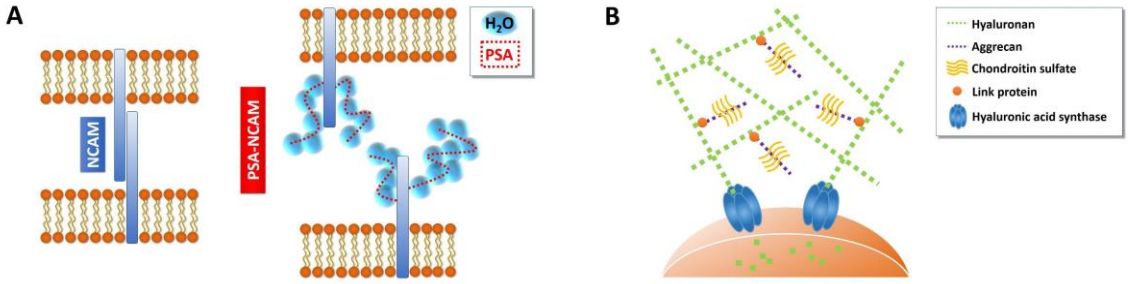

Figure 9: Plasticity-related molecules. A) Representation of the union of two membranes with homotypic binding between NCAM molecules and their separation (de-adhesion) with the incorporation of highly hydrated and negatively charged PSA-NCAM. B) Composition of the PNNs. NCAM: neural cell adhesion molecule. PSA-NCAM: polysialylated form of the neural cell adhesion molecule. PNNs: perineuronal nets. B was inspired by (Tsien, 2013).

3.2.3.2. Perineuronal nets

Perineuronal nets (PNNs) are specialized structures of the extracellular matrix that surround neurons and restrain their connectivity and plasticity. They contain several molecules, such as chondroitin sulphate proteoglycans, aggrecan or hyalunoran (figure 9B). Although they surround many cell types, they are found preferentially around PV-expressing interneurons (Nowicka *et al*, 2009; Ueno *et al*, 2016; see section 2.2.1). The apparition of PNNs occurs late in the development and is thought to end critical period plasticity (Hensch and Bilimoria, 2012; Wang and Fawcett, 2012). Furthermore, PNNs seem to regulate many forms of plasticity (McRae and Porter, 2012); their specific degradation in different brain regions induces changes that appear to revert the neuronal circuitry to an immature stage. For instance, their elimination in the visual cortex restores the ocular dominance plasticity after a monocular deprivation paradigm (Pizzorusso *et al*, 2002), whereas in the amygdala, this elimination causes the erasure of previously conditioned fear memories (Gogolla *et al*, 2009). In addition, the removal of hyaluronan

from hippocampal organotypic cultures impairs the establishment of LTP (Kochlamazashvili *et al*, 2010).

Interestingly, the ratio of PV-expressing interneurons surrounded by PNNs is altered in several neuropsychiatric disorders, including schizophrenia (see section 4.3), where variations in the PFC, amygdala (Berretta *et al*, 2015; Bitanihirwe *et al*, 2016; Mauney *et al*, 2013) and hippocampus (Castillo-Gomez *et al*, unpublished results) have been found. In addition, chronic inhibition of the 5-HTT with fluoxetine during fear-conditioning and extinction paradigms, causes a decrease in the number of PV-expressing interneurons surrounded by PNNs in the BLA nucleus of the amygdala and the hippocampal CA1, along with the proper erasure of conditioned fear memories (Karpova *et al*, 2011).

4. NEUROPSYCHIATRIC DISORDERS

4.1. Anxiety-related disorders

This classification comprises a group of diseases characterized by the common occurrence of anxiety and fear. Many events in life can have an anxiogenic component due to their stressful nature. This induces a marked release of corticosteroids that alters neural processes (Korte, 2001; Ottenweller, 2007; Russo *et al*, 2013). Although peaks of anxiety are necessary for the survival of the species, due to the fight-or-flight response, a sustained anxiety during a long period of time can lead to severe neurologic problems (Arnsten, 2015; Bauer, 2008; Brady and Sinha, 2005). As a matter of fact, chronic stress is used to model some neuropsychiatric disorders, such as major depression or some endophenotypes of schizophrenia (Arnsten, 2015; Bauer, 2008; Fone and Porkess, 2008; Negrón-Oyarzo *et al*, 2016; Pollak *et al*, 2010; Slattery and Cryan, 2017). Importantly, stress can cause alterations in the structure of the CNS and, inversely, we can obtain a behavioural readout of this structural plasticity by studying anxiety-related behaviours. For instance, in rodents, anxiety can always be detected by hyperlocomotion and thigmotaxis; two parameters that can be easily assessed in behavioural tests, such as the hole-board or the open field apparatus. On the contrary, chronic stress produces dendritic atrophy and a decrease in the spine density of pyramidal neurons of the PFC (Cook and Wellman, 2004; Radley *et al*,

2004) and the hippocampus (Sousa *et al*, 2000; Watanabe *et al*, 1992). However, chronic exposure to this aversive experience also produces the hypertrophy of pyramidal neurons in the amygdala (Vyas *et al*, 2002, 2003). Interestingly, the directions of these changes are opposite when the arborization of dendrite-targeting, SOM-expressing, interneurons is studied (see section 2.2.5): An increase can be seen in the PFC (Gilabert-Juan *et al*, 2013b), whereas a reduction has been reported in the amygdala (Gilabert-Juan *et al*, 2011).

4.2. Major depressive disorder

It is the most prevalent psychiatric disorder, characterized by an increased appearance of sadness, changes in sleep cycles, decrease in appetite or sexual desire, among others (Belmaker and Agam, 2008; Otte *et al*, 2016). As some other neuropsychiatric diseases, depression is accompanied by alterations in the structure of the CNS. In human patients, there is a decrease in the spine density of pyramidal neurons in the subiculum (hippocampal formation, Rosoklija *et al*, 2000), as well as a reduction in the total number of synapses of the PFC (Zhao *et al*, 2012). However, human post-mortem studies are highly hindered by the poor fixation of the brain, as well as the uncontrolled circumstances that the subjects intrinsically pose. This is why the development of animal models has been necessary for the study of neural structural plasticity in major depressive disorder. In fact, as has been previously described, chronic stress is a valid model of major depressive disorder: It causes several changes in the structure of both pyramidal neurons and interneurons of the PFC, hippocampus and amygdala (Cook and Wellman, 2004; Gilabert-Juan *et al*, 2011, 2013b; Radley *et al*, 2004; Sousa *et al*, 2000; Vyas *et al*, 2002, 2003; Watanabe *et al*, 1992; see sections 2 and 4.1).

The etiopathology of this disease can be partially explained by two non-excluding hypotheses closely linked to neural plasticity: The “monoamine-deficiency” and the “neurotrophic” hypotheses. The first one postulates that lower levels of monoamines, such as serotonin, are responsible (Iversen, 2008; Tran *et al*, 2003). This fact would explain why the 5-HTT inhibitors (SSRIs), such as fluoxetine, have been such a great success in treating major depression through increasing the serotonin availability in the synaptic cleft

(Krishnan and Nestler, 2008). On the other hand, the "neurotrophic" hypothesis suggests that neurotrophins, specifically BDNF, may play an important role in the development of this disorder (Brunoni *et al*, 2008; Duman and Monteggia, 2006). This idea comes from the fact that depressed patients show lower levels of BDNF (Karege *et al*, 2002, 2005; Shimizu *et al*, 2003), whereas the levels in treated patients are higher (Aydemir *et al*, 2005; Gervasoni *et al*, 2005; Shimizu *et al*, 2003). Studies of BDNF expression on animal models have also given support to this theory (Nibuya *et al*, 1995, 1996). However, both hypotheses have their limitations and do not explain totally the behavioural onset or why not every patient is susceptible to improve with SSRIs (Krishnan and Nestler, 2008).

4.3. Schizophrenia

Schizophrenia is a complex neuropsychiatric disease affecting behaviour, perception and cognition (Brunoni *et al*, 2008; Tandon *et al*, 2013), in which the PFC, hippocampus and amygdala are implicated (Bogerts *et al*, 1993; Casanova, 1997; Harrison, 2004; Keshavan *et al*, 1994; Woodruff *et al*, 2000). These areas are strongly dependent on one another, since the PFC is innervated directly by the amygdala and by the hippocampus (Jay and Witter, 1991; Krettek and Price, 1977; see section 1.4.). In fact, the disruption of this innervation is presumed to be the cause of several neuropsychiatric disorders, including schizophrenia (Keshavan *et al*, 1994; Thomases *et al*, 2014). Moreover, an important tool to diagnose properly this disease is the assessment of particular behavioural traits dependent on these areas: Impairments in working memory (Gonzalez-Burgos *et al*, 2015), which can be easily analysed in rodents with the hole-board apparatus (Kuc *et al*, 2006); and increases in anxiety (Braga *et al*, 2005; Malcolm *et al*, 2015), which can be detected as explained in section 4.1.

Additionally, different lines of evidence point to alterations in neuronal structural plasticity, especially of the PFC, as important factors in the etiopathology of this disorder, which may be caused by the improper closure of its critical period. This has already been shown in animal models (Bitanihirwe *et al*, 2016; De Luca and Papa, 2016) and in human patients (Berretta *et al*, 2015; Mauney *et al*, 2013). Regarding neuronal structure, several

changes have been already reported in both pyramidal neurons and interneurons of patients and animal models of this disorder. In fact, the dendritic spine density of corticofrontal pyramidal neurons is decreased in schizophrenic patients (Glantz and Lewis, 2000; Kolluri *et al*, 2005), as well as in animal models (Baharnoori *et al*, 2009; Flores *et al*, 2005). Moreover, the study of a rat model has shown that pyramidal neurons of the hippocampus also display decreased spine density, whereas in the BLa nucleus of the amygdala this density is increased (Lazcano *et al*, 2015). Inhibitory circuits are also altered in schizophrenic patients and animal models of this disease (Lewis *et al*, 2008). However, little is known yet on how the structure of interneurons is altered in schizophrenia.

II. OBJECTIVES

The main objective of this doctoral thesis is to study the impact of pharmacological and environmental manipulations on the structure and dynamics of excitatory and inhibitory neurons in the mouse brain, in an attempt to gain a better understanding of the plasticity of the adult nervous system and of the neurobiological bases of psychiatric disorders. In order to achieve this main target, we derive the following specific objectives:

1. **To study the role that NMDA receptors play in the structural plasticity and dynamics of SOM expressing interneurons of the hippocampus.**

    1.1. To demonstrate the presence of NMDA receptors in these interneurons.

    1.2. To study whether the blockade of these receptors with a specific antagonist alters the structure and dynamics of these interneurons, and whether it influences anxiety-related behaviours and working memory.

    1.3. To study whether the activation of NMDA receptors alters the structural dynamics of these interneurons.

2. **To develop a new mouse model of schizophrenia, which comprises social isolation stress and perinatal NMDA receptor blockade, and report its effects on the medial prefrontal cortex and amygdala.**

    2.1. To study in this model the structural plasticity of pyramidal neurons and interneurons.

    2.2. To study in this model the excitatory and inhibitory neurotransmission.

    2.3. To study in this model the expression of plasticity-related molecules.

3. **To analyse whether the chronic treatment with the antidepressant fluoxetine affects the plasticity of the hippocampus and the medial prefrontal cortex.**

    3.1. To study whether this treatment alters the structure of interneurons.

3.2. To study whether this treatment alters the expression of plasticity-related molecules.

3.3. To study whether this treatment alters the excitatory and inhibitory neurotransmission.

4. To study *in vivo*, using cranial windows and 2-photon microscopy, the effects of a chronic treatment with the TrkB agonist 7,8-dihydroxyflavone on the dynamics of pyramidal neurons in the barrel cortex.

4.1. To study the dynamics and volume of pyramidal dendritic spines prior and during this treatment.

4.2. To study the dynamics of axonal *boutons* prior and during this treatment.

4.3. To study how this treatment influences object-recognition behaviour and how this behaviour is correlated to the structural dynamics of pyramidal neurons.

III. RESEARCH

1. NMDA receptors regulate the structural plasticity of spines and axonal *boutons* in hippocampal interneurons

Perez-Rando, M., Castillo-Gómez, E., Guirado, R., Blasco Ibáñez, J. M., Crespo, C., Varea, E., Nacher J. (2017). NMDA receptors regulate the structural plasticity of spines and axonal boutons in hippocampal interneurons. Frontiers in Cellular Neuroscience

doi:10.3389/FNCEL.2017.00166.

frontiers in Cellular Neuroscience

ORIGINAL RESEARCH
published: 12 June 2017
doi: 10.3389/fncel.2017.00166

NMDA Receptors Regulate the Structural Plasticity of Spines and Axonal Boutons in Hippocampal Interneurons

*Marta Perez-Rando[1], Esther Castillo-Gómez[1], Ramon Guirado[1], José Miguel Blasco-Ibañez[1], Carlos Crespo[1], Emilio Varea[1] and Juan Nacher[1,2,3]**

[1]Neurobiology Unit, Department of Cell Biology, Interdisciplinary Research Structure for Biotechnology and Biomedicine (BIOTECMED), Universitat de València, València, Spain, [2]CIBERSAM: Spanish National Network for Research in Mental Health, Madrid, Spain, [3]Fundación Investigación Hospital Clínico de Valencia, Instituto de Investigación Sanitaria (INCLIVA), València, Spain

N-methyl-D-aspartate receptors (NMDARs) are present in both pyramidal neurons and interneurons of the hippocampus. These receptors play an important role in the adult structural plasticity of excitatory neurons, but their impact on the remodeling of interneurons is unknown. Among hippocampal interneurons, somatostatin-expressing cells located in the stratum oriens are of special interest because of their functional importance and structural characteristics: they display dendritic spines, which change density in response to different stimuli. In order to understand the role of NMDARs on the structural plasticity of these interneurons, we have injected acutely MK-801, an NMDAR antagonist, to adult mice which constitutively express enhanced green fluorescent protein (EGFP) in these cells. We have behaviorally tested the animals, confirming effects of the drug on locomotion and anxiety-related behaviors. NMDARs were expressed in the somata and dendritic spines of somatostatin-expressing interneurons. Twenty-four hours after the injection, the density of spines did not vary, but we found a significant increase in the density of their *en passant boutons (EPB)*. We have also used entorhino-hippocampal organotypic cultures to study these interneurons in real-time. There was a rapid decrease in the apparition rate of spines after MK-801 administration, which persisted for 24 h and returned to basal levels afterwards. A similar reversible decrease was detected in spine density. Our results show that both spines and axons of interneurons can undergo remodeling and highlight NMDARs as regulators of this plasticity. These results are specially relevant given the importance of all these players on hippocampal physiology and the etiopathology of certain psychiatric disorders.

Keywords: NMDAR, spine dynamics, interneurons, organotypic cultures, MK-801, axonal boutons

OPEN ACCESS

Edited by:
Laura Cancedda, Fondazione Istituto Italiano di Technologia, Italy

Reviewed by:
Cheng-Chang Lien, National Yang-Ming University, Taiwan
Norbert Hajos, Institute of Experimental Medicine (MTA), Hungary

****Correspondence:***
Juan Nacher
nacher@uv.es

Received: *03 April 2017*
Accepted: *29 May 2017*
Published: *12 June 2017*

Citation:
Perez-Rando M, Castillo-Gómez E, Guirado R, Blasco-Ibañez JM, Crespo C, Varea E and Nacher J (2017) NMDA Receptors Regulate the Structural Plasticity of Spines and Axonal Boutons in Hippocampal Interneurons. Front. Cell. Neurosci. 11:166. doi: 10.3389/fncel.2017.00166

INTRODUCTION

The study of changes in the morphology of neurons is important for understanding neural activity. In fact, changes in the dendritic arbor or the number of dendritic spines and axonal *boutons*, allow neurons to modify the strength of their synaptic input and output and to adapt to changing environments (for a review see Whitt et al., 2014).

Dendritic spines are membranous protrusions, which can establish excitatory or inhibitory synapses through different neurotransmitter receptors. Although they were thought to be a distinctive feature of principal neurons, different studies have shown that some interneuronal subpopulations also display these postsynaptic specializations (Freund and Buzsáki, 1996). In interneurons, however, the structure of the spines is slightly different: they lack the spine apparatus found in pyramidal neurons, several synapses are established per spine (in contrast with the one or two found in pyramidal neuron spines) and they are usually less numerous (Gulyás et al., 1992; Acsády et al., 1998). On the other hand, *boutons* are axonal thickenings, which contain and release the synaptic vesicles. Because of their roles as postsynaptic and presynaptic elements, spines and *boutons* have been found to be proper markers for neuronal input and output; therefore, increases in spine and axonal *bouton* density have been correlated to increases in neuronal activity (Engert and Bonhoeffer, 1999; Becker et al., 2008).

Excitatory neurons experience structural remodeling under different conditions, involving changes in the length and complexity of dendritic arbors, and in the density or morphology of their spines (Fu and Zuo, 2011) and axonal *boutons* (Florence et al., 1998; Colicos et al., 2001; Nikonenko et al., 2003). This has been shown in different conditions and disorders, including chronic stress and depression (McEwen, 1999; Qiao et al., 2016), obesity (Dingess et al., 2016), neurodevelopmental disorders (Glausier and Lewis, 2013; Flores et al., 2016) and after different pharmacological manipulations (Guirado et al., 2009; Yang et al., 2015; Castillo-Gómez et al., 2016b). By contrast, studies on the effects on interneuron morphology are scarcer, despite the important role of inhibitory networks in central nervous system physiology (Nacher et al., 2013). Most of these studies on interneuron plasticity are focused on basket interneurons and few have explored structural changes on dendrite-targeting interneurons, such as those expressing somatostatin. These interneurons are essential for the maturation of deep cortical circuits (Tuncdemir et al., 2016) and are important players in other stages of neurodevelopment, brain pathology and neuronal plasticity (for a review see Liguz-Lecznar et al., 2016). Only some recent studies have shown that these interneurons are able to undergo dendritic remodeling after chronic stress (Gilabert-Juan et al., 2011), antidepressant treatment (Guirado et al., 2014b), streptozotocin-diabetic challenge (Castillo-Gómez et al., 2015) or the depletion of plasticity related molecules (Guirado et al., 2014a; Castillo-Gómez et al., 2016a).

However, most of these structural analyses, as the majority of those in other interneuronal subtypes, have been performed on fixed tissue. Data acquired with this experimental approach is based on population analysis and does not allow for the longitudinal study of individual spines or *boutons*. Using such methods, neither transient nor homeostatic changes can be detected, i.e., changes that only alter the composition of synapses and leave the total number of spines or dendritic length intact. Structurally, these changes in network configurations are represented by the addition of one spine on one site, compensated by the pruning on another. The emergence of 2-photon microscopy and the chronic implantation of cranial windows have allowed for longitudinal analysis of individual elements of the neocortex after sensory deprivation, which have shown structural remodeling of excitatory (Hofer et al., 2009; Holtmaat and Svoboda, 2009; Cane et al., 2014), and inhibitory microcircuits (Chen et al., 2011a,b, 2012; Keck et al., 2011; van Versendaal et al., 2012; Chen and Nedivi, 2013). However, this technique is limited by the position of the cranial window and can only be used chronically, without brain damage, on studies of the neocortex. This inconvenience hinders the longitudinal study of the hippocampus, an important structure interconnected with the neocortex and responsible for spatial memory. The use of entorhino-hippocampal organotypic cultures, with their intrinsic limitations, helps to solve this problem and allows us to follow elements from a hippocampal neuron throughout an entire experiment. These cultures have been broadly used as an *in vitro* model of the rodent hippocampus (Stoppini et al., 1991), allowing the study of structural changes in real-time.

N-methyl-D-aspartate receptors (NMDARs) are a subtype of ionotropic glutamate receptors, expressed widely in both pyramidal neurons and interneurons (Collingridge et al., 1983; Nyíri et al., 2003; Alvarez et al., 2007; Oren et al., 2009). They play a key role in several events of central nervous system development, such as neuronal birth and migration (Komuro and Rakic, 1993). Antagonists to these glutamate receptors, such as MK-801, are known to interfere with the targeting and pruning of axons and the regulation of synaptogenesis during development (Cline and Constantine-Paton, 1990; Shatz, 1990; Butler et al., 1998). NMDAR antagonists also induce axonal sprouting during adulthood (Sutula et al., 1996; McKinney et al., 1999b) and are able to modulate some processes related to learning, such as LTP (Bailey et al., 1996). The blockade of these receptors does not appear to produce effects on the dendritic spine density of pyramidal neurons, neither *in vivo* (Woolley and McEwen, 1994) nor *in vitro* (McKinney et al., 1999b). However, this latter study showed the apparition of filopodia-like processes after chronic treatment with MK-801, resembling those in the developing hippocampus. Interestingly, NMDAR blockade with MK-801 increases the motility of dendritic spines of pyramidal neurons in hippocampal organotypic cultures (Alvarez et al., 2007). Regarding interneurons, little is known about the expression of NMDARs in these cells or about how the hypofunction of these receptors may affect their structure or physiology. Some studies in the prefrontal cortex have shown that MK-801 administration impairs the functional maturation of perisomatic inhibitory circuits expressing parvalbumin (Thomases et al., 2013) and affects differentially the physiology of these interneurons and pyramidal neurons (Wang and Gao, 2012). However, it is still unknown how this blockade may affect dendrite-targeting interneurons, such as those expressing somatostatin in the hippocampus. There are certain cell populations located in the *stratum oriens* sharing these characteristics, which are essential for the physiology of this region (Freund and Gulyás, 1997; Müller and Remy, 2014) and are known to present dynamic

dendritic spines (Guirado et al., 2014a). Two of the most studied of these populations are the oriens-lacunosum moleculare (O-LM), and the hippocampo-septal (HS), interneurons (Jinno and Kosaka, 2002; Gulyás et al., 2003). The former are named after their microcircuitry: they receive their inputs in the *stratum oriens* from pyramidal neurons of the *stratum pyramidale* and reciprocally inhibit these cells and other interneurons, establishing these synapses in the *stratum lacunosum moleculare* (Müller and Remy, 2014). These cells are essential for the correct functioning of the hippocampus. In fact, they appear to mediate *theta* oscillations (Katona et al., 2014) and have been postulated to be essential for the establishment of spatial context-fear conditioning (Lovett-Barron et al., 2014; Müller and Remy, 2014).

In the present study, we aim to understand the impact of NMDAR manipulation on the structure and dynamics of somatostatin-expressing interneurons in the CA1 *stratum oriens*. In order to achieve our goal, we have used a transgenic mice strain in which these interneurons are constitutively labeled with enhanced green fluorescent protein (EGFP), which allows us to study their entire morphology (Oliva et al., 2000). After demonstrating the presence of NMDARs on these interneurons and their dendritic spines, we have acutely treated adult mice with the NMDAR antagonist MK-801 and have studied its effects on the structural remodeling of their dendritic spines and axonal *en passant boutons* (EPB). To have a behavioral readout of the efficacy of the treatment, we have measured locomotor activity, anxiety-related behavior and working memory. Finally, in order to study whether NMDAR manipulation modified spine dynamics in these cells, we have acutely blocked these receptors with MK-801 in entorhino-hippocampal organotypic cultures and have observed morphological changes in real-time.

MATERIALS AND METHODS

Animals and Treatment

For both *in vivo* and *in vitro* experiments we used the EGFP-expressing inhibitory neurons (GIN), Tg(GadGFP)45704Swn mice (Jackson laboratories, Bar Harbor, ME, USA). They constitutively express the EGFP in a subpopulation of somatostatin expressing interneurons (Oliva et al., 2000).

For the experiment analyzing *in vivo* fixed tissue, we used 3-month-old male mice (n = 18). The MK-801 treatment (1 mg/kg) consisted of a single intraperitoneal injection and the perfusion was performed 24 h afterwards (**Figure 1A1**).

For the real-time analysis *in vitro*, 14 GIN pups (P7) were used to prepare the hippocampal-entorhinal organotypic cultures (Stoppini et al., 1991). MK-801 (10 μM in culture media) was administered after the second imaging session during 1 h (**Figure 1A2**).

All the animals were maintained in standard conditions of light (12 h cycles) and temperature, without restrictions of food and water. All animal experimentation was conducted in accordance with the Directive 2010/63/EU of the European Parliament and of the Council of 22 September 2010 on the protection of animals used for scientific purposes and was approved by the Committee on Bioethics of the Universitat de València. Every effort was made to minimize the number of animals used and their suffering.

Behavioral Analysis

Prior to their sacrifice, every adult GIN mouse was tested in the hole-board apparatus (ANY-maze video tracking system v4.98; Stoelting Europe, Ireland) to automatically analyze locomotor activity and anxiety-related behavior (Castilla-Ortega et al., 2010; Torres-García et al., 2012).The hole-board test measures exploration and can also be used as an initial basic screen for working memory (Karl et al., 2008). The open-field chamber (40 × 40 cm) was fitted with a hole-board floor insert for mice (16 holes, diameter = 2.8 cm). Testing of the mice took place between 1 h and 2 h after the onset of the dark phase (illumination at floor level <2 lx). Each mouse was placed in the center of the arena and was left to explore the environment for 7 min (test session). The video tracking system and the infrared photobeams provided automated measures of the: (a) total distance traveled, mean speed and immobility episodes (to study locomotor activity); (b) head dips, for the study of working memory (working memory ratio = number of head dips into novel holes/total number of head dips; Karl et al., 2008); and (c) number of entries, latency for the first entry, distance traveled and mean speed in the periphery of the arena, for the measure of anxiety and thigmotaxis (a valid index of anxiety in mice; Simon et al., 1994). The periphery zone of the area was defined as the area located between 0 cm and 10 cm from the walls of the apparatus.

Histological Procedures

For the fixed tissue experiment, adult mice were perfused transcardially under deep pentobarbital anesthesia, with NaCl 0.9% and then 4% paraformaldehyde in phosphate buffer 0.1 M, pH 7.4 (PB). Brains were then cut with a vibratome (Leica VT 1000E, Germany) in 100 μm-thick coronal sections for the study of interneuron morphology.

Nine additional adult GIN mice were transcardially perfused for the analyses of protein expression in EGFP+ interneurons (GluN1 subunit of NMDAR), or the identification of HS cells (retrograde tracing from the medial septal nucleus). The brains were then extracted and cut in 50 μm thick coronal sections to perform immunohistochemical analyses.

Analysis of Hippocampo-Septal Interneurons

In order to know whether some of the EGFP+ interneurons of the *stratum oriens* were projecting HS cells, we performed intracranial injections of a retrograde tracer in the medial septal nucleus of three GIN mice. Mice were anesthetized with a mixture of ketamine (50 mg/kg; Imalgene, Merial) and medetomidine (1 mg/kg; Sedator, Dechra). Carprofen (5 mg/kg; Rimadyl, Pfizer) was also injected intraperitoneally to

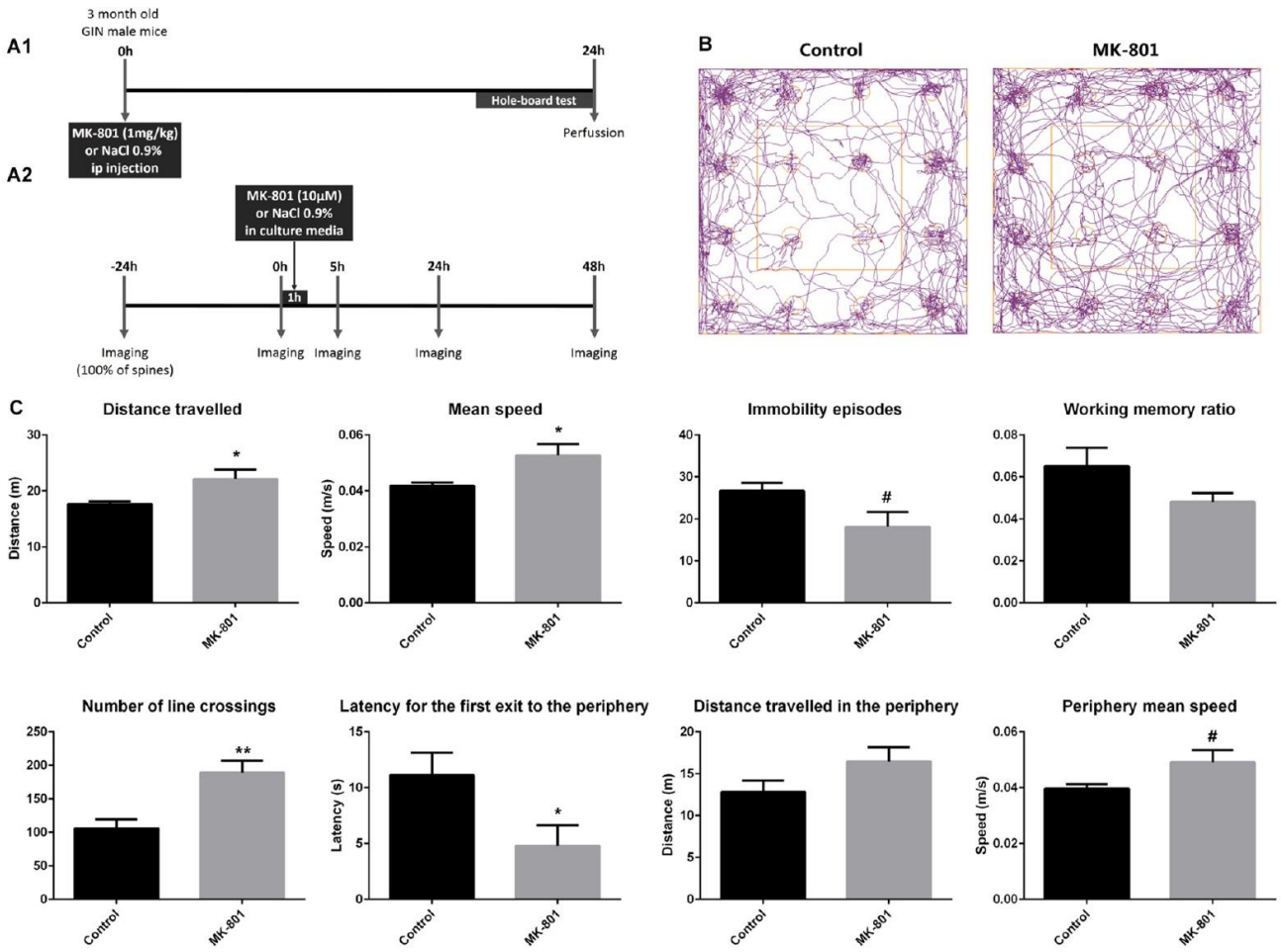

FIGURE 1 | (A1) Experimental design of the *in vivo* experiment. **(A2)** Experimental design of the real-time *in vitro* experiment. **(B,C)** Hole-board behavioral test. **(B)** Representative tracking-plots of NaCl-treated animals (control) and MK-801-treated animals (MK-801). **(C)** Graphs representing the changes observed in the behavioral parameters that were analyzed (all graphs represent mean + SEM., $^{*}p < 0.05$, $^{**}p < 0.01$, $^{\#}0.05 < p < 0.1$).

avoid inflammation and a subcutaneous injection of butorfanol (5 mg/kg; Torbugesic, Pfizer) was administered to avoid any suffering during and after the surgery. The animals were then injected with 2% Fluorogold (Molecular Probes, Thermo Fisher Scientific, Inc., Waltham, MA, USA) in the right medial septal nucleus using a stereotaxic apparatus and borosilicate glass capillaries (World Precision Instruments, Sarasota, FL, USA; tip length >10 mm, tip thickness <50 μm). The coordinates for the injection were 0.86 mm anterior from Bregma, 0.05 mm lateral from the midline, and a 3.0, 3.5 and 4.1 mm below the pial surface, according to the adult mouse atlas (Paxinos and Franklin, 2013). After 3 days, all the animals were transcardially perfused and the brains processed for histology.

In order to image the EGFP + HS interneurons in the *stratum oriens* of CA1, we used a laser scanning confocal microscope (Olympus FV10, Japan) with a 10× objective and a 2× digital zoom. We counted 100 EGFP+ interneurons and calculated the ratio of colocalization with fluorogold.

Analysis of GluN1 Expression

Sections from three non-treated animals were processed free-floating for fluorescence immunohistochemistry against the GluN1 subunit of the NMDA receptor. The fluorescence immunohistochemistry protocol was slightly modified in order to unmask the epitope. First, the sections were incubated at 70°C for 1 h in 0.1 M PBS and then incubated in 2 M HCl for 30 min at room temperature, as described previously by our laboratory (Nácher et al., 2007). The protocol followed as previously explained. Sections were incubated for 48 h at 4°C with rabbit anti-GluN1 (1:100, Millipore, USA). After rinsing with PBS, sections were incubated for 2 h at room temperature with donkey anti-rabbit A647 (1:400, Abcam, UK). Finally, sections were rinsed in PB 0.1 M, mounted on slides and coverslipped using fluorescence mounting medium (Dako, Germany). NDS, primary and secondary antibodies were diluted in PBS—0.2% Triton-X100.

Images were taken with a laser scanning confocal microscope using a 63× oil immersion objective with an additional

5× digital zoom for the analysis of GluN1 expression in somata and dendritic spines. Controls were performed omitting the anti-GluN1 antibody or incubating with this antibody pre-absorbed overnight with an excess of its immunogenic peptide (LQNQKDTVLPRRAIEREEGQLQLCSRHRES, Chemicon). No immunolabeling was observed in either control.

Analysis of the Density of Dendritic Spines and Axonal *En Passant Boutons*

The structural parameters of the GAD-EGFP+ interneurons were studied using a laser scanning confocal microscope (Leica TCS SPE, Germany), as described before (Gomez-Climent et al., 2011). Since our targets were the spiny interneurons located in the *stratum oriens*, we analyzed the dendrites arising from somata located in this *stratum* and the plexus of EGFP+ axons present in the *stratum lacunosum-moleculare* of the CA1 region.

For the spine density analysis, a 63× oil immersion objective and 3.5× digital zoom was used to image the different dendritic sections. Dendrites from EGFP interneurons were chosen at random, but they had to meet different criteria to be included in the study: (1) they should measure at least 150 or 200 μm from the soma; and (2) no other dendrites should be found crossing their trajectory. The data were expressed as the total number of spines in the proximal (0–50 μm), medial (50–100 μm) and distal (100–150 μm) segments from the soma. A total of six neurons were analyzed per animal.

For the density of EPB, we used a 63× oil immersion objective with a 2.5× digital zoom. Six axonal segments, measuring at least 10 μm, were chosen randomly per animal. In order to rigorously score the EPB and to avoid an overestimation, the axonal varicosities were only considered when they fulfilled three criteria: (1) they should be at least two times brighter than the axonal backbone; (2) they should be two times wider than the axonal backbone; and (3) they should not have any crossings from other axons nearby.

In order to analyze the functionality of EGFP + EPB, we studied the presence of gephyrin-expressing puncta (GEPH) in juxtaposition with these presynaptic structures. We performed a double fluorescence immunohistochemistry against gephyrin and EGFP in all the experimental animals. The immunohistochemical protocol is similar to those described above. In order to label gephyrin and to enhance the EGFP signal, we incubated all the sections with chicken anti-GFP (1:2000, Abcam, UK) and mouse anti-gephyrin (1:700, Synaptic Systems, Germany) primary antibodies for 48 h at 4°C. After rinsing with PBS, the sections were incubated with donkey anti-chicken CF488 (1:1000, Sigma, Germany) and donkey anti-mouse IgG A555 (1:400, Thermo Fisher Scientific, UK) for 2 h at room temperature. Sections were then rinsed with PB 0.1 M, mounted on slides and coverslipped using fluorescence mounting medium (Dako, Germany). Sera, primary and secondary antibodies were diluted in PBS—0.2% Triton-X100. All the images were taken with a laser scanning confocal microscope (Leica TCS SPE, Germany), with a 63× oil immersion objective and a 2× additional digital zoom. Six axons in the *stratum lacunosum moleculare* were analyzed per animal, following the same criteria described above for axon selection and EPB scoring. Only GEPH in juxtaposition with the EPB were counted, in order to calculate the ratio of EPB containing this synaptic marker.

Organotypic Cultures and Real-Time Analysis

Hippocampal slices (400 μm-thick) were obtained with a tissue chopper, following the protocol described by Stoppini et al. (1991). The brain was freshly extracted from P7 mice and the hippocampus dissected along with the entorhinal cortex in order to preserve the perforant pathway. Media was changed three times per week and the cultures remained 13 days *in vitro* (13DIV) until the confocal imaging started.

For the real-time analysis of organotypic cultures, short imaging sessions (10–15 min) were carried out with a 40× water immersion objective. An additional 10× digital zoom was used to analyze dendritic segments of about 35 μm in length, located between 100 μm and 150 μm from the soma (*Z* step size of 0.8 μm). Laser intensity was kept at the minimum allowing observation, and acquisition conditions maintained unchanged over the different days of observation. Control experiments showed that this procedure did not produce any deleterious effect on cell viability, such as cell death or dendritic beadings. One dendrite was analyzed per organotypic culture slice, and 16 slices from six different animals were analyzed. All the somata of the interneurons analyzed were located in the *stratum oriens* of CA1 region. The imaging took place at five different time points referenced to the beginning of the treatment: −24 h, 0 h, 5 h, 24 h and 48 h, starting on DIV 13. MK-801 was added to the media after the second imaging session (0 h) for 1 h, and then again substituted by normal culture media. The rapid effect was registered after 4 h (5 h), 24 h (24 h) and 48 h (48 h).

Statistics

After checking the normality and homoscedasticity of the data, we used a *t*-test to compare control and experimental groups. When comparing the morphological analysis in adult animals, we used an unpaired *t*-test. In the real-time longitudinal analysis, when comparing the same neuron at different time points, we used a paired *t*-test, whereas when comparing the external control (cultures receiving vehicle) to the experimental slices we used an unpaired *t*-test. In every case α was set to 0.05 and the animal or the slice was considered as the "n".

RESULTS

Increased Locomotion and Anxiety-Related Behavior on MK-801 Treated Animals

Twenty-four hours after MK-801 treatment (1 mg/kg, one i.p injection), mice showed significant alterations in locomotor activity and anxiety-related behavior when tested in the

hole-board apparatus (**Figures 1B,C**): increased distance traveled (unpaired *t*-test; $t_{(12)} = -2.515$, $p = 0.040$), increased mean speed (unpaired *t*-tests; $t_{(12)} = -2.600$, $p = 0.035$), increased number of line crossings (unpaired *t*-test; $t_{(12)} = -3.624$, $p = 0.003$), and a decreased latency to the first exit from the center zone to the periphery (unpaired *t*-test; $t_{(12)} = 2.321$, $p = 0.043$). A trend towards an increase in the mean speed in the periphery (unpaired *t*-test; $t_{(12)} = -2.027$, $p = 0.079$) and a trend towards a decrease in the number of immobility episodes (unpaired *t*-test; $t_{(12)} = 2.129$, $p = 0.061$) could also be observed. However, working memory was not affected by the treatment (unpaired *t*-test; $t_{(12)} = 1.739$, $p = 0.118$; **Figure 1C**).

Some Somatostatin Expressing Interneurons in the *Stratum Oriens* Project to the Medial Septal Nucleus

In order to know the proportion of HS cells in the *stratum oriens* of GIN mice, a retrograde tracer was injected in the medial septal nucleus. This assay revealed that at least a 6.5% of EGFP+ cells were projecting to this region (**Figure 2**). These results indicate that, although the majority of EGFP+ interneurons in the stratum oriens of the CA1 region of GIN mice can be considered O-LM cells, some HS have also their somata among these fluorescent interneurons.

Somatostatin Interneurons Coexpress NMDA Receptors on their Somata and on the Head of their Dendritic Spines

Immunohistochemistry against GluN1, the obligatory subunit of the NMDAR, showed wide expression in somatostatin-expressing interneurons throughout the hippocampus, as previously described (Nyíri et al., 2003). Specifically, in the somatostatin-expressing interneurons of the *stratum oriens* it was expressed on the surface of their somata (**Figure 3A**). Immunoreactive puncta were also found associated to the head of their dendritic spines (**Figure 3B**). Only one punctum, when present, appeared per spine.

MK-801 Treatment Increases the Density of *En Passant Boutons* from Hippocampal Somatostatin-Expressing Interneurons, whereas the Density of their Dendritic Spines Remains Unaltered

We studied the densities of dendritic spines and *EPB* of somatostatin-expressing interneurons in the *stratum oriens* of CA1 (**Figure 4A**), 1 day after an intraperitoneal injection of the MK-801. When analyzing the different segments of the dendrite (proximal, medial and distal from the soma), we did not observe any significant difference in dendritic spine density between control and MK-801-treated animals (unpaired *t*-tests; proximal: $t_{(8)} = -0.338$, $p = 0.744$; medial: $t_{(6)} = -0.736$, $p = 0.483$; distal: $t_{(8)} = -0.015$, $p = 0.988$; **Figures 4B1,B2,E1**). Likewise, there were no differences between groups when comparing the total density of dendritic spines throughout the dendrite (unpaired *t*-test; $t_{(8)} = -0.531$, $p = 0.610$; **Figure 3E2**). However, in the *stratum lacunosum moleculare*, the axonal projection field of O-LM interneurons, the linear density of *EPB* was significantly increased in MK-801-treated animals (unpaired *t*-test; $t_{(8)} = -2.220$, $p = 0.046$; **Figures 4C1,C2,F**). Interestingly, the ratio of GEPH in juxtaposition with EPB did not vary between groups. Every EPB analyzed had an associated GEPH (**Figure 4D**).

Real-Time Analysis of the Dendritic Spines of EGFP-Expressing Interneurons Reveals a Rapid Decrease on the Appearance Rate and the Dynamic Events after MK-801 Administration

Real-time analysis was performed in control conditions and after the acute addition of MK-801 (1 h in the culture medium; **Figures 5A,A′**). In control conditions, we found no alterations in the appearance, the disappearance and the stability rates, or in the rate of dynamic events. However, 24 h after the infusion of MK-801 (0–24 h), the appearance rate of new spines was significantly reduced from 46% under control conditions to a 14% of the total of pre-existing spines in treated cultures. This decrease in the appearance rate was significant when compared to both the baseline (−24 h to 0 h, paired *t*-test, $t_{(5)} = 3.492$, $p = 0.017$) and the external control (unpaired *t*-test, $t_{(8)} = 3.338$, $p = 0.010$, **Figures 5B,C**). The stability and disappearance rates did not change (unpaired *t*-tests; stability rate: unpaired *t*-test $t_{(8)} = 0.119$, $p = 0.908$; disappearance rate: unpaired *t*-test, $t_{(8)} = -0.119$; **Figures 5B,C**). In addition, there was a trend towards a decrease in the rate of dynamic events 24 h after the administration of MK-801 (unpaired *t*-test, $t_{(8)} = 2.189$, $p = 0.060$; **Figures 5B,C**).

We also imaged the dendrites 4 h after MK-801 administration (0–5 h), in order to register putative rapid effects of this compound. In the MK-801 group, we recorded an acute decrease in the spine apparition rate (unpaired *t*-test, $t_{(8)} = 2.713$, $p = 0.027$, **Figures 5D1,D2,E**). Neither the disappearance nor the stability rates varied 4 h after the treatment (unpaired *t*-tests; stability rate: $t_{(8)} = -0.273$, $p = 0.792$; disappearance rate: $t_{(8)} = 0.273$, $p = 0.792$; **Figures 5D1,D2,E**). However, there was a trend towards a decrease in the rate of dynamic events in the MK-801 group (unpaired *t*-test, $t_{(8)} = 1.894$, $p = 0.095$, **Figures 5D1,D2,E**).

Real-Time Analysis of the Dendritic Spines of EGFP-Expressing Interneurons Shows a Decrease on the Relative Spine Density after MK-801 Administration

When analyzing the relative variation of the spine density in organotypic cultures, we observed a marked decrease 24 h after the administration of MK-801 when compared to its group baseline. Just before MK-801 administration, the dendrites showed 119% of the original density of spines and statistically did not differ from the control group,

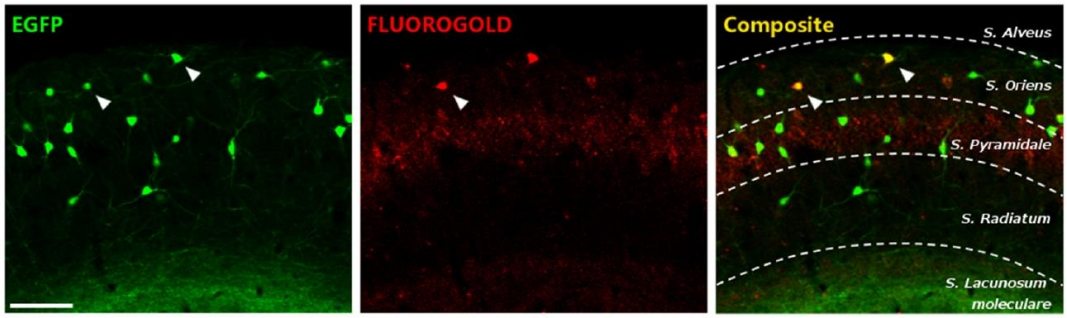

FIGURE 2 | Characterization of enhanced green fluorescent protein (EGFP)-expressing interneurons in the *stratum oriens* of CA1. EGFP+ cells (left), fluorogold retrograde tracing from the medial septal nucleus (middle) and the composite image. Scale bar: 15 μm.

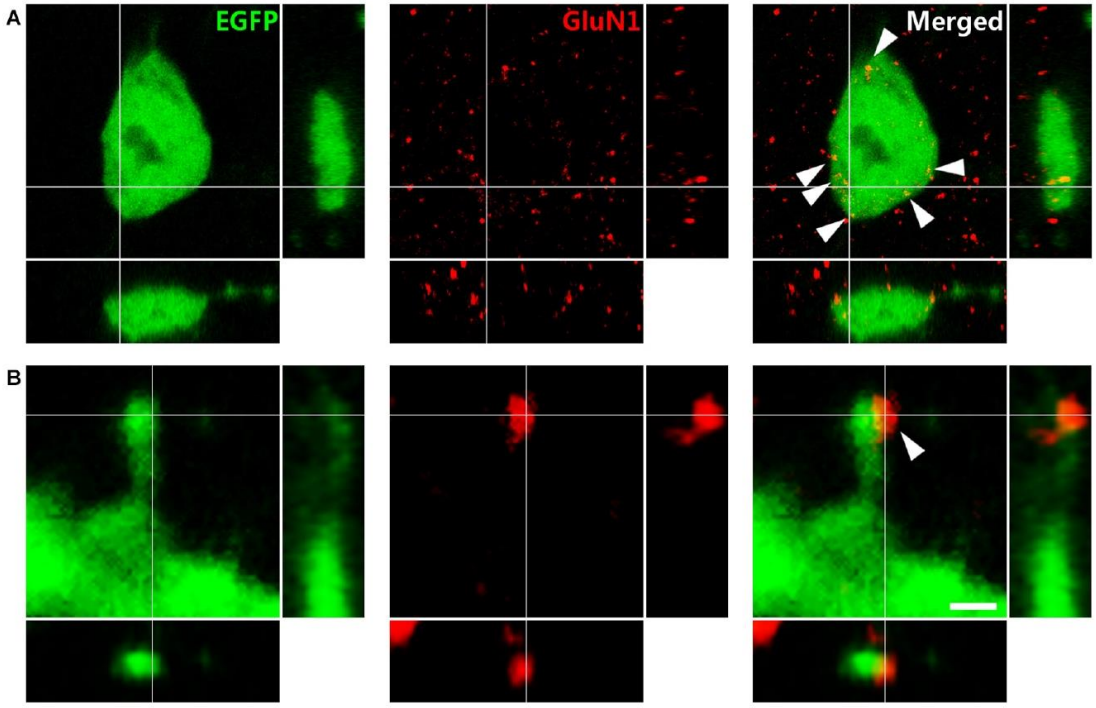

FIGURE 3 | Immunohistochemistry against the N-methyl-D-aspartate receptor (NMDAR) obligatory subunit GluN1 in GIN mice. **(A)** Puncta expressing NMDARs (arrowheads) in an EGFP labeled soma. **(B)** Dendritic spine of an EFGP-labeled interneuron. Note the expression of NMDAR on the spine head. Panels on the right and bottom are orthogonal projections of the middle panel. Scale bar: 2 μm in **(A)**, 0.50 μm in **(B)**.

which showed a 101% (unpaired *t*-test, $t_{(8)} = -1.202$, $p = 0.264$, **Figures 6A1,A2,B**). Nevertheless, 24 h after the treatment, the relative spine density was decreased to 86% in the MK-801-treated group (paired *t-test*, $t_{(5)} = 4.827$, $p = 0.005$, **Figures 6A1,A2,B**), and there was a trend towards a decrease when compared to the control group in the same time point (unpaired *t*-test, $t_{(8)} = 2.035$, $p = 0.076$; **Figures 6A1,A2,B**).

In order to analyze the acute effect of MK-801, we also studied the relative spine density 4 h after the MK-801 administration. There were no significant differences when compared to the control group (unpaired *t*-test, $t_{(8)} = 0.150$, $p = 0.884$; **Figure 6C**).

DISCUSSION

The NMDARs are among the most studied receptors in the nervous system, because of their involvement in LTP and several developmental processes (Butler et al., 1998; McKinney et al., 1999b; Nacher and McEwen, 2006; Kehoe et al., 2014). These receptors also play an important role in the activity-dependent regulation of the morphology of the dendritic spines of excitatory

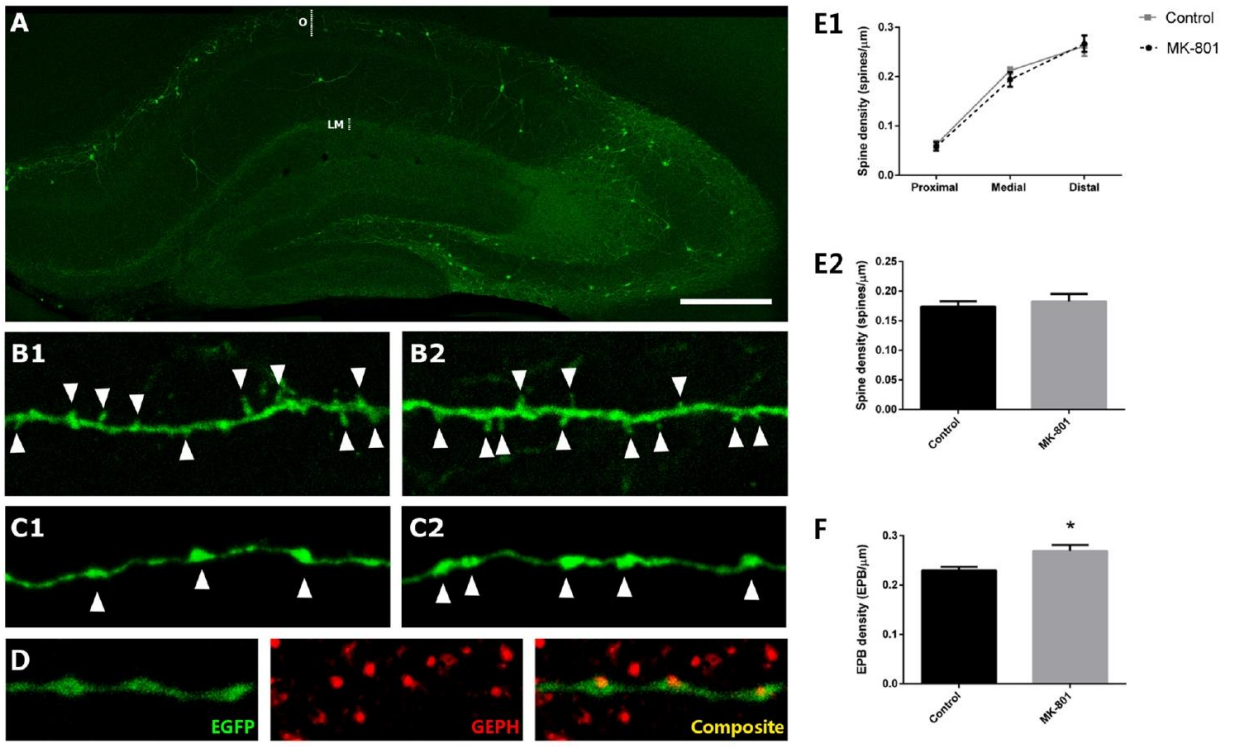

FIGURE 4 | Structural modifications in EGFP-expressing interneurons in the *stratum oriens* after MK-801 injection. **(A)** Hippocampus of a GIN mouse. The *strata oriens* (O) and *lacunosum moleculare* (LM) are indicated with dotted lines. **(B)** Segments of dendrites bearing spines (arrowheads) from a control animal **(B1)** and a MK-801-treated mouse **(B2). (C)** Segments of axons of somatostatin-expressing interneurons in the *stratum lacunosum moleculare* showing *en passant boutons* (EPBs, arrowheads) in control **(C1)** and MK-801-treated **(C2)** animals. **(D)** Axonal segment with three *EPB* in juxtaposition to gephyrin-expressing puncta (GEPH). **(E1)** Graph representing the spine density in the proximal, medial and distal dendritic segment relative to the soma. **(E2)** Graph representing the spine density in the total length of the dendrite. **(F)** Graph showing the density of EPBs in *stratum lacunosum moleculare*, where a significant increase can be observed in the MK-801 group (all graphs represent mean + SEM., $*p < 0.05$). Scale bar: 180 µm in **(A)**, 7 µm in **(B)**, 5 µm in **(C)** and 7 µm in **(D)**.

neurons (Nikonenko et al., 2002; Ultanir et al., 2007). However, despite the abundant presence of NMDARs in interneurons (Nyíri et al., 2003), little is known about their role on the structural plasticity of these cells. Interneurons also change their axonal and dendritic morphology in response to different stimuli (Chen et al., 2011b; Gilabert-Juan et al., 2011; Nacher et al., 2013). Furthermore, some interneuron populations have spines in their dendrites and they are dynamic, as the ones present on pyramidal neurons (Keck et al., 2011; Guirado et al., 2014a). Only some studies have focused on the structural plasticity of interneurons. Dr. Nedivi's laboratory, using cranial windows in transgenic mice with fluorescent interneurons, has shown the elongation/retraction of dendritic branch tips *in vivo* in different neocortical regions (for a review see Chen and Nedivi, 2013). There are scarce published studies on the turnover of interneuronal dendritic spines. In mice, these spines have a stability rate close to 98% in a 24 h time-lapse experiment (Keck et al., 2011). These results are considerable higher than the ones we describe in hippocampal interneurons in the control group, where the stability rate is around 70%. These differences may be due to a difference in the stability of different interneuronal subpopulations, the region and age studied, or, more likely, to a higher stability *in vivo* than in our organotypic cultures.

The use of NMDAR antagonists, such as MK-801 or ketamine, has increased exponentially our knowledge on the physiology of these receptors and their involvement in neurological and psychiatric disorders. They have been broadly used to model certain symptoms of schizophrenia (Gilmour et al., 2012), to produce neurotoxic insults (Beninger et al., 2002) or as a novel treatment for depression (Browne and Lucki, 2013; Yang et al., 2015). In order to obtain a behavioral readout of the effectiveness of NMDAR blockade induced by *in vivo* MK-801 administration, we used the hole-board apparatus and automatically tracked the mice to test for hyperlocomotion, anxiety-related behaviors, and effects on working memory. Our study agrees with the previously reported increase in locomotor activity in MK-801 treated mice (Zuo et al., 2006; Kalinichev et al., 2008). The working memory ratio showed a non-significant decrease in the MK-801-treated animals, which is similar to the absence of differences in head-dip counts reported by other labs (Haj-Mirzaian et al., 2015; Hirose et al., 2016).

There is some evidence of the impact of NMDAR antagonists on interneurons, particularly on those targeting the soma of pyramidal neurons (Román et al., 2011; Rotaru et al., 2011). However, little is known about the effects that NMDAR blockade

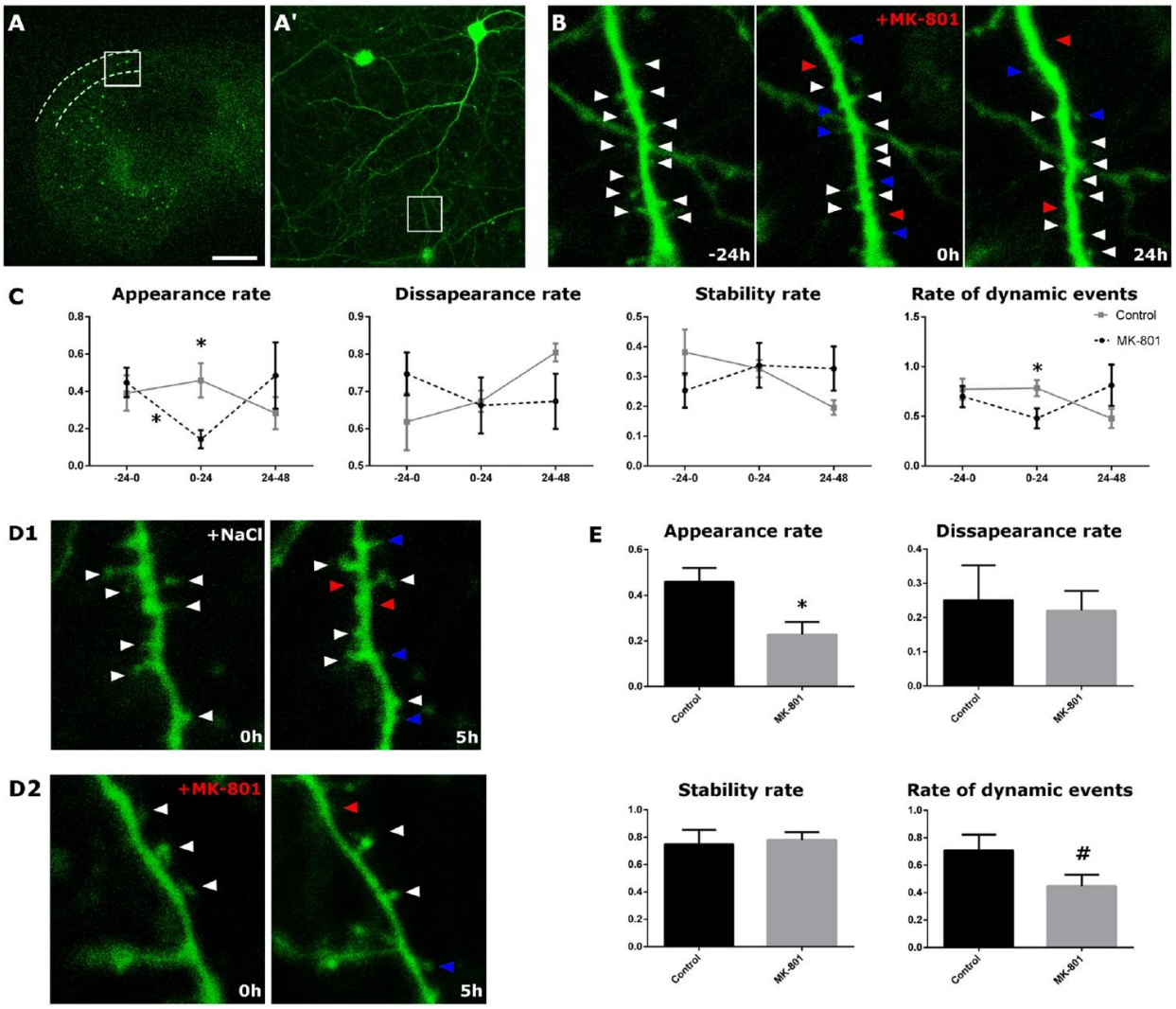

FIGURE 5 | Structural dynamics of EGFP-expressing interneurons after MK-801 administration. **(A)** Panoramic view of an organotypic entorhino-hippocampal culture, with the *stratum oriens* of CA1 delineated by dotted lines. **(A′)** Enlarged view of the squared region with an interneuron in the *stratum oriens*. **(B)** Enlarged view of the squared region in **(A,A′)**. The figure shows a dendritic segment 24 h prior (left panel), right before (middle panel) and 24 h after (right panel) the MK-801 administration. Arrowheads point to stable (white), gained (blue) and lost (red) spines. **(C)** Graphs showing different dynamic rates in control and MK-801 treated slices (appearance, disappearance, stability rate and rate of total dynamic events). **(D1,D2)** Microphotographs showing the differences in the spine appearance rate between a control slice **(D1)** and the MK-801 treated slice **(D2)** 5 h after the starting of the MK-801 administration. **(E)** Graphs showing the different rates 5 h after the beginning of the treatment (all graphs represent mean + SEM., $^{*}p < 0.05$, $^{\#}0.05 < p < 0.1$). Scale bar: 1500 μm in **(A)**, 150 μm in **(A′)**, 1.5 μm in **(B,D)**.

can exert on other types of interneurons, like those targeting the distal segments of the dendrites of pyramidal neurons. One of the best studied populations of these dendrite-targeting interneurons are the O-LM cells in the hippocampus. These interneurons are a specially interesting cell type to study structural plasticity, because they have dendritic spines (Sik et al., 1995; Katona et al., 1999; Guirado et al., 2014a), which mainly receive excitatory synapses from recurrent collaterals of local pyramidal cells (Blasco-Ibáñez and Freund, 1995). They are essential to the proper functioning of this region of the limbic system, since they appear to modulate CA3 and entorhinal inputs (Leão et al., 2012), mediate *theta* rhythm (Katona et al., 2014) and have been associated with spatial context-fear conditioning behavior (for a review see Müller and Remy, 2014). In addition to these O-LM cells, our study, using retrograde tracing has shown that a minority of the EGFP+ interneurons in the *stratum oriens* are HS cells, suggesting that NMDA receptors may also modulate the structure of these projection interneurons.

Interestingly, different studies have found that the dendritic complexity of somatostatin-expressing interneurons can change after a chronic stress paradigm (Gilabert-Juan et al., 2017)

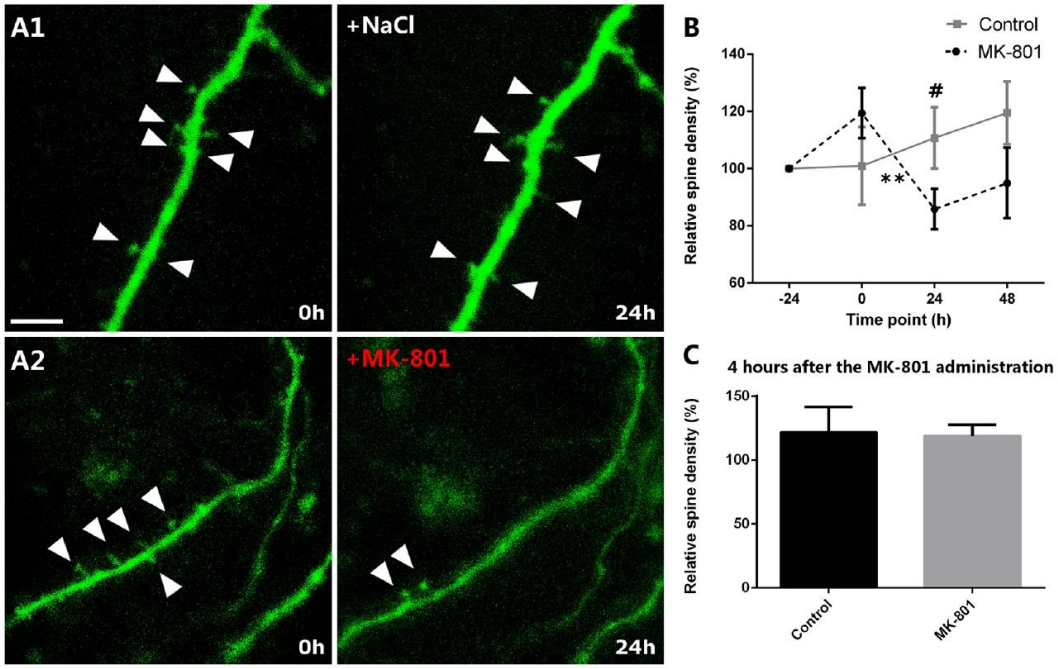

FIGURE 6 | Relative spine density after MK-801 administration. **(A)** Representative images of dendritic segments in control **(A1)** and MK-801-treated **(A2)** groups. Note the decreased relative spine density 24 h after the MK-801 treatment (**A2**, right panel). Triangles mark the dendritic spines. **(B)** Graph showing the relative spine densities in the different time points. **(C)** Graph representing the relative spine density 5 h after the beginning of the MK-801 administration. Scale bar: 6 μm (All graphs represent mean + SEM., $^{**}p < 0.01$, $^{\#}0.05 < p < 0.1$).

and that they particularly change their dendritic spine density after the chronic administration of fluoxetine (Guirado et al., 2014b).

Somatostatin-expressing interneurons in the *stratum oriens* express NMDARs in their somata and dendrites (Nyíri et al., 2003). In the present study, we increase this knowledge by showing NMDAR expression specifically in the dendritic spines of these interneurons. In hippocampal pyramidal neurons, *in vitro* studies have shown that NMDARs mediate spinogenesis during neurodevelopment (Kwon and Sabatini, 2011) and are responsible for spine structural remodeling (Matsuzaki et al., 2004; Lai and Ip, 2013). Therefore, it is not unreasonable to think that NMDARs could have a similar role in interneuronal spines and mediate these types of plasticity.

To know whether NMDARs could modulate interneuronal spine density in somatostatin-expressing interneurons of the hippocampus, we have acutely injected MK-801 to adult animals. Pyramidal neurons in the mPFC modify the density of their dendritic spines after NMDAR blockade with several drugs. Previous studies have shown that after NMDAR blockade with MK-801 *in vivo*, pyramidal spine density in the hippocampus remained unaltered (Woolley and McEwen, 1994; Han et al., 2013). In accordance with these results in excitatory neurons, we have found that the acute administration of MK-801 does not affect the density of dendritic spines of somatostatin-expressing interneurons in adult mice. However, other studies with NMDAR antagonists in pyramidal neurons have rendered positive results: studies using chronic treatments have described increases (Flores et al., 2007) or decreases (Velázquez-Zamora et al., 2011) in this parameter, and those using acute administration reported a rapid increase in spine density (Li et al., 2010; Liu et al., 2013; Phoumthipphavong et al., 2016). Discrepancies in the doses and duration of the treatment may account for these differential effects, as well as differences in the structure and physiology between the spines of pyramidal neurons and interneurons (Gulyás et al., 1992; Freund and Buzsáki, 1996; Acsády et al., 1998).

There is an apparent discrepancy between the results we obtained *in vivo* and those we found in organotypic cultures. This could be due to a higher spine stability in adult animals than in organotypic cultures (Guirado et al., 2014a). Moreover, the different results may be the consequence of a different subunit composition of their NMDARs. These receptors vary their composition during the second postnatal week, when there is a developmental switch from the subunit GluN2B to the subunit GluN2A, which have different kinetic traits (Erreger et al., 2005). Our hippocampal slices have been generated and studied during this time period, when their NMDAR still have the GluN2B subunit. The treatment of organotypic cultures with MK-801 induced significant changes in the dynamics and density of dendritic spines of somatostatin-expressing interneurons. Most of these cells are probably O-LM interneurons, since the type of organotypic culture used in our study (Stoppini et al., 1991) only preserves the perforant path and the local connections. Previous reports using this type of cultures have also shown effects of NMDAR antagonists on the structure of hippocampal

pyramidal neurons: treatment with MK-801 for 7 days did not alter pyramidal spine density on CA1, but produced an increase in the number of filopodia-like processes, which resemble the immature spines observed during synaptogenesis in the developing hippocampus (McKinney et al., 1999a). Only a piece of previous work in primary cultures has shown that the chronic exposure to ketamine produces a retraction of the dendritic arbor of interneurons in cell cultures (Vutskits et al., 2007). Although the phenotype of these interneurons was not analyzed, these results are similar to those in the present study, which show a reduction in the density of dendritic spines and thus in the area susceptible for stablishing synaptic contacts.

Even though axonal remodeling has not been as broadly studied as that involving dendrites, some studies have also highlighted the effects of NMDAR antagonists on axonal structure. Only 3 days of MK-801 treatment are enough to produce axonal sprouting in the hippocampal Schaffer collaterals *in vitro* (McKinney et al., 1999b). We have observed a similar effect in adult animals on the axonal *boutons* of somatostatin-expressing interneurons. These collaterals in the *stratum lacunosum moleculare* are most likely emerging from O-LM cells, since they are the only somatostatin-expressing interneurons innervating this area (Freund and Buzsáki, 1996). Whether a similar effect on Schaffer collaterals occurs *in vivo*, still remains to be explored. However, it is interesting to note that a recent study has found that O-LM cells facilitate the transmission of intrahippocampal information through this input from CA3 and reduce the influence of the entorhinal afferents (Leão et al., 2012); the axonal terminal field of O-LM interneurons is located precisely in the same location of the entorhinal afferents to CA1 pyramidal neurons (Freund and Buzsáki, 1996).

Treatments with MK-801 have been extensively used to model the etiopathology of schizophrenia in rodents, because NMDAR antagonists can reproduce some symptoms of schizophrenia in normal individuals. In fact, there is a NMDA hypothesis of schizophrenia, which poses that alterations in the NMDARs, particularly during development, are involved in the etiopathology of this disorder (Adell et al., 2012; Lim et al., 2012). Since these receptors are expressed in certain interneuron populations, including somatostatin-expressing cells (Nyíri et al., 2003), it has already been speculated that a NMDAR hypofunction during development would inhibit interneurons, thus producing an overexcitation of the network. Different studies point to this hypofunction as a factor contributing to alterations of fast-spiking neurons in schizophrenia (Coyle, 2006; Lisman et al., 2008), but alterations of these receptors in other interneuronal populations could also result in an abnormal functioning or connectivity. Based in our present results and previous ones describing the structural plasticity of dendrite-targeting interneurons (Guirado et al., 2014a,b; Gilabert-Juan et al., 2017), it is reasonable to speculate that a hypofunction of NMDAR might result in changes in the postsynaptic (spines) and presynaptic (EPB) elements. Whether these changes occur in schizophrenic patients still remains to be determined. However, interestingly, in a recently developed double hit model of schizophrenia using the same strain of this study, we have observed a reduction of spine density in EGFP-labeled interneurons in the mPFC (Castillo-Gómez et al., 2017).

In conclusion, our results set a promising starting point to understand the dynamics of interneuronal spines, how this structural plasticity can be regulated by NMDARs and what are the mechanisms underlying it. With a better understanding of the structural remodeling of interneurons we may predict its impact on local neuronal networks and, in time, understand better the neurobiology of complex psychiatric disorders, such as schizophrenia or major depression, in which both NMDARs and inhibitory networks are affected.

AUTHOR CONTRIBUTIONS

EC-G, RG, JN and MP-R designed the study. MP-R, EC-G and RG performed the experiments. MP-R analyzed the data prepared the figures. MP-R, EC-G, JMB-I, CC, EV and JN wrote the manuscript.

FUNDING

This research was supported by Generalitat Valenciana (Prometeo Excellence Program PROMETEO2013/069), the Fundación Alicia Koplowitz and the Spanish Ministry of Economy and Competitiveness (BFU2012-32512) projects to JN. EC-G had postdoctoral fellowship (IJCI-2015-24124) and MP-R a predoctoral fellowship (FPU12/03200, FPU) from the Spanish Ministry of Economy and Competitiveness.

REFERENCES

Acsády, L., Kamondi, A., Sík, A., Freund, T., and Buzsáki, G. (1998). GABAergic cells are the major postsynaptic targets of mossy fibers in the rat hippocampus. *J. Neurosci.* 18, 3386–3403.

Adell, A., Jiménez-Sánchez, L., López-Gil, X., and Romón, T. (2012). Is the acute NMDA receptor hypofunction a valid model of schizophrenia? *Schizophr. Bull.* 38, 9–14. doi: 10.1093/schbul/sbr133

Alvarez, V. A., Ridenour, D. A., and Sabatini, B. L. (2007). Distinct structural and ionotropic roles of NMDA receptors in controlling spine and synapse stability. *J. Neurosci.* 27, 7365–7376. doi: 10.1523/jneurosci.0956-07.2007

Bailey, C. H., Bartsch, D., and Kandel, E. R. (1996). Toward a molecular definition of long-term memory storage. *Proc. Natl. Acad. Sci. U S A* 93, 13445–13452. doi: 10.1073/pnas.93.24.13445

Becker, N., Wierenga, C. J., Fonseca, R., Bonhoeffer, T., and Nägerl, U. V. (2008). LTD induction causes morphological changes of presynaptic boutons and reduces their contacts with spines. *Neuron* 60, 590–597. doi: 10.1016/j.neuron.2008.09.018

Beninger, R. J., Jhamandas, A., Aujla, H., Xue, I., Dagnone, R. V., Boegman, R. J., et al. (2002). Neonatal exposure to the glutamate receptor antagonist MK-801: effects on locomotor activity and pre-pulse inhibition before and after sexual maturity in rats. *Neurotox. Res.* 4, 477–488. doi: 10.1080/10298420290031414

Blasco-Ibáñez, J. M., and Freund, T. F. (1995). Synaptic input of horizontal interneurons in stratum oriens of the hippocampal CA1 subfield: structural basis of feed-back activation. *Eur. J. Neurosci.* 7, 2170–2180. doi: 10.1111/j.1460-9568.1995.tb00638.x

Browne, C. A., and Lucki, I. (2013). Antidepressant effects of ketamine: mechanisms underlying fast-acting novel antidepressants. *Front. Pharmacol.* 4:161. doi: 10.3389/fphar.2013.00161

Butler, A. K., Uryu, K., and Chesselet, M. F. (1998). A role for *N*-methyl-D-aspartate receptors in the regulation of synaptogenesis and expression of the polysialylated form of the neural cell adhesion molecule in the developing striatum. *Dev. Neurosci.* 20, 253–262. doi: 10.1159/000017319

Cane, M., Maco, B., Knott, G., and Holtmaat, A. (2014). The relationship between PSD-95 clustering and spine stability *in vivo*. *J. Neurosci.* 34, 2075–2086. doi: 10.1523/JNEUROSCI.3353-13.2014

Castillo-Gómez, E., Coviello, S., Perez-Rando, M., Curto, Y., Carceller, H., Salvador, A., et al. (2015). Streptozotocin diabetic mice display depressive-like behavior and alterations in the structure, neurotransmission and plasticity of medial prefrontal cortex interneurons. *Brain Res. Bull.* 116, 45–56. doi: 10.1016/j.brainresbull.2015.06.002

Castillo-Gómez, E., Perez-Rando, M., Bellés, M., Gilabert-Juan, J., Llorens, J. V., Carceller, H., et al. (2017). Early social isolation stress and perinatal NMDA receptor antagonist treatment induce changes in the structure and neurochemistry of inhibitory neurons of the adult amygdala and prefrontal cortex. *Eneuro* 4:ENEURO.0034-17.2017. doi: 10.1523/ENEURO.0034-17.2017

Castillo-Gómez, E., Perez-Rando, M., Videira, S., and Nacher, J. (2016a). Polysialic acid acute depletion induces structural plasticity in interneurons and impairs the excitation/inhibition balance in medial prefrontal cortex organotypic cultures. *Front. Cell. Neurosci.* 10:170. doi: 10.3389/fncel.2016.00170

Castillo-Gómez, E., Varea, E., Blasco-Ibáñez, J. M., Crespo, C., and Nacher, J. (2016b). Effects of chronic dopamine D2R agonist treatment and polysialic acid depletion on dendritic spine density and excitatory neurotransmission in the mPFC of adult rats. *Neural Plast.* 2016:1615363. doi: 10.1155/2016/1615363

Castilla-Ortega, E., Sánchez-López, J., Hoyo-Becerra, C., Matas-Rico, E., Zambrana-Infantes, E., Chun, J., et al. (2010). Exploratory, anxiety and spatial memory impairments are dissociated in mice lacking the LPA1 receptor. *Neurobiol. Learn. Mem.* 94, 73–82. doi: 10.1016/j.nlm.2010.04.003

Chen, J. L., Flanders, G. H., Lee, W.-C. A., Lin, W. C., and Nedivi, E. (2011a). Inhibitory dendrite dynamics as a general feature of the adult cortical microcircuit. *J. Neurosci.* 31, 12437–12443. doi: 10.1523/jneurosci.0420-11.2011

Chen, J. L., Lin, W. C., Cha, J. W., So, P. T., Kubota, Y., and Nedivi, E. (2011b). Structural basis for the role of inhibition in facilitating adult brain plasticity. *Nat. Neurosci.* 14, 587–594. doi: 10.1038/nn.2799

Chen, J. L., and Nedivi, E. (2013). Highly specific structural plasticity of inhibitory circuits in the adult neocortex. *Neuroscientist* 19, 384–393. doi: 10.1177/1073858413479824

Chen, J. L., Villa, K. L., Cha, J. W., So, P. T. C., Kubota, Y., and Nedivi, E. (2012). Clustered dynamics of inhibitory synapses and dendritic spines in the adult neocortex. *Neuron* 74, 361–373. doi: 10.1016/j.neuron.2012.02.030

Cline, H. T., and Constantine-Paton, M. (1990). NMDA receptor agonist and antagonists alter retinal ganglion cell arbor structure in the developing frog retinotectal projection. *J. Neurosci.* 10, 1197–1216.

Colicos, M. A., Collins, B. E., Sailor, M. J., and Goda, Y. (2001). Remodeling of synaptic actin induced by photoconductive stimulation. *Cell* 107, 605–616. doi: 10.1016/s0092-8674(01)00579-7

Collingridge, G. L., Kehl, S. J., and McLennan, H. (1983). Excitatory amino acids in synaptic transmission in the Schaffer collateral-commissural pathway of the rat hippocampus. *J. Physiol. Lond.* 334, 33–46. doi: 10.1113/jphysiol.1983.sp014478

Coyle, J. T. (2006). Glutamate and schizophrenia: beyond the dopamine hypothesis. *Cell. Mol. Neurobiol.* 26, 365–384. doi: 10.1007/s10571-006-9062-8

Dingess, P. M., Darling, R. A., Kurt Dolence, E., Culver, B. W., and Brown, T. E. (2016). Exposure to a diet high in fat attenuates dendritic spine density in the medial prefrontal cortex. *Brain Struct. Funct.* 222, 1077–1085. doi: 10.1007/s00429-016-1208-y

Engert, F., and Bonhoeffer, T. (1999). Dendritic spine changes associated with hippocampal long-term synaptic plasticity. *Nature* 399, 66–70. doi: 10.1038/19978

Erreger, K., Dravid, S. M., Banke, T. G., Wyllie, D. J. A., and Traynelis, S. F. (2005). Subunit-specific gating controls rat NR1/NR2A and NR1/NR2B NMDA channel kinetics and synaptic signalling profiles. *J. Physiol.* 563, 345–358. doi: 10.1113/jphysiol.2004.080028

Florence, S. L., Taub, H. B., and Kaas, J. H. (1998). Large-scale sprouting of cortical connections after peripheral injury in adult macaque monkeys. *Science* 282, 1117–1121. doi: 10.1126/science.282.5391.1117

Flores, G., Morales-Medina, J. C., and Diaz, A. (2016). Neuronal and brain morphological changes in animal models of schizophrenia. *Behav. Brain Res.* 301, 190–203. doi: 10.1016/j.bbr.2015.12.034

Flores, C., Wen, X., Labelle-Dumais, C., and Kolb, B. (2007). Chronic phencyclidine treatment increases dendritic spine density in prefrontal cortex and nucleus accumbens neurons. *Synapse* 61, 978–984. doi: 10.1002/syn.20452

Freund, T. F., and Buzsáki, G. (1996). Interneurons of the hippocampus. *Hippocampus* 6, 347–470. doi: 10.1002/(SICI)1098-1063(1996)6:4<347::AID-HIPO1>3.0.CO;2-I

Freund, T. F., and Gulyás, A. I. (1997). Inhibitory control of GABAergic interneurons in the hippocampus. *Can. J. Physiol. Pharmacol.* 75, 479–487. doi: 10.1139/y97-33

Fu, M., and Zuo, Y. (2011). Experience-dependent structural plasticity in the cortex. *Trends Neurosci.* 34, 177–187. doi: 10.1016/j.tins.2011.02.001

Gilabert-Juan, J., Bueno-Fernandez, C., Castillo-Gomez, E., and Nacher, J. (2017). Reduced interneuronal dendritic arborization in CA1 but not in CA3 region of mice subjected to chronic mild stress. *Brain Behav.* 7:e00534. doi: 10.1002/brb3.534

Gilabert-Juan, J., Castillo-Gomez, E., Perez-Rando, M., Moltó, M. D., and Nacher, J. (2011). Chronic stress induces changes in the structure of interneurons and in the expression of molecules related to neuronal structural plasticity and inhibitory neurotransmission in the amygdala of adult mice. *Exp. Neurol.* 232, 33–40. doi: 10.1016/j.expneurol.2011.07.009

Gilmour, G., Dix, S., Fellini, L., Gastambide, F., Plath, N., Steckler, T., et al. (2012). NMDA receptors, cognition and schizophrenia—Testing the validity of the NMDA receptor hypofunction hypothesis. *Neuropharmacology* 62, 1401–1412. doi: 10.1016/j.neuropharm.2011.03.015

Glausier, J. R., and Lewis, D. A. (2013). Dendritic spine pathology in schizophrenia. *Neuroscience* 251, 90–107. doi: 10.1016/j.neuroscience.2012.04.044

Gomez-Climent, M. A., Guirado, R., Castillo-Gomez, E., Varea, E., Gutierrez-Mecinas, M., Gilabert-Juan, J., et al. (2011). The polysialylated form of the neural cell adhesion molecule (PSA-NCAM) is expressed in a subpopulation of mature cortical interneurons characterized by reduced structural features and connectivity. *Cereb. Cortex* 21, 1028–1041. doi: 10.1093/cercor/bhq177

Guirado, R., Perez-Rando, M., Sanchez-Matarredona, D., Castillo-Gomez, E., Liberia, T., Rovira-Esteban, L., et al. (2014a). The dendritic spines of interneurons are dynamic structures influenced by PSA-NCAM expression. *Cereb. Cortex* 24, 3014–3024. doi: 10.1093/cercor/bht156

Guirado, R., Perez-Rando, M., Sanchez-Matarredona, D., Castrén, E., and Nacher, J. (2014b). Chronic fluoxetine treatment alters the structure, connectivity and plasticity of cortical interneurons. *Int. J. Neuropsychopharmacol.* 17, 1635–1646. doi: 10.1017/s1461145714000406

Guirado, R., Varea, E., Castillo-Gómez, E., Gómez-Climent, M. A., Rovira-Esteban, L., Blasco-Ibáñez, J. M., et al. (2009). Effects of chronic fluoxetine treatment on the rat somatosensory cortex: activation and induction of neuronal structural plasticity. *Neurosci. Lett.* 457, 12–15. doi: 10.1016/j.neulet.2009.03.104

Gulyás, A. I., Hájos, N., Katona, I., and Freund, T. F. (2003). Interneurons are the local targets of hippocampal inhibitory cells which project to the medial septum. *Eur. J. Neurosci.* 17, 1861–1872. doi: 10.1046/j.1460-9568.2003.02630.x

Gulyás, A. I., Miettinen, R., Jacobowitz, D. M., and Freund, T. F. (1992). Calretinin is present in non-pyramidal cells of the rat hippocampus-I. A new type of neuron specifically associated with the mossy fibre system. *Neuroscience* 48, 1–27. doi: 10.1016/0306-4522(92)90334-x

Haj-Mirzaian, A., Amiri, S., Kordjazy, N., Rahimi-Balaei, M., Haj-Mirzaian, A., Marzban, H., et al. (2015). Blockade of NMDA receptors reverses the

depressant, but not anxiogenic effect of adolescence social isolation in mice. *Eur. J. Pharmacol.* 750, 160–166. doi: 10.1016/j.ejphar.2015.01.006

Han, D., Xu, L., Xiao, H., Prado Schmidt, G. C., and Shi, S. (2013). Dizocilpine reduces head diameter of dendritic spines in the hippocampus of adolescent rats. *Psychiatry Res.* 210, 351–356. doi: 10.1016/j.psychres.2013.04.025

Hirose, N., Saitoh, A., and Kamei, J. (2016). Involvement of glutamatergic *N*-methyl-D-aspartate receptors in the expression of increased head-dipping behaviors in the hole-board tests of olfactory bulbectomized mice. *Behav. Brain Res.* 312, 313–320. doi: 10.1016/j.bbr.2016.06.045

Hofer, S. B., Mrsic-Flogel, T. D., Bonhoeffer, T., and Hübener, M. (2009). Experience leaves a lasting structural trace in cortical circuits. *Nature* 457, 313–317. doi: 10.1038/nature07487

Holtmaat, A., and Svoboda, K. (2009). Experience-dependent structural synaptic plasticity in the mammalian brain. *Nat. Rev. Neurosci.* 10, 647–658. doi: 10.1038/nrn2699

Jinno, S., and Kosaka, T. (2002). Immunocytochemical characterization of hippocamposeptal projecting GABAergic nonprincipal neurons in the mouse brain: a retrograde labeling study. *Brain Res.* 945, 219–231. doi: 10.1016/s0006-8993(02)02804-4

Kalinichev, M., Bate, S. T., Coggon, S. A., and Jones, D. N. C. (2008). Locomotor reactivity to a novel environment and sensitivity to MK-801 in five strains of mice. *Behav. Pharmacol.* 19, 71–75. doi: 10.1097/fbp.0b013e3282f3cf48

Karl, T., Duffy, L., and Herzog, H. (2008). Behavioural profile of a new mouse model for NPY deficiency. *Eur. J. Neurosci.* 28, 173–180. doi: 10.1111/j.1460-9568.2008.06306.x

Katona, I., Acsády, L., and Freund, T. (1999). Postsynaptic targets of somatostatin-immunoreactive interneurons in the rat hippocampus. *Neuroscience* 88, 37–55. doi: 10.1016/s0306-4522(98)00302-9

Katona, L., Lapray, D., Viney, T. J., Oulhaj, A., Borhegyi, Z., Micklem, B. R., et al. (2014). Sleep and movement differentiates actions of two types of somatostatin-expressing GABAergic interneuron in rat hippocampus. *Neuron* 82, 872–886. doi: 10.1016/j.neuron.2014.04.007

Keck, T., Scheuss, V., Jacobsen, R. I., Wierenga, C. J., Eysel, U. T., Bonhoeffer, T., et al. (2011). Loss of sensory input causes rapid structural changes of inhibitory neurons in adult mouse visual cortex. *Neuron* 71, 869–882. doi: 10.1016/j.neuron.2011.06.034

Kehoe, L. A., Bellone, C., De Roo, M., Zandueta, A., Dey, P. N., Perez-Otano, I., et al. (2014). GluN3A promotes dendritic spine pruning and destabilization during postnatal development. *J. Neurosci.* 34, 9213–9221. doi: 10.1523/jneurosci.5183-13.2014

Komuro, H., and Rakic, P. (1993). Modulation of neuronal migration by NMDA receptors. *Science* 260, 95–97. doi: 10.1126/science.8096653

Kwon, H.-B., and Sabatini, B. L. (2011). Glutamate induces *de novo* growth of functional spines in developing cortex. *Nature* 474, 100–104. doi: 10.1038/nature09986

Lai, K.-O. O., and Ip, N. Y. (2013). Structural plasticity of dendritic spines: the underlying mechanisms and its dysregulation in brain disorders. *Biochim. Biophys. Acta* 1832, 2257–2263. doi: 10.1016/j.bbadis.2013.08.012

Leão, R. N., Mikulovic, S., Leão, K. E., Munguba, H., Gezelius, H., Enjin, A., et al. (2012). OLM interneurons differentially modulate CA3 and entorhinal inputs to hippocampal CA1 neurons. *Nat. Neurosci.* 15, 1524–1530. doi: 10.1038/nn.3235

Li, N., Lee, B., Liu, R.-J., Banasr, M., Dwyer, J. M., Iwata, M., et al. (2010). mTOR-dependent synapse formation underlies the rapid antidepressant effects of NMDA antagonists. *Science* 329, 959–964. doi: 10.1126/science.1190287

Liguz-Lecznar, M., Urban-Ciecko, J., and Kossut, M. (2016). Somatostatin and somatostatin-containing neurons in shaping neuronal activity and plasticity. *Front. Neural Circuits* 10:48. doi: 10.3389/fncir.2016.00048

Lim, A. L., Taylor, D. A., and Malone, D. T. (2012). Consequences of early life MK-801 administration: long-term behavioural effects and relevance to schizophrenia research. *Behav. Brain Res.* 227, 276–286. doi: 10.1016/j.bbr.2011.10.052

Lisman, J. E., Coyle, J. T., Green, R. W., Javitt, D. C., Benes, F. M., Heckers, S., et al. (2008). Circuit-based framework for understanding neurotransmitter and risk gene interactions in schizophrenia. *Trends Neurosci.* 31, 234–242. doi: 10.1016/j.tins.2008.02.005

Liu, R.-J., Fuchikami, M., Dwyer, J. M., Lepack, A. E., Duman, R. S., and Aghajanian, G. K. (2013). GSK-3 inhibition potentiates the synaptogenic and antidepressant-like effects of subthreshold doses of ketamine. *Neuropsychopharmacology* 38, 2268–2277. doi: 10.1038/npp.2013.128

Lovett-Barron, M., Kaifosh, P., Kheirbek, M. A., Danielson, N., Zaremba, J. D., Reardon, T. R., et al. (2014). Dendritic inhibition in the hippocampus supports fear learning. *Science* 343, 857–863. doi: 10.1126/science.1247485

Matsuzaki, M., Honkura, N., Ellis-Davies, G. C. R., and Kasai, H. (2004). Structural basis of long-term potentiation in single dendritic spines. *Nature* 429, 761–766. doi: 10.1038/nature02617

McEwen, B. S. (1999). Stress and hippocampal plasticity. *Annu. Rev. Neurosci.* 22, 105–122. doi: 10.1146/annurev.neuro.22.1.105

McKinney, R. A., Capogna, M., Dürr, R., Gähwiler, B. H., and Thompson, S. M. (1999a). Miniature synaptic events maintain dendritic spines via AMPA receptor activation. *Nat. Neurosci.* 2, 44–49. doi: 10.1038/4548

McKinney, R. A., Lüthi, A., Bandtlow, C. E., Gähwiler, B. H., and Thompson, S. M. (1999b). Selective glutamate receptor antagonists can induce or prevent axonal sprouting in rat hippocampal slice cultures. *Proc. Natl. Acad. Sci. U S A* 96, 11631–11636. doi: 10.1073/pnas.96.20.11631

Müller, C., and Remy, S. (2014). Dendritic inhibition mediated by O-LM and bistratified interneurons in the hippocampus. *Front. Synaptic Neurosci.* 6:23. doi: 10.3389/fnsyn.2014.00023

Nacher, J., Guirado, R., and Castillo-Gómez, E. (2013). Structural plasticity of interneurons in the adult brain: role of PSA-NCAM and implications for psychiatric disorders. *Neurochem. Res.* 38, 1122–1133. doi: 10.1007/s11064-013-0977-4

Nacher, J., and McEwen, B. S. (2006). The role of *N*-methyl-D-asparate receptors in neurogenesis. *Hippocampus* 16, 267–270. doi: 10.1002/hipo.20160

Nácher, J., Varea, E., Miguel Blasco-Ibáñez, J., Gómez-Climent, M. Á., Castillo-Gómez, E., Crespo, C., et al. (2007). *N*-methyl-D-aspartate receptor expression during adult neurogenesis in the rat dentate gyrus. *Neuroscience* 144, 855–864. doi: 10.1016/j.neuroscience.2006.10.021

Nikonenko, I., Jourdain, P., Alberi, S., Toni, N., and Muller, D. (2002). Activity-induced changes of spine morphology. *Hippocampus* 12, 585–591. doi: 10.1002/hipo.10095

Nikonenko, I., Jourdain, P., and Muller, D. (2003). Presynaptic remodeling contributes to activity-dependent synaptogenesis. *J. Neurosci.* 23, 8498–8505.

Nyíri, G., Stephenson, F. A., Freund, T. F., and Somogyi, P. (2003). Large variability in synaptic *n*-methyl-d-aspartate receptor density on interneurons and a comparison with pyramidal-cell spines in the rat hippocampus. *Neuroscience* 119, 347–363. doi: 10.1016/s0306-4522(03)00157-x

Oliva, A. A., Jiang, M., Lam, T., Smith, K. L., and Swann, J. W. (2000). Novel hippocampal interneuronal subtypes identified using transgenic mice that express green fluorescent protein in GABAergic interneurons. *J. Neurosci.* 20, 3354–3368.

Oren, I., Nissen, W., Kullmann, D. M., Somogyi, P., and Lamsa, K. P. (2009). Role of ionotropic glutamate receptors in long-term potentiation in rat hippocampal CA1 oriens-lacunosum moleculare interneurons. *J. Neurosci.* 29, 939–950. doi: 10.1523/JNEUROSCI.3251-08.2009

Paxinos, G., and Franklin, K. B. J. (2013). Paxinos and franklin's the mouse brain in stereotaxic coordinates. Available online at: https://books.google.de/books?id=8RJZLwEACAAJ

Phoumthipphavong, V., Barthas, F., Hassett, S., and Kwan, A. C. (2016). Longitudinal effects of ketamine on dendritic architecture *in vivo* in the mouse medial frontal cortex. *Eneuro* 3:ENEURO.0133-15.2016. doi: 10.1523/ENEURO.0133-15.2016

Qiao, H., Li, M.-X., Xu, C., Chen, H.-B., An, S.-C., Ma, X.-M., et al. (2016). Dendritic spines in depression: what we learned from animal models. *Neural Plast.* 2016:8056370. doi: 10.1155/2016/8056370

Romón, T., Mengod, G., and Adell, A. (2011). Expression of parvalbumin and glutamic acid decarboxylase-67 after acute administration of MK-801. Implications for the NMDA hypofunction model of schizophrenia.

Psychopharmacology (Berl) 217, 231–238. doi: 10.1007/s00213-011-2268-6

Rotaru, D. C., Yoshino, H., Lewis, D. A., Ermentrout, G. B., and Gonzalez-Burgos, G. (2011). Glutamate receptor subtypes mediating synaptic activation of prefrontal cortex neurons: relevance for schizophrenia. *J. Neurosci.* 31, 142–156. doi: 10.1523/JNEUROSCI.1970-10.2011

Shatz, C. J. (1990). Impulse activity and the patterning of connections during cns development. *Neuron* 5, 745–756. doi: 10.1016/0896-6273(90)90333-b

Sik, A., Penttonen, M., Ylinen, A., Buzsiki, G., and Buzsbki, G. (1995). Hippocampal CA1 interneurons: an *in vivo* intracellular labeling study. *J. Neurosci.* 75, 6651–6665.

Simon, P., Dupuis, R., and Costentin, J. (1994). Thigmotaxis as an index of anxiety in mice. Influence of dopaminergic transmissions. *Behav. Brain Res.* 61, 59–64. doi: 10.1016/0166-4328(94)90008-6

Stoppini, L., Buchs, P. A., and Muller, D. (1991). A simple method for organotypic cultures of nervous tissue. *J. Neurosci. Methods* 37, 173–182. doi: 10.1016/0165-0270(91)90128-m

Sutula, T., Koch, J., Golarai, G., Watanabe, Y., and McNamara, J. O. (1996). NMDA receptor dependence of kindling and mossy fiber sprouting: evidence that the NMDA receptor regulates patterning of hippocampal circuits in the adult brain. *J. Neurosci.* 16, 7398–7406.

Thomases, D. R., Cass, D. K., and Tseng, K. Y. (2013). Periadolescent exposure to the NMDA receptor antagonist MK-801 impairs the functional maturation of local GABAergic circuits in the adult prefrontal cortex. *J. Neurosci.* 33, 26–34. doi: 10.1523/jneurosci.4147-12.2013

Torres-García, M. E., Solis, O., Patricio, A., Rodríguez-Moreno, A., Camacho-Abrego, I., Limón, I. D., et al. (2012). Dendritic morphology changes in neurons from the prefrontal cortex, hippocampus and nucleus accumbens in rats after lesion of the thalamic reticular nucleus. *Neuroscience* 223, 429–438. doi: 10.1016/j.neuroscience.2012.07.042

Tuncdemir, S. N., Wamsley, B., Stam, F. J., Osakada, F., Goulding, M., Callaway, E. M., et al. (2016). Early somatostatin interneuron connectivity mediates the maturation of deep layer cortical circuits. *Neuron* 89, 521–535. doi: 10.1016/j.neuron.2015.11.020

Ultanir, S. K., Kim, J.-E., Hall, B. J., Deerinck, T., Ellisman, M., and Ghosh, A. (2007). Regulation of spine morphology and spine density by NMDA receptor signaling *in vivo*. *Proc. Natl. Acad. Sci. U S A* 104, 19553–19558. doi: 10.1073/pnas.0704031104

van Versendaal, D., Rajendran, R., Saiepour, M. H., Klooster, J., Smit-Rigter, L., Sommeijer, J.-P., et al. (2012). Elimination of inhibitory synapses is a major component of adult ocular dominance plasticity. *Neuron* 74, 374–383. doi: 10.1016/j.neuron.2012.03.015

Velázquez-Zamora, D. A., González-Ramírez, M. M., Beas-Zárate, C., and González-Burgos, I. (2011). Egocentric working memory impairment and dendritic spine plastic changes in prefrontal neurons after NMDA receptor blockade in rats. *Brain Res.* 1402, 101–108. doi: 10.1016/j.brainres.2011.06.018

Vutskits, L., Gascon, E., Potter, G., Tassonyi, E., and Kiss, J. Z. (2007). Low concentrations of ketamine initiate dendritic atrophy of differentiated GABAergic neurons in culture. *Toxicology* 234, 216–226. doi: 10.1016/j.tox.2007.03.004

Wang, H.-X., and Gao, W.-J. (2012). Prolonged exposure to NMDAR antagonist induces cell-type specific changes of glutamatergic receptors in rat prefrontal cortex. *Neuropharmacology* 62, 1808–1822. doi: 10.1016/j.neuropharm.2011.11.024

Whitt, J. L., Petrus, E., and Lee, H.-K. (2014). Experience-dependent homeostatic synaptic plasticity in neocortex. *Neuropharmacology* 78, 45–54. doi: 10.1016/j.neuropharm.2013.02.016

Woolley, C. S., and McEwen, B. S. (1994). Estradiol regulates hippocampal dendritic spine density via an *N*-methyl-D-aspartate receptor-dependent mechanism. *J. Neurosci.* 14, 7680–7687.

Yang, C., Shirayama, Y., Zhang, J., Ren, Q., Yao, W., Ma, M., et al. (2015). R-ketamine: a rapid-onset and sustained antidepressant without psychotomimetic side effects. *Transl. Psychiatry* 5:e632. doi: 10.1038/tp.2015.136

Zuo, D.-Y., Zhang, Y.-H., Cao, Y., Wu, C.-F., Tanaka, M., and Wu, Y.-L. (2006). Effect of acute and chronic MK-801 administration on extracellular glutamate and ascorbic acid release in the prefrontal cortex of freely moving mice on line with open-field behavior. *Life Sci.* 78, 2172–2178. doi: 10.1016/j.lfs.2005.09.022

Conflict of Interest Statement: The authors declare that the research was conducted in the absence of any commercial or financial relationships that could be construed as a potential conflict of interest.

2. Early social isolation stress and perinatal NMDA receptor antagonist treatment induce changes in the structure and neurochemistry of inhibitory neurons of the adult amygdala and prefrontal cortex

Castillo-Gómez, E., Perez-Rando, M., Bellés, M., Gilabert-Juan, J., Llorens, J.V., Carceller, H., Bueno-Fernández, C., García-Mompó, C., Ripoll-Martínez, B., Curto, Y., Sebastiá-Ortega, N., Moltó, M.D., Sanjuan, J., Juan, N. (2017). Early Social Isolation Stress and Perinatal NMDA Receptor Antagonist Treatment Induce Changes in the Structure and Neurochemistry of Inhibitory Neurons of the Adult Amygdala and Prefrontal Cortex. eNeuro 4, ENEURO.0034-17.2017

doi:10.1523/ENEURO.0034-17.2017

eNeuro

New Research

Disorders of the Nervous System

Early Social Isolation Stress and Perinatal NMDA Receptor Antagonist Treatment Induce Changes in the Structure and Neurochemistry of Inhibitory Neurons of the Adult Amygdala and Prefrontal Cortex

Esther Castillo-Gómez,[1,*] Marta Pérez-Rando,[1,*] María Bellés,[1] Javier Gilabert-Juan,[1,2,3,4] José Vicente Llorens,[2] Héctor Carceller,[1] Clara Bueno-Fernández,[1] Clara García-Mompó,[1] Beatriz Ripoll-Martínez,[1] Yasmina Curto,[1] Noelia Sebastiá-Ortega,[2,3] María Dolores Moltó,[2,3,4] Julio Sanjuan,[3,4] and Juan Nacher[1,3,4]

DOI:http://dx.doi.org/10.1523/ENEURO.0034-17.2017

[1]Neurobiology Unit, Cell Biology Department, Interdisciplinary Research Structure for Biotechnology and Biomedicine (BIOTECMED), Universitat De València, Burjassot 46100, Spain, [2]Department of Genetics, Universitat De València, Burjassot 46100, Spain, [3]CIBERSAM: Spanish National Network for Research in Mental Health, 28029 Madrid, and [4]Fundación Investigación Hospital Clínico De Valencia, INCLIVA, Valencia 46010, Spain

Abstract

The exposure to aversive experiences during early life influences brain development and leads to altered behavior. Moreover, the combination of these experiences with subtle alterations in neurodevelopment may contribute to the emergence of psychiatric disorders, such as schizophrenia. Recent hypotheses suggest that imbalances between excitatory and inhibitory (E/I) neurotransmission, especially in the prefrontal cortex and the amygdala, may underlie their etiopathology. In order to understand better the neurobiological bases of these alterations, we studied the impact of altered neurodevelopment and chronic early-life stress on these two brain regions. Transgenic mice displaying fluorescent excitatory and inhibitory neurons, received a single injection of MK801 (NMDAR antagonist) or vehicle solution at postnatal day 7 and/or were socially isolated from the age of weaning until adulthood (3 months old). We found that anxiety-related behavior, brain volume, neuronal structure, and the expression of molecules related to plasticity and E/I neurotransmission in adult mice were importantly affected by early-life stress. Interestingly, many of these effects were potentiated when the stress paradigm was applied to mice perinatally injected with MK801 ("double-hit" model). These results clearly show the impact of early-life stress on the adult brain, especially on the structure and plasticity of inhibitory networks, and highlight the double-hit model as a valuable tool to study the contribution of early-life stress in the emergence of neurodevelopmental psychiatric disorders, such as schizophrenia.

Key words: interneuron; neuronal plasticity; PSA-NCAM; schizophrenia; social isolation; stress

Significance Statement

The double-hit model constitutes a valuable tool for future experiments exploring the effects of aversive experiences during early life and the biological basis of mental disorders, such as schizophrenia. It also supports the emerging hypothesis of altered E/I balance in key brain regions as one of the underlying causes of the disease. Our study also supports the idea that such imbalances may arise from problems in initial neural circuit formation or its maintenance, because we found alterations in the structure of inhibitory circuits and also in the expression of molecules related to their plasticity and maturation.

Introduction

Aversive experiences, such as chronic stress, remodel the structure and connectivity of excitatory and inhibitory excitatory and inhibitory (E/I) neurons. These effects of stress are particularly relevant during early life and may constitute a predisposing factor for the development of psychiatric disorders, such as schizophrenia. In fact, patients show important alterations in different brain regions, including the prefrontal cortex (PFC) and the amygdala (Goghari et al. 2010). Interestingly, the structure of E/I neurons in these two regions is dramatically affected by stress (Gilabert-Juan et al. 2011, 2013b; Duman and Duman, 2015).

Different animal models have been generated to understand the impact of early-life stress on the structure of the adult brain and its influence on schizophrenia and other psychiatric disorders. The post-weaning social isolation paradigm is one of these models and reproduces some of the behavioral, structural, and neurochemical alterations found in schizophrenic patients (Geyer et al. 1993; Ferdman et al. 2007; Gilabert-Juan et al. 2012; Wang et al. 2012; Glausier and Lewis, 2013). Given the importance of altered neurodevelopment on the etiology of schizophrenia and other mental disorders, this paradigm has been lately combined with experimental interventions during early postnatal life, such as the administration of NMDA receptor (NMDAR) antagonists (i.e., MK801), which alters the latest stages of neocortical development (Hickey et al. 2012; Lim et al. 2012; Gilabert-Juan et al. 2013a). Numerous studies in humans and animal models of schizophrenia, have documented the presence of structural alterations in the basolateral amygdala (BLA) and PFC, including volume loss in both regions (Jaaro-Peled et al. 2010; Levitt et al. 2010; Gilabert-Juan et al. 2013a). These volumetric alterations may probably reflect structural changes in PFC and BLA neurons, including alterations in spine density and dendritic arborization.

The polysialylated form of the neural cell adhesion molecule (PSA-NCAM) plays a key role in structural remodeling and the connectivity of neurons in the adult brain, especially of interneurons (for review, see Bonfanti, 2006; Rutishauser, 2008; Nacher et al. 2013), which is particularly evident after chronic stress (Sandi, 2004; Nacher et al. 2013). Perineuronal nets (PNNs) also play a fundamental role in the plasticity and maturation of interneurons, particularly on those expressing parvalbumin (PV; Kinden Lensjø et al. 2017). In fact, this plasticity of inhibitory networks is crucial for brain physiology and development, which largely depend on the precise balance between E/I neurotransmission (E/I balance). The E/I balance is compromised by stress, both in adulthood and in early life (Saaltink and Vreugdenhil, 2014; Tzanoulinou et al. 2014; van der Kooij et al. 2014) and its disbalance may be one of the underlying causes of different neurodevelopmental psychiatric disorders, including schizophrenia (Curley and Lewis, 2012; Lewis et al. 2012; Inan et al. 2013; Lin et al. 2013; Sun et al. 2013; Morishita et al. 2015). Importantly, E/I balance can also be affected by changes in the expression of other molecules that influence the physiology and development of inhibitory circuits. This is the case of glutamic acid decarboxylase (GAD; Akbarian, 1995; Akbarian and Huang, 2006; Straub et al. 2007; Mitchell et al. 2015); brain-derived neurotrophic factor (BDNF), which promotes the maturation of inhibitory synapses (Weickert et al. 2003, 2005; Tao et al. 2014); the cannabinoid receptor 1 (CB1-R), which affects their development (Volk and Lewis, 2010; den Boon et al. 2015); and neuregulin 1 (Nrg1) and its receptor ErbB4, which play prominent roles in the synaptogenesis and plasticity of inhibitory networks (Rico and Marín, 2011).

The main objective of this work is to study the impact of early-life stress on E/I circuits in the adult amygdala and PFC, especially on neuronal structure. To combine this aversive experience with a neurodevelopmental alteration, which mimic those found in schizophrenia, we have developed a "double-hit" model in transgenic mice by combining a perinatal MK801 injection and post-weaning social isolation. We have used two transgenic strains expressing fluorescent proteins in E/I neurons and studied in detail the structural features of these neurons, the expression of molecules related to plasticity and E/I neurotransmission and the behavior of the animals.

Materials and Methods

Animals and Experimental Treatment

Two different transgenic mice strains, purchased from The Jackson Laboratory were used in our experiments: the GIN mice [EGFP-expressing inhibitory neurons, Tg(GadGFP)45704Swn], which express the enhanced green fluorescent protein (EGFP) in a subpopulation of interneurons of interest (Oliva et al. 2000); and the THY1 mice (Thy1-YFP line H), which express the yellow fluorescent protein (YFP) in a subset of pyramidal neurons (Feng et al. 2000). The experimental procedure was performed twice for the GIN mice and once for the THY1 mice (Fig.

Received January 29, 2017; accepted March 2, 2017; First published April 21, 2017.

All authors reported no biomedical financial interests or potential conflicts of interest.

Author contributions: E.C.-G. and J.N. designed the study; E.C.-G., M.P.-R., M.B., J.G.-J., J.V.L., H.C., C.B.-F., C.G.-M., B.R.-M., Y.C., and N.S.-O. performed the experiments; E.C.-G. and M.P.-R. analyzed the data; E.C.-G. and M.P.-R. prepared the figures; E.C.-G., M.P.-R., and J.N. wrote the paper; M.D.M. supervised the molecular part of the project; J.S. reviewed the manuscript and gave clinical advice. J.N. supervised the whole project; all authors read and approved the final paper.

This work was supported by the Spanish Ministry of Economy and Competitiveness (BFU2012-32512, SAF2015-68436-R), Generalitat Valenciana (PROMETEO2013/069) and Fundación Alicia Koplowitz (FAK2012-01). M.P.-R. and Y.C. hold pre-doctoral fellowships from the Spanish Ministry of Education (FPU12/03200, FPU13/04764) and M.B., from the University of Valencia ('Atracció de talent-VLC campus').

*E.C.-G. and M.P.-R. contributed equally to this work.

Correspondence should be addressed to either Dr. Juan Nacher or Dr. Esther Castillo-Gómez, Neurobiology Unit, Cell Biology Department, Interdisciplinary Research Structure for Biotechnology and Biomedicine (BIOTECMED), Universitat de València, Dr. Moliner, 50, Burjassot 46100, Spain. E-mail: nacher@uv.es or esther.castillo@uv.es.

DOI:http://dx.doi.org/10.1523/ENEURO.0034-17.2017

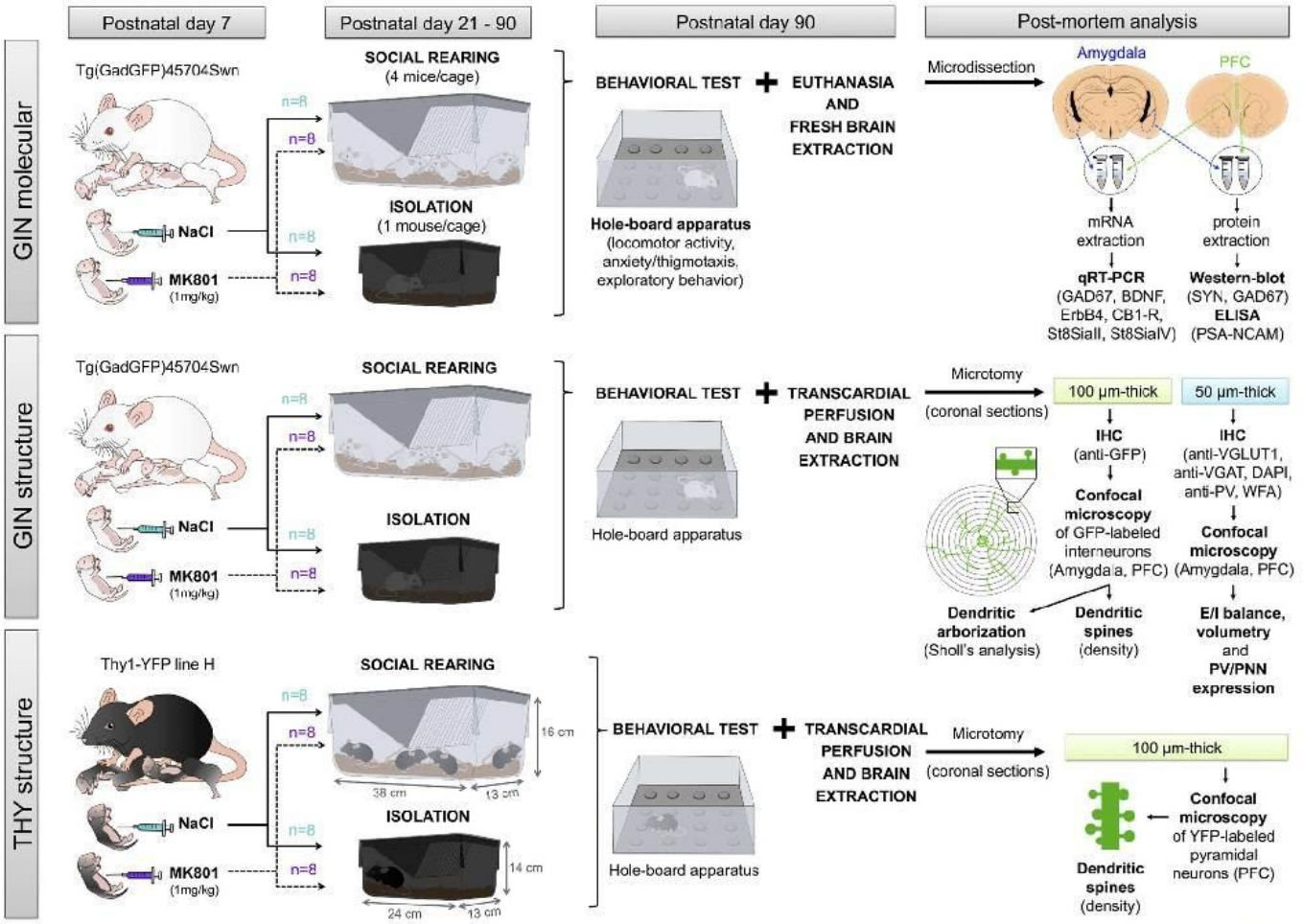

Figure 1. Experimental procedure. Seven days after birth (P7), male pups from two different transgenic strains: the GIN mice (Oliva et al. 2000), which express EGFP in interneurons, and the THY1 mice (Feng et al. 2000), which express the YFP in pyramidal neurons) were intraperitoneally injected with MK801 or NaCl (vehicle solution). After weaning (P21), mice were randomly selected and housed alone (isolation) or in groups of four mice (social rearing) for 10 weeks. At P90, all mice were tested in the hole-board apparatus. Brains from GIN molecular mice were destined to protein and gene expression studies, whereas brains from GIN structure mice were used for the structural and neurochemical analysis of interneurons. The THY structure set of mice was used to study structural alterations of pyramidal neurons. For further details, see Material and Methods.

1). One set of the GIN mice ($n = 32$) was used for the structural and neurochemical analysis of interneurons ("GIN structure"), and the other set ($n = 32$) was used for molecular analyses ("GIN molecular"). All THY mice ($n = 32$) were used for the structural analysis of pyramidal neurons ("THY structure"). The following procedure refers to any of the three sets. Breeding cages containing one male and two female mice (3 months old) were maintained in our animal facility under standard conditions of temperature and light (12 h light/dark cycle) and ad libitum access to food and water. Once the females were pregnant, they were housed individually to avoid any disturbances among mice. Seven days after birth (P7), male pups received randomly a single intraperitoneal injection of MK801 (1 mg/kg solved in NaCl 0.9%, Abcam) or the vehicle solution (NaCl 0.9%). This dose and age of administration produced alterations in PFC-dependent behavior and changes in the structure and inhibitory networks of this region (Lyall et al. 2009; Gilabert-Juan et al. 2013a). MK801, also known as dizocilpine, is a noncompetitive antagonist of NMDA receptors. After the injection, pups were returned to their cages and remained with their mother until the age of weaning (P21). At this age, eight mice from each of the former groups (NaCl or MK801) were randomly selected and housed alone (social isolation) in small polycarbonate cages ($24 \times 14 \times 13$ cm; Zoonlab-Bioscapey) or in groups of three to four mice (social housing) in standard-size cages ($38 \times 16 \times 13$ cm; Zoonlab-Bioscape) for 10 weeks (P90). Thus, at this point, the four final experimental groups ($n = 8$ mice/group) were determined: NaCl-Social (injected with vehicle at P7, and socially housed after weaning), NaCl-Isolation (injected with vehicle but isolated after weaning), MK801-Social (injected with MK-801 at P7 and reared in group), and MK801-Isolation or double-hit model (injected with MK801 at P7 and isolated after weaning). All mice were housed in the same room, sharing the same controlled-environment. Isolated mice were able to hear and smell other mice but physical or visual contact with them was not allowed (Fig. 1).

All animal experimentation was conducted in accordance with the Directive 2010/63/EU of the European

Parliament and of the Council of 22 September 2010 on the protection of animals used for scientific purposes and was approved by the Committee on Bioethics of the Universitat de València. Every effort was made to minimize the number of animals used and their suffering.

Behavioral Analyses

Before their sacrifice (P90), all mice were tested in the hole-board apparatus (ANY-maze video tracking system v4.98; Stoelting Europe). The hole-board test measures directed exploration but can also be used as an initial basic screen for working memory (Karl et al. 2008), locomotor activity, and anxiety-related behavior (Castilla-Ortega et al. 2010; Torres-García et al. 2012; Fig. 1). The open-field chamber (40 × 40 cm) was fitted with a hole-board floor insert for mice (16 holes, diameter = 2.8 cm, non-baited). Testing of male mice took place between 1 and 2 h after the onset of the dark phase (illumination at floor level <2 lx). Each mouse was placed in the center of the arena and was left to explore the environment for 7 min (test session). The video tracking system and the infrared photobeams provided automated measures of the following: (1) total distance traveled and mean speed (to study locomotor activity); (2) head dips, for the study of exploratory behavior (number of head dips into novel holes/total number of head dips; Karl et al. 2008); and (3) body rotations (360°) and number of entries and time spent in the periphery of the arena, for the measure of anxiety and thigmotaxis (a valid index of anxiety in mice; Simon et al. 1994). The periphery zone of the area was defined as the area located between 0 and 6 cm away the walls of the apparatus (Figs. 1,2A,3A).

Perfusion, Microtomy, and Immunohistochemistry

At P90, GIN structure and THY structure mice were deeply anesthetized with sodium pentobarbital and transcardially perfused with 4% paraformaldehyde solution for 20 min. Thirty minutes after perfusion, brains were extracted from the skull and their hemispheres were separated. One hemisphere was cryoprotected [30% sucrose in phosphate buffer (PB) 0.1M, 48 h] and afterward cut in 50-μm-thick coronal sections using a freezing-sliding microtome (LEICA SM2000R, Leica) for immunohistochemical analysis. The other hemisphere, destined to the study of the neuronal structure, was cut in 100-μm-thick coronal sections with a vibratome (Leica VT 1000E, Leica; Fig. 1).

After cutting, tissue was counterstained with DAPI (50-μm-thick sections for volumetric studies; see below) or processed free-floating for fluorescence immunohistochemistry as follows (Fig. 1). Briefly, sections were washed in PBS and then incubated for 1 h in 10% normal donkey serum (NDS; Abcys) in PBS with 0.2% Triton X-100 (PBST; Sigma-Aldrich). Afterward, they were incubated for 48 h at 4°C with the appropriate primary antibody or antibody cocktail diluted in PBST and 5% NDS: (a) polyclonal chicken IgY anti-GFP (1:1000, Abcam) in 100-μm-thick sections from GIN mice to enhance EGFP signal for the structural study of interneurons; (b) polyclonal guinea pig anti-vesicular glutamate transporter 1 (VGLUT1; 1:2000, Merck-Millipore) and monoclonal IgG mouse anti-vesicular GABA transporter (VGAT; 1:1000, Synaptic Systems) in 50-μm-thick sections to study excitatory and inhibitory neurotransmission in the neuropil; (c) polyclonal rabbit IgG anti-PV (1:2000, Swant) and biotin-conjugated *Wisteria floribunda* agglutinin (1:200, Sigma-Aldrich) in 50-μm-thick sections to study the coexpression of PV and PNNs in the amygdala and PFC. After washing, sections were incubated for 2 h at room temperature with matching secondary antibodies (1:400, Jackson ImmunoResearch) diluted in PBST and 5% NDS: (a) donkey anti-chicken DyLight-488-conjugated, (b) goat anti-guinea Pig DyLight-649-conjugated and goat anti-mouse IgG AlexaFluor-555-conjugated, and (c) donkey anti-rabbit IgG AlexaFluor-555-conjugated and Avidin AlexaFluor-647-conjugated. Finally, sections were washed in PB 0.1 M, mounted on slides, and coverslipped using fluorescence mounting medium (Dako Diagnósticos).

Volumetry

A volumetric analysis of the different nuclei of the amygdala (central, lateral, medial, basolateral, and basomedial) and regions of the PFC (infralimbic, prelimbic, dorsal cingulate, and ventral cingulate cortices) were performed by processing confocal images using the Volumest plugin of FIJI/ImageJ Software (NIH; Schindelin et al. 2012). To be able to differentiate the different regions of interest in the subsets of slices, 50-μm-thick sections from the GIN structure set of mice ($n = 32$) were counterstained with DAPI (1:10,000 in H_2O, Sigma-Aldrich). Images of the regions-of-interest were acquired using a confocal microscope (Olympus FV-10). Volumes were estimated using Cavalieri's principle (Gundersen and Jensen, 1987).

Analysis of Dendritic Arborization and Dendritic Spine Density

All the structural parameters of the GAD-EGFP interneurons and THY1-YFP pyramidal neurons were studied using a laser scanning confocal microscope (Leica TCS SPE). In the case of pyramidal neurons, we focused our studies on the PFC, in particular, on the cingulated cortices because, due to the straight projection of the principal dendrite of pyramidal neurons to layer 1, it is only visible coronally in these two subregions of the PFC. To be consistent, interneurons were studied in the same subregions of the PFC. In addition, we studied the arborization and dendritic spine density of interneurons in the basolateral nucleus of the amygdala, which is known to project directly to the PFC and has an abundant population of fluorescent interneurons in GIN mice. Unfortunately, due to the overwhelming expression of the YFP in the amygdala, we could not to perform these structural analyses for pyramidal neurons.

For the study of the dendritic arborization, six GAD-GFP expressing interneurons per animal and region were randomly selected (Fig. 1). Z-series of optical sections (0.8 μm step size; 40× objective) covering the dendritic tree of selected interneurons were obtained using the sequential scanning mode. To be suitable for analysis, these interneurons had to fulfill the following features: (1) the cell must not show any truncated dendrites, (2) the dendritic arbor of the cell must show at least a process with a

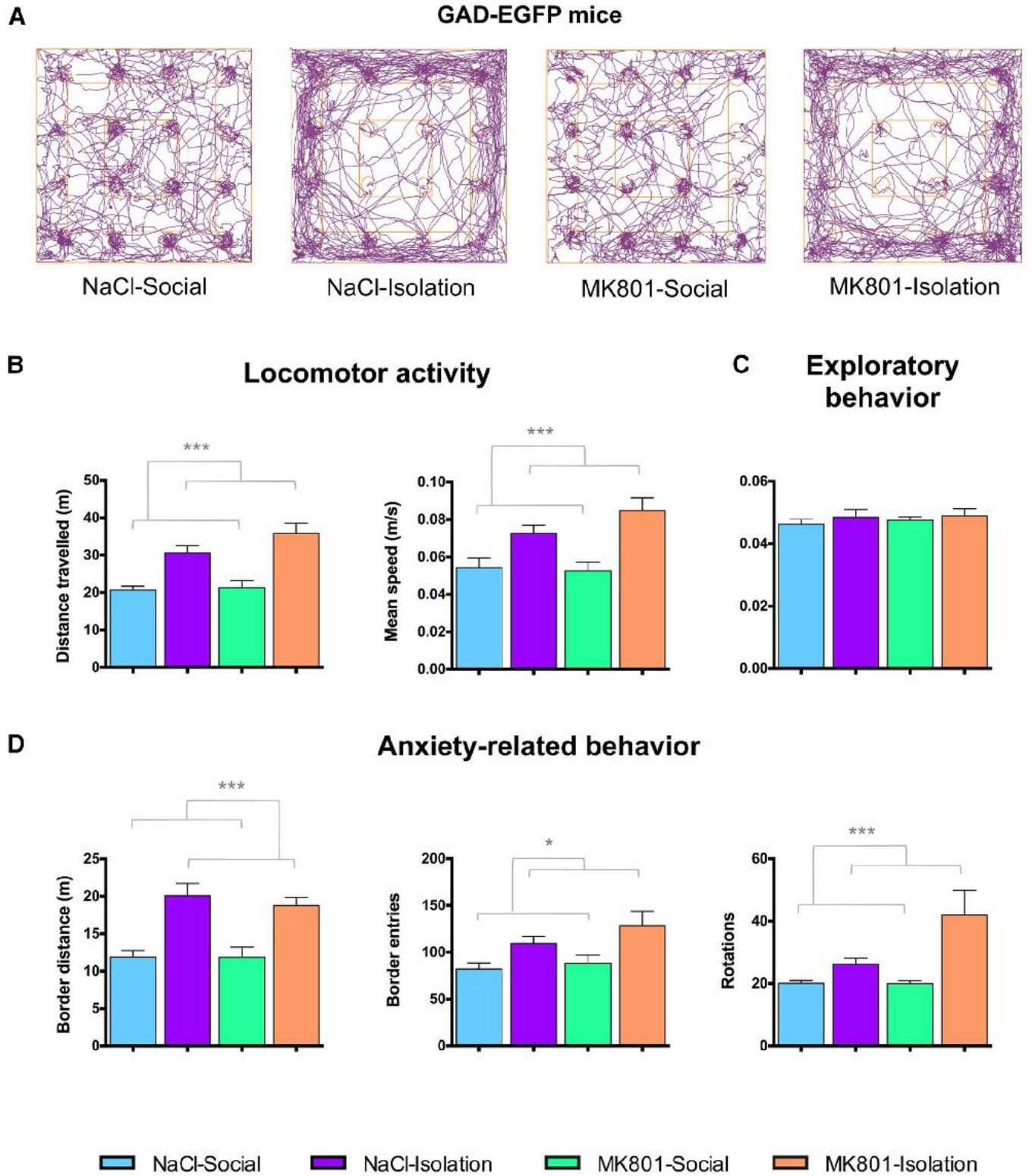

Figure 2. Behavioral analysis of GAD-EGFP expressing mice. ***A***, Representative track-plot reports recorded during the hole-board test session (ANY-maze). Observe the increased distance traveled (purple line) in the two groups subjected to post-weaning isolation, especially in the border of the apparatus. Social isolation rearing increased locomotor activity (***B***) and anxiety-related behavior (***D***) but did not change exploratory behavior (number of head dips into novel holes/total number of head dips; ***C***). Gray lines in graphs (***B–D***) represent statistically significant effects of rearing in a two-way ANOVA. $*p < 0.05$, $**p < 0.01$, $***p < 0.001$.

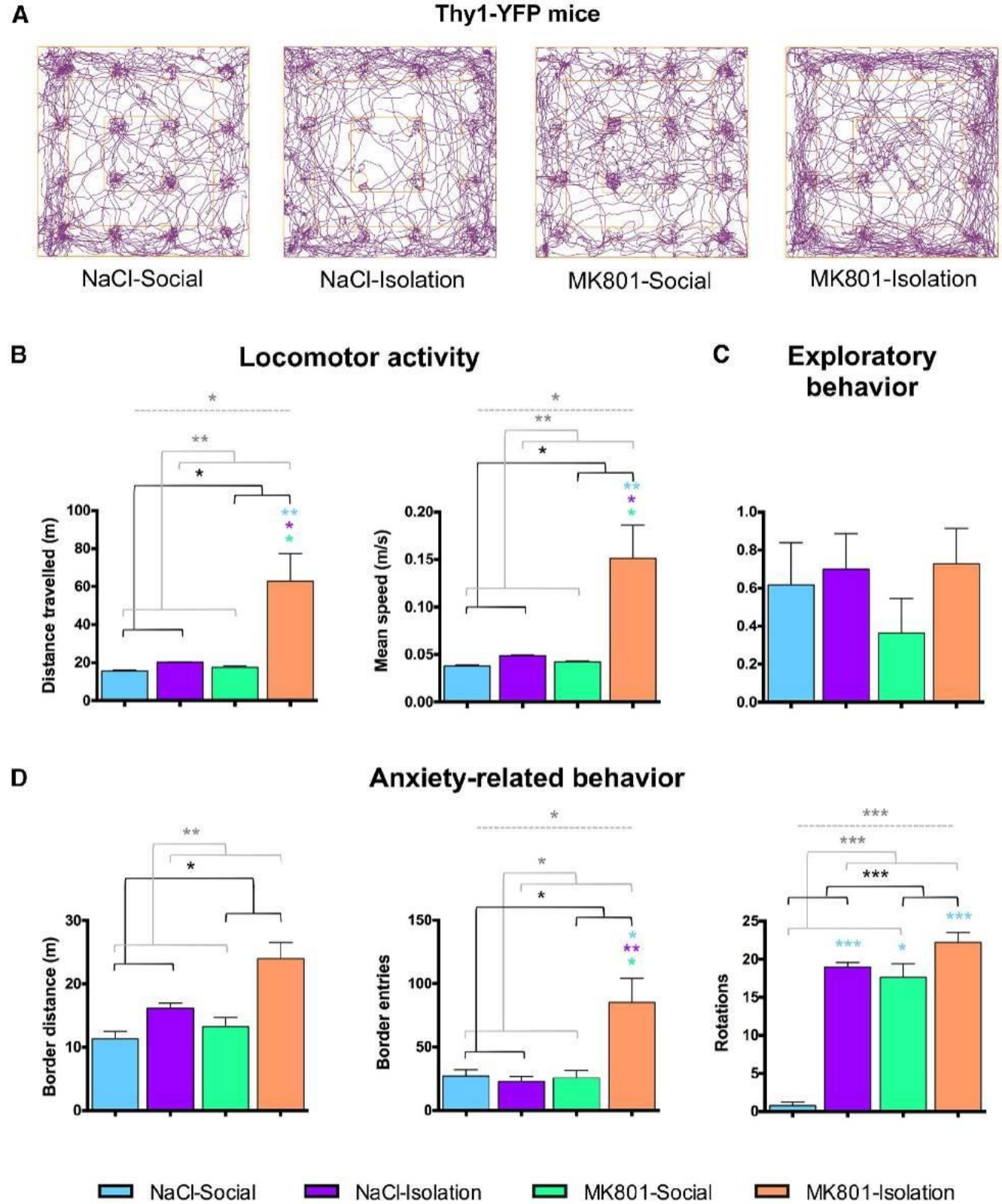

Figure 3. Behavioral analysis of Thy1-YFP expressing mice. ***A***, Representative track-plot reports showing the increased distance traveled (purple line) of double-hit mice (MK801-Isolation group) in the hole-board test compared with the other groups. Double-hit mice showed increased locomotor activity (***B***) and anxiety-related behavior (***D***) but no changes in exploratory behavior (number of head dips into novel holes/total number of head dips; ***C***). ***B–D***, Horizontal lines in graphs represent statistically significant effects of MK801 treatment (black), rearing (gray), or interaction (gray, dashed) in a two-way ANOVA. $*p < 0.05$, $**p < 0.01$, $***p < 0.001$. Colored symbols in bars represent trends and statistically significant differences among groups after *post hoc* analysis: # $0.1 > p > 0.05$, $*p < 0.05$, $**p < 0.01$, $***p < 0.001$.

length >150 μm, and (3) the soma must be located at least 30 μm deep from the surface of the tissue. The stacks obtained were then processed using FIJI (ImageJ, NIH) software to render 3D reconstructions. Neurons were traced using the "Simple neurite tracer" plugin, which also allowed us to analyze their Sholl profile in 3D (Longair et al. 2011; Fig. 1). The Sholl analysis consists on the measure of the number of intersections of the dendrites with spheres of increasing radius centered in the soma. The separation among the spheres of the analysis was set at 20 μm. For each animal, mean ± SEM was calculated and statistics were performed using the number of animals and the sample number (*n*; see below).

For the analysis of dendritic spines, six GAD-GFP expressing interneurons and six THY1-YFP expressing pyramidal neurons per animal and region were randomly selected (Fig. 1). A 63× oil immersion objective and a 3.5× additional digital zoom were used to observe the first 150 μm of the dendrite in the case of interneurons and the first 200 μm of the dendrite in the case of pyramidal neurons in segments of 50 μm (Z-step size of 0.38 μm). Dendrites within EGFP- and YFP-positive interneurons were randomly selected, but they had to meet the following criteria to be included in the study: (1) their length should be at least 150 μm (for interneurons) or 200 μm (for pyramidal neurons), and (2) no other dendrites should be found crossing their trajectory. For interneurons, data were expressed as the total number of spines in the proximal (0–50 μm), medial (50–100 μm), and distal (100–150 μm) segments of the dendrite, depending on its distance from the soma. For pyramidal neurons, four segments were established: proximal (0–50 μm), medial (50–100 μm), medial-distal (100–150 μm), and distal (150–200 μm). The total number of spines in every dendrite (sum of the spines in the entire segment) was also analyzed. For each animal, mean ± SEM was calculated and statistics were performed using the number of animals and the sample number (*n*; see below).

Analysis of VGLUT1 and VGAT Puncta Density in the Neuropil and Calculation of the E/I Ratio

The images used for the analysis of neuropil puncta expressing inhibitory (VGAT) or excitatory (VGLUT1) markers were obtained with a confocal microscope (Olympus FV-10). We analyzed layer 5 of the different regions of the PFC (infralimbic, prelimbic, dorsal cingulate, and ventral cingulate cortices). In the amygdala, the five nuclei were analyzed (central, lateral, medial, basolateral, and basomedial). Confocal *z*-stacks covering the whole depth of the sections were taken with 1 μm step size and only subsets of confocal planes with the optimal penetration level for each antibody were selected. On these planes, small regions of the neuropil (505 μm^2) were selected for analysis to avoid blood vessels and cell somata. Images were processed using FIJI/ImageJ software as described (Guirado et al. 2012): the background was subtracted with rolling value of 50, converted to 8-bit deep images and binarized using a determined threshold value. This value depended on the marker and the area analyzed and was kept the same for all images with the same marker and area. Then, the images were processed with a blur filter to reduce noise and to separate closely apposed puncta. Finally, the number of the resulting dots per region was counted. The E/I ratio was calculated as the density of VGLUT1 expressing puncta divided by the density of inhibitory VGAT expressing puncta. For each animal, mean ± SEM was calculated and statistics were performed using the number of animals and the sample number (*n*; see below).

Estimation of the Total Number of PV-Expressing Neurons, PNN, and PV-PNN Colocalization

The total number of PV-expressing (PV+) neurons, PNNs, and PV+ neurons surrounded by PNNs from the different nuclei/regions of the amygdala and PFC were estimated using a modified version of the fractionator method (West, 1993; Nacher et al. 2002). That is, within each 50-μm-thick section of one from the six systematic-random series of sections, all labeled cells covering the 100% of the sample area were counted. The images used for the analysis were obtained with a confocal microscope (Olympus FV-10) and processed afterward using FIJI/ImageJ software. For each animal, mean ± SEM was calculated and statistics were performed using the number of animals as the sample number (*n*; see below).

Sample Preparation for Molecular Studies

A total of 32 mice encompassing the four experimental groups (GIN molecular set of mice) were used for protein and gene expression analyses. Mice were sacrificed by decapitation at P90 under deep anesthesia with sodium pentobarbital. Their brains were quickly removed from the skull and the amygdala and PFC from both hemispheres were microdissected and immediately frozen in liquid nitrogen. The samples from one of the hemispheres of every animal were processed for protein extraction and the samples from the other hemisphere for mRNA extraction (Fig. 1).

For protein extraction, tissue was homogenized in 50 μl of lysis buffer using a TissueLyser (Qiagen) and Tungsten carbide beads for 5 min at 50 Hz/s and 4°C. Lysis buffer was made solving one pill of protease inhibitor cocktail (Ref. 04693124001, Roche Applied Science) in 1 ml of PBS-1% Triton X-100. Samples were afterward centrifuged at 16000 × *g* and 4°C for 4 min and supernatant was assessed for the total amount of protein using Bradford reagent at 595 nm with bovine serum albumin as the standard (Sigma-Aldrich).

Total mRNA was extracted from the tissue using Tri-Pure reagent (Roche Applied Science) and following the manufacturer's instructions. The concentration and purity of total RNA was determined with an Eppendorf BioPhotometer Plus (Eppendorf AG). cDNA synthesis was performed using the Expand Reverse Transcriptase (Roche Applied Science) and oligo-dT primers.

Protein Expression

Quantitative immunoblotting of synaptophysin and GAD67

Twenty micrograms of total protein from each sample was separated on 10% SDS–PAGE and transferred to Hybond enhanced chemiluminescence (ECL) nitrocellu-

Table 1. Sequences of gene specific primers and associated amplicon lengths for qRT-PCR

Target gene	Primers	Sequence (5′ → 3′)	Amplicon size*
GAD67	Forward	CTGGAGCTGGCTGAATACCT	120
	Reverse	TCGGAGGCTTTGTGGTATGT	
BDNF	Forward	GGTTCGAGAGGTCTGACGAC	159
	Reverse	CAAAGGCACTTGACTGCTGA	
ErbB4	Forward	CAGTCGCCCAGGGTGCAACG	133
	Reverse	GCGAACACTGTGGGGTCGGC	
CB1-R	Forward	TGTCCCTCACCCTGGGCACC	134
	Reverse	TCCCAGGAGATCGGCCACCG	
ST8SiaII	Forward	GGCAACTCAGGAGTCTTGCT	123
	Reverse	GTCAGTCTTGAGGCCCACAT	
ST8SiaIV	Forward	CCTTCATGGTCAAAGGAGGA	125
	Reverse	CCTTCATGGTCAAAGGAGGA	
Ywhaz	Forward	TTGAGCAGAAGACGGAAGGT	136
	Reverse	GAAGCATTGGGGATCAAGAA	

*Amplicon length in base pairs.

lose membranes (GE Healthcare). After saturation of nonspecific sites with blocking buffer (5% nonfat dry milk in PBS-0.025%Tween 20, overnight, 4°C), membranes were probed for 2 h at room temperature with primary antibodies against synaptophysin (1:5000, Sigma-Aldrich), GAD67 (1:1000, Merck-Millipore) or the control protein α-tubulin (1:5000, Sigma-Aldrich), all of them diluted in blocking buffer. After washing with PBS-0.025%Tween 20, membranes were incubated for 2 h with the appropriate secondary horseradish peroxidase-linked antibodies (1:2500, Sigma-Aldrich), and finally developed using ECL detection reagents (Thermo Scientific). Bands were detected using ImageQuant LAS4000 system (GE Health care) and densitometry analysis on every band was calculated using FIJI/ImageJ software (NIH). Synaptophysin and GAD67 densitometry values were normalized to within-lane α-tubulin. Every sample was immunoblotted in duplicate and mean ± SEM was then calculated. Statistics were performed using the number of animals as the sample number (*n*).

ELISA for PSA-NCAM assessment

PSA-NCAM protein levels were quantified in the same samples that were used for synaptophysin and GAD67 quantification, by performing commercially available ELISA kits (Eurobio/AbCys). A total volume of 100 μl of each sample was loaded at a concentration of 4 μg/ml per well in duplicates. PSA-NCAM levels (ng PSA/μg of total protein) were calculated according to the manufacturer's protocol. Statistics were performed using the number of animals and the sample number (*n*).

Gene Expression

qRT-PCR analyses were performed in triplicate. Specific primers for all genes (Table 1) at a concentration of 240 nM, and 4 μl of cDNA (50 ng) were used. Primers were designed between exons to avoid genomic DNA contamination when possible. *Ywhaz* was used as a reference gene based on the study of Bonefeld et al. (2008). Primers were tested for nonspecific amplification and for the correct amplicon size by electrophoresis in 1.5% agarose gel. qPCR was conducted with the ABI PRISM 7700 Sequence Detector (Applied Biosystems) using SYBR Green PCR master mix (Applied Biosystems), following a 95°C denaturation for 10 min. The reactions were cycled 40 times with a 95°C denaturation for 15 s, and a 60°C annealing step for 1 min. After this, a melt curve was performed to assess the specificity of primers.

Relative quantification was performed using the comparative threshold (C_t) method according to the $2^{-\Delta\Delta Ct}$ method (Pfaffl, 2001). Changes in gene expression were reported as fold-change relative to controls and the statistics were performed as described below.

Statistics

Group differences in all our studies were assessed using two-way ANOVA with the number of animals as the sample number (*n*). When interaction between treatment (MK801 vs vehicle) and rearing (social vs isolation) was statistically significant ($p < 0.05$), multiple pairwise comparisons between groups (Tukey HSD or Games–Howell *post hoc* analyses) were performed. Analysis were performed using the statistical package SPSS v22.0 (IBM) and graphs were created using GraphPad Prism 6. Data in the figures are expressed as mean ± SEM and $p < 0.05$ are indicated.

Results

Increased Locomotion and Anxiety-Related Behavior

Early-life stress induced hyperlocomotion and increased anxiety-related behavior in GIN mice, whereas exploratory behavior was not affected (Fig. 2; Table 2). Specifically, double-hit animals (MK801-Isolation) and isolated animals showed increased distance traveled, speed, number of body rotations, and thigmotaxis (increased distance traveled in the periphery zone of the apparatus and increased number of entries to this zone; Fig. 2*B–D*). Similar results were found when analyzing the behavior of THY1 mice, but in this case, specific significant increases were found in most of the parameters measured for locomotor activity (Fig. 3*A*,*B*) and anxiety-related behavior (Fig. 3*D*) when comparing double-hit to control mice. Exploratory behavior was also not affected in this strain (Fig. 3*C*). Detailed information on statistical tests can be found in Table 2.

Table 2. Summary of results (part I)

Parameter	Main effects (two-way ANOVA) Treatment	Rearing	Interaction	Group differences (from NaCl-Social) NaCl-Isolation	MK801-Social	MK801-Isolation
Behavior (Figs. 2, 3)						
Locomotor activity						
Total distance travelled						
Gad-EGFP mice	—	✓(1)	—	n/a	n/a	n/a
Thy1-YFP mice	✓(2)	✓(3)	✓(4)	—	—	↑ **
Mean speed						
Gad-EGFP mice	—	✓(5)	—	n/a	n/a	n/a
Thy1-YFP mice	✓(6)	✓(7)	✓(8)	—	—	↑ **
Anxiety-related behavior						
Border distance						
Gad-EGFP mice	—	✓(9)	—	n/a	n/a	n/a
Thy1-YFP mice	✓(10)	✓(11)	—	n/a	n/a	n/a
Border entries						
Gad-EGFP mice	—	✓(12)	—	n/a	n/a	n/a
Thy1-YFP mice	✓(13)	✓(14)	✓(15)	—	—	↑ *
Body rotations						
Gad-EGFP mice	—	✓(16)	—	n/a	n/a	n/a
Thy1-YFP mice	✓(17)	✓(18)	✓(19)	↑ ***	↑ *	↑ ***
Exploratory behavior						
Gad-EGFP mice	—	—	—	n/a	n/a	n/a
Thy1-YFP mice	—	—	—	n/a	n/a	n/a
Brain volume (Fig. 4)						
Amygdala						
Total volume	—	—	#(20)	n/a	n/a	n/a
Central	—	—	✓(21)	↑ *	—	—
Lateral	—	—	—	n/a	n/a	n/a
Basolateral	—	✓(22)	—	n/a	n/a	n/a
Basomedial	✓(23)	—	—	n/a	n/a	n/a
Medial	—	—	—	n/a	n/a	n/a
PFC						
Total volume	—	#(24)	—	n/a	n/a	n/a
IL	—	#(25)	—	n/a	n/a	n/a
PrL	—	—	—	n/a	n/a	n/a
Cg1	✓(26)	—	✓(27)	—	—	↓ #
Cg2	—	—	—	n/a	n/a	n/a

Symbols: (✓) statistically significant effect (two-way ANOVA); (—) no statistically significant effect (two-way ANOVA) or difference from NaCl-Social group (*post hoc*); (↑) increase; (n/a) not applicable; (↓) decrease; $*p < 0.05$; $**p < 0.01$; $***p < 0.001$; #$0.10 \geq p \geq 0.05$.
F and *p* values: (1) $F_{(1,58)} = 31.11$, $p < 10^{-6}$; (2) $F_{(1,11)} = 8.05$, $p = 0.016$; (3) $F_{(1,11)} = 9.99$, $p = 0.009$; (4) $F_{(1,11)} = 6.74$, $p = 0.025$; (5) $F_{(1,59)} = 19.38$, $p = 4.6 \times 10^{-5}$; (6) $F_{(1,11)} = 7.80$, $p = 0.018$; (7) $F_{(1,11)} = 9.90$, p = 0.009; (8) $F_{(1,11)} = 6.61$, $p = 0.026$; (9) $F_{(1,59)} = 36.48$, $p < 10^{-7}$; (10) $F_{(1,11)} = 8.22$, $p = 0.015$; (11) $F_{(1,11)} = 20.68$, $p = 0.001$; (12) $F_{(1,60)} = 6.20$, $p = 0.016$; (13) $F_{(1,11)} = 7.48$, $p = 0.019$; (14) $F_{(1,11)} = 6.11$, $p = 0.031$; (15) $F_{(1,11)} = 8.27$, $p = 0.015$; (16) $F_{(1,60)} = 5.14$, $p = 0.027$; (17) $F_{(1,11)} = 93.50$, $p = 10^{-5}$; (18) $F_{(1,11)} = 119.86$, $p < 10 - 6$; (19) $F_{(1,11)} = 42.94$, $p = 4.1 \times 10^{-5}$; (20) $F_{(1,20)} = 3.34$, $p = 0.082$; (21) $F_{(1,21)} = 4.73$, $p = 0.041$; (22) $F_{(1,21)} = 9.44$, $p = 0.0058$; (23) $F_{(1,21)} = 5.82$, $p = 0.025$; (24) $F_{(1,23)} = 3.39$, $p = 0.079$; (25) $F_{(1,23)} = 3.61$, $p = 0.07$; (26) $F_{(1,22)} = 5.062$, $p = 0.035$; (27) $F_{(1,22)} = 6.62$, $p = 0.017$.

Alterations in the Volume of Amygdala and PFC

We have performed volumetric analyses to test whether the different interventions result in changes in the volumes of the amygdala and the PFC, as some studies have described in schizophrenic patients (Jaaro-Peled et al. 2010; Levitt et al. 2010; Fig. 4). Rearing in social isolation increased the volume of the BLA (Fig. 4*B*,*C*) and induced a trend toward an increase in the volume of the infralimbic (IL) cortex (Fig. 4*D*,*E*). By contrast, MK-801 treatment decreased the volume of the basomedial amygdala (BMA) (Fig. 4*B*,*C*) and the cingulate 1 (Cg1) cortex (Fig. 4*D*,*E*). A significant effect of the interaction of both interventions could also be observed in the central (Ce) nuclei of the amygdala (Fig. 4*B*,*C*) and the Cg1 cortex (Fig. 4*D*,*E*). When performing *post hoc* analyses, the isolated group of animals showed a significant increase in the volume of the Ce amygdala compared with the control group and double-hit mice showed a significant decrease in the volume of the Cg1 cortex compared with isolated or MK-801-treated animals (Fig. 4*C*,*E*; Table 2).

Structural Alterations of E/I Neurons

Because these changes in the volume of the different regions studied could be due to changes in the structure of neurons, particularly of dendritic remodeling, we first analyzed spine density in PFC pyramidal neurons. Unfortunately, the characteristics of the strain (Porrero et al. 2010) do not allow for the analysis of dendritic arborization in these PFC neurons or any type of structural analysis in amygdaloid excitatory neurons. Treatment, rearing and their interaction affected the density of spines in different dendritic segments of pyramidal neurons in the PFC (Table 3). There was a decrease in the density of spines in the whole length of the dendrite, in double-hit mice compared with controls, but it was considered

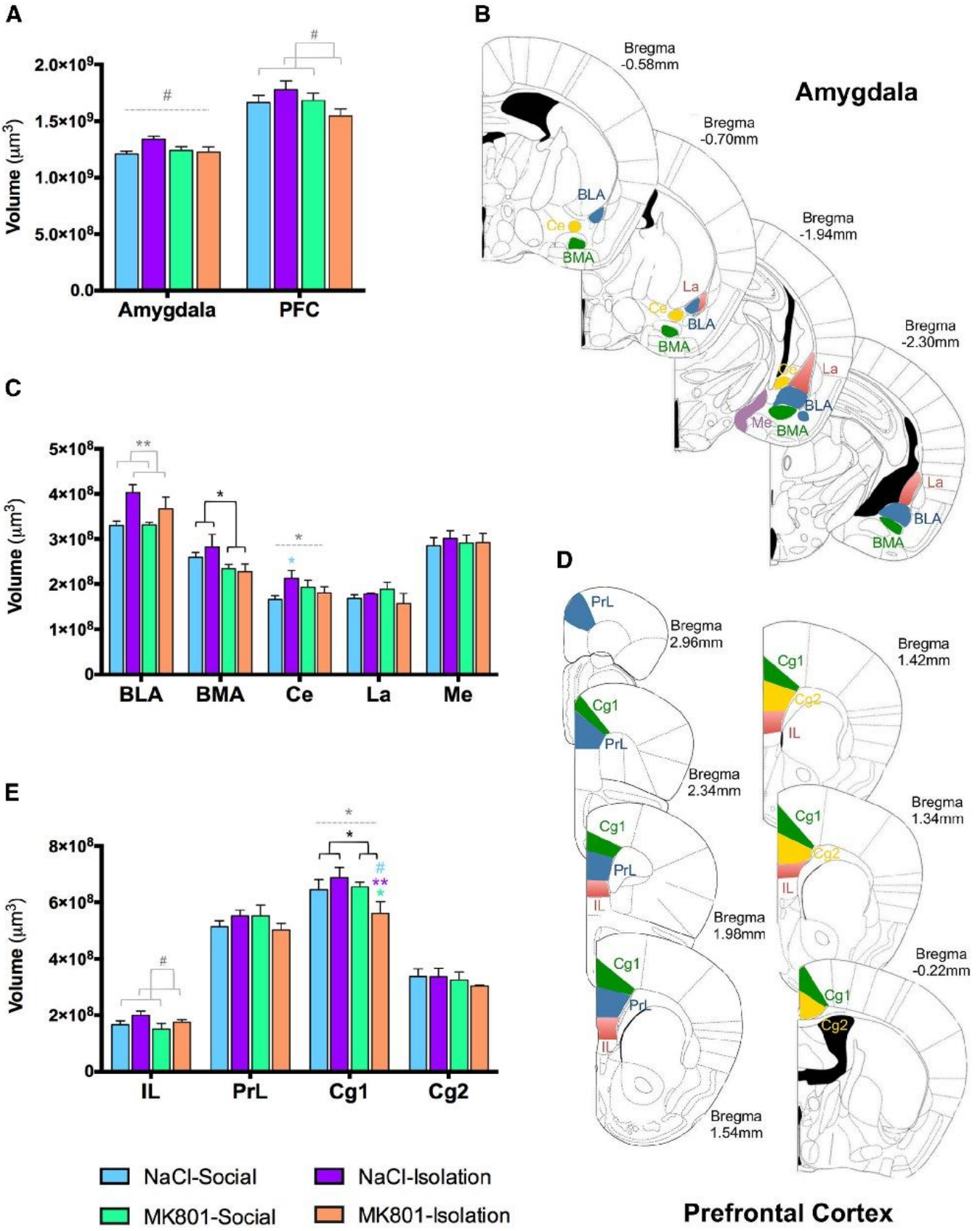

Figure 4. Volumetric analysis. Treatment, rearing, and the interaction of both treatments influenced the volume of the amygdala and the PFC. Although the total volume of both regions was not significantly affected (***A***), the volume of some nuclei of the amygdala (***B***, ***C***) and some regions of the PFC (***D***, ***E***) was affected by treatment (BMA, Cg1), rearing (BLA, IL), or their interaction (Ce, Cg1). Horizontal

continued

lines in graphs represent trends and statistically significant effects of MK801 treatment (black), rearing (gray), or interaction (gray, dashed) in a two-way ANOVA. # $0.1 > p > 0.05$, $*p < 0.05$, $**p < 0.01$, $***p < 0.001$. Colored symbols in bars represent trends and statistically significant differences among groups after *post hoc* analysis: # $0.1 > p > 0.05$, $*p < 0.05$, $**p < 0.01$, $***p < 0.001$. ***B***, ***D***, Schematic representations of the regions that were measured in our volumetric study (amygdala: all brain slices from bregma −0.58 to −2.30 mm; PFC: all brain slices from bregma +2.96 to −0.22 mm).

Table 3. Summary of results (part II)

	Main effects (two-way ANOVA)			Group differences (from NaCl-Social)		
Parameter	Treatment	Rearing	Interaction	NaCl-Isolation	MK801-Social	MK801-Isolation
Structure of pyramidal neurons (Fig. 5)						
Dendritic spines						
PFC						
50	—	—	✓(28)	—	—	—
100	—	—	—	n/a	n/a	n/a
150	—	✓(29)	—	n/a	n/a	n/a
200	✓(30)	—	—	n/a	n/a	n/a
Total	—	—	—	n/a	n/a	n/a
Structure of interneurons (Fig. 6)						
Dendritic arborization						
Amygdala						
20	—	#(31)	✓(32)	—	—	—
40	—	✓(33)	✓(34)	—	—	↑*
60	✓(35)	✓(36)	✓(37)	—	—	↑***
80	✓(38)	✓(39)	✓(40)	—	—	↑*
100	✓(41)	✓(42)	#(43)	n/a	n/a	n/a
120	✓(44)	✓(45)	✓(46)	—	—	↑*
140	#(47)	—	—	n/a	n/a	n/a
160	—	—	—	n/a	n/a	n/a
Total	✓(48)	✓(49)	✓(50)	—	—	↑***
PFC						
20	—	—	—	n/a	n/a	n/a
40	—	—	—	n/a	n/a	n/a
60	—	—	—	n/a	n/a	n/a
80	—	—	—	n/a	n/a	n/a
100	—	—	—	n/a	n/a	n/a
120	—	—	—	n/a	n/a	n/a
140	—	—	—	n/a	n/a	n/a
160	—	—	—	n/a	n/a	n/a
Total	—	—	—	n/a	n/a	n/a
Dendritic spines						
Amygdala						
50	—	—	—	n/a	n/a	n/a
100	—	—	—	n/a	n/a	n/a
150	—	#(51)	#(52)	n/a	n/a	n/a
Total	—	—	—	n/a	n/a	n/a
PFC						
50	#(53)	✓(54)	#(55)	n/a	n/a	n/a
100	✓(56)	✓(57)	✓(58)	↑*	↑**	↑**
150	✓(59)	✓(60)	—	n/a	n/a	n/a
Total	✓(61)	✓(62)	✓(63)	↑**	↑***	↑***

Symbols: (✓) statistically significant effect (two-way ANOVA); (—) no statistically significant effect (two-way ANOVA) or difference from NaCl-Social group (*post hoc*); (↑) increase; (n/a) not applicable; (↓) decrease; $*p < 0.05$; $**p < 0.01$; $***p < 0.001$; #$0.10 \geq p \geq 0.05$.

F and *p* values: (28) $F_{(1,15)} = 6.29$, $p = 0.024$; (29) $F_{(1,15)} = 4.88$, $p = 0.043$; (30) $F_{(1,18)} = 4.90$, $p = 0.043$ (31) $F_{(1,19)} = 3.81$, $p = 0.066$; (32) $F_{(1,19)} = 4.72$, $p = 0.043$; (33) $F_{(1,19)} = 9.02$, $p = 0.007$; (34) $F_{(1,19)} = 12.58$, $p = 0.002$; (35) $F_{(1,18)} = 7.53$, $p = 0.013$; (36) $F_{(1,18)} = 23.53$, $p = 12.8 \times 10^{-5}$; (37) $F_{(1,18)} = 12.62$, $p = 0.002$; (38) $F_{(1,19)} = 4.64$, $p = 0.044$; (39) $F_{(1,19)} = 6.55$, $p = 0.019$; (40) $F_{(1,19)} = 10.23$, $p = 0.005$; (41) $F_{(1,20)} = 4.43$, $p = 0.048$; (42) $F_{(1,20)} = 8.79$, $p = 0.008$; (43) $F_{(1,20)} = 3.27$, $p = 0.086$; (44) $F_{(1,20)} = 5.73$, $p = 0.027$; (45) $F_{(1,20)} = 5.32$, $p = 0.032$; (46) $F_{(1,20)} = 14.63$, $p = 0.0011$; (47) $F_{(1,20)} = 4.34$, $p = 0.050$; (48) $F_{(1,20)} = 8.31$, $p = 0.009$; (49) $F_{(1,20)} = 14.29$, $p = 0.001$; (50) $F_{(1,20)} = 18.23$, $p = 37.5 \times 10^{-5}$; (51) $F_{(1,22)} = 3.79$, $p = 0.064$; (52) $F_{(1,22)} = 3.34$, $p = 0.081$; (53) $F_{(1,22)} = 3.74$, $p = 0.066$; (54) $F_{(1,22)} = 4.53$, $p = 0.045$; (55) $F_{(1,22)} = 3.31$, $p = 0.083$; (56) $F_{(1,22)} = 11.72$, $p = 0.002$; (57) $F_{(1,22)} = 5.50$, $p = 0.029$; (58) $F_{(1,22)} = 5.18$, $p = 0.033$; (59) $F_{(1,22)} = 5.50$, $p = 0.028$; (60) $F_{(1,22)} = 7.43$, $p = 0.012$; (61) $F_{(1,22)} = 21.08$, $p = 14.2 \times 10^{-5}$; (62) $F_{(1,22)} = 6.27$, $p = 0.020$; (63) $F_{(1,22)} = 10.18$, $p = 0.004$.

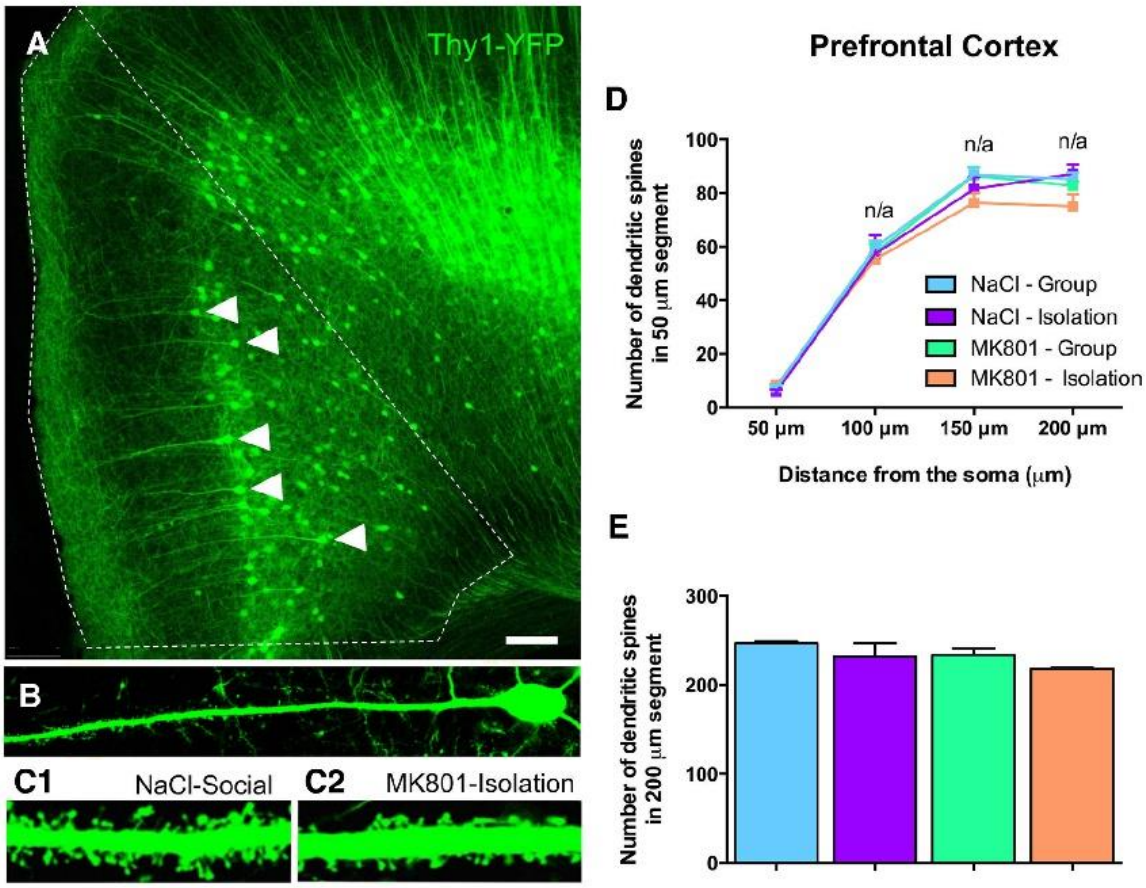

Figure 5. Structural analysis of pyramidal neurons. *A*, Panoramic view of the PFC of THY1-YFP expressing mice. Arrowheads point to fluorescent pyramidal neurons. ***B***, Representative confocal image of a pyramidal neuron from these animals. ***C1*** (NaCl-Group) and ***C2*** (MK801-Isolation) represent sections of the spiny apical dendrites of these pyramidal neurons. ***D***, ***E***, Graphs showing the results of the analysis of dendritic spine density. ***D***, The segmented analysis of the spine densities only showed a significant interaction effect in the first segment (0–50 μm of distance from the soma; Table 3) but no statistically significant differences among groups where observed after *post hoc* comparison. Despite the significant effects of treatment or rearing in some of the other segments (Table 3), the interaction (two-way ANOVA) was not significant in any of them and, therefore, *post hoc* comparisons were not applicable (n/a). ***E***, No statistical significant effects of treatment, rearing, or their interaction (two-way ANOVA) were observed when analyzing the spines density of the total length of the dendrite (200 μm). Scale bars: ***A***, 100 μm; ***B***, 20 μm; ***C1***, ***C2***, 2.5 μm.

nonsignificant because of the lack of interaction between factors (Fig. 5*E*).

Previous work from different laboratories has shown that the structure of interneurons is also susceptible to change in different paradigms, including chronic stress (Gilabert-Juan et al. 2011, 2013b). For this reason, we have also evaluated the structure of a subpopulation of these inhibitory neurons (Oliva et al. 2000). Treatment, rearing, and their interaction affected the total number of dendritic intersections in interneurons of the amygdala and the density of dendritic spines in interneurons of the PFC (Fig.6; Table 3). In particular, interneurons from double-hit mice showed significantly increased arborization in the amygdala (Fig.6*B1*,*B2*,*D*,*E*) and significantly increased density of dendritic spines in the PFC (Fig. 6*J1*,*J2*,*M*,*N*) compared with the control group.

Decreased E/I Ratio in the Amygdala but Increased in the PFC

To have another readout of the putative alterations in inhibitory networks and the balance of excitatory versus inhibitory neurotransmission, we have studied with immunohistochemistry the expression of the GABA and glutamate vesicular transporters (VGAT and VGLUT1). Almost all nuclei/regions of the amygdala and PFC showed significant effects of treatment, rearing, or their interaction when analyzing the density of VGLUT1 and VGAT expressing puncta and E/I ratio (Table 4). Regarding excitatory puncta (VGLUT1), double-hit animals showed increased density in the La and Me nuclei of the amygdala (Fig. 7*A1*,*A2*) but no changes in any of the regions of the PFC (Fig. 7*B1*,*B2*). These animals also showed decreased density of VGAT puncta in the Cg1-Cg2 region of the PFC (Fig. 7*B1*,*B3*). The E/I ratio was significantly increased in the PFC of double-hit animals (IL + PrL; (Fig. 7B4).

Expression of GAD67, SYN, and PSA-NCAM

The differences that we have found in the structure of interneurons and in the E/I ratio prompted us to study the expression of molecules related to inhibitory neurotransmission and to the plasticity of interneuronal networks, such as the polysialylated form of the neural cell adhesion

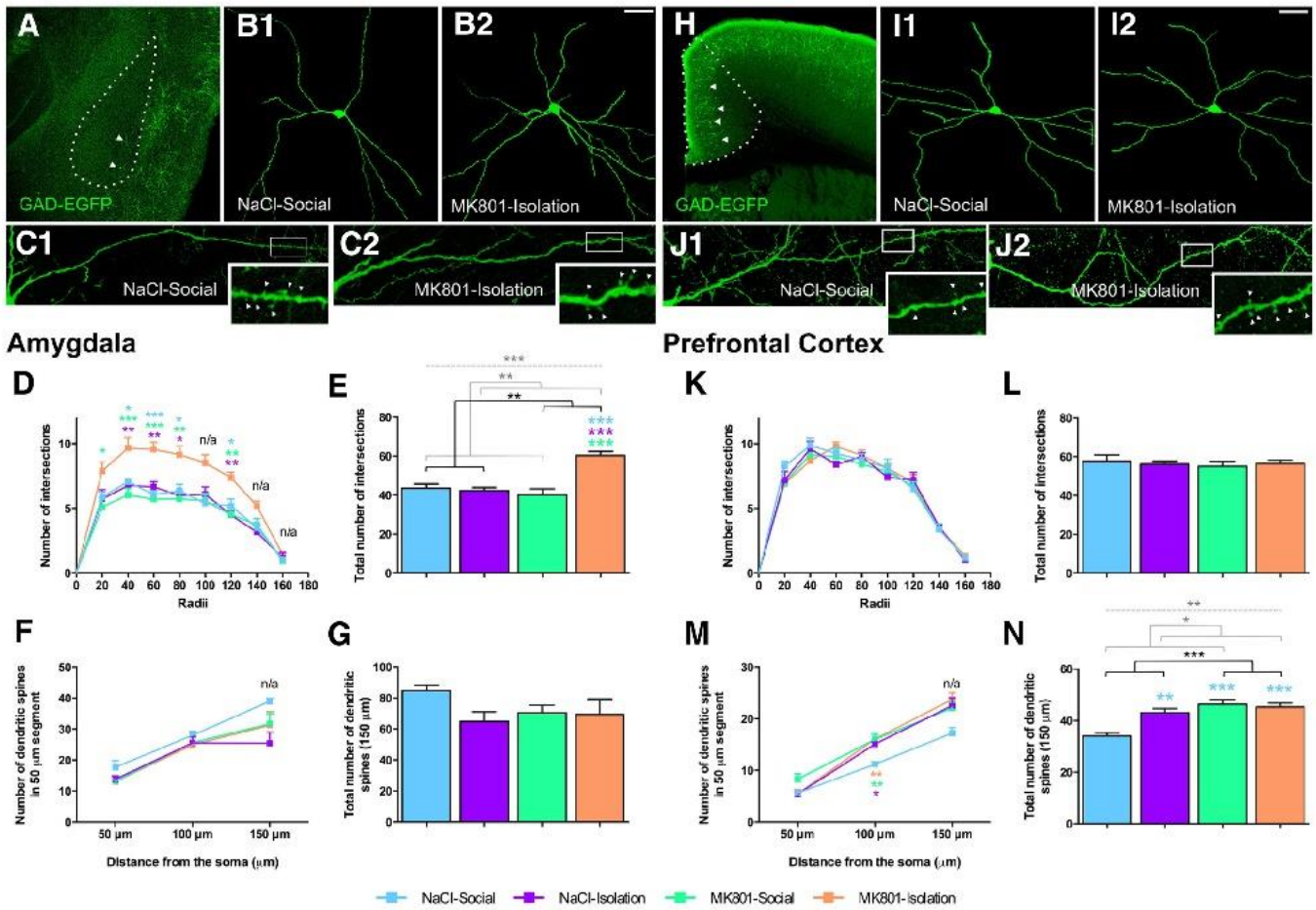

Figure 6. Structural analysis of interneurons. Panoramic view of the amygdala (***A***) and PFC (***H***) of GIN mice. ***B1***, ***B2***, ***I1***, ***I2***, Representative 3D reconstructions of the dendritic arbor of GAD-EGFP expressing interneurons. Double-hit mice showed increased dendritic arborization (number of intersections in the Sholl analysis) in interneurons form the amygdala (***D***, ***E***) but not from the PFC (***K***, ***L***). ***C1***, ***C2***, ***J1***, ***J2***, Representative images of spiny dendrites from GAD-EGFP expressing interneurons. Insets are magnified views of the squared sections of their respective images. Arrowheads point to dendritic spines. Analysis of the dendritic spines showed increased density in the PFC (***M***, ***N***) but not in the amygdala (***F***, ***G***) of double-hit mice. Horizontal lines in graphs (***E***, ***N***) represent statistically significant effects of MK801 treatment (black), rearing (gray), or interaction (gray, dashed) in a two-way ANOVA. $*p < 0.05$, $**p < 0.01$, $***p < 0.001$. Colored symbols (***D***, ***E***, ***M***, ***N***) represent statistically significant differences among groups after *post hoc* analysis: $*p < 0.05$, $**p < 0.01$, $***p < 0.001$. If the interaction (two-way ANOVA) was not significant, *post hoc* comparisons were not applicable (n/a). Scale bars: ***A***, ***H***, 800 μm; ***B***, ***I***, 40 μm; ***C***, ***J***, 14 μm; ***C***, ***J*** (insets), 2 μm.

molecule (PSA-NCAM; Nacher et al. 2013). GAD67 protein expression in the amygdala was significantly influenced by rearing (increased as a consequence of social isolation) but double-hit animals failed to show significant differences compared with the control group (Table 5; Fig. 8*A*). Synaptophysin (SYN) protein expression in both regions and GAD67 expression in the PFC were not affected by any experimental condition (Table 5; Fig. 8*A*,*B*). PSA-NCAM expression was influenced by rearing (decreased expression in the amygdala after social isolation) and treatment (after MK-801, increased expression in the amygdala and decreased expression in the PFC) but not by their interaction (Table 5; Fig. 8*B*,*D*).

Rearing Influences *BDNF, CB1-R*, and *St8SiaIV* Gene Expression

We have also studied the expression of different genes involved in the development and regulation of inhibitory networks, including the enzymes responsible for PSA synthesis. Among all the studied genes, a significant effect of rearing was found when studying BDNF (increased after social isolation) and ST8SiaIV mRNA expression (decreased after social isolation) in the PFC and CB1-R mRNA expression (increased after social isolation) in the amygdala (Table 5; Fig. 8*D–I*).

Number of PNNs and PV-Expressing Neurons Surrounded by PNNs

Different components of the extracellular matrix can play a role in the E/I imbalance and the remodeling of inhibitory networks observed in our study. Of particular interest are PNNs, which are abundant around PV-expressing interneurons (Härtig et al. 1992). The composition of these PNN is regulated dynamically in response to aversive experiences, such as fear or stress, and alterations in the expression of PNNs have been observed in the PFC of schizophrenic patients (Berretta et al. 2015). In our study, effects of treatment, isolation, and their inter-

Table 4. Summary of results (part III)

Parameter	Main effects (two-way ANOVA) Treatment	Rearing	Interaction	Group differences (from NaCl-Social) NaCl-Isolation	MK801-Social	MK801-Isolation
Density of neuropil puncta (Fig. 7)						
VGLUT1 (Amygdala)						
Central	—	—	—	n/a	n/a	n/a
Lateral	✓(64)	✓(65)	✓(66)	—	—	↑*
Basolateral	—	—	—	n/a	n/a	n/a
Basomedial	✓(67)	✓(68)	#(69)	n/a	n/a	n/a
Medial	#(70)	✓(71)	✓(72)	—	—	↑*
VGLUT1 (PFC)						
IL+PrL	—	—	—	n/a	n/a	n/a
Cg1+Cg2	✓(73)	✓(74)	#(75)	n/a	n/a	n/a
VGAT (Amygdala)						
Central	—	#(76)	—	n/a	n/a	n/a
Lateral	—	✓(77)	—	n/a	n/a	n/a
Basolateral	#(78)	#(79)	#(80)	n/a	n/a	n/a
Basomedial	#(81)	✓(82)	—	n/a	n/a	n/a
Medial	#(83)	✓(84)	#(85)	n/a	n/a	n/a
VGAT (PFC)						
IL+PrL	#(86)	#(87)	✓(88)	—	↑*	—
Cg1+Cg2	—	✓(89)	—	n/a	n/a	n/a
E/I Balance (Fig. 7)						
Amygdala						
Central	—	—	—	n/a	n/a	n/a
Lateral	#(90)	✓(91)	—	n/a	n/a	n/a
Basolateral	—	✓(92)	—	n/a	n/a	n/a
Basomedial	—	—	—	n/a	n/a	n/a
Medial	—	—	—	n/a	n/a	n/a
PFC						
IL+PrL	#(93)	✓(94)	✓(95)	—	—	↑*
Cg1+Cg2	✓(96)	✓(97)	—	n/a	n/a	n/a

Symbols: (✓) statistically significant effect (two-way ANOVA); (-) no statistically significant effect (two-way ANOVA) or difference from NaCl-Social group (*post hoc*); (↑) increase; (n/a) not applicable; (↓) decrease; $*p < 0.05$; $**p < 0.01$; $***p < 0.001$; #$0.10 \geq p \geq 0.05$.
F and p values: (64) $F_{(1,29)} = 4.58$, $p = 0.041$; (65) $F_{(1,29)} = 7.12$, $p = 0.012$; (66) $F_{(1,29)} = 4.20$, $p = 0.049$; (67) $F_{(1,28)} = 4.89$, $p = 0.036$; (68) $F_{(1,28)} = 6.08$, $p = 0.020$; (69) $F_{(1,28)} = 3.17$, $p = 0.086$; (70) $F_{(1,29)} = 3.74$, $p = 0.063$; (71) $F_{(1,29)} = 4.32$, $p = 0.047$; (72) $F_{(1,29)} = 5.01$, $p = 0.033$; (73) $F_{(1,19)} = 6.31$, $p = 0.021$; (74) $F_{(1,19)} = 8.44$, $p = 0.009$; (75) $F_{(1,19)} = 3.54$, $p = 0.075$; (76) $F_{(1,29)} = 3.45$, $p = 0.074$; (77) $F_{(1,28)} = 5.28$, $p = 0.029$; (78) $F_{(1,29)} = 3.09$, $p = 0.089$; (79) $F_{(1,29)} = 3.88$, $p = 0.058$; (80) $F_{(1,29)} = 2.91$, $p = 0.097$; (81) $F_{(1,29)} = 3.16$, $p = 0.086$; (82) $F_{(1,29)} = 4.29$, $p = 0.047$; (83) $F_{(1,29)} = 3.47$, $p = 0.073$; (84) $F_{(1,29)} = 5.88$, $p = 0.022$; (85) $F_{(1,29)} = 3.05$, $p = 0.091$; (86) $F_{(1,18)} = 3.75$, $p = 0.069$; (87) $F_{(1,18)} = 3.88$, $p = 0.065$; (88) $F_{(1,18)} = 6.53$, $p = 0.020$; (89) $F_{(1,19)} = 21.12$, $p = 2 \times 10^{-4}$; (90) $F_{(1,29)} = 3.55$, $p = 0.070$; (91) $F_{(1,29)} = 9.01$, $p = 0.005$; (92) $F_{(1,28)} = 6.75$, $p = 0.015$; (93) $F_{(1,18)} = 3.93$, $p = 0.063$; (94) $F_{(1,18)} = 6.18$, $p = 0.023$; (95) $F_{(1,18)} = 6.39$, $p = 0.021$; (96) $F_{(1,18)} = 10.72$, $p = 0.004$; (97) $F_{(1,18)} = 8.33$, $p = 0.0098$.

action were found in different regions of the mPFC and the amygdala. Specifically, in the infralimbic cortex, both isolated, and especially MK-801-treated animals, showed a significant increase in the number of PV-expressing neurons, PNNs, and PV-expressing neurons surrounded by PNNs (only MK-801; Table 6; Fig. 9). By contrast, in this region there was a tendency for a decrease in these parameters in the double-hit mice.

Discussion

In the present study, we report alterations in behavior, neuronal structural plasticity, and E/I neurotransmission in mice subjected to chronic early-life stress, consisting in a social isolation rearing from the age of weaning until adulthood. A group of animals (double-hit) was also subjected to a perinatal injection of the NMDAR antagonist MK801 to interfere with the last stages of neocortical development: the activation of the NMDA receptor is essential for neuronal differentiation, migration, and survival (Jansson and Åkerman, 2014) and perinatal treatments with NMDAR antagonists trigger apoptosis, specially in the frontal neocortex (Ikonomidou et al. 1999; Wang and Johnson, 2005).

Both interventions, isolation and MK801 treatment, have been considered animal models for schizophrenia. We have found that, especially, the isolation rearing induces a wide spectrum of alterations, including changes in neurochemical, behavioral, and structural parameters. These changes affect particularly interneurons and some of them are significant when this aversive experience is combined with the neurodevelopmental intervention. These effects are the consequence of prolonged isolation stress during a period in which the circuits are already stablished, although they still display a high degree of plasticity. Alterations on the structure and neurotransmission of interneurons can be induced even in young-adult animals when they are subjected to chronic stress (Gilabert-Juan et al. 2011). By contrast, the single injection of MK801 in P7 is a procedure that disturbs acutely ongoing neurodevelopmental processes, particularly in the frontal cortex, such as neuronal migration, neurite extension, or synaptogenesis. This is an important time

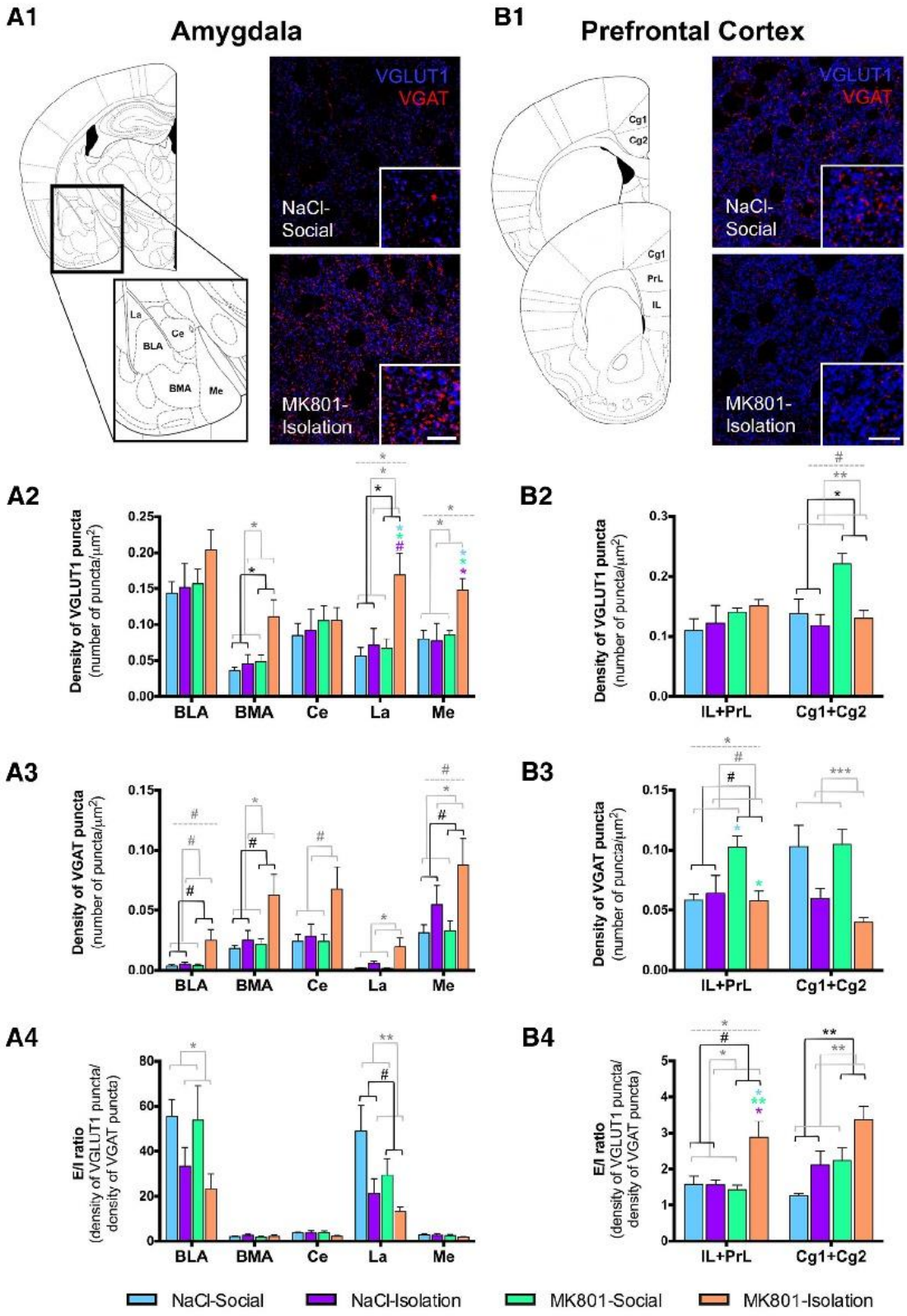

Figure 7. Excitatory and inhibitory neurotransmission. Schematic view of all the analyzed regions (***A1***, amygdala; ***B1***, PFC). Right, Representative confocal images of excitatory (blue, VGLUT1) and inhibitory (red, VGAT) puncta in the neuropil of NaCl-Social and MK801-Isolated animals. Scale bars: images, 16 μm; insets, 6 μm. Significant differences in VGLUT1 puncta density (***A2***, ***B2***), VGAT puncta density (***A3***, ***B3***), and E/I ratio (***A4***, ***B4***) among groups were observed. Horizontal lines in graphs represent trends and statistically significant effects of MK801 treatment (black), rearing (gray), or interaction (gray, dashed) in a two-way ANOVA. # $0.1 > p > 0.05$, $*p < 0.05$, $**p < 0.01$, $***p < 0.001$. Colored symbols in bars represent trends and statistically significant differences among groups after *post hoc* analysis: # $0.1 > p > 0.05$, $*p < 0.05$, $**p < 0.01$, $***p < 0.001$.

Table 5. Summary of results (part IV)

Parameter	Main effects (two-way ANOVA) Treatment	Rearing	Interaction	Group differences (from NaCl-Social) NaCl-Isolation	MK801-Social	MK801-Isolation
Protein expression (Fig.7)						
GAD67						
Amygdala	—	✓(98)	—	n/a	n/a	n/a
PFC	—	—	—	n/a	n/a	n/a
SYN						
Amygdala	—	—	—	n/a	n/a	n/a
PFC	—	—	—	n/a	n/a	n/a
PSA-NCAM						
Amygdala	✓(99)	✓(100)	#(101)	n/a	n/a	n/a
PFC	✓(102)	—	—	n/a	n/a	n/a
Gene expression (Fig.7)						
GAD67						
Amygdala	—	—	—	n/a	n/a	n/a
PFC	#(103)	—	—	n/a	n/a	n/a
BDNF						
Amygdala	—	—	—	n/a	n/a	n/a
PFC	—	✓(104)	—	n/a	n/a	n/a
ErbB4						
Amygdala	—	—	#(105)	n/a	n/a	n/a
PFC	—	—	—	n/a	n/a	n/a
CB1-R						
Amygdala	—	✓(106)	—	n/a	n/a	n/a
PFC	—	—	—	n/a	n/a	n/a
ST8SiaII						
Amygdala	#(107)	—	—	n/a	n/a	n/a
PFC	—	—	—	n/a	n/a	n/a
ST8SiaIV						
Amygdala	—	—	—	n/a	n/a	n/a
PFC	#(108)	✓(109)	—	n/a	n/a	n/a

Symbols: (✓) statistically significant effect (two-way ANOVA); (—) no statistically significant effect (two-way ANOVA) or difference from NaCl-Social group (*post hoc*); (↑) increase; (n/a) not applicable; (↓) decrease; (*) $p < 0.05$; (**) $p < 0.01$; (***) $p < 0.001$; (#) $0.10 \geq p \geq 0.05$.
F and *p* values: (98) $F_{(1,19)} = 11.74$, $p = 0.003$; (99) $F_{(1,25)} = 11.58$, $p = 0.002$; (100) $F_{(1,25)} = 107.23$, $p < 10^{-10}$; (101) $F_{(1,25)} = 4.02$, $p = 0.056$; (102) $F_{(1,32)} = 9.863$, $p = 0.004$; (103) $F_{(1,25)} = 3.94$, $p = 0.058$; (104) $F_{(1,26)} = 13.51$, $p = 0.001$; (105) $F_{(1,25)} = 4.10$, $p = 0.054$; (106) $F_{(1,26)} = 5.52$, $p = 0.027$; (107) $F_{(1,20)} = 3.07$, $p = 0.095$; (108) $F_{(1,25)} = 4.12$, $p = 0.053$; (109) $F_{(1,25)} = 5.06$, $p = 0.033$.

point for the maturation of inhibitory circuits. When animals are subjected to both alterations (MK801 injection and social isolation), we observe a cumulative effect, especially on the structure of interneurons. Probably the early effect of MK801 disturbs the construction of interneuronal morphology and connectivity. In animals reared in group, these alterations are probably compensated during infancy and puberty: for instance, in the proportion of PV-expressing neurons surrounded by PNNs in the infralimbic cortex, the significant effects of the MK801 injection appear to be reverted by the social isolation. However, if the animals are subjected to the prolonged isolation stress, the impact of this aversive experience may prevent this compensation. The social isolation stress by itself seems to be enough to produce significant changes in many parameters, but in others, like some anxiety-like and locomotor behaviors, this aversive experience is not enough to render significant alterations. Apparently, these changes only appear when the stressful event operates on a previously altered substrate, such as the subtly modified circuitry of MK801-injected animals.

Behavioral Alterations

Anxiety, hyperactivity, and working memory deficits are frequently reported in patients suffering from schizophrenia (Pallanti et al. 2013; Pallanti and Salerno, 2015; Van Snellenberg et al. 2016) and in several animal models of this disease (Jones et al. 2011; Lett et al. 2014). In our study, we used the hole-board apparatus to analyze these behaviors (Karl et al. 2008; Castilla-Ortega et al. 2010; Torres-García et al. 2012). Our results on GIN mice show that rearing in isolation induced anxiety-like behavior and locomotor hyperactivity. Therefore, the functional consequences of the molecular and structural changes affecting only the double-hit GIN mice are not yet clear. The analysis of Thy1 mice also showed these effects of rearing, but in this strain also revealed significant differences in double-hit animals compared with controls. These behavioral abnormalities may be a long-term consequence of the impairments in brain development that are induced by post-weaning social deprivation, as other authors reported before (Koike et al. 2009; Jones et al. 2011; Hickey et al. 2012; Jiang et al. 2013). No changes in exploratory behavior were observed in any of the strains when measured in the hole-board; this test can be considered as an initial basic screen for working memory (Karl et al. 2008).

Studies on schizophrenia models based on NMDAR hypofunction during early postnatal development have yielded contradictory results; whereas some authors described hyperlocomotion, anxiety-related behaviors, and

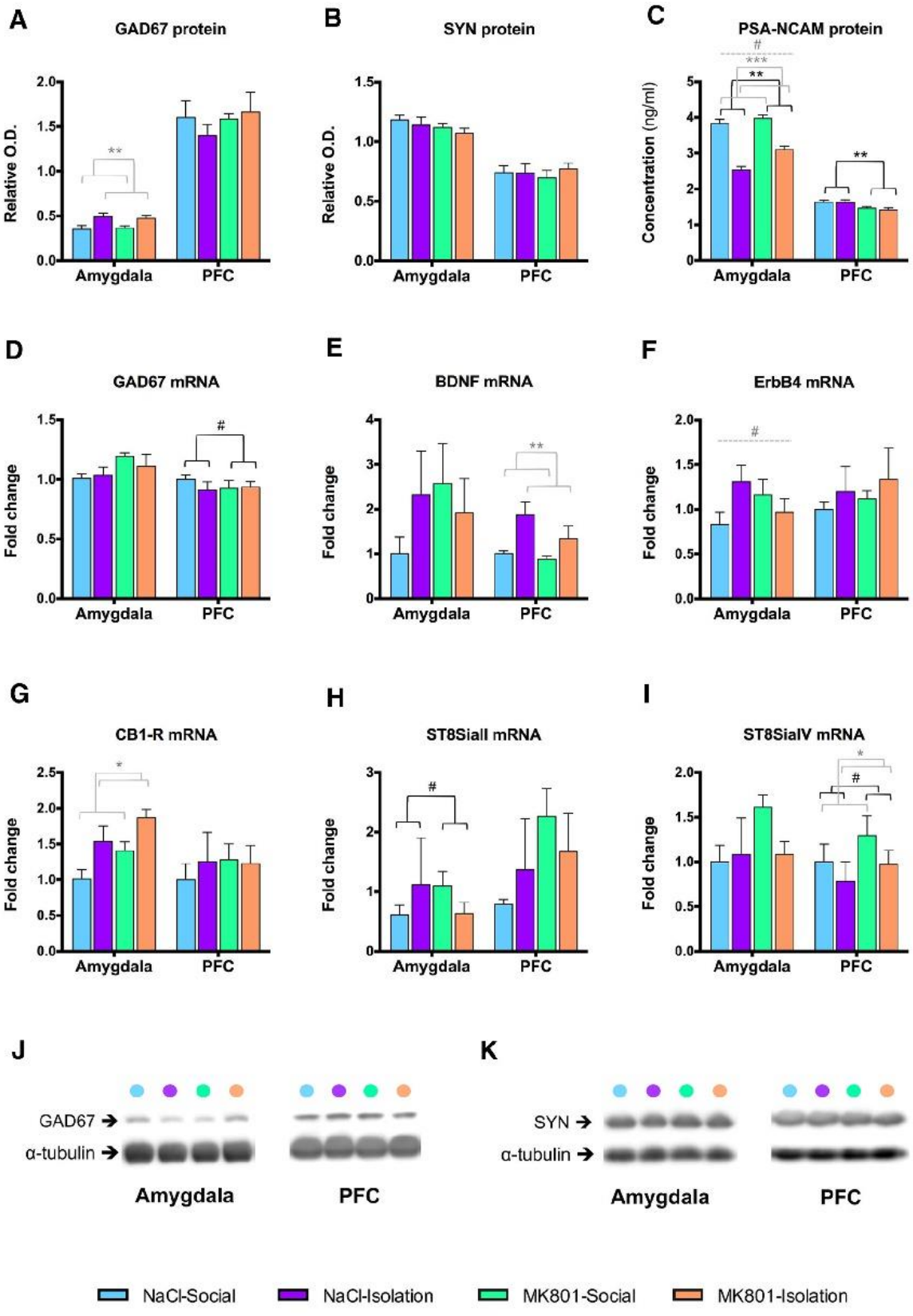

Figure 8. Protein and gene expression studies. Bar graphs showing the presence or lack of effect of the treatment, rearing, or their interaction in GAD67, SYN, and PSA-NCAM protein expression (***A–C***) and in GAD67, BDNF, ErbB4, CB1-R, ST8SiaII, and ST8SiaIV mRNA levels (***D–I***). Horizontal lines in graphs represent trends and statistically significant effects of MK801 treatment (black), rearing (gray) or interaction (gray, dashed) in a two-way ANOVA. # $0.1 > p > 0.05$, * $p < 0.05$, ** $p < 0.01$, *** $p < 0.001$. ***J*** & ***K***: Representative bands from immunoblots for GAD67 (***J***) and SYN (***K***) in the amygdala and the PFC.

Table 6. Summary of results (part V)

Parameter	Main effects (two-way ANOVA) Treatment	Rearing	Interaction	Group differences (from NaCl-Social) NaCl-Isolation	MK801-Social	MK801-Isolation
PV+ neurons (Fig. 9)						
Amygdala						
Total	—	—	#(110)	n/a	n/a	n/a
Central	—	—	—	n/a	n/a	n/a
Lateral	—	—	—	n/a	n/a	n/a
Basolateral	—	—	✓(111)	—	—	—
Basomedial	—	—	✓(112)	—	—	↑*
PFC						
Total	—	—	✓(113)	—	—	—
IL	—	✓(114)	✓(115)	↑*	↑**	—
PrL	—	—	✓(116)	—	—	—
PNNs (Fig. 9)						
Amygdala						
Total	✓(117)	—	✓(118)	—	—	—
Central	✓(119)	—	—	n/a	n/a	n/a
Lateral	—	—	—	n/a	n/a	n/a
Basolateral	✓(120)	—	✓(121)	—	—	—
Basomedial	#(122)	✓(123)	—	n/a	n/a	n/a
PFC						
Total	—	—	✓(124)	—	↑**	—
IL	✓(125)	✓(126)	✓(127)	↑*	↑***	—
PrL	—	—	—	n/a	n/a	n/a
PV-PNN colocalization (Fig. 9)						
Amygdala						
Total	—	✓(128)	✓(129)	—	↑#	—
Central	—	—	—	n/a	n/a	n/a
Lateral	—	—	—	n/a	n/a	n/a
Basolateral	—	—	✓(130)	—	—	—
Basomedial	#(131)	✓(132)	—	n/a	n/a	n/a
PFC						
Total	—	#(133)	✓(134)	—	↑**	↓#
IL	✓(135)	✓(136)	✓(137)	—	↑***	—
PrL	—	—	—	n/a	n/a	n/a

Symbols: (✓) statistically significant effect (two-way ANOVA); (—) no statistically significant effect (two-way ANOVA) or difference from NaCl-Social group (*post hoc*); (↑) increase; (n/a) not applicable; (↓) decrease; $*p < 0.05$; $**p < 0.01$; $***p < 0.001$; #$0.10 \geq p \geq 0.05$.
F values and *p* values: (110) $F_{(1,21)} = 3.99$, $p = 0.059$; (111) $F_{(1,18)} = 7.06$, $p = 0.016$; (112) $F_{(1,20)} = 4.80$, $p = 0.041$; (113) $F_{(1,14)} = 12.82$, $p = 0.003$; (114) $F_{(1,15)} = 7.22$, $p = 0.017$; (115) $F_{(1,15)} = 52.97$, $p = 3 \times 10^{-6}$; (116) $F_{(1,15)} = 7.03$, $p = 0.018$; (117) $F_{(1,20)} = 5.648$, $p = 0.028$; (118) $F_{(1,20)} = 6.70$, $p = 0.016$; (119) $F_{(1,18)} = 10.19$, $p = 0.005$; (120) $F_{(1,21)} = 4.91$, $p = 0.038$; (121) $F_{(1,21)} = 12.96$, $p = 0.002$; (122) $F_{(1,20)} = 3.39$, $p = 0.08$; (123) $F_{(1,20)} = 6.4$, $p = 0.02$; (124) $F_{(1,14)} = 10.55$, $p = 0.006$; (125) $F_{(1,15)} = 12.93$, $p = 0.003$; (126) $F_{(1,15)} = 17.92$, $p = 0.001$; (127) $F_{(1,15)} = 88.68$, $p < 10 - 7$; (128) $F_{(1,19)} = 10.95$, $p = 0.004$; (129) $F_{(1,19)} = 13.36$, $p = 0.002$; (130) $F_{(1,19)} = 6.53$, $p = 0.019$; (131) $F_{(1,21)} = 2.99$, $p = 0.098$; (132) $F_{(1,21)} = 4.97$, $p = 0.037$; (133) $F_{(1,13)} = 3.61$, $p = 0.08$; (134) $F_{(1,13)} = 15.49$, $p = 0.002$; (135) $F_{(1,15)} = 19.87$, $p = 4.61 \times 10^{-4}$; (136) $F_{(1,15)} = 47.52$, $p = 5 \times 10^{-6}$; (137) $F_{(1,15)} = 87.65$, $p < 10^{-7}$.

working memory abnormalities after these treatments (Andersen and Pouzet, 2004; Bubeníková-Valesová et al. 2008; Belforte et al. 2010; Nozari et al. 2015), others failed to find them (Bubeníková-Valesová et al. 2008; Rompala et al. 2013).

Changes in Brain Volume and Neuronal Structure

Numerous studies in humans and animal models of schizophrenia have documented the presence of structural alterations in the BLA and PFC, including volume impairments (Jaaro-Peled et al. 2010; Levitt et al. 2010). Early-life stress also has dramatic effects on brain structure, especially on the amygdala (hypertrophy, increased activity, and dendritic arborization of excitatory neurons; for review, see Coplan et al. 2014). In our study, early-life stress, but not specifically the double-hit model, has a negative effect in the volume of the PFC (as described previously in rats, Gilabert-Juan et al. 2013a), but increases the volume of CeA. To our knowledge, there are no previous studies on the effects of social isolation rearing on these nuclei, although reductions in the volume of the MeA have been described (Cooke et al. 2000).

As these volumetric alterations may probably reflect structural changes in PFC and BLA neurons, we decided to analyze their structure. In fact, a previous Golgi study in rats found that social isolation rearing reduces the length of dendritic segments of pyramidal neurons in the BLA while increasing their complexity (Wang et al. 2012). This study also found reduced dendritic arborization and spine density in mPFC pyramidal neurons, similar to what has been found after chronic stress in adult rats (Radley et al. 2004, 2006). By contrast, also with data from schizophrenic patients and rat models (Jones et al. 2011; Flores et al. 2016), we have not observed a significant reduction in spine density of the PFC pyramidal neurons in isolated or double-hit mice. This controversy could be due to species differences. However, because there is a clear trend toward a decrease in the double-hit animals, it is

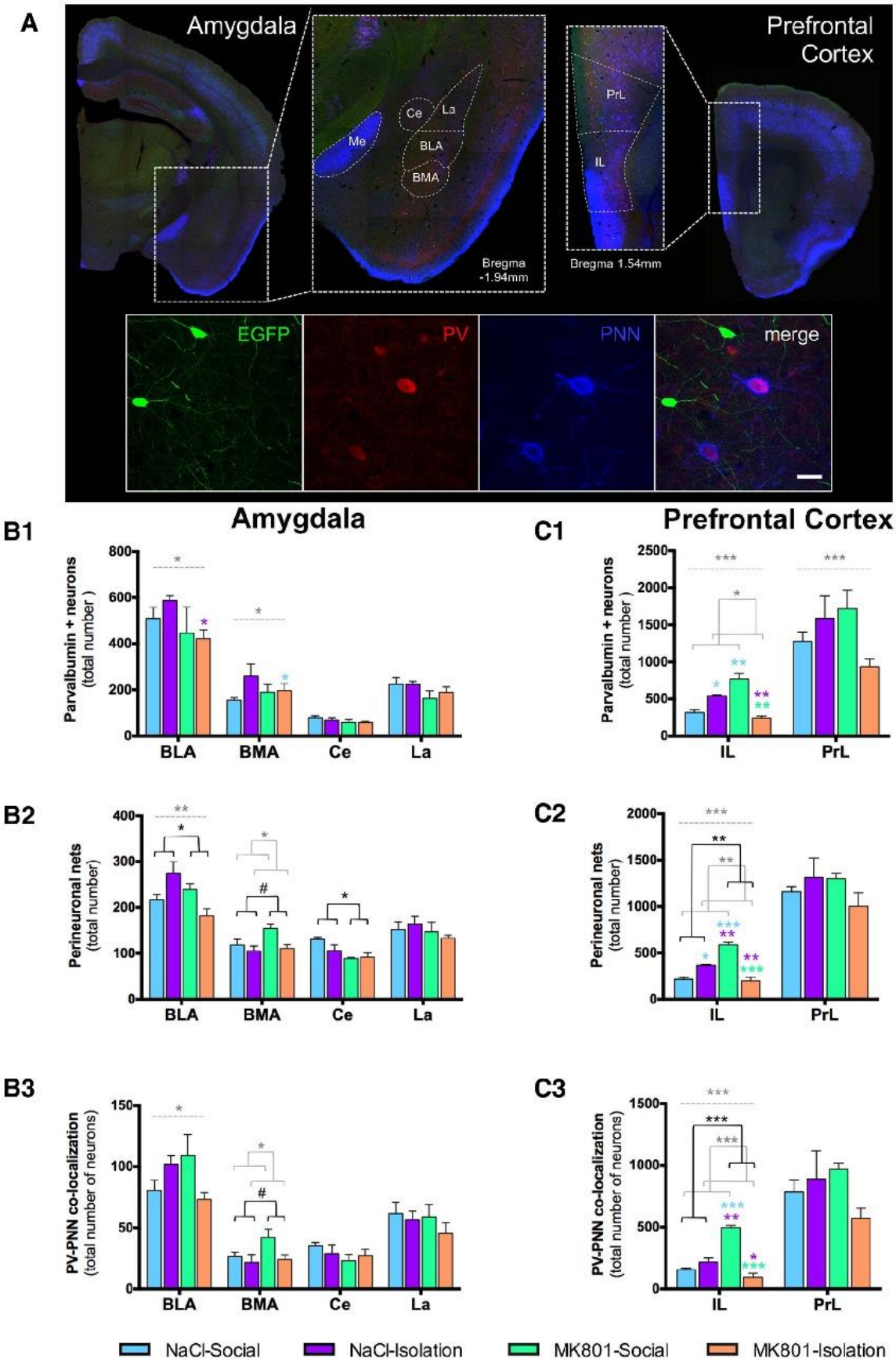

Figure 9. Expression of PNNs in PV-immunoreactive neurons. **A**, Representative confocal images showing the distribution of PV (red) and PNNs (blue) in the different nuclei of the amygdala (left) and regions of the PFC (right) of GIN mice (GAD-GFP, green). The squared

continued
section in the panoramic images was 2× magnified to show the different nuclei and areas that were analyzed. In a detailed view (below), two PV-immunoreactive neurons expressing PNN can be observed. GAD-GFP expressing interneurons do not express PNN. Scale bars: panoramic views, 875 μm; detailed view, 25 μm. ***B***, ***C***, Treatment, rearing, or their interaction affected the total number of PV neurons (***B1***, ***C1***), PNNs (***B2***, ***C2***), or their colocalization (***B3***, ***C3***) in some nuclei of the amygdala and regions of the PFC. Horizontal lines in graphs represent trends and statistically significant effects of MK801 treatment (black), rearing (gray), or interaction (gray, dashed) in a two-way ANOVA. # $0.1 > p > 0.05$, $*p < 0.05$, $**p < 0.01$, $***p < 0.001$. Colored symbols in bars represent trends and statistically significant differences among groups after *post hoc* analysis: # $0.1 > p > 0.05$, $*p < 0.05$, $**p < 0.01$, $***p < 0.001$.

possible that studies with higher number of animals would render significant results on this parameter.

An increase in dendritic spine density was found in PFC interneurons of isolated and double-hit mice, which may lead to an increased number of synaptic contacts on these interneurons. Future experiments should explore whether these new spines are active and receive excitatory and/or inhibitory contacts. We have also detected a significant increase in dendritic arborization in amygdaloid interneurons of the double-hit mice, also suggesting an increased surface for the reception of new synaptic contacts. Interestingly, the subpopulation of interneurons studied in the present paper, which mainly express somatostatin (Oliva et al. 2000), also exhibits hypertrophic changes when young adult mice are subjected to chronic stress (Gilabert-Juan et al. 2011, 2013b). These findings are especially relevant because, despite the abundant number of studies that point to interneurons as key players in neurodevelopmental mental disorders, no studies looking for dendritic abnormalities in interneurons, neither of the PFC nor the amygdala, have been conducted before.

Alterations in Structural Plasticity and E/I Neurotransmission

The impairments in the morphology and connectivity of neurons may be mediated by changes in the expression of the plasticity-related molecule PSA-NCAM (Bonfanti, 2006; Rutishauser, 2008; Nacher et al. 2013). Post-weaning social isolation rearing in rats leads to increases in the expression of PSA-NCAM during adulthood, specially in the basolateral amygdaloid nucleus (Gilabert-Juan et al. 2012). Adult rats exposed to different physical stressors during adolescence show a similar increase in this nucleus (Tsoory et al. 2008). However, in the present experiment, both the isolated and the double-hit mice showed decreased expression of PSA-NCAM in the amygdala in adult life. These apparently contradictory results could be due to species differences and/or to a different impact of stress in different amygdaloid regions, because the expression of PSA-NCAM in the present study has been studied in the whole amygdala. In fact, similar reductions in the expression of this molecule have been found after chronic stress in the central amygdala of adult mice (Gilabert-Juan et al. 2011) and rats (Cordero et al. 2005). These findings are specially relevant for inhibitory circuits, because in the amygdala and PFC, PSA-NCAM is exclusively expressed by interneurons, and therefore is able to regulate directly its structure and connectivity (Nacher et al. 2013).

PNNs were reduced in the lateral nucleus of the amygdala (Pantazopoulos et al. 2010) and the PFC in schizophrenic patients (Mauney et al. 2013). Reduced labeling of PV neurons was also observed in these patients (Enwright et al. 2016). Moreover, a recent report has described a disruption of PNNs in the mPFC after in an animal model of this disorder (maternal immune activation; Paylor et al. 2016). Our study also reveals a similar, although nonsignificant, decrease in these parameters in the infralimbic cortex of the double-hit mice. This is in accordance with previous results on PV-expressing neurons in this prefrontocortical region using the same double-hit model in rats (Gilabert-Juan et al. 2013a). However, it has to be noted that opposite effects were observed in the MK-801 group of animals. We do not have an explanation yet for these effects and there are no previous studies looking at the effects of NMDAR antagonists on PNNs.

The precise balance between excitatory and inhibitory neurotransmission is crucial for the proper maturation of the neural circuitry during development. In fact, E/I imbalances in key brain regions have been proposed as underlying causes of some neurodevelopmental psychiatric disorders, including schizophrenia (Curley and Lewis, 2012; Lewis et al. 2012; Inan et al. 2013; Lin et al. 2013; Sun et al. 2013; Morishita et al. 2015). Our data support this hypothesis, demonstrating that early-life stress strongly influences E/I balance and that alterations in this balance are particularly evident in the PFC and the amygdala of double-hit mice. E/I balance can also be affected by changes in the expression of other molecules that influence the maturation of inhibitory circuits and that have also been related to schizophrenia. This is the case of BDNF (Sánchez-Huertas and Rico, 2011), ST8SialV (Nacher et al. 2010), and CB1-R (Volk and Lewis, 2010; den Boon et al. 2015). BDNF and ST8SialV mRNA levels in the PFC are increased and decreased, respectively, by early-life stress, whereas CB1-R mRNA levels in the amygdala are increased.

Concluding remarks and future perspectives

The present results suggest an important impact of stressful events in early life on inhibitory networks, both at the structural and the neurochemical level. We still do not know whether the changes in the structure (and probably in the connectivity) of interneurons precede or are the response to alterations in the excitatory neurotransmission. Future experiments evaluating different time points should clarify this matter. The present model may constitute a powerful resource for the study of the influence of early-life aversive experiences on the adult brain and to deepen further in the understanding of the neurobiological

basis of mental disorders in which these experiences seem to play a critical role, such as schizophrenia. The model may constitute an interesting tool for testing new antipsychotic drugs or to understand how other genetic or environmental factors, particularly during the early-life stages, can impact on the development of this symptomatology. Future studies will have to expand the battery of behavioral tests, particularly those measuring prefrontal- and amygdaloid-related behaviors. Given the alterations found in the structure of interneurons and in some molecules related to inhibitory neurotransmission, it would also be interesting to analyze them in more detail.

References

Akbarian S (1995) Gene expression for glutamic acid decarboxylase is reduced without loss of neurons in prefrontal cortex of schizophrenics. Arch Gen Psychiatry 52:258. Medline

Akbarian S, Huang HS (2006) Molecular and cellular mechanisms of altered GAD1/GAD67 expression in schizophrenia and related disorders. Brain Res Rev 52:293–304. CrossRef Medline

Andersen JD, Pouzet B (2004) Spatial memory deficits induced by perinatal treatment of rats with PCP and reversal effect of D-serine. Neuropsychopharmacology 29:1080–1090. CrossRef Medline

Belforte JE, Zsiros V, Sklar ER, Jiang Z, Yu G, Li Y, Quinlan EM, Nakazawa K (2010) Postnatal NMDA receptor ablation in corticolimbic interneurons confers schizophrenia-like phenotypes. Nat Neurosci 13:76–83. CrossRef Medline

Berretta S, Pantazopoulos H, Markota M, Brown C, Batzianouli ET (2015) Losing the sugar coating: Potential impact of perineuronal net abnormalities on interneurons in schizophrenia. Schizophr Res 167:18–27. CrossRef Medline

Bonefeld BE, Elfving B, Wegener G (2008) Reference genes for normalization: a study of rat brain tissue. Synapse 62:302–309. CrossRef Medline

Bonfanti L (2006) PSA-NCAM in mammalian structural plasticity and neurogenesis. Prog Neurobiol 80:129–164. CrossRef Medline

Bubeníková-Valesová V, Horácek J, Vrajová M, Höschl C (2008) Models of schizophrenia in humans and animals based on inhibition of NMDA receptors. Neurosci Biobehav Rev 32:1014–1023. CrossRef Medline

Castilla-Ortega E, Sánchez-López J, Hoyo-Becerra C, Matas-Rico E, Zambrana-Infantes E, Chun J, De Fonseca FR, Pedraza C, Estivill-Torrús G, Santin LJ (2010) Exploratory, anxiety and spatial memory impairments are dissociated in mice lacking the LPA1 receptor. Neurobiol Learn Mem 94:73–82. CrossRef Medline

Cooke BM, Chowanadisai W, Breedlove SM (2000) Post-weaning social isolation of male rats reduces the volume of the medial amygdala and leads to deficits in adult sexual behavior. Behav Brain Res 117:107–113. Medline

Coplan JD, Fathy HM, Jackowski AP, Tang CY, Perera TD, Mathew SJ, Martinez J, Abdallah CG, Dwork AJ, Pantol G, Carpenter D, Gorman JM, Nemeroff CB, Owens MJ, Kaffman A, Kaufman J (2014) Early life stress and macaque amygdala hypertrophy: preliminary evidence for a role for the serotonin transporter gene. Front Behav Neurosci 8:342. CrossRef Medline

Cordero MI, Rodríguez JJ, Davies HA, Peddie CJ, Sandi C, Stewart MG (2005) Chronic restraint stress down-regulates amygdaloid expression of polysialylated neural cell adhesion molecule. Neuroscience 133:903–910. CrossRef Medline

Curley AA, Lewis DA (2012) Cortical basket cell dysfunction in schizophrenia. J Physiol 590:715–724. CrossRef Medline

den Boon FS, Werkman TR, Schaafsma-Zhao Q, Houthuijs K, Vitalis T, Kruse CG, Wadman WJ, Chameau P (2015) Activation of type-1 cannabinoid receptor shifts the balance between excitation and inhibition towards excitation in layer II/III pyramidal neurons of the rat prelimbic cortex. Pflu¨Gers Arch 467:1551–1564. CrossRef

Duman CH, Duman RS (2015) Spine synapse remodeling in the pathophysiology and treatment of depression. Neurosci Lett601: 20–29. CrossRef

Enwright JF, Sanapala S, Foglio A, Berry R, Fish KN, Lewis DA (2016) Reduced labeling of parvalbumin neurons and perineuronal nets in the dorsolateral prefrontal cortex of subjects with schizophrenia. Neuropsychopharmacology 41:2206–2214. CrossRef Medline

Feng G, Mellor RH, Bernstein M, Keller-Peck C, Nguyen QT, Wallace M, Nerbonne JM, Lichtman JW, Sanes JR (2000) Imaging neuronal subsets in transgenic mice expressing multiple spectral variants of GFP. Neuron 28:41–51. Medline

Ferdman N, Murmu RP, Bock J, Braun K, Leshem M (2007) Weaning age, social isolation, and gender, interact to determine adult exploratory and social behavior, and dendritic and spine morphology in prefrontal cortex of rats. Behav Brain Res 180:174–182. CrossRef Medline

Flores G, Morales-Medina JC, Diaz A (2016) Neuronal and brain morphological changes in animal models of schizophrenia. Behav Brain Res 301:190–203. CrossRef Medline

Geyer MA, Wilkinson LS, Humby T, Robbins TW (1993) Isolation rearing of rats produces a deficit in prepulse inhibition of acoustic startle similar to that in schizophrenia. Biol Psychiatry 34:361–372. Medline

Gilabert-Juan J, Belles M, Saez AR, Carceller H, Zamarbide-Fores S, Moltó MD, Nacher J (2013a) A "double hit" murine model for schizophrenia shows alterations in the structure and neurochemistry of the medial prefrontal cortex and the hippocampus. Neurobiol Dis 59:126–140.

Gilabert-Juan J, Castillo-Gomez E, Guirado R, Moltó MD, Nacher J (2013b) Chronic stress alters inhibitory networks in the medial prefrontal cortex of adult mice. Brain Struct Funct 218:1591–1605.

Gilabert-Juan J, Castillo-Gomez E, Pérez-Rando M, Moltó MD, Nacher J (2011) Chronic stress induces changes in the structure of interneurons and in the expression of molecules related to neuronal structural plasticity and inhibitory neurotransmission in the amygdala of adult mice. Exp Neurol 232:33–40. CrossRef Medline

Gilabert-Juan J, Moltó MD, Nacher J (2012) Post-weaning social isolation rearing influences the expression of molecules related to inhibitory neurotransmission and structural plasticity in the amygdala of adult rats. Brain Res 1448:129–136. CrossRef Medline

Glausier JR, Lewis DA (2013) Dendritic spine pathology in schizophrenia. Neuroscience 251:90–107. CrossRef Medline

Goghari VM, Sponheim SR, MacDonald AW (2010) The functional neuroanatomy of symptom dimensions in schizophrenia: a qualitative and quantitative review of a persistent question. Neurosci Biobehav Rev 34:468–486. CrossRef Medline

Guirado R, Sanchez-Matarredona D, Varea E, Crespo C, Blasco-Ibáñez JM, Nacher J (2012) Chronic fluoxetine treatment in middle-aged rats induces changes in the expression of plasticity-related molecules and in neurogenesis. BMC Neurosci 13:5. CrossRef Medline

Gundersen HJ, Jensen EB (1987) The efficiency of systematic sampling in stereology and its prediction. J Microsc 147:229–263. Medline

Härtig W, Brauer K, Brückner G (1992) Wisteria floribunda agglutinin-labelled nets surround parvalbumin-containing neurons. Neuroreport 3:869–872. Medline

Hickey AJ, Reynolds JN, Beninger RJ (2012) Post-weaning social isolation and subchronic NMDA glutamate receptor blockade: effects on locomotor activity and GABA signaling in the rat suggest independent mechanisms. Pharmacol Biochem Behav 101:231–238. CrossRef Medline

Ikonomidou C, Bosch F, Miksa M, Bittigau P, Vöckler J, Dikranian K, Tenkova TI, Stefovska V, Turski L, Olney JW (1999) Blockade of NMDA receptors and apoptotic neurodegeneration in the developing brain. Science 283:70–74. Medline

Inan M, Petros TJ, Anderson SA (2013) Losing your inhibition: linking cortical GABAergic interneurons to schizophrenia. Neurobiol Dis 53:36–48. CrossRef Medline

Jaaro-Peled H, Ayhan Y, Pletnikov MV, Sawa A (2010) Review of pathological hallmarks of schizophrenia: comparison of genetic models with patients and nongenetic models. Schizophr Bull 36: 301–313. CrossRef Medline

Jansson LC, Åkerman KE (2014) The role of glutamate and its receptors in the proliferation, migration, differentiation and survival of neural progenitor cells. J Neural Transm 121:819–836. CrossRef Medline

Jiang Z, Rompala GR, Zhang S, Cowell RM, Nakazawa K (2013) Social isolation exacerbates schizophrenia-like phenotypes via oxidative stress in cortical interneurons. Biol Psychiatry 73:1024–1034. CrossRef Medline

Jones CA, Watson DJ, Fone KC (2011) Animal models of schizophrenia. Br J Pharmacol 164:1162–1194. CrossRef Medline

Karl T, Duffy L, Herzog H (2008) Behavioural profile of a new mouse model for NPY deficiency. Eur J Neurosci 28:173–180. CrossRef Medline

Kinden Lensjø K, Elle Lepperød M, Dick G, Hafting T, Fyhn M (2017) Removal of perineuronal nets unlocks juvenile plasticity through network mechanisms of decreased inhibition and increased gamma activity. J Neurosci 37:1269-1283.

Koike H, Ibi D, Mizoguchi H, Nagai T, Nitta A, Takuma K, Nabeshima T, Yoneda Y, Yamada K (2009) Behavioral abnormality and pharmacologic response in social isolation-reared mice. Behav Brain Res 202:114–121. CrossRef Medline

Lett TA, Voineskos AN, Kennedy JL, Levine B, Daskalakis ZJ (2014) Treating working memory deficits in schizophrenia: a review of the neurobiology. Biol Psychiatry 75:361–370. CrossRef Medline

Levitt JJ, Bobrow L, Lucia D, Srinivasan P (2010) A selective review of volumetric and morphometric imaging in schizophrenia. Curr Top Behav Neurosci 4:243–281. Medline

Lewis DA, Curley AA, Glausier JR, Volk DW (2012) Cortical parvalbumin interneurons and cognitive dysfunction in schizophrenia. Trends Neurosci 35:57–67. CrossRef Medline

Lim AL, Taylor DA, Malone DT (2012) A two-hit model: behavioural investigation of the effect of combined neonatal MK-801 administration and isolation rearing in the rat. J Psychopharmacol 26: 1252–1264. CrossRef Medline

Lin HC, Gean PW, Wang CC, Chan YH, Chen PS (2013) The amygdala excitatory/inhibitory balance in a valproate-induced rat autism model. PLoS One 8:e55248. CrossRef Medline

Longair MH, Baker DA, Armstrong JD (2011) Simple Neurite Tracer: open source software for reconstruction, visualization and analysis of neuronal processes. Bioinformatics 27:2453–2454. CrossRef Medline

Lyall A, Swanson J, Liu C, Blumenthal TD, Turner CP (2009) Neonatal exposure to MK801 promotes prepulse-induced delay in startle response time in adult rats. Exp Brain Res 197:215–222. CrossRef Medline

Mauney SA, Athanas KM, Pantazopoulos H, Shaskan N, Passeri E, Berretta S, Woo TU (2013) Developmental pattern of perineuronal nets in the human prefrontal cortex and their deficit in schizophrenia. Biol Psychiatry 74:427–435. CrossRef Medline

Mitchell AC, Jiang Y, Peter C, Akbarian S (2015) Transcriptional regulation of GAD1 GABA synthesis gene in the prefrontal cortex of subjects with schizophrenia. Schizophr Res 167:28–34. CrossRef Medline

Morishita H, Kundakovic M, Bicks L, Mitchell A, Akbarian S (2015) Interneuron epigenomes during the critical period of cortical plasticity: Implications for schizophrenia. Neurobiol Learn Mem 124: 104–110. CrossRef Medline

Nacher J, Alonso-Llosa G, Rosell D, McEwen B (2002) PSA-NCAM expression in the piriform cortex of the adult rat: modulation by NMDA receptor antagonist administration. Brain Res 927:111–121. Medline

Nacher J, Guirado R, Castillo-Gómez E (2013) Structural plasticity of interneurons in the adult brain: role of PSA-NCAM and implications for psychiatric disorders. Neurochem Res 38:1122-1133.

Nacher J, Guirado R, Varea E, Alonso-Llosa G, Röckle I, Hildebrandt H (2010) Divergent impact of the polysialyltransferases ST8SiaII and ST8SiaIV on polysialic acid expression in immature neurons and interneurons of the adult cerebral cortex. Neuroscience 167: 825–837. CrossRef Medline

Nozari M, Mansouri FA, Shabani M, Nozari H, Atapour N (2015) Postnatal MK-801 treatment of female rats impairs acquisition of working memory, but not reference memory in an eight-arm radial maze; no beneficial effects of enriched environment. Psychopharmacology (Berl) 232:2541–2550. CrossRef Medline

Oliva AA, Jiang M, Lam T, Smith KL, Swann JW (2000) Novel hippocampal interneuronal subtypes identified using transgenic mice that express green fluorescent protein in GABAergic interneurons. J Neurosci 20:3354–3368. Medline

Pallanti S, Cantisani A, Grassi G (2013) Anxiety as a core aspect of schizophrenia. Curr Psychiatry Rep 15:354. CrossRef Medline

Pallanti S, Salerno L (2015) Raising attention to attention deficit hyperactivity disorder in schizophrenia. World J Psychiatry 5:47–55. CrossRef Medline

Pantazopoulos H, Woo TU, Lim MP, Lange N, Berretta S (2010) Extracellular matrix-glial abnormalities in the amygdala and entorhinal cortex of subjects diagnosed with schizophrenia. Arch Gen Psychiatry 67:155. CrossRef Medline

Paylor JW, Lins BR, Greba Q, Moen N, de Moraes RS, Howland JG, Winship IR (2016) Developmental disruption of perineuronal nets in the medial prefrontal cortex after maternal immune activation. Sci Rep 6:37580. CrossRef Medline

Pfaffl MW (2001) A new mathematical model for relative quantification in real-time RT-PCR. Nucleic Acids Res 29:e45. Medline

Porrero C, Rubio-Garrido P, Avendaño C, Clascá F (2010) Mapping of fluorescent protein-expressing neurons and axon pathways in adult and developing Thy1-eYFP-H transgenic mice. Brain Res 1345:59–72. CrossRef Medline

Radley JJ, Rocher AB, Miller M, Janssen WGM, Liston C, Hof PR, McEwen BS, Morrison JH (2006) Repeated stress induces dendritic spine loss in the rat medial prefrontal cortex. Cereb Cortex 16:313–320. CrossRef

Radley JJ, Sisti HM, Hao J, Rocher AB, McCall T, Hof PR, McEwen BS, Morrison JH (2004) Chronic behavioral stress induces apical dendritic reorganization in pyramidal neurons of the medial prefrontal cortex. Neuroscience 125:1–6. CrossRef Medline

Rico B, Marín O (2011) Neuregulin signaling, cortical circuitry development and schizophrenia. Curr Opin Genet Dev 21:262–270. CrossRef Medline

Rompala GR, Zsiros V, Zhang S, Kolata SM, Nakazawa K (2013) Contribution of NMDA receptor hypofunction in prefrontal and cortical excitatory neurons to schizophrenia-like phenotypes. PLoS One 8:e61278. CrossRef Medline

Rutishauser U (2008) Polysialic acid in the plasticity of the developing and adult vertebrate nervous system. Nat Rev Neurosci 9:26–35. CrossRef Medline

Saaltink DJ, Vreugdenhil E (2014) Stress, glucocorticoid receptors, and adult neurogenesis: a balance between excitation and inhibition?. Cell Mol Life Sci 71:2499–2515. CrossRef Medline

Sánchez-Huertas C, Rico B (2011) CREB-dependent regulation of GAD65 transcription by BDNF/TrkB in cortical interneurons. Cereb Cortex 21:777–788. CrossRef Medline

Sandi C (2004) Stress, cognitive impairment and cell adhesion molecules. Nat Rev Neurosci 5:917–930. CrossRef Medline

Schindelin J, Arganda-Carreras I, Frise E, Kaynig V, Longair M, Pietzsch T, Preibisch S, Rueden C, Saalfeld S, Schmid B, Tinevez JY, White DJ, Hartenstein V, Eliceiri K, Tomancak P, Cardona A (2012) Fiji: an open-source platform for biological-image analysis. Nat Methods 9:676–682. CrossRef Medline

Simon P, Dupuis R, Costentin J (1994) Thigmotaxis as an index of anxiety in mice. Influence of dopaminergic transmissions. Behav Brain Res 61:59–64. Medline

Straub RE, Lipska BK, Egan MF, Goldberg TE, Callicott JH, Mayhew MB, Vakkalanka RK, Kolachana BS, Kleinman JE, Weinberger DR (2007) Allelic variation in GAD1 (GAD67) is associated with schizophrenia and influences cortical function and gene expression. Mol Psychiatry 12:854–869. CrossRef Medline

Sun L, Castellanos N, Grützner C, Koethe D, Rivolta D, Wibral M, Kranaster L, Singer W, Leweke MF, Uhlhaas PJ (2013) Evidence for dysregulated high-frequency oscillations during sensory processing in medication-naïve, first episode schizophrenia. Schizophr Res 150:519–525. CrossRef Medline

Tao HW, Li Y, Zhang LI (2014) Formation of excitation-inhibition balance: inhibition listens and changes its tune. Trends Neurosci 37:528–530. CrossRef Medline

Torres-García ME, Solis O, Patricio A, Rodríguez-Moreno A, Camacho-Abrego I, Limón ID, Flores G (2012) Dendritic morphology changes in neurons from the prefrontal cortex, hippocampus and nucleus accumbens in rats after lesion of the thalamic reticular nucleus. Neuroscience 223:429–438. CrossRef Medline

Tsoory M, Guterman A, Richter-Levin G (2008) Exposure to stressors during juvenility disrupts development-related alterations in the PSA-NCAM to NCAM expression ratio: potential relevance for mood and anxiety disorders. Neuropsychopharmacology 33:378–393. CrossRef Medline

Tzanoulinou S, Riccio O, de Boer MW, Sandi C (2014) Peripubertal stress-induced behavioral changes are associated with altered expression of genes involved in excitation and inhibition in the amygdala. Transl Psychiatry 4:e410. CrossRef Medline

van der Kooij MA, Fantin M, Kraev I, Korshunova I, Grosse J, Zanoletti O, Guirado R, Garcia-Mompó C, Nacher J, Stewart MG, Berezin V, Sandi C (2014) Impaired hippocampal neuroligin-2 function by chronic stress or synthetic peptide treatment is linked to social deficits and increased aggression. Neuropsychopharmacology 39:1148–1158. CrossRef Medline

Van Snellenberg JX, Girgis RR, Horga G, van de Giessen E, Slifstein M, Ojeil N, Weinstein JJ, Moore H, Lieberman JA, Shohamy D, Smith EE, Abi-Dargham A (2016) Mechanisms of working memory impairment in schizophrenia. Biol Psychiatry 80:617–626.

Volk DW, Lewis DA (2010) Prefrontal cortical circuits in schizophrenia. Curr Top Behav Neurosci 4:485–508. Medline

Wang CZ, Johnson KM (2005) Differential effects of acute and subchronic administration on phencyclidine-induced neurodegeneration in the perinatal rat. J Neurosci Res 81:284–292. CrossRef

Wang YC, Ho UC, Ko MC, Liao CC, Lee LJ (2012) Differential neuronal changes in medial prefrontal cortex, basolateral amygdala and nucleus accumbens after postweaning social isolation. Brain Struct Funct 217:337–351. CrossRef Medline

Weickert CS, Hyde TM, Lipska BK, Herman MM, Weinberger DR, Kleinman JE (2003) Reduced brain-derived neurotrophic factor in prefrontal cortex of patients with schizophrenia. Mol Psychiatry 8:592–610. CrossRef Medline

Weickert CS, Ligons DL, Romanczyk T, Ungaro G, Hyde TM, Herman MM, Weinberger DR, Kleinman JE (2005) Reductions in neurotrophin receptor mRNAs in the prefrontal cortex of patients with schizophrenia. Mol Psychiatry 10:637–650. CrossRef Medline

West MJ (1993) New stereological methods for counting neurons. Neurobiol Aging 14:275–285. Medline

3. Chronic fluoxetine treatment alters the structure, connectivity and plasticity of cortical interneurons

Guirado, R., Perez-Rando, M., Sanchez-Matarredona, D., Castrén, E., Nacher, J. (2014). Chronic fluoxetine treatment alters the structure, connectivity and plasticity of cortical interneurons. International Journal of Neuropsychopharmacology. 17, 1635–1646.

doi:10.1017/S1461145714000406

International Journal of Neuropsychopharmacology (2014), **17**, 1635–1646. © CINP 2014
doi:10.1017/S1461145714000406

ARTICLE

Chronic fluoxetine treatment alters the structure, connectivity and plasticity of cortical interneurons

Ramon Guirado[1,2]*, Marta Perez-Rando[1]*, David Sanchez-Matarredona[1]†, Eero Castrén[2] and Juan Nacher[1,3,4]

[1] *Neurobiology Unit and Program in Basic and Applied Neurosciences, Cell Biology Department, Universitat de València, Spain*
[2] *Neuroscience Centre, University of Helsinki, Finland*
[3] *CIBERSAM: Spanish National Network for Research in Mental Health, Madrid, Spain*
[4] *Fundacion Investigacion Hospital Clinico de Valencia, INCLIVA, Spain*

Abstract

Novel hypotheses suggest that antidepressants, such as the selective serotonin reuptake inhibitor fluoxetine, induce neuronal structural plasticity, resembling that of the juvenile brain, although the underlying mechanisms of this reopening of the critical periods still remain unclear. However, recent studies suggest that inhibitory networks play an important role in this structural plasticity induced by fluoxetine. For this reason we have analysed the effects of a chronic fluoxetine treatment in the hippocampus and medial prefrontal cortex (mPFC) of transgenic mice displaying eGFP labelled interneurons. We have found an increase in the expression of molecules related to critical period plasticity, such as the polysialylated form of the neural cell adhesion molecule (PSA-NCAM), GAD67/65 and synaptophysin, as well as a reduction in the number of parvalbumin expressing interneurons surrounded by perineuronal nets. We have also described a trend towards decrease in the perisomatic inhibitory puncta on pyramidal neurons in the mPFC and an increase in the density of inhibitory puncta on eGFP interneurons. Finally, we have found that chronic fluoxetine treatment affects the structure of interneurons in the mPFC, increasing their dendritic spine density. The present study provides evidence indicating that fluoxetine promotes structural changes in the inhibitory neurons of the adult cerebral cortex, probably through alterations in plasticity-related molecules of neurons or the extracellular matrix surrounding them, which are present in interneurons and are known to be crucial for the development of the critical periods of plasticity in the juvenile brain.

Received 11 November 2013; Reviewed 13 December 2013; Revised 16 February 2014; Accepted 6 March 2014; First published online 30 April 2014

Key words: Critical period plasticity, fluoxetine, interneurons, perineuronal nets, PSA-NCAM.

Introduction

Neuronal plasticity is required for the adaptation of the brain to face a changing external environment. Several lines of evidence during the last decade have suggested that antidepressants may act by promoting this plasticity (Duman et al., 2000; Castrén, 2005). The antidepressant fluoxetine, a selective serotonin reuptake inhibitor, promotes different kinds of plasticity in the adult CNS, including increased hippocampal neurogenesis (Malberg et al., 2000), LTP induction (Rubio et al., 2013) or remodelling in the structure of pyramidal neurons (Hajszan et al., 2005; Guirado et al., 2009). However, to date most of the research on the effects of antidepressants has been focused on excitatory neural networks, leaving their action on inhibitory neurons almost unexplored (Chen et al., 2011).

Recent research has promoted the development of a new perspective on our understanding of the mode of action of antidepressants: The structural plasticity induced by antidepressants and particularly fluoxetine, resembles that naturally occurring during the critical periods of development. Therefore, fluoxetine may act by promoting a 'dematuration' in certain regions of the adult brain, such as the limbic system (Kobayashi et al., 2010). Moreover, research on the visual cortex has, in fact, demonstrated that the plasticity induced by fluoxetine is similar to that observed during critical periods, when the neuronal wiring of this cortical region is finally established (Maya-Vetencourt et al., 2008).

Cell adhesion molecules and several components of the extracellular matrix have been shown to be critical for structural plasticity in the CNS (Sandi, 2004; Dityatev et al., 2010; Tiraboschi et al., 2013). In this regard, the polysialylated form of the neural cell

Address for correspondence: Dr Juan Nacher, Neurobiology Unit, Cell Biology Department, Universitat de València, Dr. Moliner, 50, Burjassot, 46100, Spain.
Tel.: +34 96 354 3241 *Fax*: +34 96 354 3241
Email: nacher@uv.es
* These authors have contributed equally to the present study.
† Present address: Presynaptic Plasticity Lab, Leibniz Institute for Neurobiology, Germany.

adhesion molecule (PSA-NCAM) and the perineuronal nets (PNNs) are interesting candidates to mediate these changes. These molecules have been both demonstrated to play a key role in synaptogenesis and neurite remodelling (Rutishauser, 2008; Howell and Gottschall, 2012). While PSA-NCAM is widely considered a marker of developing neurons, which expression decreases as development progresses (Probstmeier et al., 1994; Kurosawa et al., 1997; Oltmann-Norden et al., 2008), PNNs are considered indicators of neuronal maturation and, consequently, the number of neurons expressing these specialized regions of the extracellular matrix increases with age (McRae et al., 2007; Nowicka et al., 2009).

Fluoxetine treatment induces a similar type of juvenile plasticity in the adult amygdala, allowing the erasure of fear memories. This reopening of the critical period was correlated with an increase in the expression of PSA-NCAM and with a reduction of the ratio of PNNs expressing parvalbumin (Karpova et al., 2011). In agreement with this plasticity-promoting role, the enzymatic removal of these molecules has an impact on the critical period plasticity. Removal of PSA-NCAM accelerates the maturation of the visual cortex and the closure of the critical period (Di Cristo et al., 2007), while removal of PNNs delays this maturation and maintains open the critical period for a longer time (Pizzorusso et al., 2002). However, little is known of the effect of this antidepressant in the hippocampus or the mPFC, two regions critically involved in the aetiopathology of major depression.

It is interesting to note that both PSA-NCAM and PNNs are found in subsets of interneurons in the adult cerebral cortex. PNNs mainly appear surrounding parvalbumin expressing interneurons (Brückner et al., 1994), and PSA-NCAM is expressed mainly by calbindin expressing interneurons, although it is also found in a lower proportion in the somata of other interneuronal populations and in parvalbumin expressing perisomatic puncta surrounding pyramidal neurons (Gómez-Climent et al., 2010; Castillo-Gómez et al., 2011). This suggests that interneurons may play a key role in the structural plasticity induced by the antidepressant fluoxetine. In fact, a recent report has demonstrated that chronic treatment with fluoxetine alters GABA release from synapses formed by fast-spiking cells, resulting in the disruption of γ oscillations (Méndez et al., 2012).

Thus, in order to better understand how fluoxetine influences the structural plasticity and the connectivity of interneurons in the mPFC and the hippocampus, we have analysed the effects of fluoxetine on: (i) the ratio of PNNs surrounding PV interneurons, (ii) the expression of PSA-NCAM and synaptic molecules related to inhibitory neurotransmission in the neuropil, (iii) the perisomatic innervation of pyramidal and inhibitory neurons, and (iv) the structure of interneurons in these two cortical regions.

Method

Animal treatments

Twelve male GIN (GFP-expressing inhibitory neurons, Tg(GadGFP)45704Swn) (Oliva et al., 2000), three-month-old mice were used in this study. They were maintained in standard conditions of light (12 h cycles) and temperature, with no limit in the access to food or water. All animal experimentation was conducted in accordance with the Directive 2010/63/EU of the European Parliament and of the Council of 22 September 2010 on the protection of animals used for scientific purposes and was approved by the Committee on Bioethics of the Universitat de València. Every effort was made to minimize the number of animals used and their suffering. Mice received daily i.p. injections either with the antidepressant fluoxetine (n=6, 20 mg/kg), or with saline solution (n=6), over 14 days (once daily at 10.00 am). Previous studies have shown that this dose and length of treatment produces increases in the expression of plasticity-related molecules in the regions analysed (Umathe et al., 2011; Yu et al., 2011; Méndez et al., 2012). The day after these treatments, mice were perfused transcardially under deep chloral hydrate anaesthesia (4%, 0.01 ml/g), first with saline and then with 4% paraformaldehyde in sodium phosphate buffer (PB 0.1 M, pH 7.4). After perfusion, the brains were extracted and stored in PB 0.1 M and sodium azide 0.05%. The two hemispheres were separated, then one hemisphere was cut into 50 μm thick sections, while the other was cut into 100 μm thick sections, both with a vibratome (Leica VT 1000E, Leica). The sections were collected in six and three subseries, respectively, and stored at 4 °C in PB 0.1 M and sodium azide 0.05% until used.

Immunohistochemistry

Tissue was processed free-floating for fluorescence immunohistochemistry. Sections were washed in phosphate buffered saline (PBS), then slices were incubated in 10% normal donkey serum (NDS) (Abcys SA), 0.2% Triton-X100 (Sigma) in PBS for 1 h. Sections were then incubated for 48 h at 4 °C with different primary antibody cocktails diluted in PBS – 0.2% Triton-X100 (see Table 1). After washing, sections were incubated for 2 h at room temperature with different secondary antibody cocktails also diluted in PBS – 0.2% Triton-X100 (see Table 1). Finally, sections were washed in PB 0.1 M, mounted on slides and coverslipped using fluorescence mounting medium (Dako).

In the present study we used only commercial antibodies whose specificity was proved by the provider. Additionally, when the antigen used for generating the primary antibody was available, we first co-incubated them in accordance with the immunohistochemical protocol in order to block the binding of these antibodies to the tissue antigens. In the cases of anti-GAD6 and anti-CAMKII antibodies no access was available to the

Table 1. List of primary and secondary antibodies used in the study

	Dilution	Company
Primary antibodies		
Monoclonal mouse anti-PSA-NCAM	1:2000	Millipore
Polyclonal guinea pig antivesicular glutamate transporter 1	1:2000	Millipore
Polyclonal rabbit anti-synaptophysin	1:1000	Millipore
Monoclonal mouse anti-glutamic acid decarboxylase 65/67	1:500	DSHB
Polyclonal guinea pig anti-parvalbumin	1:2000	Synaptic Systems
Polyclonal chicken anti-GFP	1:1000	Millipore
WFA lectin biotin-conjugated	1:200	Sigma
Monocolonal mouse anti-CaMKII	1:500	Abcam
Secondary antibodies		
Goat anti-mouse A555-conjugated	1:400	Invitrogen
Donkey anti-rabbit A555-conjugated	1:400	Invitrogen
Goat anti-guinea pig A647-conjugated	1:400	Invitrogen
Donkey anti-chicken A488-conjugated	1:400	Invitrogen
Streptavidin A647-conjugated	1:400	Invitrogen
Donkey anti-mouse DL649-conjugated	1:400	Jackson
Donkey anti-mouse A488-conjugated	1:400	Invitrogen

antigens used for their generation. However, these antibodies are included in the JCN AntibodyDatabase: http://onlinelibrary.wiley.com/journal/10.1002/%28ISSN%2910969861/homepage/jcn_antibody_database.htm. The antibodies on this list have been described and characterized adequately according to the strict guidelines of the journal, including appropriate controls. The primary antibodies against VGLUT1 and PV were pre-adsorbed with the peptides used for their generation by their commercial source: AG208 (Millipore) and SySy 195-0P (synaptic systems), respectively. The primary antibody against SYN was pre-adsorbed with a synaptophysin recombinant protein (H00006855-P01, Novus). The antibody against PSA-NCAM was co-incubated with alpha-2,8-sialic acid (Colominic acid, Sigma). The performance of the immunohistochemical procedure using these blocked antibodies resulted in a total absence of immunostaining. The *Wisteria floribunda* lectin was pre-adbsorbed with N-Acetyl-D-galactosamine (Sigma, A2795). The performance of the histochemical procedure using this blocked lectin also resulted in a total absence of staining.

Analysis of immunoreactive puncta in single confocal planes

We analysed the density of puncta expressing different markers in single confocal planes (Olympus FV10i) of different regions of the mouse brain, as previously described (Guirado et al., 2012). We imaged an area located within layer V of the medial prefrontal cortex (mPFC). In this layer reside the pyramidal neurons that provide the main output projection of this region, which project extensively to the striatum (Lévesque and Parent, 1998). We analysed the different regions of the mPFC in two different sections: the prelimbic (PrL) and the infralimbic cortices (IL; in sections corresponding to Bregma +1.78 mm) and the ventral and dorsal cingulate cortices (Cg1 and Cg2 respectively; Bregma +1.1 mm). Different regions and strata of the hippocampus were also analysed (Bregma −2.18 mm): the hilus and the molecular layer of the dentate gyrus, the stratum lacunosum-moleculare, radiatum and oriens of CA1 and the stratum lucidum of CA3. Confocal *z*-stacks of the superficial layers of the slices, for optimal penetration levels for antibody recognition were selected.

On these planes, three small areas of the neuropil (505 μm^2) were selected for analysis, in order to avoid blood vessels and cell somata. Images were processed using ImageJ software. The background was subtracted with a rolling value of 50, converted to 8-bit deep images and binarized using a determined threshold value. This value depended on the marker and the area analysed and was kept the same for all images with the same marker and area. The images were then processed with a blur filter to reduce noise and separate closely apposed puncta. Finally, the number of the resulting dots per region was counted (Fig. S1).

Analysis of the density of perisomatic puncta

We analysed the density of puncta surrounding the cell somata of pyramidal neurons and interneurons using a similar methodology to that described above. In the mPFC, between 20 and 30 pyramidal neurons were imaged per animal in three different sections and similar numbers where analysed in the CA1 region of the hippocampus. However, only between 10 and 15 interneurons were counted per region (also both in the mPFC and the hippocampus), since their density was more limited. Images were processed using ImageJ. The profile of the plasmatic membrane of every soma was delimited manually, and then the selection was enlarged 1 μm in order to cover the area surrounding the somata. The selected area was processed for binarization as described above.

Analysis of spine density

To study the spine density of interneurons we selected individual dendrites from eGFP-expressing neurons in deep layers of the mPFC and in the CA1 region of the hippocampus. Stacks of confocal images were obtained with a 63×objective and an additional 3.5 digital zoom. The spines were counted in three dendritic fragments (around 60 μm each) expanding until 180 μm from the soma. The length of every dendritic fragment was measured and the data was expressed in density of spines per 10 μm.

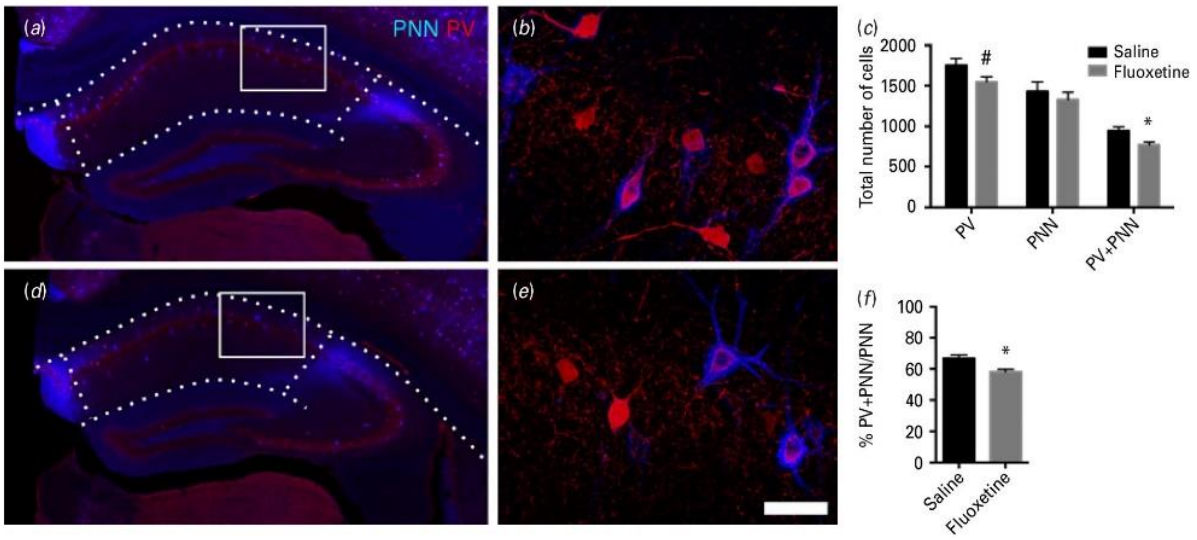

Fig. 1. Expression of PV and PNNs, after chronic fluoxetine treatment, in the hippocampus. (*a* & *d*): Single confocal planes showing the expression of PV and the presence of PNNs in the CA1 region of the hippocampus of mice treated either with saline (*a*) or fluoxetine (*d*). (*b* & *e*): Higher magnification microphotographs showing differences in the number of neurons co-expressing both markers. (*c* & *f*): Graphs showing the changes in cells expressing each of the markers, expressing both markers and the ratio of total PNNs surrounding PV-expressing neurons (Unpaired *T*-test, *p*-values: #<0.1, *<0.05). Scale bar 377 μm in A and D, 41 μm in (*b*) and (*e*). PNNs: perineuronal nets; PV: parvalbumin.

Estimation of number of cells

We also estimated the number of cells expressing parvalbumin (PV) or surrounded by perineuronal nets (PNN) as previously described (Nacher et al., 2002b). In brief, we analysed sections selected by a 1:6 fractionator sampling covering the whole rostral to caudal extension of the mPFC and the hippocampus CA1.

Statistics

We have used two-way ANOVAs to analyse the data whenever we had to consider more than one factor, as in the analysis of the density of immunoreactive puncta in different subregions or the density of spines at different distances from the soma. For comparing two means with only one factor, we used unpaired *t*-tests, as in the study of the perisomatic innervation and the total number of cells expressing PV, surrounded by PNNs, PV/PNNs positive cells, or the ratio of PNNs surrounding PV immunoreactive neurons. For all statistics the number of animals in each group was considered as the '*n*'.

Results

Chronic fluoxetine treatment alters the expression of plasticity-related molecules in interneurons of the mPFC and the hippocampus

We found that animals treated with fluoxetine displayed a non-significant trend towards a decreased number of PV-expressing interneurons in the CA1 region of the hippocampus (p=0.098; Fig. 1). In addition, the number of PV interneurons expressing PNNs was significantly reduced (p=0.014). Moreover, another parameter typically measured to evaluate the maturation degree of a cerebral region (Karpova et al., 2011) was also affected—the ratio of neurons surrounded by PNNs that co-expressed PV—was significantly reduced (p=0.016). In the mPFC of mice treated with fluoxetine we found a non-significant trend towards a decrease in the number of neurons surrounded by PNNs (p=0.094; Fig. 2) and a significant reduction in the number of PV interneurons expressing PNN (p=0.042). However, the ratio mentioned above was not affected in this region.

We found that after chronic fluoxetine treatment there are significant increases in the density of PSA-NCAM-expressing puncta in the strata lacunosum-moleculare (p=0.040; Fig. 3), radiatum (p=0.048) and oriens (p=0.002). Similar increases were found in the density of synaptophysin (SYN)-expressing puncta in the strata lucidum (p=0.045), moleculare (p=0.008), oriens (p=0.027) and radiatum (p=0.016). We also found a significant increase (p=0.016) in the density of glutamic acid decarboxylase 67/65 (GAD6)-expressing puncta in the hilus. However, we did not find any change in the density of the vesicular glutamate transporter 1 (VGluT1)-expressing puncta in any of the areas analysed. In the mPFC we only found a non-significant trend towards an increase in the density of neuropil-expressing PSA-NCAM (p=0.060; Fig. 3) and SYN (p=0.073) in the Cg2 region, in animals chronically treated with fluoxetine. Furthermore, we did not find any changes in the expression of GAD6 or of VGluT1 in any region of the mPFC.

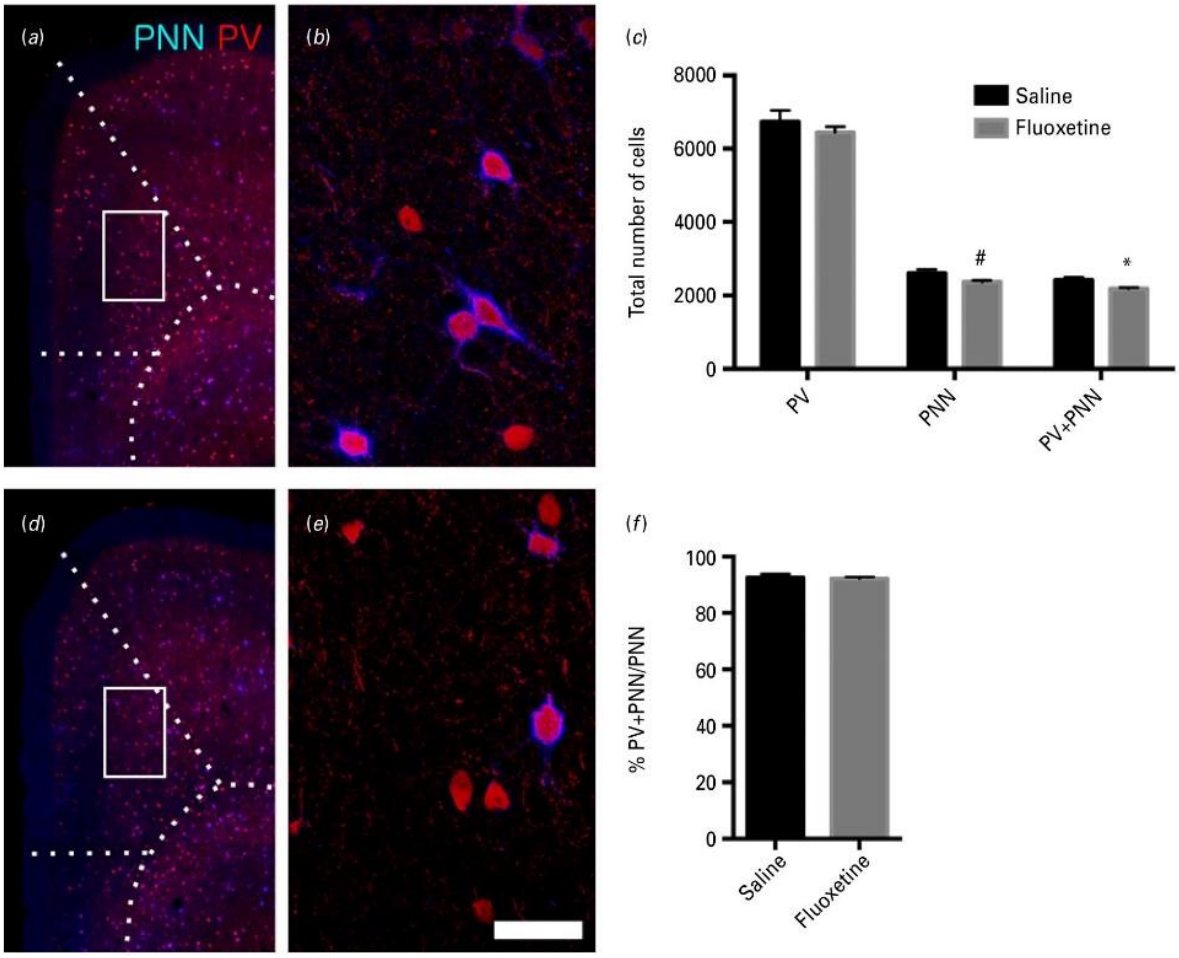

Fig. 2. Expression of PV and PNN after chronic fluoxetine treatment in the mPFC. (*a* & *d*): Single confocal planes showing the expression of PV and the presence of PNNs in the mPFC of mice treated either with saline (*a*) or fluoxetine (*d*). (*b* & *e*): Higher magnification microphotographs showing differences in the number of neurons co-expressing both markers. (*c* & *f*): Graphs showing the changes in cells expressing each of the markers, both markers and the ratio of total PNNs surrounding PV-expressing neurons (Unpaired *T*-test, *p*-values: #<0.1, *<0.05). Scale bar 286 μm in (*a*) and (*d*), 41 μm in (*b*) and (*e*). PNNs: perineuronal nets; PV: parvalbumin.

Chronic fluoxetine treatment increases the number of inhibitory perisomatic puncta on interneurons but not on pyramidal neurons

We analysed the density of PV positive puncta surrounding the somata of pyramidal neurons and its co-localization with SYN (Fig. 4). In the hippocampus we did not observe any change in the density of PV- or SYN- expressing puncta or in the density of PV puncta expressing SYN after fluoxetine treatment. However, in the mPFC we found a non-significant trend towards a decrease in the density of perisomatic-PV-puncta-expressing SYN (p=0.080; Fig. 4).

We observed an increase in the density of GAD6-expressing puncta surrounding the somata of interneurons expressing eGFP in the CA1 region of the hippocampus of animals treated with fluoxetine (p=0.015; Fig. 4). Although there were no changes in the density of puncta expressing SYN surrounding the somata of these interneurons, we also found an increase in the density of perisomatic-GAD6-puncta-expressing SYN (p=0.028; Fig. 4). However, in the mPFC we found no changes in the density of perisomatic puncta on interneurons.

Chronic fluoxetine treatment increases the dendritic spine density in interneurons of the mPFC

We described recently that this subpopulation of eGFP interneurons display spines on their dendrites (Gómez-Climent et al., 2010), whose dynamics are influenced by PSA-NCAM expression (Guirado et al., 2013). As some of these interneurons co-express PSA-NCAM, we studied both subpopulations: eGFP interneurons expressing PSA-NCAM and those lacking this molecule. We compared the dendritic spine density of interneurons expressing PSA-NCAM in animals treated with fluoxetine and those injected with saline and we found that, in our paradigm, fluoxetine does not affect the dendritic spine density of these interneurons in the

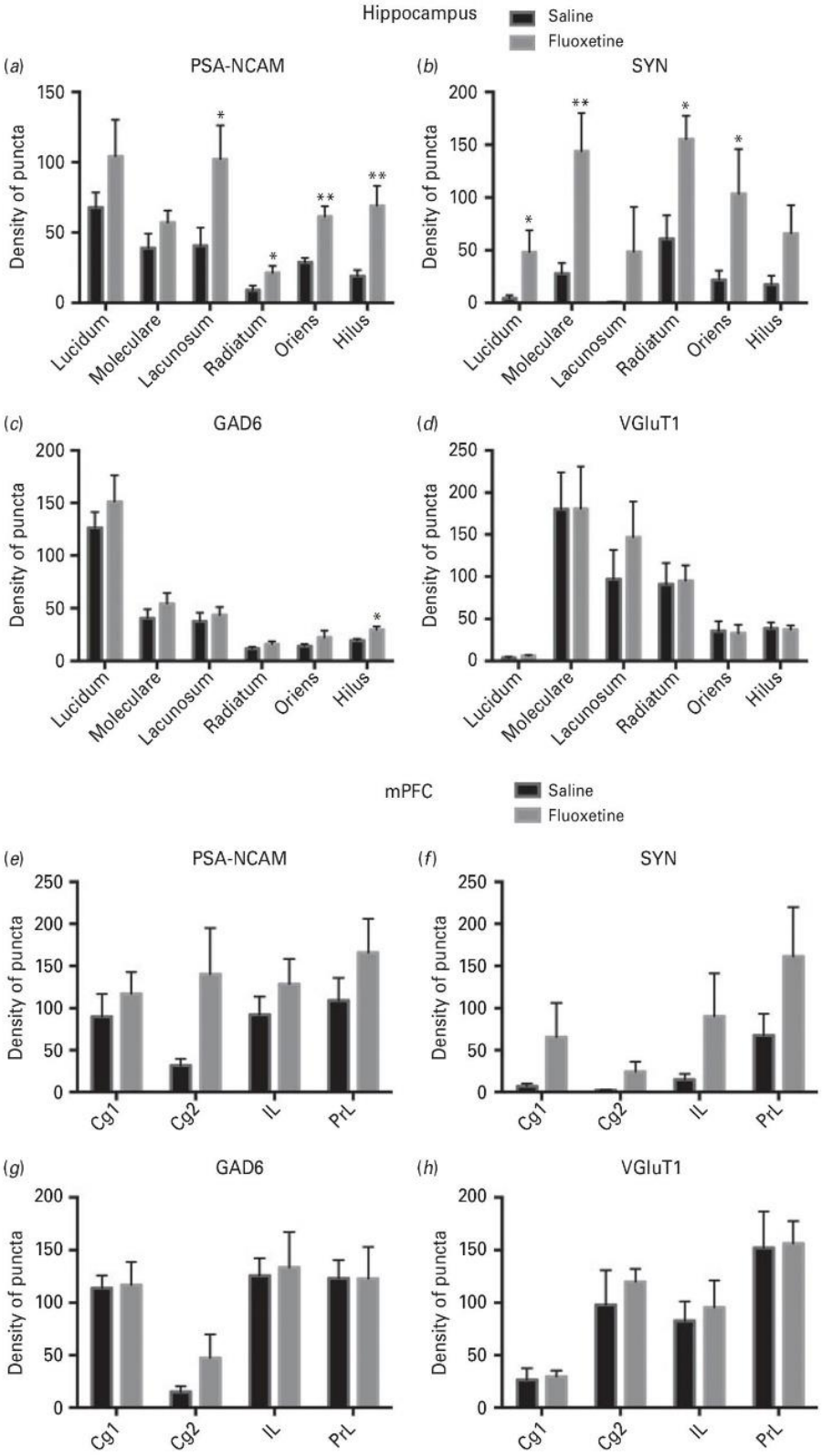

Fig. 3. Expression of molecules related to neuronal plasticity in the different strata of the hippocampus (*a–d*) and the mPFC (*e–h*). (*a*): Graphs showing the density of puncta-expressing PSA-NCAM. (*b*): Graphs showing the density of puncta-expressing SYN. (*c*): Graphs showing the density of puncta-expressing GAD6. (*d*): Graphs showing the density of puncta-expressing VGluT1 (One-way ANOVA, *p*-values: *<0.05, **<0.01). (*e*): Graphs showing the density of puncta-expressing PSA-NCAM. (*f*): Graphs showing the density of puncta-expressing SYN. (*g*): Graphs showing the density of puncta-expressing GAD6. (*h*): Graphs showing the density of puncta-expressing VGluT1. (One-way ANOVA, *p*-values: #<0.1). GAD6: Glutamic acid decarboxylase 65/67; SYN: synaptophysin; VGluT1: vesicular glutamate transporter 1.

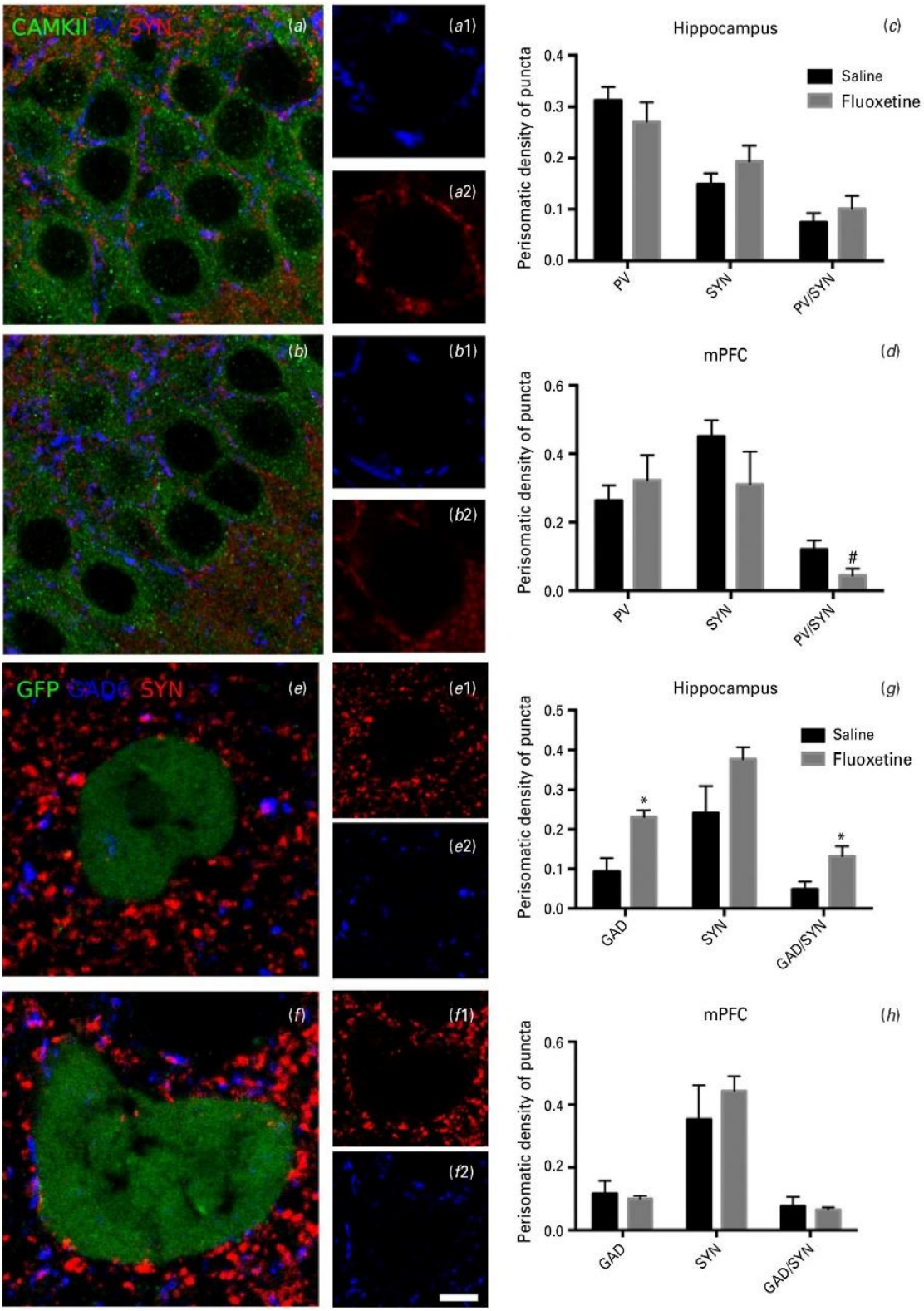

Fig. 4. (*a* & *b*): Effects of chronic fluoxetine treatment on the perisomatic innervation of pyramidal neurons. Single confocal planes of the CA1 stratum pyramidale of the hippocampus showing CAMKIIα-expressing pyramidal neuron somata (green) and perisomatic-puncta-expressing PV (blue) or SYN (red) in saline (*a*) and fluoxetine treated (*b*) mice. (*a1–a2* & *b1–b2*): Single confocal planes showing PV- (*a1, b1*), and SYN- (*a2, b2*) expressing puncta surrounding the somata of a pyramidal neuron of saline (*a* series) and fluoxetine treated (*b* series) mice. (*c* & *d*): Histograms showing the perisomatic density of the puncta-expressing the different markers surrounding pyramidal neurons in the hippocampus and the mPFC. (Unpaired *T*-test, *p*-values: #<0.1). (*e* & *f*): Effects of chronic fluoxetine treatment on the perisomatic innervation of interneurons. Single confocal planes of eGFP-expressing interneurons

hippocampus. Similarly, we did not find changes when comparing eGFP-expressing interneurons lacking PSA-NCAM, after fluoxetine treatment. However, we replicated our previous results, confirming that interneurons expressing PSA-NCAM have a reduced dendritic spine density compared with interneurons lacking this molecule (Fig. S2).

However, in the mPFC, where eGFP-expressing interneurons always lack PSA-NCAM expression, we found that animals treated with fluoxetine had a significant increase in dendritic spine density in these interneurons ($p=0.005$). When analysing the different segments, we found that these changes were especially more intense in the distal segment of the dendrites ($p=0.008$; Fig. 5).

Discussion

In the current study, we described the effects of chronic treatment with fluoxetine on different parameters affecting inhibitory networks in the hippocampus and the mPFC. This antidepressant increases the number of inhibitory perisomatic puncta on interneurons, but not on pyramidal neurons, and increases the density of dendritic spines in interneurons of the mPFC. Fluoxetine induces these changes in inhibitory networks and through putative mechanisms alters the expression of the polysialylated form of the neural cell adhesion molecule (PSA-NCAM) and the number of perineuronal nets (PNNs). Both molecules (PSA-NCAM and PNNs) play an important role in the plasticity associated with the development and closure of critical period plasticity, are mainly associated with interneurons in the adult cerebral cortex and are considered markers of neuronal development and of neuronal maturation, respectively.

We have found that the chronic fluoxetine treatment used in our study does not induce significant alterations in the density of perisomatic puncta on the mPFC pyramidal neurons, although there was a trend for a decrease in the number of puncta co-expressing PV and SYN. These results are in contrast to those of a recent report, which has found that chronic treatment with fluoxetine alters GABA release from synapses formed by hippocampal fast-spiking cells, resulting in the disruption of γ oscillations (Méndez et al., 2012). It is possible that the lack of significant differences in the density of perisomatic puncta found in our study may be due to the fact that, despite the fact that the doses used were the same, our mice were treated with fluoxetine for two weeks only while the rats in Méndez et al. (2012) study received the treatment for three weeks.

We found that, similar to pyramidal neurons, the somata of interneurons expressing eGFP are also surrounded by puncta expressing the inhibitory marker GAD6 and that chronic fluoxetine treatment induces a dramatic increase in the density of these perisomatic puncta in the hippocampus, but not in the mPFC. Although the co-localization with synaptophysin indicates that these perisomatic inhibitory puncta may correspond to active synapses, it is still complicated to discuss the functional implications of their increase via fluoxetine. It would be necessary to perform new experiments including electron microscopy to clarify which subpopulation/s are affected by this putative increase in perisomatic inhibition.

Our study shows for the first time that chronic treatment with fluoxetine alters the structure of interneurons. Previous studies have demonstrated that fluoxetine treatment increases the dendritic spine density in pyramidal neurons of the hippocampus (Hajszan et al., 2005) and the somatosensory cortex (Guirado et al., 2009), but there is no information on its effect on the mPFC. We found that fluoxetine induces an increase in the density of dendritic spines in eGFP-labelled interneurons in the mPFC, but not in those of the hippocampal CA1 region. A recent report by our laboratory has revealed that these spines receive mainly excitatory synapses (Guirado et al., 2013). In the mPFC of the strain of mice used in the present study, eGFP-labelled interneurons correspond to Martinotti cells (Gilabert-Juan et al., 2013), which innervate the distal portion of the dendritic arbour of pyramidal neurons (Markram et al., 2004). If the new synapses that these interneurons receive on their spines are functional, then they may enhance the excitatory input that these interneurons receive and, in turn, enhance the inhibition produced on mPFC pyramidal neurons. This would be in accordance with previous reports describing increased expression of molecules involved in inhibitory neurotransmission in rats chronically treated with fluoxetine (Varea et al., 2007a; Guirado et al., 2012; Tiraboschi et al., 2013). Since a previous report has described decreased cortical inhibition in the visual cortex of rats chronically treated with fluoxetine (Maya-Vetencourt et al., 2008), it is possible that the changes in the structure of interneurons and the

located in the CA1 region of the hippocampus showing eGFP in their somata (green) and perisomatic-puncta-expressing GAD6 (blue) or SYN (red) in saline (*e*) and fluoxetine treated (*f*) mice. (*e1–e2* & *f1–f2*): Single confocal planes showing SYN- (*e1, f1*) and GAD6- (*e2, f2*) expressing puncta surrounding the somata of an eGFP-expressing interneuron of saline (*e* series) and fluoxetine treated (*f* series) mice. (*g* & *h*): Histograms showing the perisomatic density of the puncta-expressing the different markers surrounding eGFP-expressing interneurons in the hippocampus and the mPFC. (Unpaired *T*-test, *p*-values: *<0.05). Scale bar 5 μm in (*a*) and (*b*), 2.5 μm in (*a1–a2* and *b1–b2*), 20 μm in (*e*) and (*f*), 6.4 μm in (*e1–e2* and *f1–f2*). CAMKIIα: anti-a subunit of the Ca2 +/calmodulin dependent protein kinase II; GAD6: glutamic acid decarboxylase 65/67; PV: parvalbumin; SYN: synaptophysin.

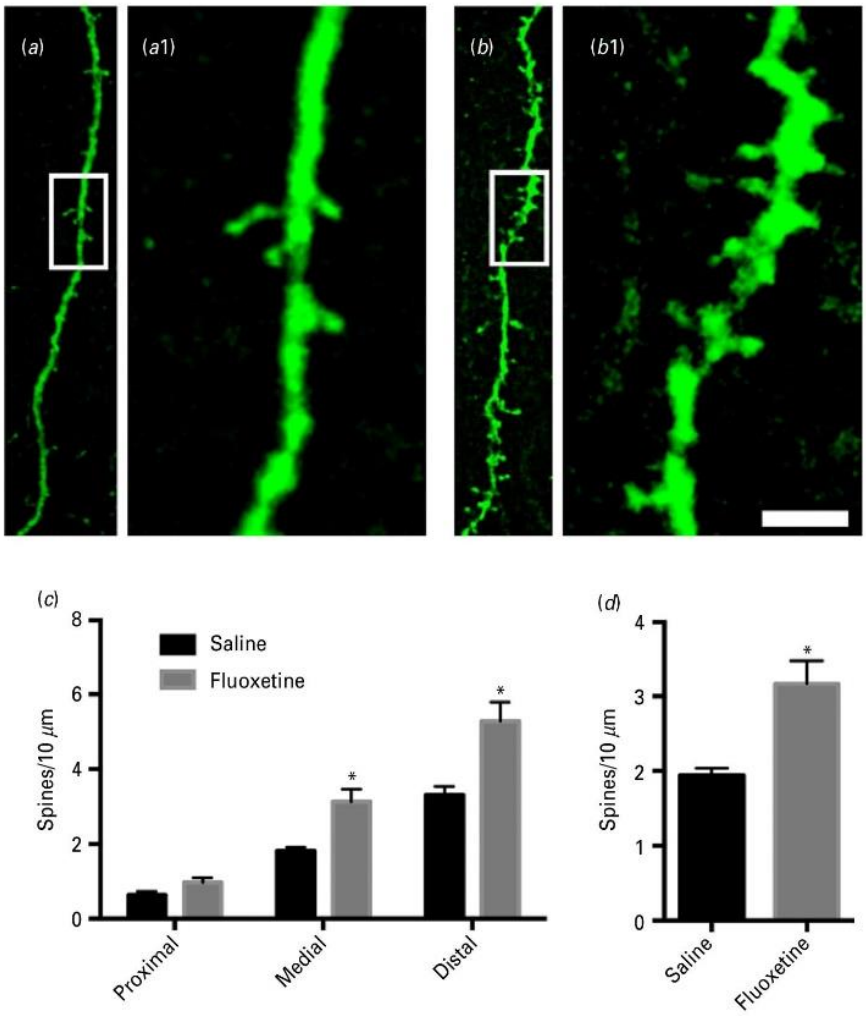

Fig. 5. Effects of fluoxetine on the spine density of interneurons in the mPFC. (*a* & *b*): Reconstruction of focal planes showing a dendrite carrying spines of an eGFP-expressing interneuron of animals treated with saline (*a*) or fluoxetine (*b*). (*a1* & *b1*): Higher magnification images showing the difference in dendritic spine density observed between both groups. (*c*): Histograms showing the dendritic spine density per 10 μm at three different segments of 60 μm each, considering their distance to the cell soma. (*d*): Graph showing the total spine density after fluoxetine treatment. (Two-way ANOVA; *p*-values *<0.05). Scale bar 8 μm in (*a*) and (*b*), 2.1 μm in (*a1* and *b1*).

expression of molecules related to inhibitory neurotransmission correspond to a compensatory mechanism.

We also confirm that this increase in the expression of molecules related to cortical inhibition in the hippocampus and mPFC is correlated with significant increases in SYN and PSA-NCAM (Varea et al., 2007a, b; Guirado et al., 2012) suggesting the formation of new inhibitory synapses after fluoxetine treatment. In fact, previous studies from our laboratory have demonstrated that PSA-NCAM is exclusively expressed by a subpopulation of interneurons in the mPFC of both humans and mice (Varea et al., 2005, 2007a). In the hippocampus PSA-NCAM is found in a subpopulation of interneurons (Nacher et al., 2002a; Gómez-Climent et al., 2010) but is also intensely expressed in the axons of a subset of granule neurons (Seki and Arai, 1999). In the rest of hippocampal structures, PSA-NCAM expression is mainly restricted to inhibitory elements (Gómez-Climent et al., 2010). Interestingly, interneurons expressing PSA-NCAM showed more reduced density of synaptic inputs, dendritic arborisation and dendritic spine density (corroborated in the present study, Fig. S2) compared to interneurons lacking this molecule (Gómez-Climent et al., 2010). However, its long-term specific ablation decreases the spine density of interneurons (Guirado et al., 2013). Indicating that an altered expression of PSA-NCAM, as that found after fluoxetine treatments (Varea et al., 2007a; Karpova et al., 2011; Guirado et al., 2012), might influence the structure of interneurons.

However, the present results suggest that PSA-NCAM may not be directly implicated in the structural changes we have described in the mPFC interneurons. The GAD67- EGFP expressing interneurons in which the structural features have been analysed normally do not show PSA-NCAM expression in their somata, neurites or in the puncta located in their projection fields in layers

I and II (Gilabert-Juan et al., 2013). Moreover, we did not find an increase in the expression of PSA-NCAM in the mPFC as we expected (only a non-significant trend). This contrast in the ability to up-regulate PSA-NCAM expression after fluoxetine treatment between hippocampal and mPFC interneurons may be due to differences in the phenotype (differential expression of calcium binding proteins and neuropeptides) of these subsets of inhibitory neurons. In fact, in control animals the interneurons that express PSA-NCAM in basal conditions belong to different phenotypic subpopulations in these two regions (Gómez-Climent et al., 2010).

Finally, we found significant reductions in the number of PV-expressing interneurons surrounded by PNN, both in the mPFC and the CA1 region of the hippocampus. This is in accordance with a previous report, which found similar reductions in the CA1 region and the basolateral amygdala (Karpova et al., 2011). The presence of PNNs is considered a marker of the maturation degree of PV-expressing interneurons and, in fact, the appearance of PNNs during late development has been used as an indication of critical period closure (Hensch, 2005; Bavelier et al., 2010; Yamada and Jinno, 2013), in which PV-expressing interneurons and their afferent connections play a critical role. In fact, removal of PNNs produces a dematuration of the axonal boutons innervating the pyramidal neurons, which results in a reopening of the critical periods (McRae et al., 2007; Nowicka et al., 2009). These results suggest that this same type of plasticity might be occurring in the mPFC and hippocampus after fluoxetine treatment. However, as mentioned above, we only found a non-significant trend for a decrease in the density of perisomatic puncta expressing PV and SYN in the mPFC and no changes in the hippocampus, suggesting that, despite its effects on PNNs, the duration of this chronic fluoxetine treatment (two weeks) is not sufficient to induce changes in the perisomatic innervation of pyramidal neurons.

Summarizing, the effects of antidepressants, affecting the structure and connectivity of certain interneuronal subpopulations, probably through the alteration in the specific expression of PSA-NCAM in interneurons and the relationship of these inhibitory cells with PNNs, may induce a window of plasticity resembling that of the critical periods. These changes may contribute in reverting the alterations of GABAergic neurotransmission in major depression patients (Sanacora et al., 2002, 2004) and, consequently, new therapeutic approaches directed to the modulation of PNNs or PSA-NCAM may constitute promising strategies to the development of innovative antidepressant drugs.

Supplementary material

For supplementary material accompanying this paper, visit http://dx.doi.org/10.1017/S1461145714000406.

Acknowledgments

Spanish Ministry of Economy and Competitiveness BFU2012-32512, MICINN-PIM2010ERN-00577/NEUCONNECT in the frame of ERA-NET NEURON, Generalitat Valenciana ACOMP/ 2012/229 and Prometeo Excellence Program PROMETEO2013/069 and the Fundación Alicia Koplowitz to JN. RG had a FPI pre-doctoral fellowship from the Spanish Ministry of Education and Science (BES 2007-15757). MPR had a FPU pre-doctoral fellowship from the Spanish Ministry of Economy and Competitiviness (FPU12/03200). EC is supported by the ERC (Project Number: 322742 iPlasticity), Sigrid Juselius Foundation and Academy of Finland Centre of Excellence program.

Statement of Interest

None.

References

Bavelier D, Levi DM, Li RW, Dan Y, Hensch TK (2010) Removing brakes on adult brain plasticity: from molecular to behavioral interventions. J Neurosci 30:14964–14971.

Brückner G, Seeger G, Brauer K, Härtig W, Kacza J, Bigl V (1994) Cortical areas are revealed by distribution patterns of proteoglycan components and parvalbumin in the Mongolian gerbil and rat. Brain Res 658:67–86.

Castillo-Gómez E, Varea E, Blasco-Ibáñez JM, Crespo C, Nacher J (2011) Polysialic acid is required for dopamine D2 receptor-mediated plasticity involving inhibitory circuits of the rat medial prefrontal cortex. PLoS ONE 6:e29516.

Castrén E (2005) Is mood chemistry? Nat Rev Neurosci 6:241–246.

Chen JL, Lin WC, Cha JW, So PT, Kubota Y, Nedivi E (2011) Structural basis for the role of inhibition in facilitating adult brain plasticity. Nat Neurosci 14:587–594.

Di Cristo G, Chattopadhyaya B, Kuhlman SJ, Fu Y, Bélanger M-C, Wu CZ, Rutishauser U, Maffei L, Huang ZJ (2007) Activity-dependent PSA expression regulates inhibitory maturation and onset of critical period plasticity. Nat Neurosci 10:1569–1577.

Dityatev A, Schachner M, Sonderegger P (2010) The dual role of the extracellular matrix in synaptic plasticity and homeostasis. Nat Rev Neurosci 11:735–746.

Duman RS, Malberg J, Nakagawa S, D'Sa C (2000) Neuronal plasticity and survival in mood disorders. Biol Psychiat 48:732–739.

Gilabert-Juan J, Castillo-Gomez E, Guirado R, Moltó MD, Nacher J (2013) Chronic stress alters inhibitory networks in the medial prefrontal cortex of adult mice. Brain Struct Funct 218:1591–1605.

Gómez-Climent MÁ, Guirado R, Castillo-Gómez E, Varea E, Gutierrez-Mecinas M, Gilabert-Juan J, García-Mompó C, Vidueira S, Sanchez-Mataredona D, Hernández S, Blasco-Ibáñez JM, Crespo C, Rutishauser U, Schachner M, Nacher J (2010) The polysialylated form of the neural cell adhesion molecule (PSA-NCAM) is expressed in a subpopulation of mature cortical interneurons characterized

by reduced structural features and connectivity. Cereb Cortex 21:1028–1041.

Guirado R, Varea E, Castillo-Gómez E, Gómez-Climent MA, Rovira-Esteban L, Blasco-Ibáñez JM, Crespo C, Martínez-Guijarro FJ, Nàcher J (2009) Effects of chronic fluoxetine treatment on the rat somatosensory cortex: activation and induction of neuronal structural plasticity. Neurosci Lett 457:12–15.

Guirado R, Sanchez-Matarredona D, Varea E, Crespo C, Blasco-Ibáñez JM, Nacher J (2012) Chronic fluoxetine treatment in middle-aged rats induces changes in the expression of plasticity-related molecules and in neurogenesis. BMC Neurosci 13:5.

Guirado R, Perez-Rando M, Sanchez-Matarredona D, Castillo-Gómez E, Liberia T, Rovira-Esteban L, Varea E, Crespo C, Blasco-Ibáñez JM, Nacher J (2013) The dendritic spines of interneurons are dynamic structures influenced by PSA-NCAM expression. Cereb Cortex. Epub ahead of print. Retrieved 17 June 2013. Doi:10.1093/cercor/bht156.

Hajszan T, MacLusky NJ, Leranth C (2005) Short-term treatment with the antidepressant fluoxetine triggers pyramidal dendritic spine synapse formation in rat hippocampus. Eur J Neurosci 21:1299–1303.

Hensch TK (2005) Critical period plasticity in local cortical circuits. Nat rev Neurosci 6:877–888.

Howell MD, Gottschall PE (2012) Lectican proteoglycans, their cleaving metalloproteinases, and plasticity in the central nervous system extracellular microenvironment. Neuroscience 217:6–18.

Karpova NN, Pickenhagen A, Lindholm J, Tiraboschi E, Kulesskaya N, Agustsdottir A, Antila H, Popova D, Akamine Y, Sullivan R, Hen R, Drew LJ, Castren E (2011) Fear erasure in mice requires synergy between antidepressant drugs and extinction training. Science 334:1731–1734.

Kobayashi K, Ikeda Y, Sakai A, Yamasaki N, Haneda E, Miyakawa T, Suzuki H (2010) Reversal of hippocampal neuronal maturation by serotonergic antidepressants. Proc Natl Acad Sci USA 107:8434–8439.

Kurosawa N, Yoshida Y, Kojima N, Tsuji S (1997) Polysialic acid synthase (ST8Sia II/STX) mRNA expression in the developing mouse central nervous system. J Neurochem 69:494–503.

Lévesque M, Parent A (1998) Axonal arborization of corticostriatal and corticothalamic fibers arising from prelimbic cortex in the rat. Cereb Cortex 8:602–613.

Malberg JE, Eisch AJ, Nestler EJ, Duman RS (2000) Chronic antidepressant treatment increases neurogenesis in adult rat hippocampus. J Neurosci 20:9104–9110.

Markram H, Toledo-rodriguez M, Wang Y, Gupta A, Silberberg G, Wu C (2004) Interneurons of the neocortical inhibitory system. Nat Rev Neurosci 5:793–807.

Maya-Vetencourt JF, Sale A, Viegi A, Baroncelli L, De Pasquale R, O'Leary OF Castrén E, Maffei L (2008) The antidepressant fluoxetine restores plasticity in the adult visual cortex. Science 320:385–388.

McRae PA, Rocco MM, Kelly G, Brumberg JC, Matthews RT (2007) Sensory deprivation alters aggrecan and perineuronal net expression in the mouse barrel cortex. J Neurosci 27:5405–5413.

Méndez P, Pazienti A, Szabó G, Bacci A (2012) Direct alteration of a specific inhibitory circuit of the hippocampus by antidepressants. J Neurosci 32:16616–16628.

Nacher J, Blasco-Ibáñez JM, McEwen BS (2002a) Non-granule PSA-NCAM immunoreactive neurons in the rat hippocampus. Brain Res 930:1–11.

Nacher J, Lanuza E, McEwen BS (2002b) Distribution of PSA-NCAM expression in the amygdala of the adult rat. Neuroscience 113:479–484.

Nowicka D, Soulsby S, Skangiel-Kramska J, Glazewski S (2009) Parvalbumin-containing neurons, perineuronal nets and experience-dependent plasticity in murine barrel cortex. Eur J Neurosci 30:2053–2063.

Oliva AA, Jiang M, Lam T, Smith KL, Swann JW (2000) Novel hippocampal interneuronal subtypes identified using transgenic mice that express green fluorescent protein in GABAergic interneurons. J Neurosci 20:3354–3368.

Oltmann-Norden I, Galuska SP, Hildebrandt H, Geyer R, Gerardy-Schahn R, Geyer H, Mühlenhoff M (2008) Impact of the polysialyltransferases ST8SiaII and ST8SiaIV on polysialic acid synthesis during postnatal mouse brain development. J Biol Chem 283:1463–1471.

Pizzorusso T, Medini P, Berardi N, Chierzi S, Fawcett JW, Maffei L (2002) Reactivation of ocular dominance plasticity in the adult visual cortex. Science 298:1248–1251.

Probstmeier R, Bilz A, Schneider-Schaulies J (1994) Expression of the neural cell adhesion molecule and polysialic acid during early mouse embryogenesis. J Neurosci Res 37:324–335.

Rubio FJ, Ampuero E, Sandoval R, Toledo J, Pancetti F, Wyneken U (2013) Long-term fluoxetine treatment induces input-specific LTP and LTD impairment and structural plasticity in the CA1 hippocampal subfield. Front Cell Neurosci 7:66.

Rutishauser U (2008) Polysialic acid in the plasticity of the developing and adult vertebrate nervous system. Nat Rev Neurosci 9:26–35.

Sanacora G, Mason GF, Rothman DL, Krystal JH (2002) Increased occipital cortex GABA concentrations in depressed patients after therapy with selective serotonin reuptake inhibitors. Am J Psychiat 159:663–665.

Sanacora G, Berman RM, Cappiello A, Oren DA, Kugaya A, Liu N, Gueorguieva R, Fasula D, Charney DS (2004) Addition of the alpha2-antagonist yohimbine to fluoxetine: effects on rate of antidepressant response. Neuropsychopharmacol 29:1166–1171.

Sandi C (2004) Stress, cognitive impairment and cell adhesion molecules. Nat Rev Neurosci 5:917–930.

Seki T, Arai Y (1999) Different polysialic acid-neural cell adhesion molecule expression patterns in distinct types of mossy fiber boutons in the adult hippocampus. J Comp Neurol 410:115–125.

Tiraboschi E, Guirado R, Greco D, Auvinen P, Maya-Vetencourt JF, Maffei L, Castrén E (2013) Gene expression patterns underlying the reinstatement of plasticity in the adult visual system. Neural Plast 2013:605079.

Umathe SN, Manna SSS, Jain NS (2011) Involvement of endocannabinoids in antidepressant and anti-compulsive effect of fluoxetine in mice. Behav Brain Res 223:125–134.

Varea E, Nácher J, Blasco-Ibáñez JM, Gómez-Climent MA, Castillo-Gómez E, Crespo C, Martínez-Guijarro FJ (2005) PSA-NCAM expression in the rat medial prefrontal cortex. Neuroscience 136:435–443.

Varea E, Blasco-Ibáñez JM, Gómez-Climent MA, Castillo-Gómez E, Crespo C, Martínez-Guijarro FJ, Nácher J

(2007a) Chronic fluoxetine treatment increases the expression of PSA-NCAM in the medial prefrontal cortex. Neuropsychopharmacol 32:803–812.

Varea E, Castillo-Gómez E, Gómez-Climent MA, Blasco-Ibáñez JM, Crespo C, Martínez-Guijarro FJ, Nácher J (2007b) Chronic antidepressant treatment induces contrasting patterns of synaptophysin and PSA-NCAM expression in different regions of the adult rat telencephalon. Eur Neuropsychopharm 17:546–557.

Yamada J, Jinno S (2013) Spatio-temporal differences in perineuronal net expression in the mouse hippocampus, with reference to parvalbumin. Neuroscience 253C:368–379.

Yu H-L, Deng X-Q, Li Y-J, Li Y-C, Quan Z-S, Sun X-Y (2011) N-palmitoylethanolamide, an endocannabinoid, exhibits antidepressant effects in the forced swim test and the tail suspension test in mice. Pharmacol Rep PR 63:834–839.

4. The activation of NMDA receptors alters the structural dynamics of hippocampal interneurons

The Activation of NMDA Receptors Alters the Structural Dynamics of Hippocampal Interneurons

Perez-Rando M.[1], Castillo-Gomez E.[1], Belles M[1]., Carceller H[1]., Nacher J[1,2,3*].

1. Neurobiology Unit, Cell Biology Dpt., Interdisciplinary Research Structure for Biotechnology and Biomedicine (BIOTECMED), Universitat de València, Spain

2. CIBERSAM: Spanish National Network for Research in Mental Health

3. Fundación Investigación Hospital Clínico de Valencia, INCLIVA, Spain

*CORRESPONDING AUTHOR: Dr. Juan Nacher, Neurobiology Unit, Cell Biology Dpt., Universitat de València. Dr. Moliner, 50. Burjassot, 46100. Spain. Telf: 34 96 354 3241. e-mail: nacher@uv.es

ABSTRACT

N-Methyl-D-Aspartate receptors (NMDARs) are present in both pyramidal neurons and interneurons of the hippocampus. These receptors play a key role in the structural plasticity of excitatory neurons in the adult brain, but to date little is known about their influence on the remodelling of interneurons. Among hippocampal interneurons, the somatostatin expressing cells in the CA1 stratum oriens are of special interest because of their functional importance and structural characteristics: they display dendritic spines, which change their density in response to different stimuli. In order to understand the role of NMDAR activation on the structural dynamics of these interneurons, we have studied entorhino-hippocampal cultures of mice in which this subpopulation express constitutively EGFP, and have imaged the same neurons in real-time. We have acutely infused the culture with NMDA, a strong NMDAR agonist, and have analysed the structural dynamics of somatostatin expressing interneurons, prior and after its administration. There were several alterations of their dynamic parameters: the appearance and disappearance rates of their dendritic spines increased 24 hours after the NMDA infusion and returned to baseline levels 48 hours afterwards, whereas their stability rate decreased in this same time point and also returned to control levels after 48 hours. The relative density of dendritic spines remained unaltered throughout the assay. Altogether, our results help to shed light on how NMDARs modulate the structural dynamics of interneurons. This is especially important because of the involvement of these receptors in neuronal potentiation/depression, and their putative role in the etiopathology of certain neuropsychiatric disorders, such as schizophrenia.

INTRODUCTION

NMDA receptors (NMDARs) have been extensively studied regarding neural potentiation and synaptic plasticity (Volianskis et al. 2015). These receptors also play crucial roles in different neurodevelopmental events, such as neurogenesis, neuronal migration and synaptogenesis (Contestabile 2000). In recent years, we have learnt that some of these plastic events persist during adulthood and that they are important contributors to cognition and to the response of the brain to aversive experiences. Neurons in the adult brain can modify their morphology and connectivity in response to different stimuli, especially by altering the complexity of their dendritic arbor and the density of their dendritic spines. These postsynaptic structures have been mainly studied in pyramidal neurons, although they are also present in some interneuronal populations (Freund and Buzsáki 1996). Furthermore, they have been found to be proper markers for neural activity as they increase their density when the neuron is potentiated (Engert and Bonhoeffer 1999).

However, the study of changes in spine density does not always provide all the information on the structural plasticity of these elements. In fact, events that result in null alterations in this density can also affect the

network by changing the synaptic configuration: the appearance of one spine in one site –and its new synapse- can structurally shadow the disappearance of another spine elsewhere, but the new connection still represents novel information. This has been commonly known as structural dynamics, and it appears to be the force underlying adaptation in the nervous system (Holtmaat et al. 2006; Chen et al. 2012). Structural remodelling of excitatory (Holtmaat and Svoboda 2009) and inhibitory (Chen and Nedivi 2013) microcircuits can be observed in real-time after sensory deprivation. However, studies directed to observe this plasticity *in vivo* can only be performed in the neocortex, due to the limitations of the method: imaging through a cranial window. This restriction limits the study of other important areas, such as the hippocampus. Entorhino-hippocampal organotypic cultures, with their intrinsic limitations, are an alternative to solve this issue. They allow us to follow the same neuron and report changes in real-time. Furthermore, they have been broadly used as an *in vitro* model of the rodent hippocampus (Stoppini et al. 1991).

Most structural studies focus on the morphology of excitatory neurons and leave aside inhibitory circuits and interneurons, important players on the central nervous system physiology. Reports on dendrite-targeting interneurons are particularly scarce, specifically on somatostatin (SOM) expressing cells. These interneurons are critical for the maturation of deep cortical circuits (Tuncdemir et al. 2016) and are important players in other stages of neurodevelopment, brain pathology and neuronal plasticity (for a review see Liguz-Lecznar et al., 2016). In addition, their structure is altered after different manipulations, such as chronic stress (Gilabert-Juan et al. 2011), antidepressant treatment (Guirado et al. 2014a), streptozotocin-diabetic challenge (Castillo-Gómez et al. 2015) or the depletion of plasticity related molecules (Guirado et al. 2014b). In the hippocampus, specifically in the *stratum oriens, two subpopulations of* SOM expressing interneurons can be found: those projecting to extrahippocampal areas, such as the HS cells (Gulyás et al. 2003) and those projecting locally to the *stratum lacunosum moleculare.* These hippocampal interneurons are essential for the proper functioning of the hippocampus (Müller and Remy 2014) and their dendrites present dynamic dendritic spines (Guirado et al. 2014b).

Glutamate NMDARs are widely expressed in both pyramidal neurons and interneurons, including the SOM expressing cells of the *stratum oriens* (Nyíri et al. 2003). The pyramidal neurons of knock-out mice lacking these receptors show altered neuromorphological characteristics, such as modifications in the size and density of their dendritic spines and axonal *boutons* (Ultanir et al. 2007). However, little is known about the role of these receptors in interneuronal structure and dynamics.

In the present study, we aim to understand the impact of NMDAR manipulation on the structural dynamics of SOM expressing interneurons in the *stratum oriens* of the hippocampal CA1 region. In order to achieve our goal, we have used a transgenic mice strain with these interneurons constitutively labelled with EGFP, which allows us to study their entire morphology (Oliva et al. 2000). Using organotypic cultures, we have studied their structure under the confocal microscope in real-time and have determined how acute NMDA administration alters the dynamic parameters of these cells.

MATERIAL AND METHODS

Animals and treatment

For the real-time in vitro analyses we have used the EGFP-expressing inhibitory neurons (GIN) Tg(GadGFP)45704Swn mice (Jackson laboratories, Bar Harbor, Maine, USA) (Oliva et al. 2000). Six GIN pups (P7) were used to prepare hippocampal-entorhinal organotypic cultures (Stoppini et al. 1991). NMDA (10 µM in culture media) was added to the media after the second imaging session and remained there for 1 hour (figure 1A).

All the animals were maintained in standard conditions of light (12h cycles) and temperature, without restrictions in food and water. All animal experimentation was conducted in accordance with the Directive 2010/63/EU of the European Parliament and of the Council of 22 September 2010 on the protection of animals used for scientific purposes and was approved by the Committee on Bioethics of the Universitat de València. Every effort was made to minimize the number of animals used and their suffering.

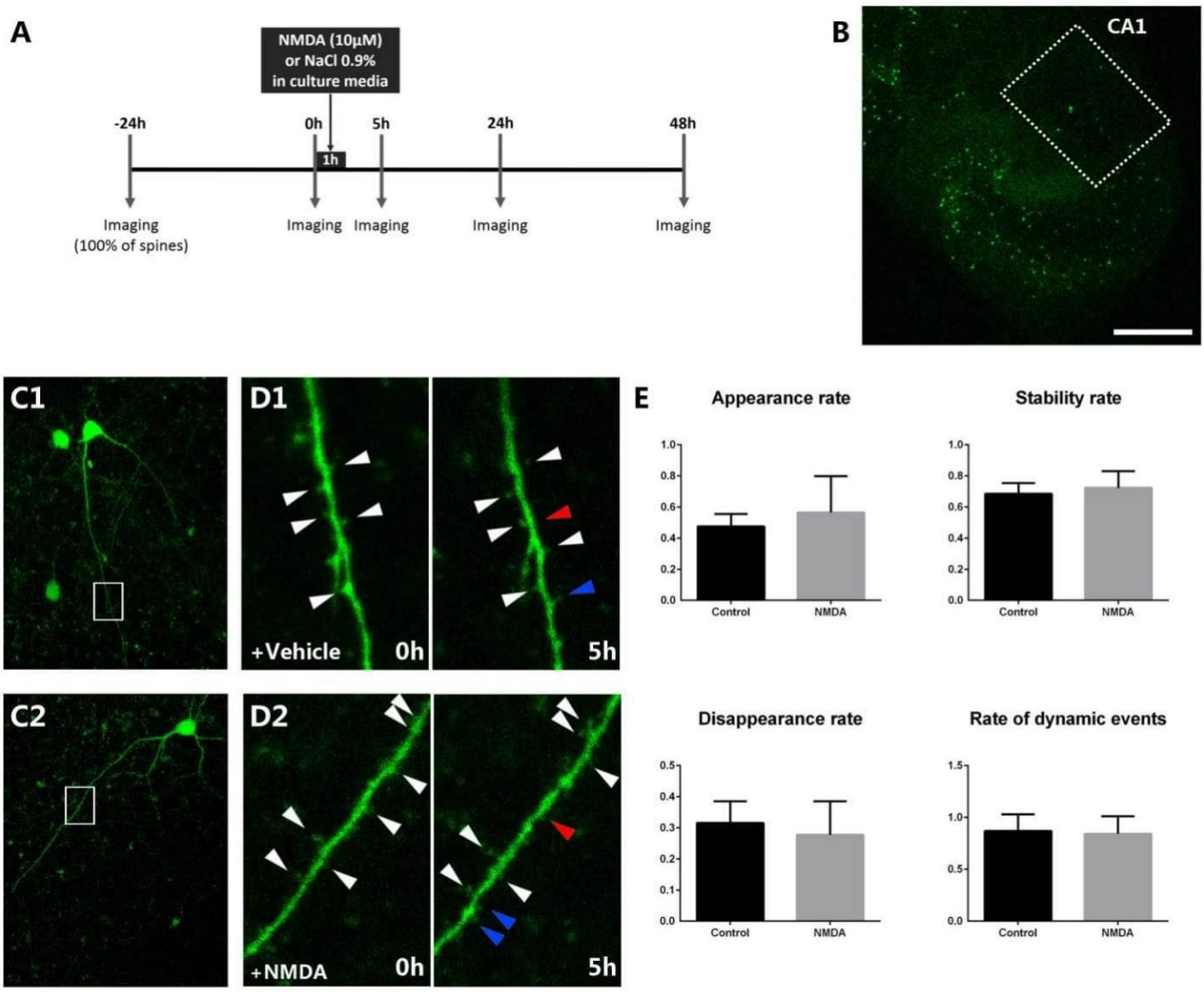

Fig. 1 Experimental design and fast effects of the NMDA administration on the structural dynamics. **(A)** Scheme of the real-time design. **(B)** A panoramic view of the entorhino-hippocampal culture with the CA1 region squared. **(C)** Low magnification images of the interneurons of interest in control **(C1)** and NMDA-infused **(C2)** conditions. **(D)** Representative dendrites analysed in real-time from the squared areas from **(C)** in control **(D1)** and NMDA-infused **(D2)** conditions. The dendritic spines are pointed by arrows with a colour legend: white arrows: dendritic spines that were present in the previous imaging session; blue arrows: dendritic spines that appear in that very imaging session; red arrows: dendritic spines that were present in the previous imaging session but are lost in the current one. **(E)** Graphs representing the different dynamic traits. Scale bar: 500 µm in (A), 60 µm in (B) and 8 µm in (C).

Organotypic culture preparation

The brain was freshly extracted from P7 mice and the hippocampus dissected along with the entorhinal cortex in order to preserve the perforant path. Hippocampal slices (400 µm-thick) were obtained with a tissue chopper following a previously described protocol (Stoppini et al. 1991; Guirado et al. 2014b). Media was changed 3 times per week and the cultures remained 13 days in vitro (DIV) until the confocal imaging started.

Real-time imaging

For the real-time imaging of organotypic cultures, short imaging sessions (10-15 minutes) were carried out with a 40X water immersion objective in a laser scanning confocal microscope (Leica TCS SPE, Germany). An additional 10X digital zoom was used to analyse dendritic segments of about 35 µm in length, located between 100 and 150 µm from the soma (Z step size of 0.8 µm). Laser intensity was kept at the minimum allowing observation, and acquisition conditions maintained unchanged over the different days of observation. Control experiments showed that this procedure did not produce any deleterious effect on

cell viability, such as cell death or dendritic beadings. One dendrite was analysed per organotypic culture slice, and 14 slices from 6 different animals were analysed. All the somata of the interneurons analysed were located in the *stratum oriens* of CA1 region. The imaging took place at five different time points referenced to the beginning of the treatment: -24h, 0h, 5h, 24h and 48h, starting on DIV 13. The treatment was administered after the second imaging session (0h) for one hour, and then it was again substituted by normal culture media. The rapid effect of the compound was registered after 4 hours (5h), 24 hours (24h) and 48 hours (48h).

Real-time analysis

The same dendrite was studied linearly to calculate the 4 dynamic parameters: appearance, disappearance and stability rates, and the rate of dynamic events. These parameters were calculated relative to the prior number of spines. Appearance rate: number of gained spines/total number of previous spines; disappearance rate: number of disappear spines/total number of previous spines; stability rate: number of stable spine/total number of previous spines. Therefore, both disappearance and stability rates are linked. The rate of dynamic events is the sum of gained and lost spines relative to the previous number of spines.

Statistics

After checking the normality and homoscedasticity of the data, we used repeated measures ANOVA to compare control and experimental groups in the 24 hour-sparse experiment. In order to compare both the linear effects within and between groups, we performed *post hoc* analyses (LSD). To compare the 5-hour time point between NMDA and control groups, we used an unpaired t-test. In every case α was set to 0.05 and the slice was considered the "n".

RESULTS

No effect in spine turnover 4 hours after NMDA administration

Real-time analysis was performed in control conditions and after the acute administration of NMDA (1 hour in the culture medium). In order to register fast effects of the NMDAR activation, we imaged the dendrites 4 hours after the 1h-treatment (0h to 5h). There were no significant changes in the NMDA group in the appearance ($p=0.568$), disappearance and stability rates (both $p=0.763$), or the rate of dynamic events ($p=0.797$, figure 1C1, 1D1, 1C2, 1D2 and 1E).

Increased appearance and disappearance rates of dendritic spines 24 hours after NMDA administration

In control conditions, we found no alterations in the appearance, the disappearance, the stability rates, or in the rate of dynamic events. However, 24 hours after NMDA administration (0h to 24h), the appearance rate of new spines was significantly increased from 40% under control conditions to a 100% of the total of pre-existing spines in treated cultures. This increase in the appearance rate was significant when compared to both its baseline (-24h to 0h, $p=0.036$) and the control group ($p= 0.018$, figure 2A1, 2B1, 2A2, 2B2 and 2C). In addition, this increase was reverted to its baseline levels 48 hours after the treatment (24h to 48h, $p=0.039$, figure 2A1, 2B1, 2A2, 2B2 and 2C). The disappearance and stability rates were also altered significantly 24 hours after the treatment. In this time point the disappearance rate was higher in the NMDA group than in the control group ($p= 0.045$, figure 2A1, 2B1, 2A2, 2B2 and 2C). Therefore, the stability rate was decreased in the treated group ($p=0.045$, figure 2A1, 2B1, 2A2, 2B2 and 2C). Furthermore, there was a trend towards an increase in the rate of dynamic events 24 hours after the administration of NMDA, both when compared to its baseline (-24h to 0h, $p=0.063$) and to the control group ($p=0.061$, figure 2A1, 2B1, 2A2, 2B2 and 2C). As reported in the appearance rate, this increase in the NMDA group was reverted to baseline levels 48 hours after the treatment (24h to 48h, $p=0.016$, figure 2A1, 2B1, 2A2, 2B2 and 2C).

No alteration in the dendritic spine density after NMDA administration

When analysing the relative variation of the spine density, there was no effect 24h after the NMDAR activation ($p=0.352$) and both control and treated groups showed similar distributions prior to and after the treatment (24h: $p=0.524$; 48h: $p=0.846$; figure 3A1,

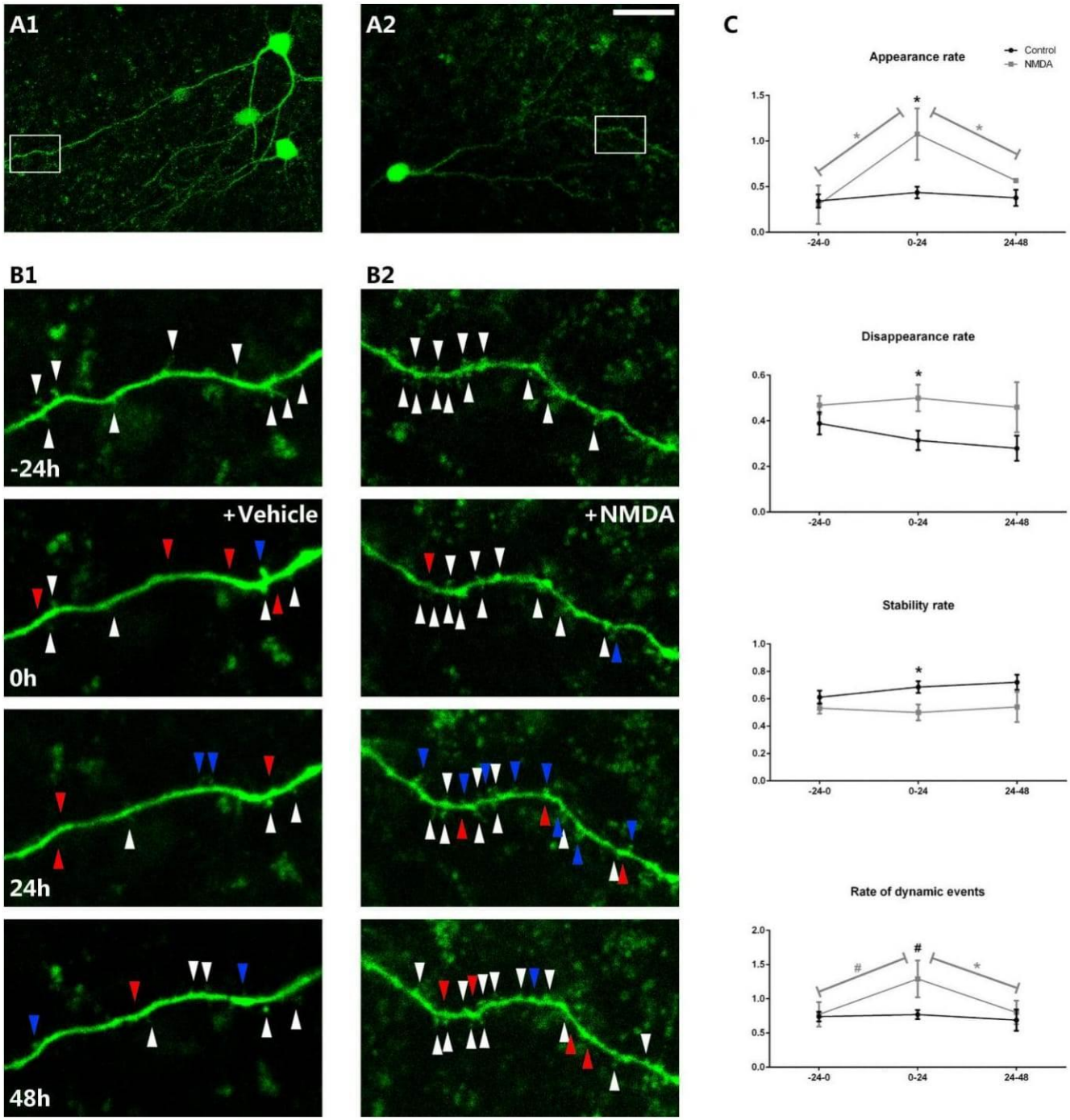

Fig. 2 Real-time analysis of the structural dynamics of SOM-expressing interneurons. (A) Low magnification images of the interneurons of interest in control **(A1)** and NMDA-infused **(A2)** conditions. **(B)** Representative dendrites analysed in real-time from the squared areas from **(A)** in control **(B1)** and NMDA-infused **(B2)** conditions. The dendritic spines are pointed by arrows with a colour legend: white arrows: dendritic spines that were present in the previous imaging session; blue arrows: dendritic spines that appear in that very imaging session; red arrows: dendritic spines that were present in the previous imaging session but are lost in the current one. **(C)** Graphs representing the different dynamic traits. Scale bar: 36 µm in (A) and 10 µm in (B).

3A2 and 3B1). In order to analyse the acute effect of NMDAR activation, we also studied the relative spine density 4 hours after the NMDA administration, and there were no significant differences when it was compared to that of the control group (p=0.559; figure 3B2).

No alteration in the dendritic spine density after NMDA administration

When analysing the relative variation of the spine density, there was no effect 24h after the NMDAR activation (p=0.352) and both control and treated groups showed similar distributions prior to and after

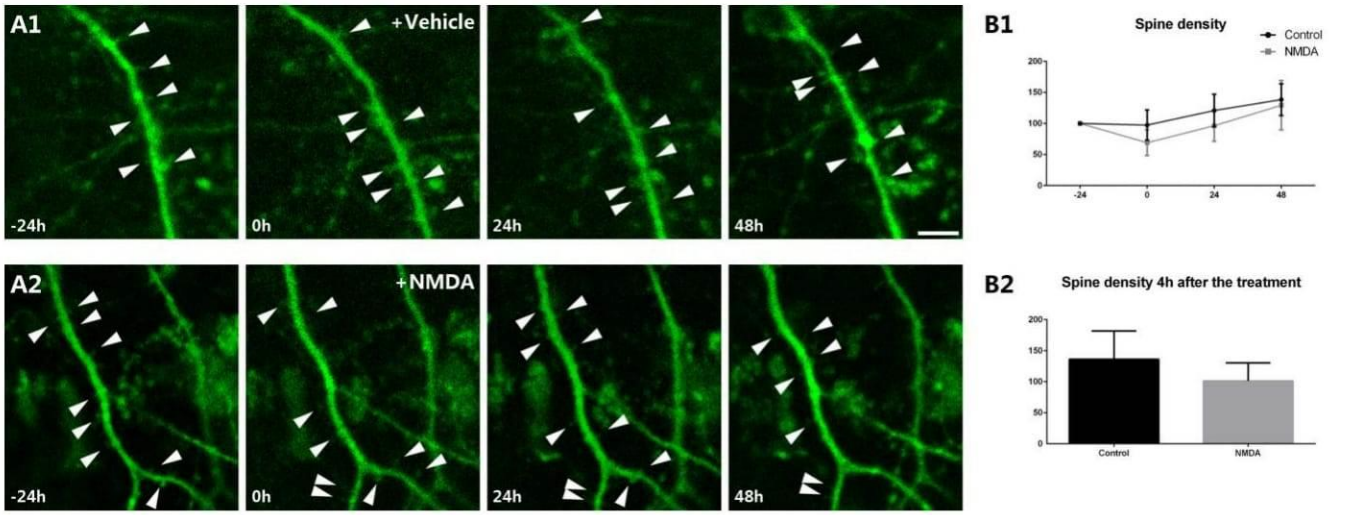

Fig. 3 Real-time analysis of the dendritic spine density of SOM-expressing interneurons. (A) Representative dendrites of interest analysed in real-time in control **(A1)** and NMDA-infused **(A2)** conditions. The dendritic spines are pointed by white arrows. **(B)** Graphs representing the linear **(B1)** and fast **(B2)** effects of the NMDA infusion on the dendritic spine density. Scale bar: 7 µm.

the treatment (24h: p=0.524; 48h: p=0.846; figure 3A1, 3A2 and 3B1). In order to analyse the acute effect of NMDAR activation, we also studied the relative spine density 4 hours after the NMDA administration, and there were no significant differences when it was compared to that of the control group (p=0.559; figure 3B2).

DISCUSSION

In the present study, we have shown that NMDAR activation causes an increase in the spine dynamics of SOM expressing interneurons. These changes are observable 24 hours after the NMDA administration, but the effect is rapidly reverted to baseline levels afterwards. Despite these alterations in dynamic parameters, the spine density of these interneurons remained unaffected throughout the entire experiment.

The present results, focused on the dendrite-targeting SOM expressing interneurons, are based on experiments performed on hippocampal-entorhinal organotypic cultures. We have previous evidence that in these cultures the SOM expressing cells have a similar distribution and morphology to those observed in the adult hippocampus and they constitute a valid model to study their structural dynamics (Guirado et al. 2014b). In fact, we have observed that the enzymatic removal of polysialic acid (PSA), a plasticity-related molecule expressed in cortical interneurons (Gomez-Climent et al. 2011), in these cultures also increases the density and apparition rate of spines (Guirado et al. 2014b). Furthermore, we have also observed similar effects after PSA depletion from the hippocampus *in vivo* (Guirado et al. 2014b). The manipulation of serotoninergic neurotransmission through the antidepressant fluoxetine also induces changes in the density of spines of a similar interneuronal population of dendrite-targeting SOM expressing cells in the medial prefrontal cortex (Guirado et al. 2014a). Moreover, a recent study has described a significant effect of chronic stress on the structure of SOM expressing interneurons in the CA1 *stratum oriens*, reducing their dendritic arborization, but not affecting their spine density (Gilabert-Juan et al. 2017). These effects of stress are interesting because it is known that this aversive experience increases glutamate release in the hippocampus (Popoli et al. 2012), which could exert an effect through NMDARs.

There is abundant data on the involvement of NMDARs in the structural plasticity of dendritic spines in pyramidal neurons. Most of this evidence comes from the observation that LTP is associated with increased production of dendritic spines through an NMDAR-dependent mechanism (Hering and Sheng 2001). In concordance with the present results describing an increase in the appearance rate of spines in interneurons, previous reports on pyramidal neurons have shown that activation of NMDARs induces spine lengthening (Maletic-Savatic et al. 1999). Recent results from our laboratory have shown that an NMDAR antagonist produces opposite results on the

dynamics of SOM expressing interneurons in the *stratum oriens* of CA1, decreasing the apparition rate and the density of their dendritic spines (Perez-Rando et al. unpublished results).

Our study shows that the application of 10 μM NMDA induces structural alterations in the SOM expressing interneurons of the *stratum oriens*, without causing dendrite beadings or cell death. However, we have also found an increase in the disappearance rate and a concomitant decrease in the stability rate, 24 hours after the NMDA infusion. Several reports have described excitotoxic properties for this agonist (Kristensen et al. 2001). Consequently, although the selected neurons did not appear blobbed or damaged in any way, it is still possible that Ca^{2+} influx may cause a mild localized excitotoxicity, resulting in the loss of dendritic spines and therefore, the decrease in the spine stability rate. Another reason for this loss in the stability rate may be the NMDA-induced destabilization of the spine F-actin cytoskeleton, as it has been shown in other reports (Halpain et al. 1998). We have also reported an increase in the appearance and disappearance rates 24 hours –although not 4 hours- after the NMDA administration. This delay in the effect might be due to a putative compensatory mechanism exerted by the interneurons to maintain the homeostasis of the system, which may buffer alterations elicited initially in pyramidal neurons. It is reasonable that these excitatory neurons would show earlier effects after the activation of the receptor because they present a higher proportion of NMDARs in their plasmatic membranes (Nyíri et al. 2003). In accordance with this hypothesis, it is known that NMDA administration increases rapidly the density of dendritic spines, and the proportion of mushroom-shaped spines (which are synaptically more active), in primary cultures of hippocampal pyramidal neurons (Tian et al. 2007).

Considering both dynamic parameters altogether, our results showed a trend towards an increase in the rate of dynamic events 24 hours after the NMDA infusion. This is a more direct measure of dynamism, which would indicate a neuronal structural availability for a putative increase in synaptogenesis (Trachtenberg et al. 2002; Knott and Holtmaat 2008). All the dynamic parameters, including the rate of dynamic events, returned to basal levels 48 hours after the treatment. This finding agrees with previously reported recovery times for NMDA administration in hippocampal organotypic cultures, where the dendritic swelling and the decreased EPSC of pyramidal cells were recovered 48 hours after NMDA administration (Ikegaya et al. 2001). Altogether, our results help to shed light on how NMDARs modulate the structural dynamics of the SOM expressing interneurons in the hippocampus. The study of these receptors is important, since their activation can lead to neuronal potentiation or depression, and alterations in their physiology may underlie major neuropsychiatric disorders, such as schizophrenia.

CONCLUSIONS

NMDA administration alters the spine dynamics of hippocampal SOM expressing interneurons in organotypic cultures.

The apparition rate of dendritic spines in these interneurons is increased 24 hours after the NMDA infusion.

NMDA administration increases the disappearance rate and decreases the stability rate 24 hours after the NMDA infusion.

AUTHOR CONTRIBUTIONS

MP, HC & MB performed the experiments. MP, EC & JN designed the experiment. MP, EC & JN wrote the manuscript.

FUNDING

This work was supported by Generalitat Valenciana (Prometeo Excellence Program ROMETEO2013/069) and the Fundación Alicia Koplowitz to JN and by the Spanish Ministry of Economy and Competitiveness to JN (BFU2012-32512), EC-G (IJCI-2015-24124) and MP-R (FPU12/03200, FPU predoctoral fellowship).

REFERENCES

Castillo-Gómez E, Coviello S, Perez-Rando M, et al (2015) Streptozotocin diabetic mice display depressive-like behavior and alterations in the structure, neurotransmission and plasticity of medial prefrontal cortex interneurons. Brain Res

Bull 116:45–56. doi: 10.1016/j.brainresbull.2015.06.002

Chen JL, Nedivi E (2013) Highly Specific Structural Plasticity of Inhibitory Circuits in the Adult Neocortex. Neurosci 19:384–393. doi: 10.1177/1073858413479824

Chen JL, Villa KL, Cha JW, et al (2012) Clustered dynamics of inhibitory synapses and dendritic spines in the adult neocortex. Neuron 74:361–73. doi: 10.1016/j.neuron.2012.02.030

Contestabile A (2000) Roles of NMDA receptor activity and nitric oxide production in brain development. Brain Res Rev 32:476–509. doi: 10.1016/S0165-0173(00)00018-7

Engert F, Bonhoeffer T (1999) Dendritic spine changes associated with hippocampal long-term synaptic plasticity. Nature 399:66–70. doi: 10.1038/19978

Freund TF, Buzsáki G (1996) Interneurons of the hippocampus. Hippocampus 6:347–470. doi: 10.1002/(SICI)1098-1063(1996)6:4<347::AID-HIPO1>3.0.CO;2-I

Gilabert-Juan J, Bueno-Fernandez C, Castillo-Gomez E, Nacher J (2017) Reduced interneuronal dendritic arborization in CA1 but not in CA3 region of mice subjected to chronic mild stress. Brain Behav 7:e00534. doi: 10.1002/brb3.534

Gilabert-Juan J, Castillo-Gomez E, Perez-Rando M, et al (2011) Chronic stress induces changes in the structure of interneurons and in the expression of molecules related to neuronal structural plasticity and inhibitory neurotransmission in the amygdala of adult mice. Exp Neurol 232:33–40. doi: 10.1016/j.expneurol.2011.07.009

Gomez-Climent MA, Guirado R, Castillo-Gomez E, et al (2011) The Polysialylated Form of the Neural Cell Adhesion Molecule (PSA-NCAM) Is Expressed in a Subpopulation of Mature Cortical Interneurons Characterized by Reduced Structural Features and Connectivity. Cereb Cortex 21:1028–1041. doi: 10.1093/cercor/bhq177

Guirado R, Perez-Rando M, Sanchez-Matarredona D, et al (2014a) Chronic fluoxetine treatment alters the structure, connectivity and plasticity of cortical interneurons. Int J Neuropsychopharmacol 17:1635–1646. doi: 10.1017/S1461145714000406

Guirado R, Perez-Rando M, Sanchez-Matarredona D, et al (2014b) The Dendritic Spines of Interneurons Are Dynamic Structures Influenced by PSA-NCAM Expression. Cereb Cortex 24:3014–3024. doi: 10.1093/cercor/bht156

Gulyás AI, Hájos N, Katona I, Freund TF (2003) Interneurons are the local targets of hippocampal inhibitory cells which project to the medial septum. Eur J Neurosci 17:1861–1872. doi: 10.1046/j.1460-9568.2003.02630.x

Halpain S, Hipolito A, Saffer L (1998) Regulation of F-actin stability in dendritic spines by glutamate receptors and calcineurin. J Neurosci 18:9835–44.

Hering H, Sheng M (2001) Dendritic spines: structure, dynamics and regulation. Nat Rev Neurosci 2:880–8. doi: 10.1038/35104061

Holtmaat A, Svoboda K (2009) Experience-dependent structural synaptic plasticity in the mammalian brain. Nat Rev Neurosci 10:647–58. doi: 10.1038/nrn2699

Holtmaat A, Wilbrecht L, Knott GW, et al (2006) Experience-dependent and cell-type-specific spine growth in the neocortex. Nature 441:979–983. doi: 10.1038/nature04783

Ikegaya Y, Kim J a, Baba M, et al (2001) Rapid and reversible changes in dendrite morphology and synaptic efficacy following NMDA receptor activation: implication for a cellular defense against excitotoxicity. J Cell Sci 114:4083–93.

Knott G, Holtmaat A (2008) Dendritic spine plasticity—Current understanding from in vivo studies. Brain Res Rev 58:282–289. doi: 10.1016/j.brainresrev.2008.01.002

Kristensen BW, Noraberg J, Zimmer J (2001) Comparison of excitotoxic profiles of ATPA, AMPA, KA and NMDA in organotypic hippocampal slice cultures. Brain Res 917:21–44. doi: 10.1016/S0006-8993(01)02900-6

Liguz-Lecznar M, Urban-Ciecko J, Kossut M (2016) Somatostatin and Somatostatin-Containing Neurons in Shaping Neuronal Activity and

Plasticity. Front Neural Circuits 10:48. doi: 10.3389/fncir.2016.00048

Maletic-Savatic M, Malinow R, Svoboda K (1999) Rapid Dendritic Morphogenesis in CA1 Hippocampal Dendrites Induced by Synaptic Activity. Science (80-) 283:1923–1927. doi: 10.1126/science.283.5409.1923

Müller C, Remy S (2014) Dendritic inhibition mediated by O-LM and bistratified interneurons in the hippocampus. Front Synaptic Neurosci 6:23. doi: 10.3389/fnsyn.2014.00023

Nyíri G, Stephenson F. A, Freund T. F, Somogyi P (2003) Large variability in synaptic n-methyl-d-aspartate receptor density on interneurons and a comparison with pyramidal-cell spines in the rat hippocampus. Neuroscience 119:347–363. doi: 10.1016/S0306-4522(03)00157-X

Oliva AA, Jiang M, Lam T, et al (2000) Novel hippocampal interneuronal subtypes identified using transgenic mice that express green fluorescent protein in GABAergic interneurons. J Neurosci 20:3354–68.

Popoli M, Yan Z, McEwen BS, Sanacora G (2012) The stressed synapse: the impact of stress and glucocorticoids on glutamate transmission. Nat Rev Neurosci 13:22–37. doi: 10.1038/nrn3138

Stoppini L, Buchs PA, Muller D (1991) A simple method for organotypic cultures of nervous tissue. J Neurosci Methods 37:173–82.

Tian L, Stefanidakis M, Ning L, et al (2007) Activation of NMDA receptors promotes dendritic spine development through MMP-mediated ICAM-5 cleavage. J Cell Biol 178:687–700. doi: 10.1083/jcb.200612097

Trachtenberg JT, Chen BE, Knott GW, et al (2002) Long-term in vivo imaging of experience-dependent synaptic plasticity in adult cortex. Nature 420:788–94. doi: 10.1038/nature01273

Tuncdemir SN, Wamsley B, Stam FJ, et al (2016) Early Somatostatin Interneuron Connectivity Mediates the Maturation of Deep Layer Cortical Circuits. Neuron 89:521–535. doi: 10.1016/j.neuron.2015.11.020

Ultanir SK, Kim J-E, Hall BJ, et al (2007) Regulation of spine morphology and spine density by NMDA receptor signaling in vivo. Proc Natl Acad Sci 104:19553–19558. doi: 10.1073/pnas.0704031104

Volianskis A, France G, Jensen MS, et al (2015) Long-term potentiation and the role of N-methyl-D-aspartate receptors. Brain Res 1621:5–16. doi: 10.1016/j.brainres.2015.01.016

5. The TrkB agonist 7,8-dihydroxyflavone changes the structural dynamics of neocortical pyramidal neurons and improves recognition memory in mice

The TrkB agonist 7,8-dihydroxyflavone changes the structural dynamics of neocortical pyramidal neurons and improves recognition memory in mice

Marta Pérez-Rando[1#], Esther Castillo-Gomez[1,2 # *], Clara Bueno-Fernández[1], Juan Nacher [1,2,3, *]

[1]. Neurobiology Unit, Program in Neurosciences and Interdisciplinary Research Structure for Biotechnology and Biomedicine (BIOTECMED), Universitat de València, Burjassot, Spain

[2]. CIBERSAM: Spanish National Network for Research in Mental Health, Burjassot, Spain

[3]. Fundación Investigación Hospital Clínico de Valencia, INCLIVA, Burjassot, Spain

[#] Both authors have contributed equally to this work.

[*] CORRESPONDING AUTHORS: Dr. Juan Nacher & Dr. Esther Castillo-Gómez. Neurobiology Unit. Cell Biology Dpt. Interdisciplinary Research Structure for Biotechnology and Biomedicine (BIOTECMED). Universitat de València. Dr. Moliner, 50. Burjassot, 46100. Spain. Telf: (+34) 963543241. e-mails: nacher@uv.es, esther.castillo@uv.es

ABSTRACT

BDNF and its receptor TrkB have important roles in neurodevelopment, neural plasticity and learning and memory. Alterations in TrkB expression have been described in different neurological and psychiatric disorders, including major depression and Alzheimer's disease. Therefore, drugs interacting with TrkB, specially agonists, are promising therapeutic tools. Among them, the recently described 7,8-dihydroxyflavone (DHF), an orally bioactive compound, is one of the best candidates, which has already been successfully tested in some animal models of diseases. Recent studies have also shown the influence of this drug on the structure of pyramidal neurons, specifically on dendritic spine density. However, to date, there is no information on how DHF may alter the structural dynamics of these neurons (i.e. real time study of the addition/elimination of dendritic spines and axonal boutons). The correlation between these structural parameters and memory improvements related to this drug has also not been studied yet. In order to understand these under-researched aspects of DHF, we performed a longitudinal analysis of spine and axonal dynamics of neocortical pyramidal neurons during a chronic oral treatment with this drug. Simultaneously, these results were correlated with changes in recognition memory. A cranial window surgery was performed in transgenic mice with fluorescently labelled pyramidal neurons. The expression of TrkB was confirmed in these excitatory neurons. The same dendrites and axons were imaged every four days before and during the treatment, using a 2-photon microscope. Recognition memory was assessed before and after treatment. The gain functions of spines and axonal boutons were increased at the beginning of the treatment but returned to baseline levels at the end. These changes were positively correlated with increased recognition memory in treated animals. These results help to understand how the activation of the BDNF-TrkB system can enhance basic behavioural tasks through changes in the dynamics of pyramidal neurons. Moreover, they highlight DHF as a promising therapeutic vector for treating certain brain disorders in which this system is altered.

INTRODUCTION

The brain-derived neurotrophic factor (BDNF) and its receptor, the tropomyosin receptor kinase B (TrkB), appear to be expressed in all the pyramidal neurons of the central nervous system (Yan et al. 1997). The interaction of this neurotrophin and its receptor is not only essential for neural growth and

survival, but also for neural plasticity (Yoshii and Constantine-Paton 2010), where, among other functions, it promotes synaptic potentiation through the establishment of LTP in the cerebral cortex (Kang et al. 1997; Escobar et al. 2003). However, its malfunction underlies the etiopathology of different neuropsychiatric disorders, including major depression (Castrén and Rantamäki 2010) or schizophrenia (Pandya et al. 2013). Therefore, it is important to develop strategies to activate TrkB that could be clinically implemented. In this regard, the 7,8-dihydroxyflavone (DHF), a potent and specific TrkB agonist, has recently emerged as a promising therapeutic treatment (Jang et al. 2010). This drug is especially interesting because it is orally bioactive and can easily cross the blood-brain barrier (Du and Hill 2015). In fact, recent research has already proven its effectiveness in animal models of Parkinson's disease (Jang et al. 2010), Alzheimer's disease (Zhang et al. 2014; Castello et al. 2014), major depression (Zhang et al. 2015; Zhang et al. 2016) or schizophrenia (Yang et al. 2014). Given the involvement of BDNF/TrkB in neuronal plasticity it is thought that DHF would increase this parameter. However, the neurobiological bases of these positive effects are still not fully understood.

Although neural plasticity can be studied from different points of view, changes in neuronal structure should represent the rearrangement of synapses and, therefore, in the neural circuitry (Caroni et al. 2012). Regarding this, DHF reverts the structural alterations that some disorders produce on pyramidal neurons: It returns to control levels the decreased spine density in mouse models of Alzheimer's disease (Castello et al. 2014) and major depression (Zhang et al. 2015). In healthy rats, DHF reverts the functional decline produced by ageing, probably by increasing the spine density in the amygdala, hippocampus and prefrontal cortex (Zeng et al. 2012a). However, the study of structural plasticity goes beyond these analyses of dendritic spine density. With the emergence of structural dynamics we have increased our knowledge on how neuronal networks are finely modulated by different treatments. In order to perform such experiments, it is necessary to chronically implant cranial windows in mice that express a fluorescent protein in their pyramidal neurons and to image these cells in real-time with a 2-photon microscope (Holtmaat et al. 2009). These studies give us information in real-time of the addition, elimination or stability of dendritic spines and axonal *boutons* in the same structure throughout an entire experiment (Holtmaat and Svoboda 2009; Chen and Nedivi 2013). They also allow us to differentiate transient alterations from persistent ones. This represents valuable information for understanding long lasting changes in the network (Holtmaat et al. 2006; Holtmaat and Svoboda 2009; Chen and Nedivi 2013), since the spines that remain stable for at least 4 days are the ones that always bear a synapse (Knott et al. 2006). In addition, these analyses are linear and consequently may allow us to establish the proper treatment course for further clinical research on the drug tested. Alterations in structural dynamics have been proposed to be underlying adaptation to changing environments, as has been shown after sensorial deprivation in both excitatory (Hofer et al. 2009; Holtmaat and Svoboda 2009; Cane et al. 2014) and inhibitory (Chen et al. 2011c; Chen et al. 2011b; Keck et al. 2011; Chen et al. 2012; van Versendaal et al. 2012) circuits.

We have developed an experiment to understand how BDNF/TrkB regulates in real time the neuronal structural plasticity of pyramidal neurons in the barrel cortex and to correlate these changes with behavioural responses. Thy1-YFP transgenic mice, in which a subset of layer V pyramidal neurons constitutively express YFP (Feng et al. 2000; Porrero et al. 2010) were used in this study. We have imaged in real-time the same dendrites and axons before and during a 14-day treatment with the DHF and have tested behaviours related to anxiety and dependent on the barrel cortex.

MATERIAL AND METHODS

Animals and 7,8-Dihydroxyflavone treatment

Twenty-six adult transgenic mice Thy1-YFP, line H (Jackson Laboratories; Bar Harbor, Maine, USA) were used for all the experiments. In this strain, layer V cortical pyramidal neurons are densely labelled with EYFP (Feng et al. 2000) (Fig. 1). Two of these mice were destined to the analysis of TrkB expression in Thy1-YFP expressing neurons (see. All 24 mice were implanted with a cranial window and subjected to 3 consecutive 2-photon imaging sessions before starting the DHF treatment and 3 sessions during the treatment (see below and Fig. 1). The oral

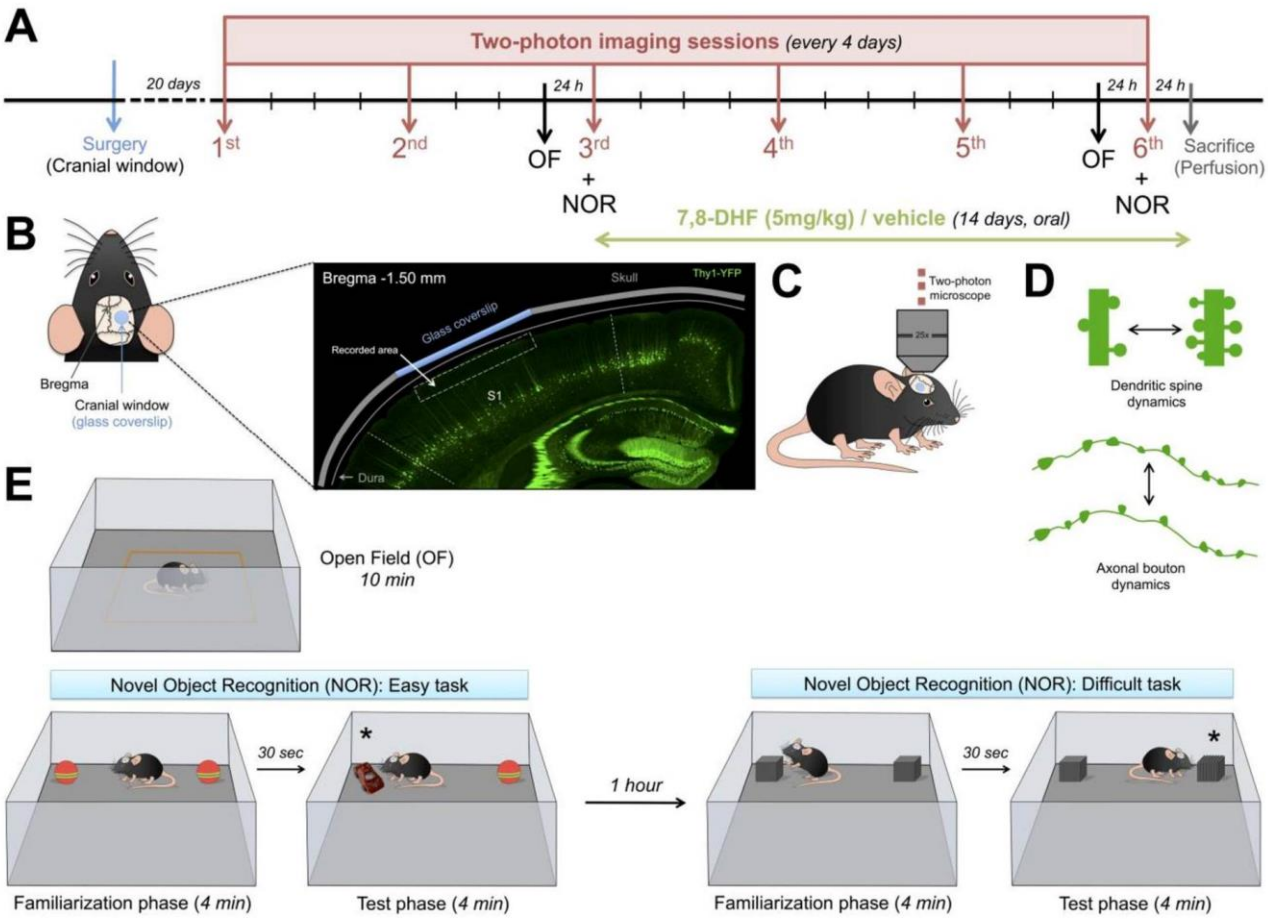

Figure 1. Experimental design. (A) Timeline of the experimental procedure **(B)** To allow long-term and high-resolution imaging of *in vivo* neuronal morphology of pyramidal neurons, a cranial window was unilaterally implanted over the primary somatosensory cortex (S1; Bregma -1.5 mm, Lateral 3.5 mm) of Thy1-YFP mice (2-month-old). **(C)** Twenty days after surgery, 2-photon imaging sessions started. **(D)** The same dendrites and axons of every animal were imaged every 4 days to study spine and *en passant bouton* (EPB) dynamics. Every animal was recorded 3 sessions before and 3 sessions after DHF or vehicle treatment. **(E)** To test locomotion and anxiety related behaviour, all animals were evaluated in the OF test, 24 hours before starting the treatment and on the 12th day of treatment. A modified version of the novel object recognition test was used to evaluate recognition memory in mice before (day 0) and after treatment (day 13). Novel objects are indicated in the scheme with an asterisk (see material and methods' section for further details).

treatment with DHF or with vehicle solution started right after the end of the 3rd imaging session. Eighty microliters of a DHF solution (100 mg/ml in DMSO; Abcam) or vehicle solution (DMSO; Sigma-Aldrich, San Luis, MO, USA) were added to 100 ml of drinking water containing 1% of sucrose (pH=7.4). These solutions were replaced every 3-4 days during the 14 days of duration of the treatment and bottle content was measured to monitor liquid intake. Animals were also weighted every 3-4 days. The average liquid intake was 2 ml/day/mouse and the average weight of mice was 32 g. Therefore, DHF dose was approximately 5mg/kg/day.

Animals were reared in groups of 3-4, in standard-size polycarbonate cages, in a temperature- and humidity-controlled environment and maintained on a 12 h light/dark cycle with food and water available *ad libitum*.

All animal experimentation was conducted in accordance with the Directive 2010/63/EU of the European Parliament and of the Council of 22 September 2010 on the protection of animals used for scientific purposes and was approved by the Committee on Bioethics of the Universitat de València. Every effort was made to minimize the number of animals used and their suffering.

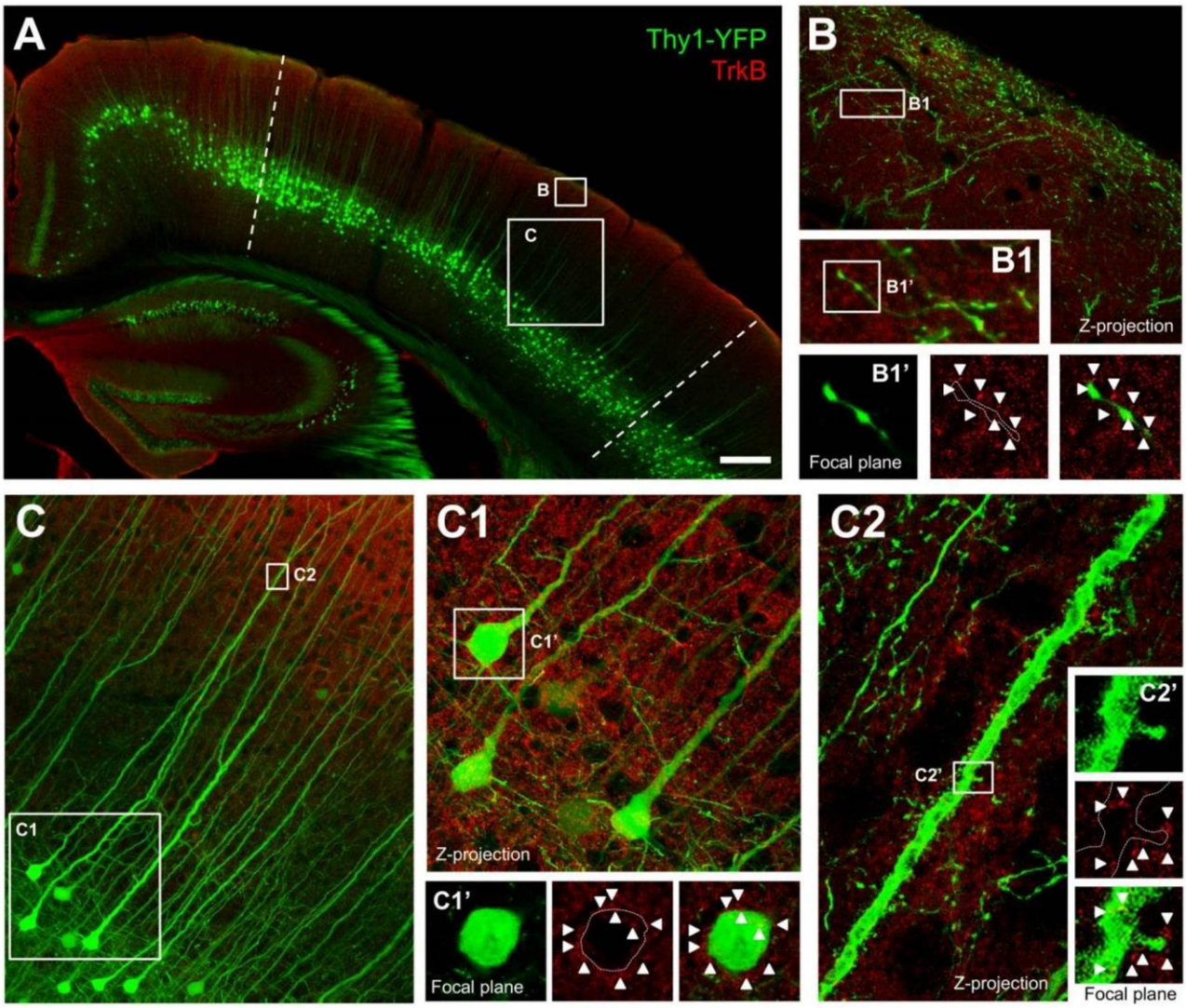

Figure 2. TrkB receptor expression in Thy1-YFP expressing neurons. (A) Confocal panoramic view of a Thy1-YFP brain slice (Bregma -1.22 mm) immunostained for TrkB receptor (red). Our region of interest, the primary somatosensory cortex (S1) is delimited by the 2 dotted lines. Scale bar: 800 µm. (B) Magnified view (12x) of the squared section in A, showing TrkB expressing puncta (arrowheads in B1') co-localizing or in close apposition to YFP expressing axonal boutons (green). (C) 4.5x magnification of the squared area in A, showing layer V YFP-expressing pyramidal neurons. TrkB receptors were found surrounding and in close apposition to the somata of these neurons (arrowheads in C1') as well as to the spine head (C2').

TrkB immunohistochemistry

The 2 Thy1-YFP mice destined to the analysis of TrkB expression in Thy1-YFP expressing neurons were transcardially perfused with 4% paraformaldehyde solution and their brains were cut in 50 µm-thick coronal sections using a vibratome (Leica VT1000E, Leica, Wetzlar, Germany). Free-floating sections were first blocked with 10% normal donkey serum solution and then incubated overnight at room temperature with goat anti-TrkB receptor primary antibody (1:400; R&D systems, Minneapolis, MN, USA). The day after, sections were incubated with donkey anti-goat secondary antibody conjugated with AlexaFluor®647 (1:400, LifeTechnologies, Carlsbad, CA, USA) for 2 hours and then mounted on slides and covered with mounting media (Dako, Glostrup, Denmark). Images were acquired with a Leica TCS SPE confocal microscope using a 63X oil objective and 2X digital zoom magnification.

Cranial window implantation

To allow long-term high-resolution imaging of *in vivo* neuronal morphology, a cranial window was unilaterally implanted over the primary somatosensory cortex (barrel field; Bregma -1.5 mm, Lateral 3.5 mm) of 24 Thy1-YFP mice (2-month-

old). Animals were first anesthetized with an intraperitoneal injection of a mixture of ketamine (50 mg/kg; Imalgene, Merial, Lyon, France) and medetomidine (1 mg/kg; Sedator, Dechra, Barcelona, Spain); carprofen (5 mg/kg; Rimadyl, Pfizer, New York, NY, USA) was also injected intraperitoneally to avoid inflammation, and a subcutaneous injection of butorfanol (5 mg/kg; Torbugesic, Pfizer) was administered to avoid any suffering during and after the surgery. Animals were placed afterwards in a stereotaxic device. After cutting a flap of skin (approx. 1 cm^2), the periosteum was gently removed from the skull using fine tweezers and the *temporalis* muscle was separated with a blunt spatula. A thin layer of cyanoacrylate was applied to the *temporalis* muscle, wound margins and skull, with the exception of the region of interest in the skull. Once it dried, a thin layer of dental acrylic was applied on top of the glue. A circular groove around the area of interest was pierced using a biopsy punch with a diameter of 3 mm (Aesthetic Group, Puiseux-le-Hauberger, France) leaving an island of skull in the centre that was removed afterwards using the tip of sharp forceps. To clean the area, drops of cortex buffer (Holtmaat et al. 2009) were applied regularly after the island of skull was removed. Finally, the unblemished dura was covered with a circular cover glass (3 mm diameter, 1 mm thick; Harvard Apparatus, Holliston, MA, USA) and the borders were sealed with cyanoacrylate and dental acrylic. Finally, animals were intraperitoneally injected with atipamezole (0.5 mg/kg; Antisedan, Esteve, Barcelona, Spain) to revert the anaesthesia and returned to individual cages for recovery. The day after surgery, mice were returned to their home cages (social rearing) and left undisturbed for 2 weeks to allow complete recovery before imaging.

In vivo 2-photon imaging

In vivo 2-photon imaging was achieved using an Olympus FV1000MPE microscope and its acquisition software (Olympus fluoview FV1000 v4.0.1.10, Olympus, Tokyo, Japan). The light source for 2-photon excitation was a commercial Ti:Sapphire laser (Mai-Tai HP DeepSee, Spectra Physics, Santa Clara, CA, USA). The excitation wavelength was set to 930 nm, with the excitation signal passing through an XLPLN25XWMP 25×/1.05 NA water-immersion objective (Olympus) and collected after a barrier filter by a photomultiplier tube. The same cells could be identified and re-imaged for up to 20 days using local fiduciary landmarks of the brain's surface vasculature.

Image acquisition and analysis

Adult mice (3-month-old) previously implanted with cranial windows were anesthetized with a mixture of ketamine (50 mg/kg; Imalgene, Merial) and medetomidine (1 mg/kg; Sedator, Dechra). Anaesthesia was monitored by breathing rate and foot-pinch reflex. The head was positioned in a custom-made stereotaxic restraint. In the first imaging session, a panoramic z-stack was obtained in order to identify all the landmarks and regions of interest (512x512, z step-size 3 μm). Afterwards, 4 regions of interest were imaged per animal, each of them containing several dendrites and axons. These images were obtained with a digital zoom of 8X and comprised only layer I of the neocortex (512x512, z step-size 1 μm). Raw scanner data were processed in ImageJ (National Institutes of Health, Bethesda, MD, USA) and the 6 four-dimensional (x, y, z, t) stacks of each animal were analysed blind to the experimenter using this software.

The real-time analysis included 6 dendrites and 6 axons of pyramidal cells per mouse, so that each animal would present uniform data regarding their dynamics, resulting in a total of 344 axonal *boutons* and 1699 dendritic spines in 90 axons and 90 dendrites (approximately 23 axonal *boutons* and 113 spines per animal). The regions of interest were arbitrarily named with a two-letter code to avoid any bias from the experimenter. Dendritic and axonal branches were distinguished by their morphology. Axons were typified as thin tubular processes, often scattered with varicosities (EBP) whose fluorescence were at least 2 times higher than that of the axonal backbone. Dendrites were distinguished by thicker diameters (generally >2 μm), smooth, gradually tapering processes, and characteristic branching patterns.

In order to study the structural dynamics, several parameters were analysed. Gain, loss and stability functions were respectively the new, lost and stable spines/EPB in a given time point related to the previous number of spines/EPB. The turnover rate

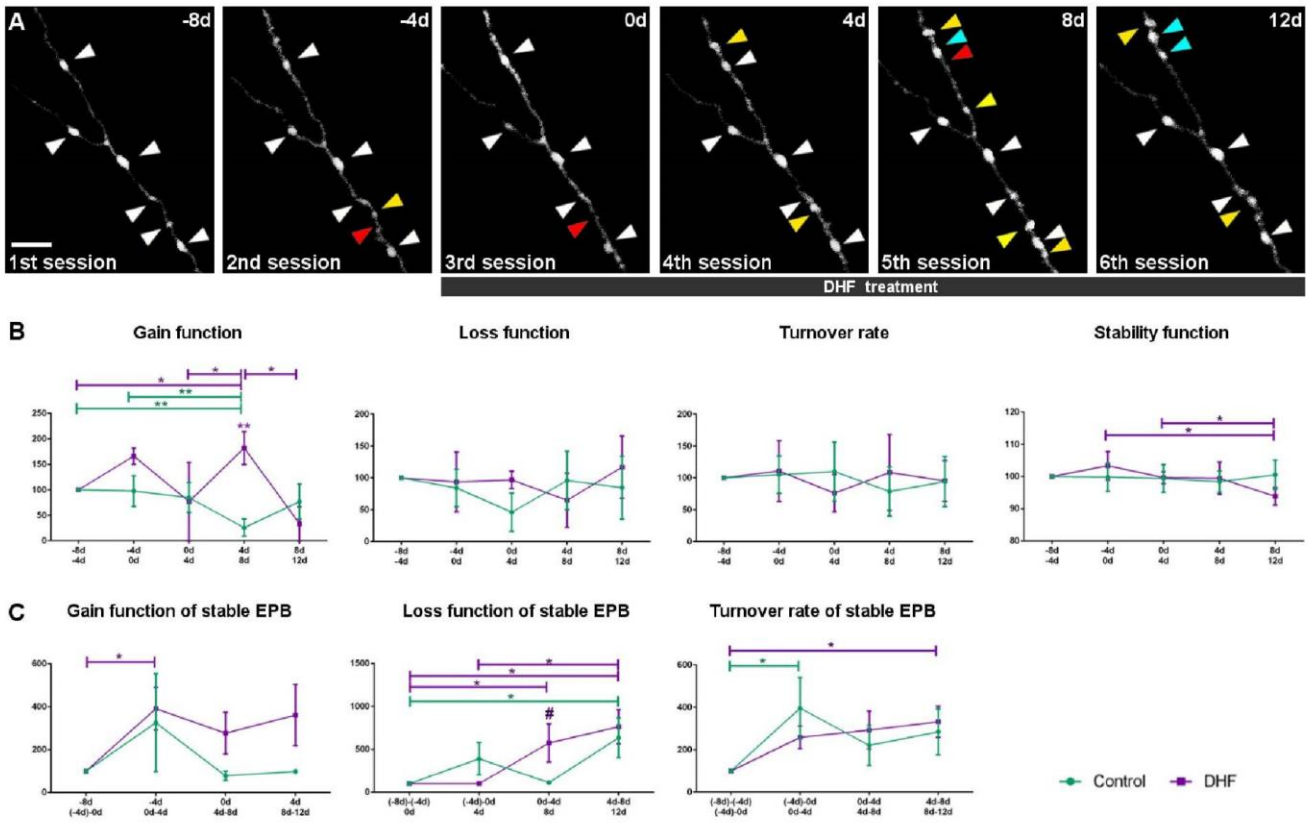

Figure 3. Structural dynamics of EPB prior and during the chronic DHF treatment. (A) Real-time 2-photon images of a representative axon from a DHF-treated mouse. Arrows point to EPB with a colour legend to clarify the effect on the dynamic parameters. White arrows point to EPB that are present from the beginning of the experiment. Yellow arrows point to EPB that are gained in that imaging session. Blue arrows point to those EPB gained in the previous imaging session that have become stable. Red arrows point to EPB that were present in the previous imaging session but have disappeared in the current one. Scale bar: 5 µm (B) Graphs representing the different dynamic parameters (gain, loss and stability functions; and turnover rate). (C) Graphs representing the different dynamic parameters studied only on stable EPB (gain and loss functions of stable EPB, and turnover rate of stable EPB). (*) $p<0.05$; (**) $p<0.01$.

was the sum of the gain and loss function divided by 2, which provided us with a more accurate idea about the dynamism. The stable functions were also studied because of their importance for the network, since structures lasting longer than 4 days have been shown to always bear at least one synapse (Knott et al. 2006; De Paola et al. 2006; Grillo et al. 2013). The stable gain function represented the number of structures (spines and EPBs) added in a time point and lasting for at least 4 days (2 consecutive imaging sessions), related to their previous number. Likewise, the stable loss function of spines/EPB represented the structures that have lasted longer than 4 days (2 consecutive imaging sessions) and were then lost, related to their previous number. The turnover rate of stable spines/EPB was the sum of the stable gain and stable loss functions divided by 2 and, again, provides us with a more accurate idea about the dynamism.

Volume analysis

It has already been shown that the fluorescent brightness of a spine is positively correlated to its volume (Holtmaat et al. 2005). In fact, increases in spine volume are related to potentiation via LTP, whereas the dendritic shaft remains unaffected (Matsuzaki et al. 2004). Therefore, we analysed whether the dendritic spines that were stable throughout the experiment would alter their volume during the DHF treatment. 6 stable spines were studied per animal (a total of 90 spines). This procedure diminished intra-group variability. Additionally, all the images had to contain no saturated pixels in order allow for the detection of variations in brightness intensity (pixel value). Because the brightness intensity of the overall image could be altered due to changes in the conditions of 2-photon imaging or the cranial window, the

brightness intensity of the dendritic shaft, whose volume remains unaffected, was also taken into account. We chose the best focal plane for a given dendritic spine and calculated the ratio between its mean pixel value and the mean pixel value of a similar portion of the adjacent dendritic shaft.

Behavioural tests

Twenty-four hours before starting the *Novel Object Recognition* (NOR) test, all animals were exposed for 10 minutes to the empty apparatus (*Open Field chamber,* OF*, 40x40cm)* (Fig. 1). This habituation procedure was also used to evaluate the locomotor activity and the anxiety levels of the animals (ANY-maze video tracking system v4.98; Stoelting Europe, Dublin, Ireland), in order to remove from the experiment those mice showing abnormal behaviours. The video tracking system provided automated measures of the total distance travelled and mean speed, to study locomotor activity, and number of entries and time spent in the periphery of the arena, for the measurement of anxiety and thigmotaxis (a valid index of anxiety in mice; (Simon et al. 1994)). The periphery zone of the arena was defined as the area located between 0 and 6 cm from the walls of the apparatus. All animals were subjected to the OF and NOR tests before and after the treatment with DHF or vehicle solution (Fig. 1).

Every NOR test was divided in 2 sessions or phases: "*familiarization*" and "*test*" (Fig. 1). During the *familiarization phase*, two identical objects were placed in 2 opposite corners of the open field (5 cm away from the walls) and the animal was allowed to explore the arena for 4 minutes. During the *test phase* (30 seconds after the familiarization phase), a novel object replaced one of the familiar objects and mice were allowed to explore again the open field arena for 4 minutes. Between sessions, the apparatus and all objects were cleaned with 70% ethanol solution. In this experiment, all mice participated in 2 familiarization phases and 2 test phases, one for every level of perceptual difficulty ("Easy" and "Difficult"; Fig. 1). In the "*Easy task*" the novel and familiar object did not share any common features, that is, they were different in shape, texture and size (Figs. 2A&B). For the *"Difficult task"*, the objects were identical in shape and colour and only 1 of the sides of the objects had a different texture (Figs. 2A&B). Object exploration was scored whenever the mouse sniffed the object or touched the object while looking at it (when the distance between the nose and the object was less than 2 cm). Climbing onto the object or chewing the object did not quantify as exploration (Leger et al. 2013). The time spent exploring each object was recorded and the difference in time spent exploring the novel object compared with the familiar object divided by the time spent exploring both objects was calculated to obtain the "discrimination ratio" (Burke et al. 2011; Burke et al. 2012).

Statistics

All the dynamic parameters were normalized to time -8d prior to the statistical analysis. For all the linear studies, a repeated-measures ANOVA was performed with treatment (DHF vs control) as between-subjects factor and time (imaging sessions) as within-subjects factor, followed by *post hoc* tests (Fisher's least significant difference) for pairwise comparisons. The unit of observation was always the animal, and each data in the linear analysis of structural dynamics was the mean of the dynamics of 6 different structures (dendrites, axons or dendritic spines), which diminished the intra-group variability. Only mice that finished all the imaging sessions were taken into account (6 control and 9 DHF).

Behavioural data were analysed using repeated measures ANOVA followed by post-hoc test. When analysing the OF data, treatment (DHF vs control) and time (before treatment vs after treatment) were considered as a between-subjects and within-subjects factors respectively. In the NOR test, an extra within-sub jects factor (Difficulty: easy vs difficult task) was added to the analysis.

The correlations between the structural dynamics and the behavioural traits were also analysed by using the Pearson's correlation coefficient (r).

All the statistical analyses were performed using the statistical package SPSS v22.0 (IBM) and graphs were created using GraphPad Prism 6. Data in the figures were expressed as mean ± SEM and $p<0.05$ were indicated.

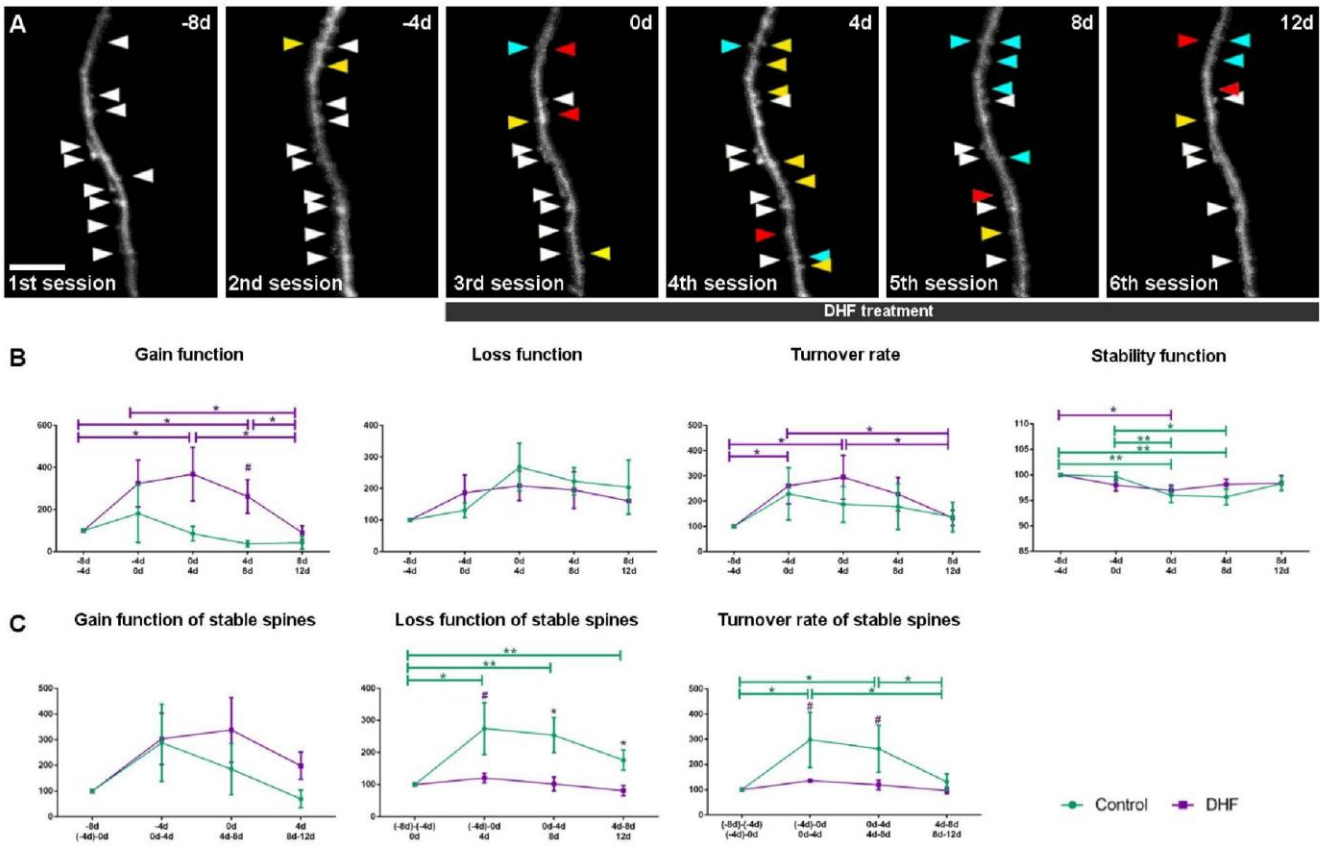

Figure 4. Structural dynamics of dendritic spines prior and during the chronic DHF treatment. (A) Real-time 2-photon images of a representative dendrite from a DHF-treated mouse. Arrows point to dendritic spines with a colour legend to clarify the effect on the dynamic parameters. White arrows point to spines that are present from the beginning of the experiment. Yellow arrows point to spines that are gained in that imaging session. Blue arrows point to those spines gained in the previous imaging session that have become stable. Red arrows point to spines that were present in the previous imaging session but have disappeared in the current one. Scale bar: 8 µm. (B) Graphs representing the different dynamic parameters (gain, loss and stability functions; and turnover rate). (C) Graphs representing the different dynamic parameters performed only on stable spines (gain and loss functions of stable spines, and turnover rate of stable spines). (*) $p<0.05$; (**) $p<0.01$.

RESULTS

Pyramidal neurons of the barrel cortex express TrkB in their somata, dendritic spines and axonal boutons

We performed immunohistochemistry to prove that TrkB was expressed by pyramidal neurons of the barrel cortex in the Thy1-YFP mice (Fig. 2). We found that, indeed, TrkB expressing puncta were abundant in the axonal *boutons* (Fig. 2B), around the cell somata (Fig. 2C1), as well as in the spine head (Fig. 2C2).

Chronic DHF treatment alters the dynamics of axonal boutons in pyramidal neurons of the barrel cortex

Different dynamic and stability parameters were analysed and found altered during the DHF treatment (Fig. 3). The gain function of EPB was altered during the experiment in both experimental and control conditions, although in a different direction (Fig. 3B). In control conditions the gain function diminished gradually throughout the experiment (Control -8d/-4d vs 4d/8d: p=0.009; -4d/0d vs 4d/8d: p=0.09), whereas in DHF-treated mice it was firstly increased (DHF -8d/-4d vs 4d/8d: p=0.033; 0d/4d vs 4d/8d: p=0.047) and finally decreased to baseline levels (DHF 4d/8d to 8d/12d: p=0.019). The difference between groups reached its peak in the middle of the DHF treatment (4d/8d Control vs DHF: p=0.005). Neither the loss function nor the turnover rate were altered during the experiment. However, in the DHF group the stability function of their EPB decreased gradually through the treatment (DHF -4d/0d vs 8d/12d: p=0.018; 0d/4d vs 8d/12d: p=0.028).

We next asked whether the stable EPB (those that last longer than 4 days) presented altered

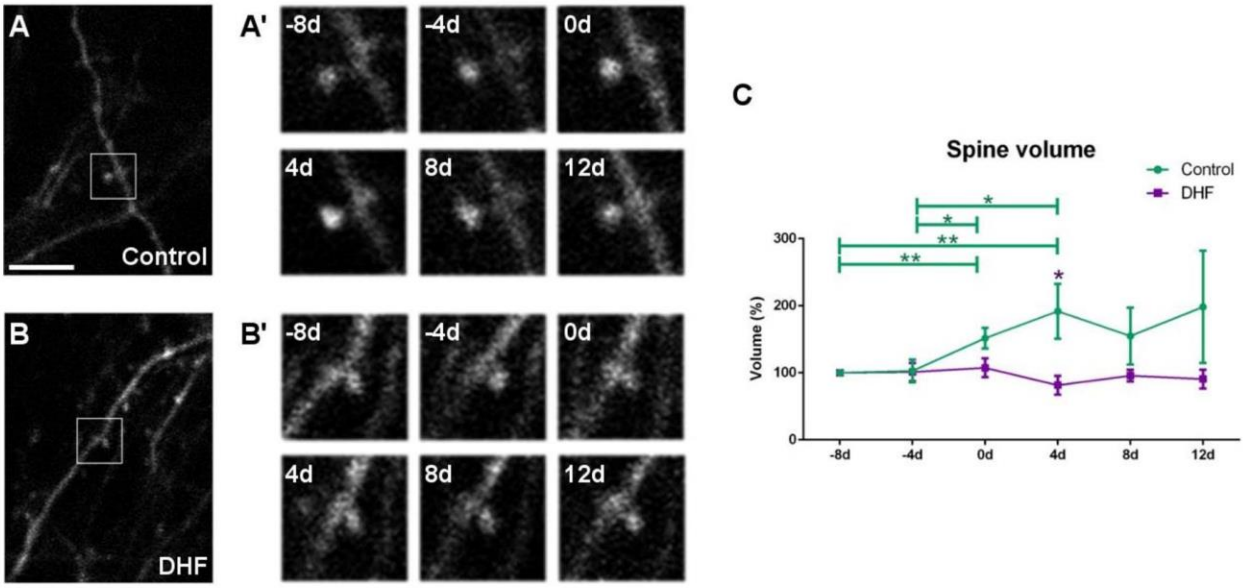

Figure 5. Real-time analysis of the dendritic spine volume prior and during the DHF treatment. (A) & (B) Low magnification images of representative dendrites in Control (A) and DHF-treated (B) animals. Scale bar: 6 µm. (A') & (B') High magnification images from the squared spines from Control (A') and DHF-treated (B') animals. Scale bar: 3 µm. (C) Graph representing the variation (%) in dendritic spine volume. (*) $p<0.05$; (**) $p<0.01$.

dynamics due to the DHF treatment, and found several interesting variations (Fig. 3C). First, the gain function of stable EPB increased rapidly only in the beginning of the DHF treatment (DHF -8d/-4d-0d vs -4d/0d-4d: p=0.037), whereas it remained unchanged in control conditions. Second, the loss function increased gradually throughout the experiment in both conditions, although in the DHF-treated mice this increase was more consistent [Control -8d-(-4d)/0d vs 4d-8d/12d: p=0.038; DHF -8d-(-4d)/0d vs 0d-4d/8d: p=0.016, -8d-(-4d)/0d vs 4d-8d/12d: p=0.015, -4d-0d/4d vs 4d-8d/12d: p=0.015], and there was a trend towards an increase in the DHF group in the middle of the treatment (0d-4d/8d Control vs DHF: p=0.071). Finally, the turnover rate of stable EPB was increased in the beginning of the experiment in control conditions [Control -8d-(-4d)/(-4d)-0d vs (-4d)-0d/0d-4d p=0.018], whilst in the DHF group this augment was significant from its baseline to the end of the DHF treatment [DHF -8d-(-4d)/(-4d)-0d vs 4d-8d/8d-12d p=0.021].

Chronic DHF treatment alters the dynamics of dendritic spines in pyramidal neurons of the barrel cortex

In order to further understand the dynamics of pyramidal neurons under the influence of DHF, we analysed the dendritic spine dynamics throughout the treatment (Fig. 4B). We found that the gain function rapidly increased in the beginning of the DHF treatment [DHF -8d/-4d vs 0d-4d p=0.032, -8d/-4d vs 4d/8d p=0.037], but later decreased to baseline and control levels [DHF -4d/0d vs 8d/12d p=0.018, 0d/4d vs 8d/12d p=0.018, 4d/8d vs 8d/12d p=0.016]. There was also a trend towards an increase in the control group in the middle of the treatment (4d/8d Control vs DHF p=0.095). The loss function remained unchanged in both control and experimental conditions, whereas the turnover rate was first increased (DHF -8d/-4d vs -4d/0d p=0.050, -8d/-4d vs 0d/4d p=0.027), to return finally to control and baseline levels (DHF –4d/0d vs 8d/12d p=0.036, 0d/4d vs 8d/12d p=0.027). Furthermore, the stability function was also reduced in both Control and DHF groups, although more prominently in the former (Control -8d/-4d vs 0d/4d: p=0.009; -8d/-4d vs 4d/8d: p=0.007; -4d/0d vs 0d/4d: p=0.005; -4d/0d vs 4d/8d: p=0.042; DHF -8d/-4d vs 0d/4d: p=0.014).

Chronic DHF treatment protects stable pyramidal spines from dynamic changes

We next asked whether the stable spines (those that last longer than 4d) had their dynamics altered under the DHF treatment (Fig. 4C). The gain function remained unaltered. However, the loss function and the turnover rate of stable spines varied in control

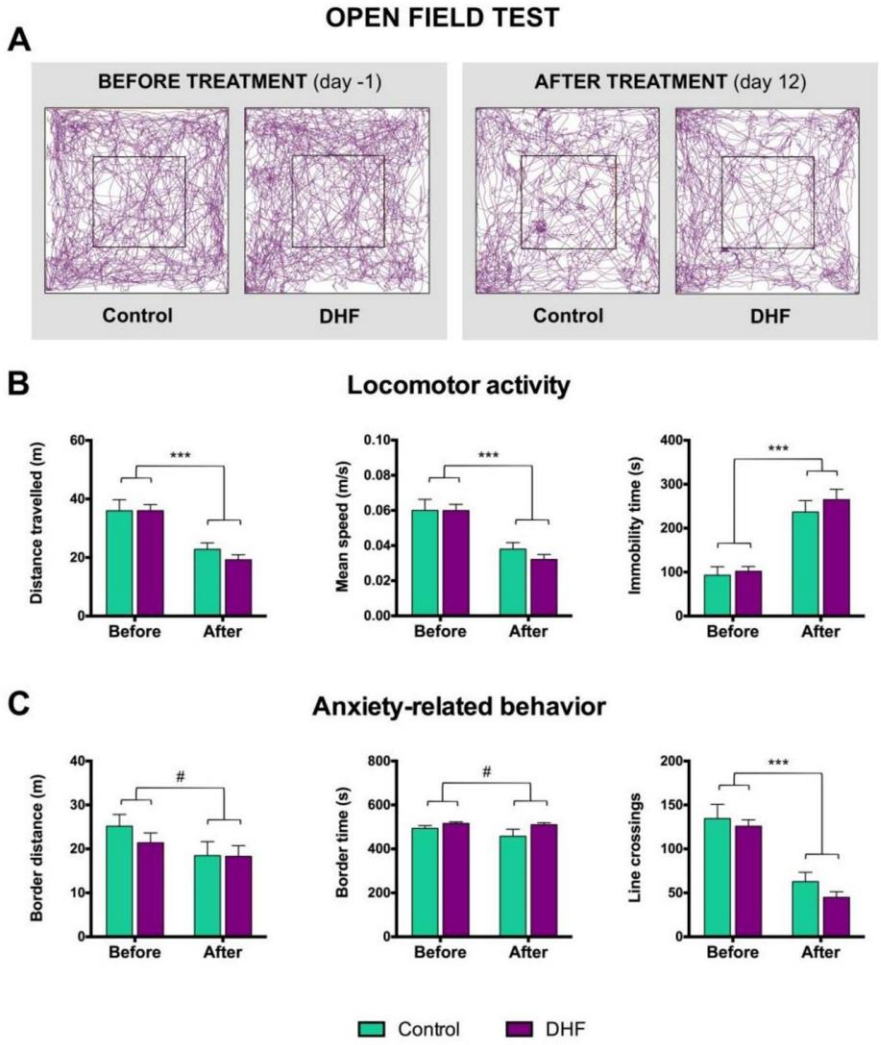

Figure 6. Open field test (OF). (A) Representative track-plot reports recorded during the 10 min test sessions (ANY-maze). The central square was denominated "central zone" and the periphery, "border zone". Observe the decrease in the distance travelled (purple line) by both groups (DHF and control) after the treatment. Locomotor activity (B) and anxiety-related behaviour (C) were decreased in both groups after the treatment, but no significant differences were found between them. (***) $p<0.001$; (#) $0.1>p>0.05$.

conditions: The loss function of stable spines increased throughout the experiment [Control -8d-(-4d)/0d vs (-4d)-0d/4d p=0.010, -8d-(-4d)/0d vs 0d-4d/8d p=0.004, -8d-(-4d)/0d vs 4d-8d/12d p=0.006]. These increases were also significant when comparing DHF and Control groups (0d-4d/8d Control vs DHF p=0.022, 4d-8d/12d p=0.010], and there was also a trend towards an increase at the beginning of the treatment (-4d-0d/4d Control vs DHF p=0.078). Similarly, the turnover rate of stable spines was altered only in control conditions, first increasing [Control -8d-(-4d)/(-4d)/0d vs (-4d)-0d/0d-4d p=0.013, -8d-(-4d)/(-4d)/0d vs 0d-4d/4d-8d p=0.019] and later returning to baseline levels [Control (-4d)-0d/0d-4d vs 4d-8d/8d-12d p=0.012, 0d-4d/4d-8d vs 4d-8d/8d-12d p=0.016]. Similarly, there were trends towards an increase when comparing both groups in the middle of the treatment [(-4d)-0d/0d-4d Control vs DHF p=0.090, 0d-4d/4d-8d Control vs DHF p=0.091].

The volume of pyramidal spines remains unaltered throughout the DHF treatment

In order to better u nderstand the changes experimented by stable spines under DHF and control conditions, we estimated the volume of the spines that were present throughout the entire experiment (Fig. 5). Surprisingly, we found that the stable spines of the control group increased their volume whereas in DHF-treated mice this parameter remained stable. These increases were significant within the control group (Control -8d vs 0d p=0.007, -8d vs 4d p=0.008, -4d vs 0d p=0.023, -4d vs 4d p=0.037) and when comparing both groups (4d Control vs DHF p=0.014).

DHF treatment does not affect locomotion or anxiety-related behaviour

We analysed the distance travelled, mean speed and immobility time during the OF test, before and

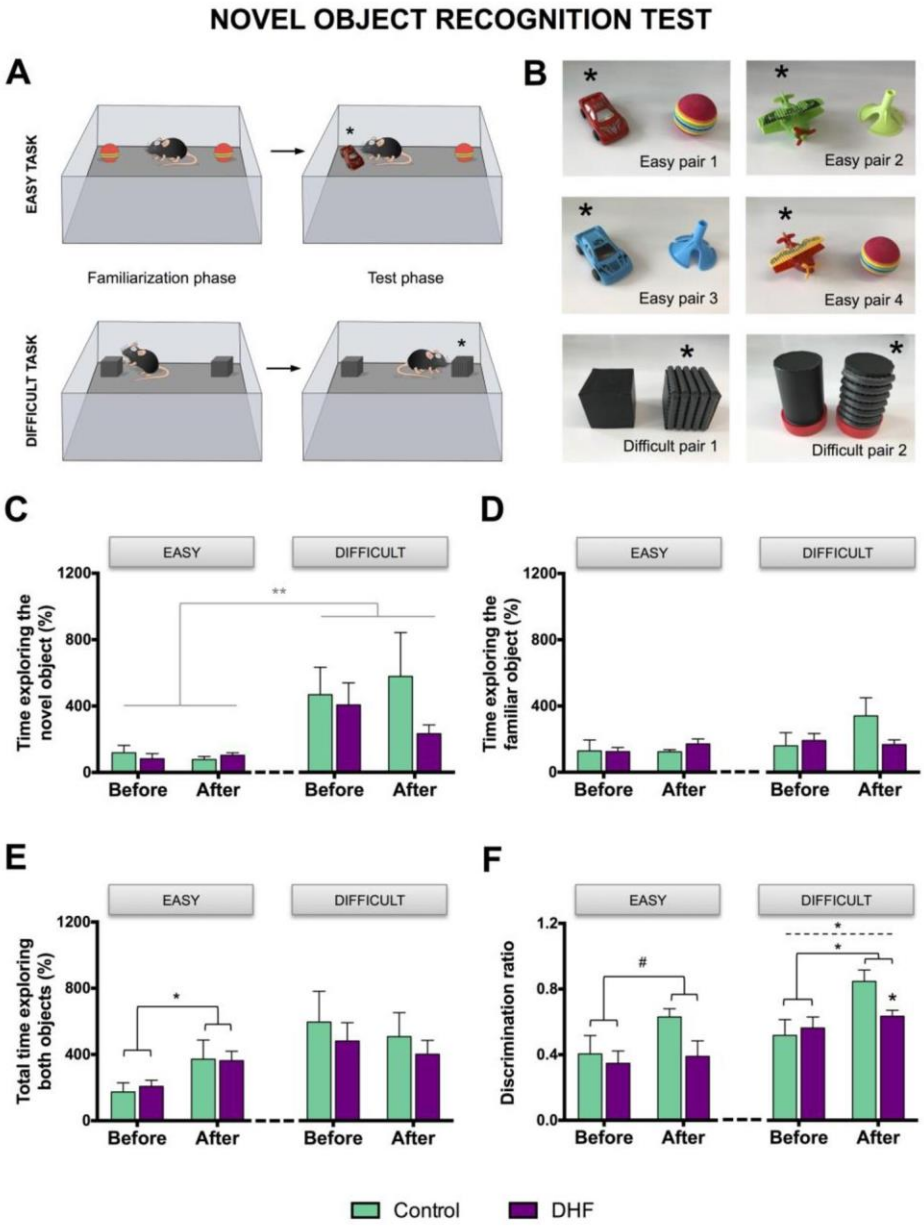

Figure 7. Novel object recognition test (NOR). (A) Schematic drawings of the 2 types of NOR tests performed in our experiment and their phases (familiarization: 2 identical objects; test: 1 familiar and 1 novel object). (B) Photographs of the pairs of objects that were randomly used during the NOR test. The asterisk marks the novel object. (C) Bar graphs representing an increased percentage of time exploring the novel object in the difficult task (easy vs difficult) but no difference due to the treatment (DHF vs. control) or time (before vs. after). (D) No statistically significant differences were observed in the exploration of the familiar object. (E) The total time exploring both objects (novel + familiar) was significantly increased after the treatment in the easy task, but no differences were observed among groups. (F) When analysing the discrimination ratio [(time spent exploring the novel object) - (time exploring the familiar object)/ time spent exploring both objects] only DHF treated mice showed decreased object discrimination ratio in the difficult task. Black Horizontal lines in graphs represent statistically significant effects of time (black), difficulty (grey), or interaction (grey, dashed) in a repeated-measures ANOVA (*p<0.05, **p<0.01, ***p<0.001, # 0.1<p<0.05).

after treatment, as an index of locomotor activity (Figs. 6A&B). Although decreased locomotion was found to occur after the treatment (distance travelled: $p= 1.2*10^{-5}$; mean speed: $p=1.3*10^{-5}$; immobility time, $p= 1.0*10^{-6}$; Fig. 6B), no statistically significant differences were found between DHF and vehicle-treated mice [distance travelled (before: p=0.994; after: p=0.234; Figs. 6A&B), mean speed (before: p=0.990; after: p=0.240; Fig. 6B) and immobility time (before: p=0.673; after: p=0.472; Fig. 6B)].

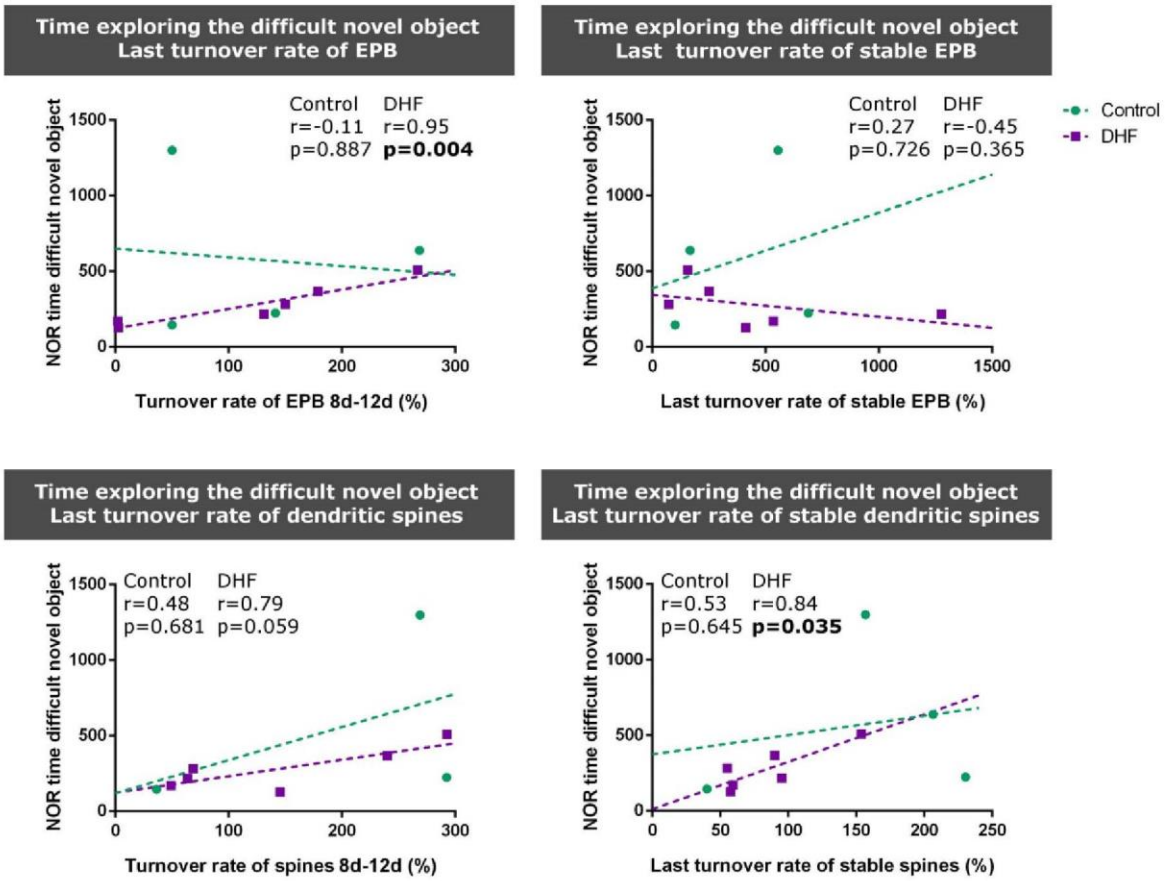

Figure 8. Correlation analysis between behavioural and dynamic parameters. Pearson's coefficient (r) for the "time exploring the difficult novel object" and the last turnover rate of dendritic spines and EPB in Control and DHF-treated animals.

A similar situation occurred when we analysed anxiety-related behaviour (Fig. 6C), with an apparent decrease of anxiety after treatment (border distance: p=0.051, border time: p=0.095, line crossings: p=0.008), but no statistically significant differences among DHF and control groups [border distance (before: p=0.324; after: p=0.966), border time (before: p=0.112; after: p=0.060) and line crossings (before: p=0.068; after: p=0.427)].

DFH treatment improves object recognition memory

As expected, the percentage of time exploring the novel object was significantly increased when performing the difficult task (easy vs difficult: p=0.008; Figs. 7A-C), with independence of the treatment (DHF vs. Control) or time (before vs. after). But interestingly, when we analysed the discrimination ratio [(time spent exploring the novel object) - (time exploring the familiar object)/ time spent exploring both objects] only DHF treated mice showed a decreased object discrimination ratio in this task (p=0.028). This can be interpreted as an increased recognition memory to difficult objects (the novel and familiar objects were identical in shape and colour and only 1 of the sides of the objects had a different texture; Fig 7B).

The time exploring the difficult novel object is correlated with the turnover rate of en passant boutons *and dendritic* spines *only in animals treated with DHF*

Finally, in order to comprehend the relationship between the behavioural performance and the structural dynamics of pyramidal neurons, we executed a correlation analysis. We found that the turnover rate of both EPB and dendritic spines was positively correlated with the time exploring the difficult novel object, only in DHF-treated mice (Fig. 8). Regarding the EPB, this correlation was significant only with the last normal turnover rate (8d/12d, DHF r=0.95 p=0.004). However, when

studying dendritic spines, we found that the time exploring the difficult novel object was only correlated with the last turnover rate of stable spines (4d-8d/8d-12d, DHF r=0.84 p=0.035).

DISCUSSION

In the current study, we show, in real-time, how the structure of neocortical pyramidal neurons is altered during a chronic treatment with DHF, a TrkB agonist that has an important clinical potential. Furthermore, we show that this treatment also enhances object recognition memory of complex items and that these improvements are correlated with the structural dynamics of dendritic spines and axonal *boutons*.

Our findings are in agreement with previous reports that showed the expression of TrkB in layer V pyramidal neurons of the rat somatosensory cortex (Miller and Pitts 2000). Moreover, we expand this knowledge by describing the presence of the receptor in the somata, dendritic spines and axonal *boutons* of these neurons in mice. We next asked whether a chronic activation of TrkB would alter the dynamics of these neuronal structures (gain, loss, stability functions of dendritic spines and axonal *boutons* in a longitudinal, chronic real-time study). We also wondered whether it would impact behaviours related to this brain area, uncovering some important alterations. The gain function of dendritic spines was increased 4 days after the beginning of the treatment, persisted after 8 days and returned to baseline levels 12 days afterwards. Our findings are not surprising, since LTP can be induced by TrkB activation (Minichiello et al. 2002; Minichiello 2009) and this form of synaptic plasticity promotes the apparition of dendritic spines in pyramidal neurons (Engert and Bonhoeffer 1999). In addition, pyramidal spine density increases in the rat hippocampus after BDNF administration (Tyler and Pozzo-Miller 2003), and even after a chronic treatment with DHF (Zeng et al. 2012b). However, although our results might seem similar, these previous findings were performed in post-mortem tissue and thus alterations in spine dynamics cannot be inferred.

We have also studied the dynamics of stable spines, which are those present at least for 4 days (two consecutive imaging sessions). These spines are particularly important because they have been shown to always bear a synapse (Knott et al. 2006) and, therefore, are the ones modifying the network. The loss function of stable spines was incremented during the experiment only in the control group, whereas the DHF protected against these changes. Surprisingly, only in the control group, we have also shown that the spines that remained stable during the whole experiment increased their volume. Increases in volume have been previously correlated to spine potentiation (Matsuzaki et al. 2004). This spine enlargement may be the consequence of the synaptic loss caused by the elimination of stable spines. Therefore, in order to compensate and maintain synaptically the circuit, the remaining stable spines increase their volumes. We have also shown that the stability function of dendritic spines was gradually reduced throughout the experiment, more remarkably in control animals. This appears to be a consequence of real-time imaging: similar reductions have already been shown in the same mice strain that we used (Grutzendler et al. 2002). All these facts suggest that the DHF protects against the intrinsic damage that real-time imaging produces, which is in agreement with the known neuroprotective properties of this drug against glutamate excitotoxicity (Chen et al. 2011a), neonatal hypoxia, ischemia (Uluc et al. 2013), degeneration of dopaminergic neurons in animal models of Parkinson's disease (Luo et al. 2016) or staurosporine-induced apoptosis (Jang et al. 2010).

The dynamics of axonal *boutons* were also analysed before and during the DHF treatment, showing increases in their gain function 8 days after its onset. The dynamics of stable EPB were also analysed and we found that their gain function increases. Both results agree with the increases in axonal arborization, and consequently in the presynaptic surface, that BDNF infusion produces in other species (Cohen-Cory and Fraser 1995; Lom and Cohen-Cory 1999; Bing et al. 2005; Granseth et al. 2013).

We have also wondered whether a chronic treatment with DHF might improve sensory perception dependent on the barrel cortex, the region of our structural analysis. In order to achieve so, we have performed a modified NOR test with easy and difficult novel objects that varied in their texture, so that they may be mostly recognizable by their

whiskers (Guić-Robles et al. 1989; Arabzadeh et al. 2005; Brecht 2007; von Heimendahl et al. 2007). Consequently, this test would allow us to link behavioural and structural alterations. We have found that, indeed, animals treated with this drug displayed a lower discrimination ratio, which means that they discriminated better the difficult novel object. These results agree with multiple studies correlating BDNF or TrkB manipulation with object recognition memory: BDNF expression has been positively linked to object recognition memory (Hopkins and Bucci 2010), whereas a lesser activation of TrkB with anti-BDNF causes opposite results (Callaghan and Kelly 2013). In addition, DHF has already been shown to improve memory consolidation in both rats and mice also in a NOR test (Bollen et al. 2013). Our results go further and show that DHF also enhances object recognition behaviour and sensory discrimination. Moreover, these behavioural effects are correlated with the turnover of dendritic spines and axonal *boutons* of layer V pyramidal neurons of the barrel cortex.

In conclusion, we provide real-time *in vivo* evidence of how the chronic activation of TrkB has beneficial behavioural effects in healthy animals and alters the structural plasticity and dynamics of neocortical pyramidal neurons, mainly by protecting them from deleterious alterations. Our results also highlight the timeline of these structural changes, so that further research can pinpoint the optimal duration of the treatment. This is not unimportant since the malfunction of the BDNF-TrkB system has been suggested to underlie several neuropsychiatric disorders, including Alzheimer's disease or schizophrenia (Angelucci et al. 2005; Zuccato and Cattaneo 2009), and currently its manipulation is being tested to provide new therapeutic vectors for these diseases (Nagahara and Tuszynski 2011; Lu et al. 2013).

FUNDING

This work was supported by Generalitat Valenciana (Prometeo Excellence Program PROMETEO2013/069) and the Fundación Alicia Koplowitz to JN, and by the Spanish Ministry of Economy and Competitiveness to JN (SAF2015-68436-R), EC-G (IJCI-2015-24124) and MP-R (FPU12/03200).

REFERENCES

Angelucci F, Brenè S, Mathé a a (2005) BDNF in schizophrenia, depression and corresponding animal models. Mol Psychiatry 10:345–52. doi: 10.1038/sj.mp.4001637

Arabzadeh E, Zorzin E, Diamond ME (2005) Neuronal encoding of texture in the whisker sensory pathway. PLoS Biol 3:e17. doi: 10.1371/journal.pbio.0030017

Bing H, Nikolakopoulou AM, Cohen-Cory S (2005) BDNF stabilizes synapses and maintains the structural complexity of optic axons in vivo. Development 132:4285–4298. doi: 10.1242/dev.02017

Bollen E, Vanmierlo T, Akkerman S, et al (2013) 7,8-Dihydroxyflavone improves memory consolidation processes in rats and mice. Behav Brain Res 257:8–12. doi: 10.1016/j.bbr.2013.09.029

Brecht M (2007) Barrel cortex and whisker-mediated behaviors. Curr Opin Neurobiol 17:408–416. doi: 10.1016/j.conb.2007.07.008

Burke SN, Ryan L, Barnes CA (2012) Characterizing cognitive aging of recognition memory and related processes in animal models and in humans. Front Aging Neurosci 4:1–13. doi: 10.3389/fnagi.2012.00015

Burke SN, Wallace JL, Hartzell AL, et al (2011) Age-Associated Deficits in Pattern Separation Functions of the Perirhinal Cortex : A Cross-Species Consensus. Behav Neurosci 125:836–847. doi: 10.1037/a0O25238

Callaghan CK, Kelly ÁM (2013) Neurotrophins play differential roles in short and long-term recognition memory. Neurobiol Learn Mem 104:39–48. doi: 10.1016/j.nlm.2013.04.011

Cane M, Maco B, Knott G, Holtmaat A (2014) The relationship between PSD-95 clustering and spine stability in vivo. J Neurosci 34:2075–86. doi: 10.1523/JNEUROSCI.3353-13.2014

Caroni P, Donato F, Muller D (2012) Structural plasticity upon learning: regulation and functions. Nat Rev Neurosci 13:478–490. doi: 10.1038/nrn3258

Castello NA, Nguyen MH, Tran JD, et al (2014) 7,8-Dihydroxyflavone, a Small Molecule TrkB Agonist, Improves Spatial Memory and Increases Thin Spine Density in a Mouse Model of Alzheimer Disease-Like Neuronal Loss. PLoS One 9:e91453. doi: 10.1371/journal.pone.0091453

Castrén E, Rantamäki T (2010) The role of BDNF and its receptors in depression and antidepressant drug action: Reactivation of developmental plasticity. Dev Neurobiol 70:289–297. doi: 10.1002/dneu.20758

Chen J, Chua KW, Chua CC, et al (2011a) Antioxidant activity of 7,8-dihydroxyflavone provides neuroprotection against glutamate-induced toxicity. Neurosci Lett 499:181–185. doi: 10.1016/j.neulet.2011.05.054

Chen JL, Flanders GH, Lee W-CA, et al (2011b) Inhibitory Dendrite Dynamics as a General Feature of the Adult Cortical Microcircuit. J Neurosci 31:12437–12443. doi: 10.1523/JNEUROSCI.0420-11.2011

Chen JL, Lin WC, Cha JW, et al (2011c) Structural basis for the role of inhibition in facilitating adult brain plasticity. Nat Neurosci 14:587–94. doi: 10.1038/nn.2799

Chen JL, Nedivi E (2013) Highly Specific Structural Plasticity of Inhibitory Circuits in the Adult Neocortex. Neurosci 19:384–393. doi: 10.1177/1073858413479824

Chen JL, Villa KL, Cha JW, et al (2012) Clustered dynamics of inhibitory synapses and dendritic spines in the adult neocortex. Neuron 74:361–73. doi: 10.1016/j.neuron.2012.02.030

Cohen-Cory S, Fraser SE (1995) Effects of brain-derived neurotrophic factor on optic axon branching and remodelling in vivo. Nature 378:192–196.

De Paola V, Holtmaat A, Knott G, et al (2006) Cell type-specific structural plasticity of axonal branches and boutons in the adult neocortex. Neuron 49:861–875. doi: 10.1016/j.neuron.2006.02.017

Du X, Hill RA (2015) 7,8-Dihydroxyflavone as a pro-neurotrophic treatment for neurodevelopmental disorders. Neurochem Int 89:170–180. doi: 10.1016/j.neuint.2015.07.021

Engert F, Bonhoeffer T (1999) Dendritic spine changes associated with hippocampal long-term synaptic plasticity. Nature 399:66–70. doi: 10.1038/19978

Escobar ML, Figueroa-Guzmán Y, Gómez-Palacio-Schjetnan A (2003) In vivo insular cortex LTP induced by brain-derived neurotrophic factor. Brain Res 991:274–279. doi: 10.1016/j.brainres.2003.08.015

Feng G, Mellor RH, Bernstein M, et al (2000) Imaging neuronal subsets in transgenic mice expressing multiple spectral variants of GFP. Neuron 28:41–51.

Granseth B, Fukushima Y, Sugo N, et al (2013) Regulation of thalamocortical axon branching by BDNF and synaptic vesicle cycling. Front Neural Circuits 7:202. doi: 10.3389/fncir.2013.00202

Grillo FW, Song S, Teles-Grilo Ruivo LM, et al (2013) Increased axonal bouton dynamics in the aging mouse cortex. Proc Natl Acad Sci 110:E1514–E1523. doi: 10.1073/pnas.1218731110

Grutzendler J, Kasthuri N, Gan WW-B (2002) Long-term dendritic spine stability in the adult cortex. Nature 420:812–816. doi: 10.1038/nature01151.1.

Guić-Robles E, Valdivieso C, Guajardo G (1989) Rats can learn a roughness discrimination using only their vibrissal system. Behav Brain Res 31:285–289. doi: 10.1016/0166-4328(89)90011-9

Hofer SB, Mrsic-Flogel TD, Bonhoeffer T, Hübener M (2009) Experience leaves a lasting structural trace in cortical circuits. Nature 457:313–317. doi: 10.1038/nature07487

Holtmaat A, Bonhoeffer T, Chow DK, et al (2009) Long-term, high-resolution imaging in the mouse neocortex through a chronic cranial window. Nat Protoc 4:1128–1144. doi: 10.1038/nprot.2009.89

Holtmaat A, Svoboda K (2009) Experience-dependent structural synaptic plasticity in the mammalian brain. Nat Rev Neurosci 10:647–58. doi: 10.1038/nrn2699

Holtmaat A, Wilbrecht L, Knott GW, et al (2006) Experience-dependent and cell-type-specific spine growth in the neocortex. Nature 441:979–983. doi: 10.1038/nature04783

Holtmaat AJGD, Trachtenberg JT, Wilbrecht L, et al (2005) Transient and persistent dendritic spines in the neocortex in vivo. Neuron 45:279–291. doi: 10.1016/j.neuron.2005.01.003

Hopkins ME, Bucci DJ (2010) BDNF expression in perirhinal cortex is associated with exercise-induced improvement in object recognition memory. Neurobiol Learn Mem 94:278–284. doi: 10.1016/j.nlm.2010.06.006

Jang S-W, Liu X, Yepes M, et al (2010) A selective TrkB agonist with potent neurotrophic activities by 7,8-dihydroxyflavone. Proc Natl Acad Sci U S A 107:2687–92. doi: 10.1073/pnas.0913572107

Kang H, Welcher AA, Shelton D, Schuman EM (1997) Neurotrophins and time: Different roles for

TrkB signaling in hippocampal long-term potentiation. Neuron 19:653–664. doi: 10.1016/S0896-6273(00)80378-5

Keck T, Scheuss V, Jacobsen RI, et al (2011) Loss of sensory input causes rapid structural changes of inhibitory neurons in adult mouse visual cortex. Neuron 71:869–82. doi: 10.1016/j.neuron.2011.06.034

Knott GW, Holtmaat A, Wilbrecht L, et al (2006) Spine growth precedes synapse formation in the adult neocortex in vivo. Nat Neurosci 9:1117–1124. doi: 10.1038/nn1747

Leger M, Quiedeville A, Bouet V, et al (2013) Object recognition test in mice. Nat Protoc 8:2531–2537. doi: 10.1038/nprot.2013.155

Lom B, Cohen-Cory S (1999) Brain-Derived Neurotrophic Factor Differentially Regulates Retinal Ganglion Cell Dendritic and Axonal Arborization In Vivo. J Neurosci 19:9928–9938.

Lu B, Nagappan G, Guan X, et al (2013) BDNF-based synaptic repair as a disease-modifying strategy for neurodegenerative diseases. Nat Rev Neurosci 14:401–416. doi: 10.1038/nrn3505

Luo D, Shi Y, Wang J, et al (2016) 7,8-dihydroxyflavone protects 6-OHDA and MPTP induced dopaminergic neurons degeneration through activation of TrkB in rodents. Neurosci Lett 620:43–49. doi: 10.1016/j.neulet.2016.03.042

Matsuzaki M, Honkura N, Ellis-Davies GCR, Kasai H (2004) Structural basis of long-term potentiation in single dendritic spines. Nature 429:761–6. doi: 10.1038/nature02617

Miller MW, Pitts AF (2000) Neurotrophin receptors in the somatosensory cortex of the mature rat: Co-localization of p75, trk, isoforms and c-neu. Brain Res 852:355–366. doi: 10.1016/S0006-8993(99)02176-9

Minichiello L (2009) TrkB signalling pathways in LTP and learning. Nat Rev Neurosci 10:850–60. doi: 10.1038/nrn2738

Minichiello L, Calella AM, Medina DL, et al (2002) Mechanism of TrkB-mediated hippocampal long-term potentiation. Neuron 36:121–137. doi: 10.1016/S0896-6273(02)00942-X

Nagahara AH, Tuszynski MH (2011) Potential therapeutic uses of BDNF in neurological and psychiatric disorders. Nat Rev Drug Discov 10:209–219. doi: 10.1038/nrd3366

Pandya CD, Kutiyanawalla A, Pillai A (2013) BDNF-TrkB signaling and neuroprotection in schizophrenia. Asian J Psychiatr 6:22–28. doi: 10.1016/j.ajp.2012.08.010

Porrero C, Rubio-Garrido P, Avendaño C, Clascá F (2010) Mapping of fluorescent protein-expressing neurons and axon pathways in adult and developing Thy1-eYFP-H transgenic mice. Brain Res 1345:59–72. doi: 10.1016/j.brainres.2010.05.061

Simon P, Dupuis R, Costentin J (1994) Thigmotaxis as an index of anxiety in mice. Influence of dopaminergic transmissions. Behav Brain Res 61:59–64.

Tyler WJ, Pozzo-Miller L (2003) Miniature synaptic transmission and BDNF modulate dendritic spine growth and form in rat CA1 neurones. J Physiol 553:497–509. doi: 10.1113/jphysiol.2003.052639

Uluc K, Kendigelen P, Fidan E, et al (2013) TrkB receptor agonist 7, 8 dihydroxyflavone triggers profound gender- dependent neuroprotection in mice after perinatal hypoxia and ischemia. CNS Neurol Disord Drug Targets 12:360–70. doi: CDTCNSND-EPUB-20130227-13 [pii]

van Versendaal D, Rajendran R, Saiepour MH, et al (2012) Elimination of inhibitory synapses is a major component of adult ocular dominance plasticity. Neuron 74:374–83. doi: 10.1016/j.neuron.2012.03.015

von Heimendahl M, Itskov PM, Arabzadeh E, Diamond ME (2007) Neuronal Activity in Rat Barrel Cortex Underlying Texture Discrimination. PLoS Biol 5:e305. doi: 10.1371/journal.pbio.0050305

Yan Q, Radeke MJ, Matheson CR, et al (1997) Immunocytochemical localization of TrkB in the central nervous system of the adult rat. J Comp Neurol 378:135–157. doi: 10.1002/(SICI)1096-9861(19970203)378:1<135::AID-CNE8>3.0.CO;2-5

Yang YJ, Li YK, Wang W, et al (2014) Small-molecule TrkB agonist 7,8-dihydroxyflavone reverses cognitive and synaptic plasticity deficits in a rat model of schizophrenia. Pharmacol Biochem Behav 122:30–36. doi: 10.1016/j.pbb.2014.03.013

Yoshii A, Constantine-Paton M (2010) Postsynaptic BDNF-TrkB signaling in synapse maturation, plasticity, and disease. Dev Neurobiol 70:304–22. doi: 10.1002/dneu.20765

Zeng Y, Liu Y, Wu M, et al (2012a) Activation of TrkB by 7,8-dihydroxyflavone prevents fear memory defects and facilitates amygdalar synaptic plasticity in aging. J Alzheimer's Dis 31:765–778.

doi: 10.3233/JAD-2012-120886

Zeng Y, Lv F, Li L, et al (2012b) 7,8-Dihydroxyflavone Rescues Spatial Memory and Synaptic Plasticity in Cognitively Impaired Aged Rats. J Neurochem 122:800–811. doi: 10.1111/j.1471-4159.2012.07830.x

Zhang J, Wu J, Fujita Y, et al (2015) Antidepressant effects of TrkB ligands on depression-like behavior and dendritic changes in mice after inflammation. Int J Neuropsychopharmacol 18:1–12. doi: 10.1093/ijnp/pyu077

Zhang MW, Zhang S feng, Li ZH, Han F (2016) 7,8-Dihydroxyflavone reverses the depressive symptoms in mouse chronic mild stress. Neurosci Lett 635:33–38. doi: 10.1016/j.neulet.2016.10.035

Zhang Z, Liu X, Schroeder JP, et al (2014) 7,8-Dihydroxyflavone Prevents Synaptic Loss and Memory Deficits in a Mouse Model of Alzheimer's Disease. Neuropsychopharmacology 39:638–650. doi: 10.1038/npp.2013.243

Zuccato C, Cattaneo E (2009) Brain-derived neurotrophic factor in neurodegenerative diseases. Nat Rev Neurol 5:311–322. doi: 10.1038/nrneurol.2009.54

IV. DISCUSSION

1. NMDA RECEPTORS REGULATE THE STRUCTURAL DYNAMICS OF SOMATOSTATIN EXPRESSING INTERNEURONS OF THE HIPPOCAMPUS

The NMDA type of glutamate receptors has been extensively studied regarding neural potentiation and depression (Bear and Malenka, 1994; Bliss and Collingridge, 1993). These receptors have also a well-described role in spinogenesis during development (Kwon and Sabatini, 2011) and in the remodelling of dendritic spines during adulthood (Lai and Ip, 2013; Matsuzaki *et al*, 2004). All these data come from studies focused on pyramidal neurons. However, these receptors are expressed also in other neurons, including interneurons such as the SOM expressing cells in the *stratum oriens* of the hippocampus, a very well characterized interneuronal subpopulation (Freund and Buzsáki, 1996; Nyíri *et al*, 2003). Very little is known about the effects of the activation of these receptors on the structure of interneurons, particularly of these hippocampal cells. In the present thesis, I have aimed to understand the effects that the acute NMDAR blockade produce in the density of dendritic spines and axonal *boutons* of hippocampal SOM expressing interneurons of the *stratum oriens*. Although structural dynamics appear to be the force underlying adaptation to changing environments (Bhatt *et al*, 2009; Holtmaat and Svoboda, 2009), to date few experiments focusing on inhibitory circuits have been published (Chen *et al*, 2012; Hofer *et al*, 2011; Keck *et al*, 2011; van Versendaal *et al*, 2012), but none of them on SOM expressing interneurons. Therefore, I next asked how NMDAR activation and inhibition might alter the spine dynamics of these cells. Altogether, these experiments have provided several interesting results, which have helped to shed light into understanding the role of these receptors on the structural plasticity of SOM expressing interneurons.

1.1. Acute MK-801 treatment does not change spine density but increases the density of axonal boutons *of somatostatin expressing interneurons and alters anxiety-related behaviours*

In order to understand how NMDAR blockade affects the density of dendritic spines and axonal *boutons* of the hippocampal SOM expressing interneurons in the *stratum*

oriens, we have acutely injected mice, which express constitutively EGFP in these cells (GIN mice, Oliva et al., 2000), with the NMDAR antagonist MK-801. Twenty-four hours after the injection, a hole-board test was performed to obtain a readout of anxiety-related behaviours and working memory alterations.

The use of agonists, antagonists and genetic deletions are frequently employed experimental approaches when studying the role of NMDARs in different neuronal processes. They have been particularly important to unravel the impact of these receptors on neuronal morphology and connectivity. The knock-out of the obligatory GluN1 subunit causes an increase in the volumes of axonal *boutons* and dendritic spines of neocortical pyramidal neurons in young mice, whereas their dendritic spine density is decreased (Ultanir *et al*, 2007). However, the blockade of these receptors with several antagonists has rendered a wider spectrum of results: While some reports describe that MK-801 has no effect in the spine density of pyramidal neurons *in vivo* (Han *et al*, 2013; Woolley and McEwen, 1994), other studies have revealed that the acute administration of ketamine – another NMDAR antagonist- produces a rapid increase in spine density (Li *et al*, 2010b; Liu *et al*, 2013; Phoumthipphavong *et al*, 2016). Conversely, chronic exposures to other antagonists have yielded contradictory results regarding this parameter: An increase in the case of phencyclidine (PCP, Flores et al., 2007), or a decrease when treated with 3-(2-carboxypiperazin-4-yl) propyl-1-phosphonic acid (CPP, Velázquez-Zamora et al., 2011). The activation of the receptor with a sustained low concentration of NMDA causes an increase in the density of mushroom spines and even in the total spine density (Tian *et al*, 2007).

In the present thesis I show that the acute blockade of NMDARs with an MK-801 injection causes no variations in the spine density of SOM expressing interneurons of the *stratum oriens*. The discrepancies between our results and the ones obtained in pyramidal neurons from other experiments may be explained by the structural and physiological differences between these cells and interneurons (Acsády *et al*, 1998; Freund and Buzsáki, 1996; Gulyás *et al*, 1992), and probably by the differences in doses and duration of the treatment. However, we have found interesting alterations induced by the MK-801 in the axonal *bouton* density of these interneurons. Even though axonal remodelling has not been

as broadly studied as that involving dendrites, some studies have also highlighted the effects of NMDAR antagonists on axonal structure. Only 3 days of MK-801 treatment are enough to produce axonal sprouting in the hippocampal Schaffer collaterals *in vitro* (McKinney *et al*, 1999b). We have observed a similar effect in adult animals on the axonal *boutons* of SOM expressing interneurons of the *stratum oriens*. Whether a similar effect on Schaffer collaterals occurs *in vivo*, still remains to be explored.

Moreover, we have found strong alterations in anxiety-related behaviours in MK-801-treated mice, including increased locomotor activity, which is in accordance with previous studies (Kalinichev *et al*, 2008; Zuo *et al*, 2006). By contrast, we have failed to find significant differences in the working memory ratio (number of head dips into non-previously explored holes divided by the total number of head dips) of treated animals, which is also in agreement with previous studies that were unable to find alterations in the head-dip count after MK-801 administration using the same apparatus (Haj-Mirzaian *et al*, 2015; Hirose *et al*, 2016). Interestingly, the increases that we show in anxiety-related behaviours but not in the density of dendritic spines agree with a previous study from our laboratory analysing the structural remodelling of SOM expressing interneurons in CA1 under a chronic stress paradigm (Gilabert-Juan *et al*, 2017); however, this report did not explore how their axons were remodelled.

1.2. MK-801 and NMDA alter the structural dynamics of somatostatin expressing interneurons

As it has previously been discussed, SOM expressing interneurons do not change their spine density after the acute NMDAR blockade with MK-801. However, we have performed additional assays that show alterations in their structural dynamics after the administration of this antagonist, or after the infusion of a NMDAR agonist, namely the NMDA molecule. These results have been obtained by using entorhino-hippocampal organotypic cultures from the same mice strain (GIN mice, Oliva et al., 2000), followed by real-time imaging. Only few studies have focused on neuronal structural dynamics after the treatment with an NMDAR antagonist, and most of them have been performed on

pyramidal neurons. For instance, in the hippocampal CA1, although pyramidal spine density is not altered after a 7-day treatment with MK-801, there is an increase in the number of filopodia-like processes, structures that resemble the immature spines of the developing hippocampus (McKinney *et al*, 1999a). Concerning interneuronal structure, only a study in primary cultures has revealed that a chronic treatment with the NMDAR antagonist ketamine causes a retraction of the dendritic arbour of interneurons (Vutskits *et al*, 2007). Although in this study the authors did not characterize the subpopulation of interneurons that was analysed, their results agree with the ones presented in this thesis: A decrease in the density of dendritic spines and, therefore, in the area available for establishing synapses. As a matter of fact, 4 hours after the MK-801 administration, the appearance rate of dendritic spines is decreased in SOM expressing interneurons. However, NMDA administration does not produce any alteration in such a short period. Nevertheless, we report concordant alterations 24 hours after the MK-801 and NMDA administration: MK-801 produces a decrease in the appearance rate, whilst NMDA causes an increase in this parameter. Furthermore, NMDA administration leads also to an increase in the disappearance rate and a decrease in the stability rate, whereas MK-801 shows no effect. These alterations caused by the NMDA infusion may be due to the destabilization that the NMDAR activation produces on the F-actin cytoskeleton (Halpain *et al*, 1998) or the glutamate excitotoxicity caused by the opening of NMDARs (Kristensen *et al*, 2001; Mody and MacDonald, 1995; Shimono *et al*, 2002).

In addition, the relative spine density has also been analysed in both experiments. When studying the NMDAR antagonism, there is a significant decrease in this parameter 24 hours after the MK-801 infusion when comparing to the group baseline, and a trend towards a decrease when comparing to the control group; probably a consequence of the reduced appearance rate reported also in this time point. However, when the cultures are treated with NMDA, the relative spine density remains unchanged throughout the experiment.

Regarding the stability rates reported in both experiments, there is an apparent discrepancy when comparing the *in vitro* and *in vivo* assays. In fact, previous real-time reports with cranial windows on mice have shown that, in control conditions,

interneuronal spines in the visual cortex have a stability rate close to 98% (Keck *et al*, 2011). However, the stability rate of the SOM expressing interneurons in both our assays had a value around 70%. These discrepancies may be caused by a difference in the stability of different interneuronal subpopulations, the region and age studied, or, more likely, to a higher stability *in vivo* than in our organotypic cultures.

Even though antagonists of the NMDARs are a great tool to understand how these receptors work and how they can modulate neuronal structure, not only basic science profits from them. In fact, neurodevelopmental diseases, including schizophrenia, are believed to be caused by the improper function of NMDARs during neural development (Cohen *et al*, 2015; Gonzalez-Burgos and Lewis, 2012; Inan *et al*, 2013; Paoletti *et al*, 2013). Therefore, disruption of these receptors in specific periods provides excellent animal models of some endophenotypes of this important disease, such as the perinatal injection with MK-801 (Adell *et al*, 2012; Li *et al*, 2015; Rompala *et al*, 2013; Rung *et al*, 2005; Thomases *et al*, 2013, 2014). For this reason, my next goal has been to understand how NMDAR disruption during postnatal development, together with aversive experiences, affects the structure of SOM-expressing interneurons, as well as other plasticity-related parameters, in adult mice.

2. THE STRUCTURE OF INTERNEURONS AND THE EXPRESSION OF PLASTICITY-RELATED MOLECULES IS ALTERED IN A MOUSE MODEL OF SCHIZOPHRENIA

Schizophrenia is a neuropsychiatric multifactorial disease that affects several brain areas and their interconnections. Despite that it is only found and diagnosed in human beings, there are several animal models that can emulate some endophenotypes of this disease, including early-life stress and, as commented before, MK-801 perinatal treatment. Among these endophenotypes, different structural alterations have been reported in pyramidal neurons of the amygdala and the mPFC. However, few studies have focused on how this disease affects the structure of interneurons and inhibitory circuits, and they have been always performed on PV-expressing cells (Beneyto and Lewis, 2011; Lewis *et al*, 2012;

Rotaru *et al*, 2012). In the current thesis, I have aimed for an integrative approach performing behavioural, structural and molecular analysis using a double-hit mouse model of the disorder that combines a postnatal MK-801 injection with post-weaning isolation, which has already rendered satisfactory results when performed in rats (Gilabert-Juan *et al*, 2013a). We have studied how the structure of both pyramidal neurons (fluorescent in Thy1-YFP mice, Feng et al., 2000)) and dendrite-targeting, SOM-expressing, interneurons (fluorescent in GIN mice, Oliva et al., 2000), alter their structure in the amygdala and the mPFC. In addition, we have tested anxiety-related behaviours and working memory and have examined the expression of molecules related to plasticity and the excitatory/inhibitory neurotransmission in these areas. Interestingly, we have found that this mouse model of schizophrenia positively emulates some endophenotypes of this disease and alters most of the analysed parameters. This knowledge is not unimportant, since we still do not know the neurodevelopmental causes of this disorder and the neural changes that it produces in adults. Understanding the cellular and molecular alterations associated to the disease is one of the first steps to properly treat its symptoms and, in time, even avoid their onset.

2.1. Anxiety-related behaviours were increased in schizophrenic mice

In the schizophrenia model developed in this thesis, mice were also subjected to the hole-board apparatus prior to their sacrifice, in order to analyse anxiety-related behaviours, hyperactivity and working memory alterations. Changes in these parameters are fairly common in human patients (Pallanti *et al*, 2013; Pallanti and Salerno, 2015; Van Snellenberg *et al*, 2016) and in animal models of this disease (Jones *et al*, 2011; Lett *et al*, 2014). In our experiment, Thy1-YFP mice from the double-hit group and all GIN mice reared in isolation (single and double-hit model) show increased anxiety-related behaviours, such as the time spent in the periphery of the apparatus, the mean speed or the number of body rotations. These results are in agreement with similar increases reported in other models of schizophrenia based on the hypofunction of the NMDARs (Belforte *et al*, 2010; Bubeníková-Valešová *et al*, 2008). However, we report no changes in

working memory in any of our models and strains analysed. This controversy regarding changes in working memory is a reflection of the field, in which some researchers have found alterations in this parameter (Andersen and Pouzet, 2004; Nozari *et al*, 2015) whilst others have reported none (Bubeníková-Valešová *et al*, 2008; Rompala *et al*, 2013).

2.2. The expression of molecules related to plasticity and the excitatory and inhibitory neurotransmission is altered in a mouse model of schizophrenia

In the present thesis I show that both the isolated and the double-hit mice have a reduced expression of PSA-NCAM in the amygdala. This is in apparent contradiction with previous reports describing increases in PSA-NCAM expression in the amygdaloid basolateral nucleus after the exposure to different stressors during adolescence (Tsoory *et al*, 2008). It is also in contrast to the results described using this same model of post-weaning isolation in rats (Gilabert-Juan *et al*, 2012a). These differences could be due to the use of different species or to the fact that the present experiment has measured the expression in all the amygdaloid nuclei together and not their different subnuclei. In fact, similar decreases have been shown in the central nucleus of the amygdala of mice and rats after a chronic stress paradigm (Cordero *et al*, 2005; Gilabert-Juan *et al*, 2011). The alterations of PSA-NCAM in the amygdala appear to relate directly to inhibitory circuits since this molecule is expressed by interneurons in this region (Nacher *et al*, 2002b, 2013), fact that makes our discoveries especially important in order to understand how schizophrenia alters this area.

Complementarily, in this experiment no significant alterations have been observed in the expression of PNNs surrounding PV-expressing interneurons in the amygdala, and only a trend towards a decrease has been found in the IL area of the mPFC. This latter result is in accordance with similar reductions detected in this area in schizophrenic patients (Mauney *et al*, 2013) or in a mouse model of this disease (Paylor *et al*, 2016). Likewise, the reduced number of PV-expressing interneurons in the PFC and the amygdala of our double-hit mice, which has also been observed in human patients (Enwright *et al*, 2016), agrees

with our previously published results in the PFC using the same model in rats (Gilabert-Juan *et al*, 2013a).

In the current thesis, I report a decreased E/I balance in the mPFC and the amygdala in our models of schizophrenia: In the post-weaning isolation and in the double-hit paradigm (postnatal MK-801 injection and post-weaning social isolation). This balance can also be affected by the expression of other molecules related to the excitatory-inhibitory neurotransmission, which have been also related to this disease. This is the case of BDNF, CB1-R, ST8SiaII and St8SiaIV. We find, in accordance with previous reports from humans and other mouse models of schizophrenia, an increase in the expression of BDNF (Sánchez-Huertas and Rico, 2011) and a decrease in the expression of ST8SiaIV (Nacher *et al*, 2010), both in the PFC; whereas the CB1-R increases its expression in the amygdala (den Boon *et al*, 2014; Volk and Lewis, 2010).

2.3. The structure of interneurons in the amygdala and the mPFC is altered in a mouse model of schizophrenia

In the current thesis, the structure of pyramidal neurons and SOM-expressing interneurons has been analysed in the reported mouse model of schizophrenia. Regarding pyramidal neurons, only those of the mPFC could be studied because of the dense labelling that Thy1-YFP mice presented in the amygdala. A previous Golgi study in a rat model of this disease (post-weaning isolation) has shown that pyramidal neurons have reduced arborisation and spine density in the mPFC (Wang *et al*, 2012). However, in the current experiment, there are no statistically significant differences in the dendritic spine density of prefrontocortical pyramidal neurons, neither in the single nor in the double-hit model, although a trend towards a decrease is reported in the latter. These discrepancies could be due to differences between species (rat versus mice) or to methodological variations, since different techniques were used to label constitutively the neurons (Golgi's method versus constitutive expression of fluorescent molecules). On the other hand, it may be also possible that augmenting the number of animals could yield statistically significant results.

The structure of dendrite-targeting, SOM-expressing, interneurons, has been analysed in the mPFC (Martinotti cells) and the amygdala. Prefrontocortical Martinotti cells show increased dendritic spine density in the single and in the double-hit models of schizophrenia. Most of the synapses established on the dendritic spines of SOM-expressing interneurons are excitatory ones (Guirado *et al*, 2014). Therefore, this increase may represent a gain of their active synaptic surface and, consequently, an augment in the excitatory input received by these cells, which may finally lead to increases in the inhibitory neurotransmission in order to compensate the overexcitation of the system. This result agrees with the increased excitation reported in this cortical region in schizophrenic patients (Starc *et al*, 2017; Sun *et al*, 2013) and animal models of this disorder (Li *et al*, 2015; Rotaru *et al*, 2011; Yizhar *et al*, 2011). In addition, we have also found an increase in the dendritic arborisation of dendrite-targeting interneurons expressing SOM in the amygdala. Interestingly, these changes are similar to those found after chronic stress in mice of the same strain (Gilabert-Juan *et al*, 2011, 2013b).

In fact, chronic stress is also an extensively validated model for major depression, that has been shown to alter the structure, plasticity and connectivity of excitatory (McEwen *et al*, 2016; McEwen and Morrison, 2013; Popoli *et al*, 2012; Sandi, 2004) and inhibitory (Ehrlich *et al*, 2009; Herman and Cullinan, 1997) circuits, with relevant contributions from our laboratory regarding the SOM-expressing interneurons (Gilabert-Juan *et al*, 2011, 2013b, 2017). Some cognitive symptoms of this disorder can be fought with the use of antidepressants; however, even though they are widely used in western society, little is known of their effects on the structure of interneurons and how they might revert the alterations that major depression causes on inhibitory circuits. Among these drugs, the extensively prescribed fluoxetine (Prozac, Lily), not only has been extremely useful to treat the symptomology, but also appears, as other antidepressants, to have a role in the reopening of critical period plasticity (Karpova *et al*, 2011; Vetencourt *et al*, 2008). Because of these reasons, I next asked how a chronic fluoxetine treatment could alter the structure of SOM-expressing interneurons and the expression of plasticity-related molecules.

3. CHRONIC FLUOXETINE ALTERS THE STRUCTURE OF INTERNEURONS AND THE EXPRESSION OF PLASTICITY-RELATED MOLECULES OF THE HIPPOCAMPUS AND THE PREFRONTAL CORTEX

In the last decades, fluoxetine has been one of the most prescribed antidepressants in the western society. Due to its effect as an inhibitor of the 5-HTT, it acts directly on the serotonergic system, increasing the extracellular presence of this neurotransmitter available to activate 5-HT receptors. Although it has been primarily used as an antidepressant, recent research points to the chronic use of fluoxetine as a valid mechanism to enhance neural plasticity and even reopen critical period plasticity (Karpova *et al*, 2011; Vetencourt *et al*, 2008). However, little is known about the effect that fluoxetine has on neuronal structure, specifically on that of interneurons and inhibitory circuits. In the current thesis, I have aimed to understand how a chronic treatment with fluoxetine alters the structure and connectivity of SOM-expressing interneurons, and the expression of plasticity-related molecules, in the hippocampus and the mPFC. In doing so, I have uncovered several interesting alterations. These effects of fluoxetine are especially important because of the wide range of use that this drug and other similar antidepressants have in our society.

3.1. Fluoxetine increases the dendritic spine density of prefrontocortical Martinotti interneurons

Few studies have shown the effects of fluoxetine on the structure of pyramidal neurons: It increases their dendritic spine density in the hippocampus (Hajszan *et al*, 2005) and in the somatosensory cortex (Guirado *et al*, 2009), but we still do not know how it affects pyramidal neurons in other cerebral regions, such as the mPFC, or its effect on the structure of interneurons. In order to achieve this knowledge, we have injected for 14 days fluoxetine in the GIN mice, in which a subpopulation of SOM-expressing interneurons express constitutively EGFP (Oliva *et al*, 2000). In the hippocampus, we have found that the dendritic spine density of SOM expressing interneurons in the *stratum oriens* remains unaltered, whereas in the mPFC this density increases in Martinotti interneurons. Because

SOM-expressing cells receive mostly excitatory inputs on their dendritic spines (Guirado *et al*, 2014), and they innervate the distal dendritic portion of pyramidal neurons (Markram *et al*, 2004), this increase in dendritic spine density may produce a gain of the excitatory input that Martinotti interneurons receive and, therefore, an increase in the inhibition that these cells exert on pyramidal neurons. This increment in inhibition agrees with the known augment in the expression of molecules related to inhibitory neurotransmission in this cortical region after a chronic fluoxetine treatment (Guirado *et al*, 2012; Tiraboschi *et al*, 2013; Varea *et al*, 2007a).

3.2. Fluoxetine alters the expression molecules related to plasticity and inhibitory neurotransmission

In the current thesis, I report an increase in the expression of PSA-NCAM in the hippocampus of animals treated chronically with fluoxetine. Previous studies from our laboratory using rats have already shown that a chronic treatment with this drug causes an increase in PSA-NCAM expression in several brain regions (Guirado *et al*, 2012; Varea *et al*, 2007a, 2007b), similar to the one described in this thesis. In addition, our laboratory has found that interneurons expressing PSA-NCAM have reduced dendritic arborisation and spine density when compared with those lacking this molecule (Gomez-Climent *et al*, 2011). Moreover, in organotypic cultures of the PFC, PSA depletion causes alterations in the spine density of the same subpopulation of interneurons: An increase in the proximal dendritic segment and a decrease in the distal dendritic segment (Castillo-Gómez *et al*, 2016a), strongly linking the expression of this sugar with the structure of these interneurons. Therefore, the alteration of PSA-NCAM expression found after chronic fluoxetine treatment (Guirado *et al*, 2012; Karpova *et al*, 2011; Varea *et al*, 2007c) influences directly the structure of these cells. The variations in the expression of PSA-NCAM may be also influencing the perisomatic innervation that basket cells exert on pyramidal neurons, since some of these baskets also express PSA-NCAM (Castillo-Gómez *et al*, 2011). In fact, after the chronic administration of fluoxetine, we have found an increase in the expression of PSA-NCAM, together with a trend towards a decrease of the

density of perisomatic puncta expressing PV and SYN in the mPFC, which suggests a decrease in the density of these synapses. These results agree with previous ones from our laboratory, which have already shown that PSA depletion in the mPFC causes an increase in the number of inhibitory puncta around the somata of pyramidal cells (Castillo-Gómez *et al*, 2011, 2016a).

Our results also show that the ratio of PV-expressing cells surrounded by PNNs is decreased in the hippocampal CA1 and in the mPFC of fluoxetine treated animals. These results agree with the reported alterations in this parameter in other cerebral areas, such as the basolateral amygdala after a chronic treatment with this drug (Karpova *et al*, 2011). The appearance of PNNs coincides with the closure of the critical period plasticity (Hensch, 2005; Wang and Fawcett, 2012; Yamada and Jinno, 2013), and their depletion causes a dematuration of the axonal *boutons* that innervate pyramidal neurons and, therefore, the reopening of critical periods (McRae *et al*, 2007; Nowicka *et al*, 2009). We hypothesized that our chronic fluoxetine treatment might be producing this same type of plasticity in both the mPFC and the hippocampus. However, we have not found significant effects in the density of perisomatic puncta expressing PV and SYN around pyramidal neurons in the hippocampus, and only a trend towards a decrease in the case of the mPFC. The reduced density of PV-expressing puncta, which correspond to the inhibitory innervation from basket cells (Freund and Katona, 2007), may indicate a partial disinhibition of the mPFC excitatory neurons. This inhibition may eventually lead to alterations in their synchronization. In fact, a recent report has found that a chronic treatment with fluoxetine alters GABA release from synapses formed by hippocampal fast-spiking cells, resulting in the disruption of γ oscillations (Mendez *et al*, 2012). This treatment also reduces intracortical inhibition in the visual cortex, an effect blocked by the administration of the $GABA_A$ receptor agonist diazepam (Vetencourt *et al*, 2008). These results appear to be in consonance with the data obtained in this thesis. However, experiments with a higher number of animals per group are necessary to confirm whether the tendencies obtained would become significant. It is also possible that the lack of significant differences in the density of perisomatic puncta found in our study may be due to the fact that, despite the use of identical doses, our mice were treated with fluoxetine only for 2 weeks, whilst the

rats in the Mendez et al. (2012) study received the treatment for 3 weeks. We have also analysed the perisomatic innervation of EGFP-expressing interneurons, which mainly co-express SOM (Martinotti cells in the mPFC and SOM expressing interneurons of the *stratum oriens* in the hippocampus). In these cells, the density of perisomatic GAD6 expressing puncta (an inhibitory synapse marker) is increased after the chronic treatment with fluoxetine in the hippocampus, but no effects have been found in the mPFC. However, despite the fact that these puncta are co-expressing SYN, which is a marker for active synapses, further studies should address the functional implications these alterations can cause. In this regard, electron microscopy could shed light into understanding which interneuronal subpopulations are being influenced by this increase in perisomatic innervation.

Finally, we have also analysed how a chronic fluoxetine treatment affects the expression density of SYN, GAD6 and VGlut-1 in the neuropil by measuring the density of puncta expressing these synaptic molecules. We have found that chronic fluoxetine increases the expression of molecules related to inhibitory neurotransmission (SYN, GAD6) in the neuropil of the hippocampus, but no effect can be seen in the mPFC. Because there are no changes in the expression of the excitatory synaptic marker VGlut-1, these results suggest the net formation of new inhibitory synapses. Altogether, these increases are in consonance with a strong augment of the PSA-NCAM expression discussed earlier, since in the hippocampus the expression of this plasticity-related molecule is mostly associated to interneurons (Guirado *et al*, 2014; Nacher *et al*, 2002a).

Despite the great importance of the serotonergic system in neural development and plasticity (Andrews *et al*, 2015; Kepser and Homberg, 2014; Miceli *et al*, 2013; Rubio *et al*, 2013), this monoamine is not a sole participant in such crucial processes. In fact, the neurotrophin BDNF, and its receptor TrkB, appear also to be critical (Bekinschtein *et al*, 2014; Gonzalez *et al*, 2016; Horch and Katz, 2002; Huang and Reichardt, 2001; Rocamora *et al*, 1996; Shen and Cowan, 2010; Yoshii and Constantine-Paton, 2010), and their malfunction is suggested to be underlying some neuropsychiatric diseases, including schizophrenia and major depression (Cannon et al., 2008; Chen et al., 2006; Guilloux et al., 2012; Pandya et al., 2013; Torrey et al., 2005, for reviews see Angelucci et al., 2005;

Binder and Scharfman, 2004; Castrén and Rantamäki, 2010; Duman and Monteggia, 2006; Green et al., 2011; Yoshii and Constantine-Paton, 2010; Zuccato and Cattaneo, 2009). For these reasons, the use of agonists to increase the activation of TrkB is an excellent strategy to understand the role of this neurotrophin in these disorders and to enhance the activation of the related molecular cascades (Lu *et al*, 2013; Nagahara and Tuszynski, 2011). In consequence, my next goal has been to learn how a TrkB agonist, the 7,8-dihydroxyflavone (DHF), alters the dynamics of dendritic spines and axonal *boutons* of neocortical pyramidal neurons. In parallel I also have explored how this TrkB agonist influences object recognition behaviour.

4. CHRONIC ACTIVATION OF TRKB ALTERS THE STRUCTURAL DYNAMICS OF CORTICAL PYRAMIDAL NEURONS AND IMPROVES OBJECT RECOGNITION IN MICE

BDNF and its receptor TrkB have been extensively studied regarding neuronal growth and survival (Horch and Katz, 2002; McAllister *et al*, 1997; Murphy *et al*, 1998; Tolwani *et al*, 2002), LTP establishment (Escobar *et al*, 2003; Kang *et al*, 1997; Meis *et al*, 2012) or neural plasticity (Gonzalez *et al*, 2016; Lai and Ip, 2013; Mariga *et al*, 2015; Tolwani *et al*, 2002; Yoshii and Constantine-Paton, 2010). Alterations in TrkB and TrkB signalling have been described in different neurological and psychiatric disorders, including schizophrenia and major depression (Cannon et al., 2008; Chen et al., 2006; Guilloux et al., 2012; Pandya et al., 2013; Torrey et al., 2005, for reviews see Angelucci et al., 2005; Binder and Scharfman, 2004; Castrén and Rantamäki, 2010; Duman and Monteggia, 2006; Green et al., 2011; Yoshii and Constantine-Paton, 2010; Zuccato and Cattaneo, 2009). Therefore, drugs interacting with TrkB, specially agonists, are promising therapeutic tools (Lu *et al*, 2013; Nagahara and Tuszynski, 2011). Among them, the recently described 7,8-dihydroxyflavone (DHF) is one of the best candidates since it is orally bioactive and can cross freely the blood-brain barrier, a common problem for those drugs intended to reach the CNS. This flavone has been shown to induce TrkB dimerization and its phosphorylation, as well as the activation of the related downstream cascades, similarly to

the BDNF itself (Jang *et al*, 2010). In addition, it has already rendered successful results when tested in animal models of different diseases (Liu *et al*, 2016). Alterations of the BDNF-TrkB system produce structural changes in pyramidal neurons. In fact, BDNF infusion to organotypic cultures increases the spine density of CA1 pyramidal neurons in the hippocampus (Tyler and Pozzo-Miller, 2003) and the dendritic arborisation of pyramidal neurons in the visual cortex (McAllister *et al*, 1995). This treatment also causes an increase in the spine density of Purkinje cells in primary cultures (Shimada *et al*, 1998). Interestingly, DHF also appears to increase pyramidal spine density in the amygdala, hippocampus and PFC (Zeng *et al*, 2012b). However, to date, there is no information on how DHF may alter the structural dynamics of neocortical pyramidal neurons (i.e. real-time study of the addition/elimination of dendritic spines and axonal *boutons*). The correlation between these structural parameters and memory improvements related to this drug has also not been studied yet. In the current thesis I describe different alterations in the structural dynamics of these neurons after a chronic treatment of 12 days with DHF. As it has been stated before, this type of analysis has become extremely important, since changes in these dynamics have been suggested to be the force underlying adaptation of neural circuits to changing environments (Bhatt *et al*, 2009; Caroni *et al*, 2012; Chen *et al*, 2012; Holtmaat and Svoboda, 2009; Keck *et al*, 2011; Knott and Holtmaat, 2008). Although these studies can be performed with organotypic cultures (*in vitro,* as discussed before) and surgically with the implantation of chronic cranial windows (in living animals: *in vivo,* Holtmaat et al., 2009), the latter provides the greater valuable clinical information, since physiologically the animal remains undisturbed and the brain maintains all its connections. For these reasons, I have tried to understand how a chronic treatment with DHF alters the structural dynamics *in vivo* by implanting cranial windows to Thy1-YFP mice (Feng *et al*, 2000; Porrero *et al*, 2010) and imaging in real-time, with a 2-photon microscope, the same dendrites and axons. In addition, we have performed a behavioural analysis related to the neocortical brain area of interest (barrel cortex), in order to correlate structural alterations with functional ones.

4.1. Alterations of the structural dynamics

We report different structural alterations in the dendritic spine dynamics of neocortical pyramidal neurons: An increase in the gain function of spines 4 days after the beginning of the treatment, which persists after 8 days, and a return to baseline levels by the end of the treatment. The increase may be explained by the induction of LTP by the DHF treatment, a consequence that has been demonstrated with other flavones (Maher *et al*, 2006; Vauzour *et al*, 2007). In fact, the activation of TrkB by itself also induces LTP (Minichiello, 2009; Minichiello *et al*, 2002). Since this form of synaptic plasticity causes the apparition of dendritic spines (Engert and Bonhoeffer, 1999), the reported increase of the gain function is not surprising. In fact, several reports relate BDNF infusions to increases in dendritic spine density, when administered either acutely to pyramidal neurons of the hippocampus (Tyler and Pozzo-Miller, 2003) or chronically to Purkinje cells (Shimada *et al*, 1998). Although these results from other laboratories may seem similar to ours, we cannot infer how the spine dynamics might be altered in their experiments (performed on post-mortem tissue), because they do not provide linear information of the same structure and only present results at the end of the treatment. In the same line, another study has also reported an increase in the dendritic spine density of hippocampal pyramidal neurons after a 34 day-long treatment with DHF in rats (Zeng *et al*, 2012b), using the same dose that has been used in this thesis. However, these increases –as those discussed earlier- cannot be related directly to the altered dynamics that we report during our DHF treatment. We can only speculate that they may be also the consequence of the enhanced gain function of the pyramidal dendritic spines in the hippocampus.

On the other hand, the stability function of dendritic spines is gradually reduced through the whole experiment in both groups, although more remarkably in the control animals. This tendency appears to obey to the natural stability loss reported in the same strain of mice when performing real-time imaging (Grutzendler *et al*, 2002). However, the decreases shown in Grutzendler et al. (2002) were not as prominent as the ones we report, probably because they chose to perform thinned skull surgery (instead of the open skull surgery we executed), a technique that generally provides higher dendritic stability functions (Xu *et al*, 2007).

We have also studied the dynamics of stable (present at least for 4 days) dendritic spines, parameters that are specially relevant because they ensure the presence of at least one synapse (Holtmaat *et al*, 2006; Knott *et al*, 2006) and, therefore, are the ones influencing the network. Interestingly, the loss function of stable spines increases significantly in the control group, whereas the DHF treatment appears to protect from these deleterious changes. In addition, we have shown that the spines that are stable throughout the whole experiment increase their volume only in the control group. Both results suggest that the continuous handling and imaging of the animal has a deleterious effect on the network, leading to a loss of stable connections. However, the spines that remained stable would increase their volume, and consequently their potentiation, in order to synaptically maintain the circuit (Matsuzaki *et al*, 2004). We suggest that DHF, due to its neurotrophic properties, may exert a fast protective effect against the deleterious repercussions conveyed by the real-time imaging. This agrees with the fact that DHF has already been shown to protect against glutamate excitotoxicity (Chen *et al*, 2011a), neonatal hypoxia and ischemia (Uluc *et al*, 2013), or even degeneration of dopaminergic neurons in animal models of Parkinson's disease (Luo *et al*, 2016) or staurosporine-induced apoptosis (Jang *et al*, 2010).

The changes in structural dynamics are not only restricted to alterations of the dendritic spines; the '*en passant boutons*' (EPB), membranous varicosities that form the presynaptic elements located in the axon, also show alterations in their dynamics during the DHF treatment. Other studies have already pointed out the important role of TrkB in proper axonal *bouton* formation (Martínez *et al*, 1998). Here, we report an increased gain function of EPB 8 days after the beginning of the treatment. We also show an increase in the gain function of EPB that will become stable –this is, those that will be present for at least 4 days (two consecutive imaging sessions). Because the EPB that were scored showed a fluorescence at least 2 times higher than the one of the axonal backbone, all the *boutons* studied are presumed to bear a synapse (Grillo *et al*, 2013; Qiao *et al*, 2016b). However, the EPB that remain stable probably are more likely to reflect the synaptic remodelling of the network. In accordance with these results, BDNF has already been shown to increase axonal arborization in other species (Bing *et al*, 2005; Cohen-Cory and Fraser, 1995; Lom

and Cohen-Cory, 1999). We also describe an increase in the loss function of EPB that were stable (EPB that were present for at least 4 days and were lost afterwards), and a decrease in the stability function, in animals treated with DHF. The time frame of these alterations overlaps with the increase in the gain function of dendritic spines.

4.2. DHF improves object recognition

In the current study we have also aimed to understand whether the activation of TrkB with DHF affects behaviour dependent on the barrel cortex. The sensory input from vibrissae in rodents is received by the barrel field of the somatosensory cortex (also known as barrel cortex). Since these animals rely on their tactile structures in order to discriminate different textures (Arabzadeh *et al*, 2005; Brecht, 2007; Guić-Robles *et al*, 1989; von Heimendahl *et al*, 2007), we have performed a modified novel object recognition task (NOR, Leger et al., 2013) which could serve as a correlate for alterations in this region. We have changed the protocol by shortening the period between familiar and novel objects (Burke *et al*, 2011, 2012), to properly distinguish between object recognition behaviour (dependent on the barrel cortex, Brecht, 2007; Kleinfeld et al., 2006), and long-term memory (dependent on other cortical areas, Simons and Spiers, 2003; Wiltgen et al., 2004). We have also adapted the objects with different textures to be mainly detected by the mice wishers, which allow us to link the structural changes reported in the barrel cortex with the behavioural ones. Furthermore, mice have been presented with an easy and a difficult novel object, so that we could test whether the DHF enhanced sensorial perception dependent on the barrel cortex.

Our results have shown that, indeed, mice treated with DHF display a lower discrimination ratio of the difficult novel object than the control group, meaning that they are able to discriminate better between difficult objects after being treated with DHF. Previous studies in other cortical areas have already linked the expression of BNDF and its receptor, TrkB, with learning (Kesslak *et al*, 1998; Klintsova *et al*, 2004). Moreover, they have positively correlated BDNF expression with novel object recognition memory (Hopkins and Bucci, 2010). In the barrel cortex, whisker stimulation produces an

upregulation of the BDNF expression (Rocamora *et al*, 1996) and tactile experience causes increases in neuronal activity, probably mediated by this neurotrophin (Filipkowski *et al*, 2000). However, fewer studies have focused on the direct action of TrkB manipulation in these behaviours. In concordance with the present results, the inhibition of TrkB receptors with anti-BDNF causes an increase in the discrimination ratio in the NOR in rats (Callaghan and Kelly, 2013), which means that these animals with a decreased function of TrkB have more difficulties in recognizing the novel object than control animals. Furthermore, a previous study, using also a NOR test, has demonstrated that the activation of TrkB with DHF improves memory consolidation in both rats and mice (Bollen *et al*, 2013). In this thesis, I show that, not only DHF boosts memory consolidation, but it also improves the object recognition behaviour through an enhanced sensory discrimination in this task, probably by altering the structural dynamics of layer V pyramidal neurons of the barrel cortex. Our results are a necessary addition to the growing knowledge of how the activation of the TrkB signalling alters the structure of neocortical pyramidal neurons. This has become increasingly important in the last decade, not only for improving the knowledge of cortical physiology, but also due to the thriving evidence linking the malfunction of the BDNF-TrkB system with the onset of several neurodegenerative and psychiatric disorders (Angelucci *et al*, 2005; Binder and Scharfman, 2004; Castrén and Rantamäki, 2010; Duman and Monteggia, 2006; Green *et al*, 2011; Yoshii and Constantine-Paton, 2010; Zuccato and Cattaneo, 2009). With our current findings, we expect to promote further research on DHF and how a treatment with this drug can ameliorate such impeding diseases (Lu *et al*, 2013; Nagahara and Tuszynski, 2011).

V. CONCLUSIONS

1. Hippocampal somatostatin expressing interneurons of the *stratum oriens* express NMDA receptors on their somata and on the head of their dendritic spines.

2. The acute treatment of adult mice with the NMDA receptor antagonist MK-801 increases locomotion and anxiety-related behaviours.

3. The acute treatment of adult mice with MK-801 increases the density of *en passant boutons* from hippocampal somatostatin expressing interneurons of the *stratum oriens*, whereas the density of their dendritic spines remains unaltered.

4. The real-time analysis of the dendritic spines of somatostatin expressing interneurons of the *stratum oriens* in hippocampal organotypic cultures reveals a fast decrease on their gain function after the MK-801 administration.

5. The real-time analysis of the dendritic spines of somatostatin expressing interneurons of the *stratum oriens* in hippocampal organotypic cultures shows a decrease on their relative density after MK-801 administration.

6. The real-time analysis of the dendritic spines of somatostatin expressing interneurons of the *stratum oriens* in hippocampal organotypic cultures reveals increases in their gain and loss functions 24 hours after NMDA administration.

7. The double-hit model of schizophrenia shows increased locomotion and anxiety-related behaviours.

8. Interneurons in the amygdala of the double-hit model of schizophrenia have an increased dendritic arborization when compared to controls.

9. The double-hit and each of the simple models of schizophrenia present increased dendritic spine density in prefrontocortical interneurons.

10. The expression of excitatory neurotransmission markers in the lateral and medial amygdala is increased in the double-hit model of schizophrenia.

11. The perinatal injection of MK-801, a simple model of schizophrenia, increases the expression of the inhibitory marker VGAT and the excitatory-inhibitory balance in the infralimbic and prelimbic regions of the prefrontal cortex.

12. The perinatal injection of MK-801 increases the density of parvalbumin expressing interneurons surrounded by perineuronal nets in the infralimbic region of the prefrontal cortex.

13. A chronic fluoxetine treatment increases the dendritic spine density in interneurons of the medial prefrontal cortex.

14. A chronic fluoxetine treatment decreases the density of parvalbumin expressing interneurons surrounded by perineuronal nets in the medial prefrontal cortex and the hippocampus.

15. A chronic fluoxetine treatment increases the expression of PSA-NCAM and synaptophysin in different regions of the hippocampus.

16. A chronic fluoxetine treatment increases the density of inhibitory perisomatic puncta on interneurons but not on pyramidal neurons of the medial prefrontal cortex.

17. Pyramidal neurons in the barrel cortex express TrkB in their somata, dendritic spines and axonal *boutons*.

18. A chronic 7,8-dihydroxyflavone treatment increases the gain function of axonal *boutons* and dendritic spines in neocortical pyramidal neurons, as observed in vivo with cranial windows and multiphoton microscopy.

19. The loss function and the volume of stable pyramidal spines remains unaltered during a chronic 7,8-dihydroxyflavone treatment, whereas it is increased in control animals.

20. A chronic treatment with 7,8-dihydroxyflavone improves the discrimination ratio of difficult objects.

21. The time exploring a difficult novel object is positively correlated with the spine turnover rate in animals treated with the 7,8-dihydroxyflavone, but not in controls.

VI. REFERENCES

Acsády L, Kamondi A, Sík A, Freund T, Buzsáki G (1998). GABAergic cells are the major postsynaptic targets of mossy fibers in the rat hippocampus. *J Neurosci* **18**: 3386–403.

Adell A, Jiménez-Sánchez L, López-Gil X, Romón T (2012). Is the acute NMDA receptor hypofunction a valid model of schizophrenia? *Schizophr Bull* **38**: 9–14.

Aerde KI Van, Feldmeyer D (2015). Morphological and physiological characterization of pyramidal neuron subtypes in rat medial prefrontal cortex. *Cereb Cortex* **25**: 788–805.

Afroz S, Parato J, Shen H, Smith SS (2016). Synaptic pruning in the female hippocampus is triggered at puberty by extrasynaptic GABA A receptors on dendritic spines. *Elife* **5**: 1–23.

Afroz S, Shen H, Smith SS (2017). α4βδ GABAA Receptors Reduce Dendritic Spine Density In CA1 Hippocampus And Impair Relearning Ability Of Adolescent Female Mice: Effects Of A Gaba Agonist And A Stress Steroid. *Neuroscience* doi:10.1016/j.neuroscience.2017.01.051.

Akbarian S (1995). Gene Expression for Glutamic Acid Decarboxylase Is Reduced Without Loss of Neurons in Prefrontal Cortex of Schizophrenics. *Arch Gen Psychiatry* **52**: 258.

Akbarian S, Huang H-S (2006). Molecular and cellular mechanisms of altered GAD1/GAD67 expression in schizophrenia and related disorders. *Brain Res Rev* **52**: 293–304.

Aleman A, Kahn RS (2005). Strange feelings: Do amygdala abnormalities dysregulate the emotional brain in schizophrenia? *Prog Neurobiol* **77**: 283–298.

Alger BE, Nicoll RA (1982). Pharmacological evidence for two kinds of GABA receptors on rat hippocampal pyramidal cells studied in vitro. *J Physiol* **328**: 125–141.

Allen Y, Adrian T, Allen J, Tatemoto K, Crow T, Bloom, *et al* (1983). Neuropeptide Y distribution in the rat brain. *Science (80-)* **221**: 877–879.

Alvarez VA, Ridenour DA, Sabatini BL (2007). Distinct structural and ionotropic roles of NMDA receptors in controlling spine and synapse stability. *J Neurosci* **27**: 7365–7376.

Amaral DG, Scharfman HE, Lavenex P (2007). The dentate gyrus: fundamental neuroanatomical organization (dentate gyrus for dummies). *Prog Brain Res* **163**: 3–22.

Andersen JD, Pouzet B (2004). Spatial memory deficits induced by perinatal treatment of rats with PCP and reversal effect of D-serine. *Neuropsychopharmacology* **29**: 1080–90.

Andersen P, Morris R, Amaral D, Bliss T, O'Keefe J (Oxford University Press: 2007). *The Hippocampus book*. *Oxford* doi:10.1093/acprof:oso/9780195100273.001.0001.

Andrews PW, Bharwani A, Lee KR, Fox M, Thomson JA (2015). Is serotonin an upper or a

downer? The evolution of the serotonergic system and its role in depression and the antidepressant response. *Neurosci Biobehav Rev* **51**: 164–188.

Angelucci F, Brenè S, Mathé a a (2005). BDNF in schizophrenia, depression and corresponding animal models. *Mol Psychiatry* **10**: 345–52.

Arabzadeh E, Zorzin E, Diamond ME (2005). Neuronal encoding of texture in the whisker sensory pathway. *PLoS Biol* **3**: e17.

Arai M, Yamada K, Toyota T, Obata N, Haga S, Yoshida Y, *et al* (2006). Association between polymorphisms in the promoter region of the sialyltransferase 8B (SIAT8B) gene and schizophrenia. *Biol Psychiatry* **59**: 652–9.

Arnsten AFT (2015). Stress weakens prefrontal networks: molecular insults to higher cognition. *Nat Neurosci* **18**: 1376–1385.

Asan E, Steinke M, Lesch KP (2013). Serotonergic innervation of the amygdala: Targets, receptors, and implications for stress and anxiety. *Histochem Cell Biol* **139**: 785–813.

Ascoli G a, Alonso-Nanclares L, Anderson S a, Barrionuevo G, Benavides-Piccione R, Burkhalter A, *et al* (2008). Petilla terminology: nomenclature of features of GABAergic interneurons of the cerebral cortex. *Nat Rev Neurosci* **9**: 557–568.

Atz ME, Rollins B, Vawter MP (2007). NCAM1 association study of bipolar disorder and schizophrenia: polymorphisms and alternatively spliced isoforms lead to similarities and differences. *Psychiatr Genet* **17**: 55–67.

Aydemir O, Deveci A, Taneli F (2005). The effect of chronic antidepressant treatment on serum brain-derived neurotrophic factor levels in depressed patients: a preliminary study. *Prog Neuro-Psychopharmacology Biol Psychiatry* **29**: 261–265.

Baharnoori M, Brake WG, Srivastava LK (2009). Prenatal immune challenge induces developmental changes in the morphology of pyramidal neurons of the prefrontal cortex and hippocampus in rats. *Schizophr Res* **107**: 99–109.

Barde YA, Edgar D, Thoenen H (1982). Purification of a new neurotrophic factor from mammalian brain. *EMBO J* **1**: 549–53.

Barnes NM, Sharp T (1999). A review of central 5-HT receptors and their function. *Neuropharmacology* **38**: 1083–1152.

Baroncelli L, Braschi C, Spolidoro M, Begenisic T, Maffei L, Sale A (2011). Brain Plasticity and Disease: A Matter of Inhibition. *Neural Plast* **2011**: 1–11.

Barria A, Malinow R (2002). Subunit-specific NMDA receptor trafficking to synapses. *Neuron* **35**: 345–353.

Bauer ME (2008). Chronic Stress and Immunosenescence: A Review. *Neuroimmunomodulation* **15**: 241–250.

Bear MF, Malenka RC (1994). Synaptic plasticity: LTP and LTD. *Curr Opin Neurobiol* **4**: 389–99.

Becker N, Wierenga CJ, Fonseca R, Bonhoeffer T, Nägerl UV (2008). LTD Induction

Causes Morphological Changes of Presynaptic Boutons and Reduces Their Contacts with Spines. *Neuron* **60**: 590–597.

Bekinschtein P, Cammarota M, Medina JH (2014). BDNF and memory processing. *Neuropharmacology* **76**: 677–683.

Belforte JE, Zsiros V, Sklar ER, Jiang Z, Yu G, Li Y, *et al* (2010). Postnatal NMDA receptor ablation in corticolimbic interneurons confers schizophrenia-like phenotypes. *Nat Neurosci* **13**: 76–83.

Belmaker RH, Agam G (2008). Major Depressive Disorder. *N Engl J Med* **358**: 55–68.

Beneyto M, Lewis DA (2011). Insights into the neurodevelopmental origin of schizophrenia from postmortem studies of prefrontal cortical circuitry. *Int J Dev Neurosci* **29**: 295–304.

Berlucchi G, Buchtel HA (2009). Neuronal plasticity: Historical roots and evolution of meaning. *Exp Brain Res* **192**: 307–319.

Berretta S, Pantazopoulos H, Markota M, Brown C, Batzianouli ET (2015). Losing the sugar coating: Potential impact of perineuronal net abnormalities on interneurons in schizophrenia. *Schizophr Res* **167**: 18–27.

Bettler B, Mulle C (1995). AMPA and kainate receptors. *Neuropharmacology* **34**: 123–139.

Bhatt DH, Zhang S, Gan W-B (2009). Dendritic Spine Dynamics. *Annu Rev Physiol* **71**: 261–282.

Bicks LK, Koike H, Akbarian S, Morishita H (2015). Prefrontal cortex and social cognition in mouse and man. *Front Psychol* **6**: 1805.

Binder DK, Scharfman HE (2004). Brain-derived Neurotrophic Factor. *Growth Factors* **22**: 123–131.

Bing H, Nikolakopoulou AM, Cohen-Cory S (2005). BDNF stabilizes synapses and maintains the structural complexity of optic axons in vivo. *Development* **132**: 4285–4298.

Bitanihirwe BKY, Mauney SA, Woo TUW (2016). Weaving a Net of Neurobiological Mechanisms in Schizophrenia and Unraveling the Underlying Pathophysiology. *Biol Psychiatry* **80**: 589–598.

Blank M, Petry FS, Lichtenfels M, Valiati FE, Dornelles AS, Roesler R (2016). TrkB blockade in the hippocampus after training or retrieval impairs memory: protection from consolidation impairment by histone deacetylase inhibition. *J Neural Transm* **123**: 159–165.

Blasco-Ibáñez JM, Freund TF (1995). Synaptic Input of Horizontal Interneurons in Stratum Oriens of the Hippocampal CA1 Subfield: Structural Basis of Feed-back Activation. *Eur J Neurosci* **7**: 2170–2180.

Bliss TVP, Collingridge GL (1993). A synaptic model of memory: long-term potentiation in the hippocampus. *Nature* **361**: 31–39.

Bogerts B, Lieberman JA, Ashtari M, Bilder RM, Degreef G, Lerner G, *et al* (1993). Hippocampus-amygdala volumes and psychopathology in chronic schizophrenia. *Biol Psychiatry* **33**: 236–246.

Bollen E, Vanmierlo T, Akkerman S, Wouters C, Steinbusch HMW, Prickaerts J (2013). 7,8-Dihydroxyflavone improves memory consolidation processes in rats and mice. *Behav Brain Res* **257**: 8–12.

Bonfanti L (2006). PSA-NCAM in mammalian structural plasticity and neurogenesis. *Prog Neurobiol* **80**: 129–64.

Boon FS den, Werkman TR, Schaafsma-Zhao Q, Houthuijs K, Vitalis T, Kruse CG, *et al* (2014). Activation of type-1 cannabinoid receptor shifts the balance between excitation and inhibition towards excitation in layer II/III pyramidal neurons of the rat prelimbic cortex. *Pflugers Arch Eur J Physiol* **467**: 1551–1564.

Brady KT, Sinha R (2005). Co-Occurring Mental and Substance Use Disorders: The Neurobiological Effects of Chronic Stress. *Am J Psychiatry* **162**: 1483–1493.

Braga RJ, Mendlowicz M V., Marrocos RP, Figueira IL (2005). Anxiety disorders in outpatients with schizophrenia: Prevalence and impact on the subjective quality of life. *J Psychiatr Res* **39**: 409–414.

Brecht M (2007). Barrel cortex and whisker-mediated behaviors. *Curr Opin Neurobiol* **17**: 408–416.

Brunoni AR, Lopes M, Fregni F (2008). A systematic review and meta-analysis of clinical studies on major depression and BDNF levels: implications for the role of neuroplasticity in depression. *Int J Neuropsychopharmacol* **11**: 1169–1180.

Bubeníková-Valešová V, Horáček J, Vrajová M, Höschl C (2008). Models of schizophrenia in humans and animals based on inhibition of NMDA receptors. *Neurosci Biobehav Rev* **32**: 1014–1023.

Buddhala C, Hsu CC, Wu JY (2009). A novel mechanism for GABA synthesis and packaging into synaptic vesicles. *Neurochem Int* **55**: 9–12.

Burke SN, Barnes CA (2006). Neural plasticity in the ageing brain. *Nat Rev Neurosci* **7**: 30–40.

Burke SN, Ryan L, Barnes CA (2012). Characterizing cognitive aging of recognition memory and related processes in animal models and in humans. *Front Aging Neurosci* **4**: 1–13.

Burke SN, Wallace JL, Hartzell AL, Nematollahi S, Plange K, Barnes CA (2011). Age-Associated Deficits in Pattern Separation Functions of the Perirhinal Cortex : A Cross-Species Consensus. *Behav Neurosci* **125**: 836–847.

Butler AK, Uryu K, Chesselet MF (1998). A role for N-methyl-D-aspartate receptors in the regulation of synaptogenesis and expression of the polysialylated form of the neural cell adhesion molecule in the developing striatum. *Dev Neurosci* **20**: 253–262.

Byatt N, Deligiannidis KM, Freeman MP (2013). Antidepressant use in pregnancy: a

critical review focused on risks and controversies. *Acta Psychiatr Scand* **127**: 94–114.

Cabelli RJ, Shelton DL, Segal RA, Shatz CJ (1997). Blockade of endogenous ligands of TrkB inhibits formation of ocular dominance columns. *Neuron* **19**: 63–76.

Callaghan CK, Kelly ÁM (2013). Neurotrophins play differential roles in short and long-term recognition memory. *Neurobiol Learn Mem* **104**: 39–48.

Cane M, Maco B, Knott G, Holtmaat A (2014). The relationship between PSD-95 clustering and spine stability in vivo. *J Neurosci* **34**: 2075–86.

Cannon TD, Yolken R, Buka S, Torrey EF (2008). Decreased Neurotrophic Response to Birth Hypoxia in the Etiology of Schizophrenia. *Biol Psychiatry* **64**: 797–802.

Caroni P, Donato F, Muller D (2012). Structural plasticity upon learning: regulation and functions. *Nat Rev Neurosci* **13**: 478–490.

Casanova MF (1997). Functional and anatomical aspects of prefrontal pathology in schizophrenia. *Schizophr Bull* **23**: 517–519.

Castello NA, Nguyen MH, Tran JD, Cheng D, Green KN, LaFerla FM (2014). 7,8-Dihydroxyflavone, a Small Molecule TrkB Agonist, Improves Spatial Memory and Increases Thin Spine Density in a Mouse Model of Alzheimer Disease-Like Neuronal Loss. *PLoS One* **9**: e91453.

Castillo-Gómez E, Perez-Rando M, Videira S, Nacher J (2016a). Polysialic Acid Acute Depletion Induces Structural Plasticity in Interneurons and Impairs the Excitation/Inhibition Balance in Medial Prefrontal Cortex Organotypic Cultures. *Front Cell Neurosci* **10**: 170.

Castillo-Gómez E, Varea E, Blasco-Ibáñez JM, Crespo C, Nacher J (2011). Polysialic Acid Is Required for Dopamine D2 Receptor-Mediated Plasticity Involving Inhibitory Circuits of the Rat Medial Prefrontal Cortex. *PLoS One* **6**: e29516.

Castillo-Gómez E, Varea E, Blasco-Ibáñez JM, Crespo C, Nacher J (2016b). Effects of Chronic Dopamine D2R Agonist Treatment and Polysialic Acid Depletion on Dendritic Spine Density and Excitatory Neurotransmission in the mPFC of Adult Rats. *Neural Plast* **2016**: 1–12.

Castrén E, Rantamäki T (2010). The role of BDNF and its receptors in depression and antidepressant drug action: Reactivation of developmental plasticity. *Dev Neurobiol* **70**: 289–297.

Cazorla M, Jouvenceau A, Rose C, Guilloux J-P, Pilon C, Dranovsky A, *et al* (2010). Cyclotraxin-B, the first highly potent and selective TrkB inhibitor, has anxiolytic properties in mice. *PLoS One* **5**: e9777.

Chen J, Chua KW, Chua CC, Yu H, Pei A, Chua BHL, *et al* (2011a). Antioxidant activity of 7,8-dihydroxyflavone provides neuroprotection against glutamate-induced toxicity. *Neurosci Lett* **499**: 181–185.

Chen JL, Flanders GH, Lee W-CA, Lin WC, Nedivi E (2011b). Inhibitory Dendrite Dynamics as a General Feature of the Adult Cortical Microcircuit. *J Neurosci* **31**:

12437–12443.

Chen JL, Lin WC, Cha JW, So PT, Kubota Y, Nedivi E (2011c). Structural basis for the role of inhibition in facilitating adult brain plasticity. *Nat Neurosci* **14**: 587–94.

Chen JL, Nedivi E (2013). Highly Specific Structural Plasticity of Inhibitory Circuits in the Adult Neocortex. *Neurosci* **19**: 384–393.

Chen JL, Villa KL, Cha JW, So PTC, Kubota Y, Nedivi E (2012). Clustered dynamics of inhibitory synapses and dendritic spines in the adult neocortex. *Neuron* **74**: 361–73.

Chen Z-Y, Jing D, Bath KG, Ieraci A, Khan T, Siao C-J, *et al* (2006). Genetic Variant BDNF (Val66Met) Polymorphism Alters Anxiety-Related Behavior. *Science (80-)* **314**: 140–143.

Clark RE, Squire LR (2013). Similarity in form and function of the hippocampus in rodents, monkeys, and humans. *Proc Natl Acad Sci* **110**: 10365–10370.

Cline HT, Constantine-Paton M (1990). NMDA receptor agonist and antagonists alter retinal ganglion cell arbor structure in the developing frog retinotectal projection. *J Neurosci* **10**: 1197–216.

Cohen-Cory S, Fraser SE (1995). Effects of brain-derived neurotrophic factor on optic axon branching and remodelling in vivo. *Nature* **378**: 192–196.

Cohen SM, Tsien RW, Goff DC, Halassa MM (2015). The impact of NMDA receptor hypofunction on GABAergic neurons in the pathophysiology of schizophrenia. *Schizophr Res* **167**: 98–107.

Colicos MA, Collins BE, Sailor MJ, Goda Y (2001). Remodeling of Synaptic Actin Induced by Photoconductive Stimulation. *Cell* **107**: 1–12.

Collingridge GL, Kehl SJ, McLennan H (1983). Excitatory amino acids in synaptic transmission in the Schaffer collateral-commissural pathway of the rat hippocampus. *J Physiol* **334**: 33–46.

Constandil L, Goich M, Hernández A, Bourgeais L, Cazorla M, Hamon M, *et al* (2012). Cyclotraxin-B, a New TrkB Antagonist, and Glial Blockade by Propentofylline, Equally Prevent and Reverse Cold Allodynia Induced by BDNF or Partial Infraorbital Nerve Constriction in Mice. *J Pain* **13**: 579–589.

Cook SC, Wellman CL (2004). Chronic stress alters dendritic morphology in rat medial prefrontal cortex. *J Neurobiol* **60**: 236–248.

Cordero MI, Rodríguez JJ, Davies HA, Peddie CJ, Sandi C, Stewart MG (2005). Chronic restraint stress down-regulates amygdaloid expression of polysialylated neural cell adhesion molecule. *Neuroscience* **133**: 903–10.

Curley A a, Lewis D a (2012). Cortical basket cell dysfunction in schizophrenia. *J Physiol* **590**: 715–24.

Curto Y, Garcia-Mompo C, Bueno-Fernandez C, Nacher J (2016). Chronic benzodiazepine treatment decreases spine density in cortical pyramidal neurons. *Neurosci Lett* **613**:

41–46.

Desmond NL, Scott CA, Jane JA, Levy WB (1994). Ultrastructural identification of entorhinal cortical synapses in CA1 stratum lacunosum-moleculare of the rat. *Hippocampus* **4**: 594–600.

Dingess PM, Darling RA, Kurt Dolence E, Culver BW, Brown TE (2017). Exposure to a diet high in fat attenuates dendritic spine density in the medial prefrontal cortex. *Brain Struct Funct* **222**: 1077–1085.

Doherty P, Fruns M, Seaton P, Dickson G, Barton CH, Sears TA, *et al* (1990). A threshold effect of the major isoforms of NCAM on neurite outgrowth. *Nature* **343**: 464–466.

Dore K, Aow J, Malinow R (2016). The Emergence of NMDA Receptor Metabotropic Function: Insights from Imaging. *Front Synaptic Neurosci* **8**: 20.

Du X, Hill RA (2015). 7,8-Dihydroxyflavone as a pro-neurotrophic treatment for neurodevelopmental disorders. *Neurochem Int* **89**: 170–180.

Duman RS, Malberg J, Nakagawa S, D'Sa C (2000). Neuronal plasticity and survival in mood disorders. *Biol Psychiatry* **48**: 732–739.

Duman RS, Monteggia LM (2006). A Neurotrophic Model for Stress-Related Mood Disorders. *Biol Psychiatry* **59**: 1116–1127.

Dumas TC (2005). Developmental regulation of cognitive abilities: Modified composition of a molecular switch turns on associative learning. *Prog Neurobiol* **76**: 189–211.

Eggan SM, Hashimoto T, Lewis DA (2008). Reduced Cortical Cannabinoid 1 Receptor Messenger RNA and Protein Expression in Schizophrenia. *Arch Gen Psychiatry* **65**: 772.

Ehrlich I, Humeau Y, Grenier F, Ciocchi S, Herry C, Lüthi A (2009). Amygdala Inhibitory Circuits and the Control of Fear Memory. *Neuron* **62**: 757–771.

Elliott SB, Harvey-Girard E, Giassi ACC, Maler L (2017). Hippocampal-like circuitry in the pallium of an electric fish: Possible substrates for recursive pattern separation and completion. *J Comp Neurol* **525**: 8–46.

Engert F, Bonhoeffer T (1999). Dendritic spine changes associated with hippocampal long-term synaptic plasticity. *Nature* **399**: 66–70.

Enwright JF, Sanapala S, Foglio A, Berry R, Fish KN, Lewis DA (2016). Reduced Labeling of Parvalbumin Neurons and Perineuronal Nets in the Dorsolateral Prefrontal Cortex of Subjects with Schizophrenia. *Neuropsychopharmacology* **41**: 2206–2214.

Erlander MG, Tobin AJ (1991). The structural and functional heterogeneity of glutamic acid decarboxylase: a review. *Neurochem Res* **16**: 215–26.

Escobar ML, Figueroa-Guzmán Y, Gómez-Palacio-Schjetnan A (2003). In vivo insular cortex LTP induced by brain-derived neurotrophic factor. *Brain Res* **991**: 274–279.

Fava M, Kendler KS (2000). Major depressive disorder. *Neuron* **28**: 335–41.

Fazzari P, Paternain A V, Valiente M, Pla R, Luján R, Lloyd K, *et al* (2010). Control of cortical GABA circuitry development by Nrg1 and ErbB4 signalling. *Nature* **464**: 1376–80.

Feng G, Mellor RH, Bernstein M, Keller-Peck C, Nguyen QT, Wallace M, *et al* (2000). Imaging neuronal subsets in transgenic mice expressing multiple spectral variants of GFP. *Neuron* **28**: 41–51.

Filipkowski RK, Rydz M, Berdel B, Morys J, Kaczmarek L (2000). Tactile Experience Induces c-fos Expression in Rat Barrel Cortex. *Learn Mem* **7**: 116–122.

Fish K, Sweet R, Lewis D (2011). Differential distribution of proteins regulating GABA synthesis and reuptake in axon boutons of subpopulations of cortical interneurons. *Cereb Cortex* **21**: 1–11.

Florence SL, Taub HB, Kaas JH (1998). Large-scale sprouting of cortical connections after peripheral injury in adult macaque monkeys. *Science* **282**: 1117–21.

Flores C, Wen X, Labelle-Dumais C, Kolb B (2007). Chronic phencyclidine treatment increases dendritic spine density in prefrontal cortex and nucleus accumbens neurons. *Synapse* **61**: 978–984.

Flores G, Alquicer G, Silva-Gómez a. B, Zaldivar G, Stewart J, Quirion R, *et al* (2005). Alterations in dendritic morphology of prefrontal cortical and nucleus accumbens neurons in post-pubertal rats after neonatal excitotoxic lesions of the ventral hippocampus. *Neuroscience* **133**: 463–470.

Flores G, Morales-Medina JC, Diaz A (2016). Neuronal and brain morphological changes in animal models of schizophrenia. *Behav Brain Res* **301**: 190–203.

Fone KCF, Porkess MV (2008). Behavioural and neurochemical effects of post-weaning social isolation in rodents-relevance to developmental neuropsychiatric disorders. *Neurosci Biobehav Rev* **32**: 1087–102.

Fox K (2008). Summary for Policymakers. *Clim Chang 2013 - Phys Sci Basis* **1**: 1–30.

Freund TF (2003). Interneuron Diversity series: Rhythm and mood in perisomatic inhibition. *Trends Neurosci* **26**: 489–495.

Freund TF, Buzsáki G (1996). Interneurons of the hippocampus. *Hippocampus* **6**: 347–470.

Freund TF, Katona I (2007). Perisomatic Inhibition. *Neuron* **56**: 33–42.

Fu M, Zuo Y (2011). Experience-dependent structural plasticity in the cortex. *Trends Neurosci* **34**: 177–87.

Fuller RW, Wong DT (1990). Serotonin uptake and serotonin uptake inhibition. *Ann N Y Acad Sci* **600**: 68-78-80.

Fuster JM (2015). *The Prefrontal Cortex*. *Elsevier* at <http://linkinghub.elsevier.com/retrieve/pii/B978012407815400009X>.

Gähwiler BH, Capogna M, Debanne D, McKinney R a, Thompson SM (1997). Organotypic

slice cultures: a technique has come of age. *Trends Neurosci* **20**: 471–7.

Garcia R, Vouimba RM, Baudry M, Thompson RF (1999). The amygdala modulates prefrontal cortex activity relative to conditioned fear. *Nature* **402**: 294–296.

Gavish M, Snyder SH (1980). Benzodiazepine recognition sites on GABA receptors. *Nature* **287**: 651–652.

Gervasoni N, Aubry J-M, Bondolfi G, Osiek C, Schwald M, Bertschy G, *et al* (2005). Partial normalization of serum brain-derived neurotrophic factor in remitted patients after a major depressive episode. *Neuropsychobiology* **51**: 234–8.

Gilabert-Juan J, Belles M, Saez AR, Carceller H, Zamarbide-Fores S, Moltó MD, *et al* (2013a). A "double hit" murine model for schizophrenia shows alterations in the structure and neurochemistry of the medial prefrontal cortex and the hippocampus. *Neurobiol Dis* **59**: 126–140.

Gilabert-Juan J, Bueno-Fernandez C, Castillo-Gomez E, Nacher J (2017). Reduced interneuronal dendritic arborization in CA1 but not in CA3 region of mice subjected to chronic mild stress. *Brain Behav* **7**: e00534.

Gilabert-Juan J, Castillo-Gomez E, Guirado R, Moltó MD, Nacher J (2013b). Chronic stress alters inhibitory networks in the medial prefrontal cortex of adult mice. *Brain Struct Funct* **218**: 1591–605.

Gilabert-Juan J, Castillo-Gomez E, Perez-Rando M, Moltó MD, Nacher J (2011). Chronic stress induces changes in the structure of interneurons and in the expression of molecules related to neuronal structural plasticity and inhibitory neurotransmission in the amygdala of adult mice. *Exp Neurol* **232**: 33–40.

Gilabert-Juan J, Moltó MD, Nacher J (2012a). Post-weaning social isolation rearing influences the expression of molecules related to inhibitory neurotransmission and structural plasticity in the amygdala of adult rats. *Brain Res* **1448**: 129–36.

Gilabert-Juan J, Varea E, Guirado R, Blasco-Ibáñez JM, Crespo C, Nácher J (2012b). Alterations in the expression of PSA-NCAM and synaptic proteins in the dorsolateral prefrontal cortex of psychiatric disorder patients. *Neurosci Lett* **530**: 97–102.

Glantz L a., Lewis DA (2000). Decreased Dendritic Spine Density on Prefrontal Cortical Pyramidal Neurons in Schizophrenia. *Arch Gen Psychiatry* **57**: 65.

Glausier JR, Lewis D a. (2013). Dendritic spine pathology in schizophrenia. *Neuroscience* **251**: 90–107.

Gogolla N, Caroni P, Luethi A, Herry C (2009). Perineuronal Nets Protect Fear Memories from Erasure. *Science (80-)* **325**: 1258–1261.

Golgi C (1873). Sulla struttura della sostanza grigia del cervello. *Gazetta medica Lomb IV* .

Gomez-Climent MA, Guirado R, Castillo-Gomez E, Varea E, Gutierrez-Mecinas M, Gilabert-Juan J, *et al* (2011). The Polysialylated Form of the Neural Cell Adhesion Molecule (PSA-NCAM) Is Expressed in a Subpopulation of Mature Cortical Interneurons Characterized by Reduced Structural Features and Connectivity. *Cereb*

Cortex **21**: 1028–1041.

Gonçalves JT, Schafer ST, Gage FH (2016). Adult Neurogenesis in the Hippocampus: From Stem Cells to Behavior. *Cell* **167**: 897–914.

Gonzalez-Burgos G, Cho RY, Lewis DA (2015). Alterations in Cortical Network Oscillations and Parvalbumin Neurons in Schizophrenia. *Biol Psychiatry* **77**: 1031–1040.

Gonzalez-Burgos G, Lewis DA (2012). NMDA receptor hypofunction, parvalbumin-positive neurons, and cortical gamma oscillations in schizophrenia. *Schizophr Bull* **38**: 950–957.

Gonzalez A, Moya-Alvarado G, Gonzalez-Billaut C, Bronfman FC (2016). Cellular and molecular mechanisms regulating neuronal growth by brain-derived neurotrophic factor. *Cytoskeleton* **73**: 612–628.

Gorba T, Wahle P (1999). Expression of TrkB and TrkC but not BDNF mRNA in neurochemically identified interneurons in rat visual cortex in vivo and in organotypic cultures. *Eur J Neurosci* **11**: 1179–1190.

Gould E (2007). How widespread is adult neurogenesis in mammals? *Nat Rev Neurosci* **8**: 481–488.

Green MJ, Matheson SL, Shepherd a, Weickert CS, Carr VJ (2011). Brain-derived neurotrophic factor levels in schizophrenia: a systematic review with meta-analysis. *Mol Psychiatry* **16**: 960–972.

Grillo FW, Song S, Teles-Grilo Ruivo LM, Huang L, Gao G, Knott GW, *et al* (2013). Increased axonal bouton dynamics in the aging mouse cortex. *Proc Natl Acad Sci* **110**: E1514–E1523.

Grutzendler J, Kasthuri N, Gan WW-B (2002). Long-term dendritic spine stability in the adult cortex. *Nature* **420**: 812–816.

Guić-Robles E, Valdivieso C, Guajardo G (1989). Rats can learn a roughness discrimination using only their vibrissal system. *Behav Brain Res* **31**: 285–289.

Guilloux J, Douillard-Guilloux G, Kota R, Wang X, Gardier AM, Martinowich K, *et al* (2012). Molecular evidence for BDNF- and GABA-related dysfunctions in the amygdala of female subjects with major depression. *Mol Psychiatry* **17**: 1130–1142.

Guirado R, Perez-Rando M, Sanchez-Matarredona D, Castillo-Gomez E, Liberia T, Rovira-Esteban L, *et al* (2014). The Dendritic Spines of Interneurons Are Dynamic Structures Influenced by PSA-NCAM Expression. *Cereb Cortex* **24**: 3014–3024.

Guirado R, Sanchez-Matarredona D, Varea E, Crespo C, Blasco-Ibáñez J, Nacher J (2012). Chronic fluoxetine treatment in middle-aged rats induces changes in the expression of plasticity-related molecules and in neurogenesis. *BMC Neurosci* **13**: 5.

Guirado R, Varea E, Castillo-Gómez E, Gómez-Climent M a., Rovira-Esteban L, Blasco-Ibáñez JM, *et al* (2009). Effects of chronic fluoxetine treatment on the rat somatosensory cortex: Activation and induction of neuronal structural plasticity.

Neurosci Lett **457**: 12–15.

Gulyás AI, Miettinen R, Jacobowitz DM, Freund TF (1992). Calretinin is present in non-pyramidal cells of the rat hippocampus-I. A new type of neuron specifically associated with the mossy fibre system. *Neuroscience* **48**: 1–27.

Haj-Mirzaian A, Amiri S, Kordjazy N, Rahimi-Balaei M, Haj-Mirzaian A, Marzban H, *et al* (2015). Blockade of NMDA receptors reverses the depressant, but not anxiogenic effect of adolescence social isolation in mice. *Eur J Pharmacol* **750**: 160–166.

Hajszan T, MacLusky NJ, Leranth C (2005). Short-term treatment with the antidepressant fluoxetine triggers pyramidal dendritic spine synapse formation in rat hippocampus. *Eur J Neurosci* **21**: 1299–303.

Halpain S, Hipolito A, Saffer L (1998). Regulation of F-actin stability in dendritic spines by glutamate receptors and calcineurin. *J Neurosci* **18**: 9835–44.

Han D, Xu L, Xiao H, Prado Schmidt GC, Shi S (2013). Dizocilpine reduces head diameter of dendritic spines in the hippocampus of adolescent rats. *Psychiatry Res* **210**: 351–356.

Harrison P (2004). The hippocampus in schizophrenia: a review of the neuropathological evidence and its pathophysiological implications. *Psychopharmacology (Berl)* **174**: 151–162.

Heimendahl M von, Itskov PM, Arabzadeh E, Diamond ME (2007). Neuronal Activity in Rat Barrel Cortex Underlying Texture Discrimination. *PLoS Biol* **5**: e305.

Hensch TK (2004). Critical Period Regulation. *Annu Rev Neurosci* **27**: 549–579.

Hensch TK (2005). Critical period plasticity in local cortical circuits. *Nat Rev Neurosci* **6**: 877–88.

Hensch TK, Bilimoria PM (2012). Re-opening Windows: Manipulating Critical Periods for Brain Development. *Cerebrum* **2012**: 11.

Hensch TK, Fagiolini M (2005). Excitatory–inhibitory balance and critical period plasticity in developing visual cortex. *Prog Brain Res* **147**: 115–124.

Hering H, Sheng M (2001). Dendritic spines: structure, dynamics and regulation. *Nat Rev Neurosci* **2**: 880–8.

Herkenham M (1980). Laminar organization of thalamic projections to the rat neocortex. *Science (80-)* **207**: 532–535.

Herman JP, Cullinan WE (1997). Neurocircuitry of stress: Central control of the hypothalamo-pituitary-adrenocortical axis. *Trends Neurosci* **20**: 78–84.

Hildebrandt H, Mühlenhoff M, Gerardy-Schahn R (2008). WITHDRAWN: Polysialylation of NCAM. *Neurochem Res* doi:10.1007/s11064-008-9724-7.

Hirose N, Saitoh A, Kamei J (2016). Involvement of glutamatergic N-methyl-D-aspartate receptors in the expression of increased head-dipping behaviors in the hole-board tests of olfactory bulbectomized mice. *Behav Brain Res* **312**: 313–320.

Hofer SB, Ko H, Pichler B, Vogelstein J, Ros H, Zeng H, *et al* (2011). Differential connectivity and response dynamics of excitatory and inhibitory neurons in visual cortex. *Nat Neurosci* **14**: 1045–52.

Hofer SB, Mrsic-Flogel TD, Bonhoeffer T, Hübener M (2009). Experience leaves a lasting structural trace in cortical circuits. *Nature* **457**: 313–317.

Holtmaat A, Bonhoeffer T, Chow DK, Chuckowree J, Paola V De, Hofer SB, *et al* (2009). Long-term, high-resolution imaging in the mouse neocortex through a chronic cranial window. *Nat Protoc* **4**: 1128–1144.

Holtmaat A, Svoboda K (2009). Experience-dependent structural synaptic plasticity in the mammalian brain. *Nat Rev Neurosci* **10**: 647–58.

Holtmaat A, Wilbrecht L, Knott GW, Welker E, Svoboda K (2006). Experience-dependent and cell-type-specific spine growth in the neocortex. *Nature* **441**: 979–983.

Hopkins ME, Bucci DJ (2010). BDNF expression in perirhinal cortex is associated with exercise-induced improvement in object recognition memory. *Neurobiol Learn Mem* **94**: 278–284.

Horch HW, Katz LC (2002). BDNF release from single cells elicits local dendritic growth in nearby neurons. *Nat Neurosci* **5**: 1177–1184.

Huang EJ, Reichardt LF (2001). NEUROTROPHINS: Roles in Neuronal Development and Function. *Annu Rev Neurosci* **24**: 677–736.

Humpel C (2015). Organotypic brain slice cultures: A review. *Neuroscience* **305**: 86–98.

Hunt WA (1983). The Effect of Ethanol on GABAergic Transmission. *Neurosci Biobehav Rev* **7**: 87–95.

Inan M, Petros TJ, Anderson S a (2013). Losing your inhibition: linking cortical GABAergic interneurons to schizophrenia. *Neurobiol Dis* **53**: 36–48.

Iñiguez SD, Alcantara LF, Warren BL, Riggs LM, Parise EM, Vialou V, *et al* (2014). Fluoxetine exposure during adolescence alters responses to aversive stimuli in adulthood. *J Neurosci* **34**: 1007–21.

Isacsson G, Holmgren P, Ahlner J (2005). Selective serotonin reuptake inhibitor antidepressants and the risk of suicide: a controlled forensic database study of 14,857 suicides. *Acta Psychiatr Scand* **111**: 286–90.

Ishikawa A, Nakamura S (2003). Convergence and Interaction of Hippocampal and Amygdalar Projections within the Prefrontal Cortex in the Rat. *J Neurosci* **23**: 9987–9995.

Iversen L (2008). The Monoamine Hypothesis of Depression. *Biol Depress From Nov Insights to Ther Strateg* 71–86doi:10.1002/9783527619672.ch5.

Jacobs BL, Azmitia EC (1992). Structure and function of the brain serotonin system. *Physiol Rev* **72**: 165–229.

Jang S-W, Liu X, Yepes M, Shepherd KR, Miller GW, Liu Y, *et al* (2010). A selective TrkB

agonist with potent neurotrophic activities by 7,8-dihydroxyflavone. *Proc Natl Acad Sci U S A* **107**: 2687–92.

Jasnow AM, Ressler KJ, Hammack SE, Chhatwal JP, Rainnie DG (2009). Distinct subtypes of cholecystokinin (CCK)-containing interneurons of the basolateral amygdala identified using a CCK promoter-specific lentivirus. *J Neurophysiol* **101**: 1494–1506.

Jay TM, Witter MP (1991). Distribution of hippocampal CA1 and subicular efferents in the prefrontal cortex of the rat studied by means of anterograde transport ofPhaseolus vulgaris-leucoagglutinin. *J Comp Neurol* **313**: 574–586.

Jones CA, Watson DJG, Fone KCF (2011). Animal models of schizophrenia. *Br J Pharmacol* **164**: 1162–94.

Jonnakuty C, Gragnoli C (2008). What do we know about serotonin? *J Cell Physiol* **217**: 301–306.

Kalinichev M, Bate ST, Coggon SA, Jones DNC (2008). Locomotor reactivity to a novel environment and sensitivity to MK-801 in five strains of mice. *Behav Pharmacol* **19**: 71–75.

Kandel ER, Schwartz JH, Jessell TM, Siegelbaum SA, Hudspeth AJ (2012). *Principles of Neural Science, Fifth edition*. doi:10.1007/s13398-014-0173-7.2.

Kang H, Welcher AA, Shelton D, Schuman EM (1997). Neurotrophins and time: Different roles for TrkB signaling in hippocampal long-term potentiation. *Neuron* **19**: 653–664.

Karege F, Perret G, Bondolfi G, Schwald M, Bertschy G, Aubry JM (2002). Decreased serum brain-derived neurotrophic factor levels in major depressed patients. *Psychiatry Res* **109**: 143–148.

Karege F, Vaudan G, Schwald M, Perroud N, Harpe R La (2005). Neurotrophin levels in postmortem brains of suicide victims and the effects of antemortem diagnosis and psychotropic drugs. *Mol Brain Res* **136**: 29–37.

Karetko M, Skangiel-Kramska J (2009). Diverse functions of perineuronal nets. *Acta Neurobiol Exp (Wars)* **69**: 564–77.

Karnani MM, Jackson J, Ayzenshtat I, Hamzehei Sichani A, Manoocheri K, Kim S, *et al* (2016). Opening Holes in the Blanket of Inhibition: Localized Lateral Disinhibition by VIP Interneurons. *J Neurosci* **36**: 3471–3480.

Karpova NN, Pickenhagen A, Lindholm J, Tiraboschi E, Kulesskaya N, Agustsdottir A, *et al* (2011). Fear Erasure in Mice Requires Synergy Between Antidepressant Drugs and Extinction Training. *Science (80-)* **334**: 1731–1734.

Katona L, Lapray D, Viney TJ, Oulhaj A, Borhegyi Z, Micklem BR, *et al* (2014). Sleep and Movement Differentiates Actions of Two Types of Somatostatin-Expressing GABAergic Interneuron in Rat Hippocampus. *Neuron* **82**: 872–886.

Kawaguchi Y, Kubota Y (1997). GABAergic cell subtypes and their synaptic connections in rat frontal cortex. *Cereb Cortex* **7**: 476–486.

Keck T, Scheuss V, Jacobsen RI, Wierenga CJ, Eysel UT, Bonhoeffer T, *et al* (2011). Loss of sensory input causes rapid structural changes of inhibitory neurons in adult mouse visual cortex. *Neuron* **71**: 869–82.

Kepser L-J, Homberg JR (2014). The neurodevelopmental effects of serotonin: A behavioural perspective. *Behav Brain Res* **277**: 1–10.

Keshavan MS, Anderson S, Pettergrew JW (1994). Is Schizophrenia due to excessive synaptic pruning in the prefrontal cortex? The Feinberg hypothesis revisited. *J Psychiatr Res* **28**: 239–265.

Kesslak JP, So V, Choi J, Cotman CW, Gomez-Pinilla F (1998). Learning upregulates brain-derived neurotrophic factor messenger ribonucleic acid: A mechanism to facilitate encoding and circuit maintenance? *Behav Neurosci* **112**: 1012–1019.

Kevenaar JT, Hoogenraad CC (2015). The axonal cytoskeleton: from organization to function. *Front Mol Neurosci* **8**: 1–12.

Kew JNC, Kemp JA (2005). Ionotropic and metabotropic glutamate receptor structure and pharmacology. *Psychopharmacology (Berl)* **179**: 4–29.

Kleinfeld D, Ahissar E, Diamond ME (2006). Active sensation: insights from the rodent vibrissa sensorimotor system. *Curr Opin Neurobiol* **16**: 435–444.

Klintsova AY, Dickson E, Yoshida R, Greenough WT (2004). Altered expression of BDNF and its high-affinity receptor TrkB in response to complex motor learning and moderate exercise. *Brain Res* **1028**: 92–104.

Knott G, Holtmaat A (2008). Dendritic spine plasticity—Current understanding from in vivo studies. *Brain Res Rev* **58**: 282–289.

Knott GW, Holtmaat A, Wilbrecht L, Welker E, Svoboda K (2006). Spine growth precedes synapse formation in the adult neocortex in vivo. *Nat Neurosci* **9**: 1117–1124.

Kobayashi K, Ikeda Y, Sakai A, Yamasaki N, Haneda E, Miyakawa T, *et al* (2010). Reversal of hippocampal neuronal maturation by serotonergic antidepressants. *Proc Natl Acad Sci U S A* **107**: 8434–9.

Kochlamazashvili G, Henneberger C, Bukalo O, Dvoretskova E, Senkov O, Lievens PMJ, *et al* (2010). The extracellular matrix molecule hyaluronic acid regulates hippocampal synaptic plasticity by modulating postsynaptic L-type Ca2+ channels. *Neuron* **67**: 116–128.

Kokaia Z, Bengzon J, Metsis M, Kokaia M, Persson H, Lindvall O (1993). Coexpression of neurotrophins and their receptors in neurons of the central nervous system. *Proc Natl Acad Sci* **90**: 6711–6715.

Kolluri N, Sun Z, Sampson AR, Lewis DA (2005). Lamina-specific reductions in dendritic spine density in the prefrontal cortex of subjects with schizophrenia. *Am J Psychiatry* **162**: 1200–2.

Komuro H, Rakic P (1993). Modulation of neuronal migration by NMDA receptors. *Science* **260**: 95–7.

Korkmaz OT, Aytan N, Carreras I, Choi J-K, Kowall NW, Jenkins BG, *et al* (2014). 7,8-Dihydroxyflavone improves motor performance and enhances lower motor neuronal survival in a mouse model of amyotrophic lateral sclerosis. *Neurosci Lett* **566**: 286–91.

Korte SM (2001). Corticosteroids in relation to fear, anxiety and psychopathology. *Neurosci Biobehav Rev* **25**: 117–142.

Krettek JE, Price JL (1977). Projections from the amygdaloid complex to the cerebral cortex and thalamus in the rat and cat. *J Comp Neurol* **172**: 687–722.

Krishnan V, Nestler EJ (2008). The molecular neurobiology of depression. *Nature* **455**: 894–902.

Kristensen BW, Noraberg J, Zimmer J (2001). Comparison of excitotoxic profiles of ATPA, AMPA, KA and NMDA in organotypic hippocampal slice cultures. *Brain Res* **917**: 21–44.

Kuc K a, Gregersen BM, Gannon KS, Dodart J-C (2006). Holeboard discrimination learning in mice. *Genes, Brain Behav* **5**: 355–363.

Kullmann DM (2011). Interneuron networks in the hippocampus. *Curr Opin Neurobiol* **21**: 709–16.

Kwon H-B, Sabatini BL (2011). Glutamate induces de novo growth of functional spines in developing cortex. *Nature* **474**: 100–4.

LaBar KS, Cabeza R (2006). Cognitive neuroscience of emotional memory. *Nat Rev Neurosci* **7**: 54–64.

Lai K-OO, Ip NY (2013). Structural plasticity of dendritic spines: The underlying mechanisms and its dysregulation in brain disorders. *Biochim Biophys Acta - Mol Basis Dis* **1832**: 2257–2263.

Lam YW, Sherman SM (2010). Functional organization of the somatosensory cortical layer 6 feedback to the thalamus. *Cereb Cortex* **20**: 13–24.

Lazcano Z, Solis O, Díaz A, Brambila E, Aguilar-Alonso P, Guevara J, *et al* (2015). Dendritic morphology changes in neurons from the ventral hippocampus, amygdala and nucleus accumbens in rats with neonatal lesions into the prefrontal cortex. *Synapse* **69**: 314–25.

Leão RN, Mikulovic S, Leão KE, Munguba H, Gezelius H, Enjin A, *et al* (2012). OLM interneurons differentially modulate CA3 and entorhinal inputs to hippocampal CA1 neurons. *Nat Neurosci* **15**: 1524–30.

Lee KFH, Soares C, Béïque J-C (2012). Examining Form and Function of Dendritic Spines. *Neural Plast* **2012**: 1–9.

Lee W-CA, Huang H, Feng G, Sanes JR, Brown EN, So PT, *et al* (2005). Dynamic Remodeling of Dendritic Arbors in GABAergic Interneurons of Adult Visual Cortex. *PLoS Biol* **4**: e29.

Leger M, Quiedeville A, Bouet V, Haelewyn B, Boulouard M, Schumann-Bard P, *et al* (2013). Object recognition test in mice. *Nat Protoc* **8**: 2531–2537.

Lett TA, Voineskos AN, Kennedy JL, Levine B, Daskalakis ZJ (2014). Treating working memory deficits in schizophrenia: a review of the neurobiology. *Biol Psychiatry* **75**: 361–70.

Levi-Montalcini R, Hamburger V (1951). Selective growth stimulating effects of mouse sarcoma on the sensory and sympathetic nervous system of the chick embryo. *J Exp Zool* **116**: 321–361.

Lewis DA, Curley AA, Glausier JR, Volk DW (2012). Cortical parvalbumin interneurons and cognitive dysfunction in schizophrenia. *Trends Neurosci* **35**: 57–67.

Lewis DA, Gonzalez-Burgos G, González-Burgos G (2008). Neuroplasticity of neocortical circuits in schizophrenia. *Neuropsychopharmacology* **33**: 141–165.

Li J-T, Zhao Y-Y, Wang H-L, Wang X-D, Su Y-A, Si T-M (2015). Long-term effects of neonatal exposure to MK-801 on recognition memory and excitatory–inhibitory balance in rat hippocampus. *Neuroscience* **308**: 134–143.

Li L, Tasic B, Micheva KD, Ivanov VM, Spletter ML, Smith SJ, *et al* (2010a). Visualizing the Distribution of Synapses from Individual Neurons in the Mouse Brain. *PLoS One* **5**: e11503.

Li N, Lee B, Liu R-J, Banasr M, Dwyer JM, Iwata M, *et al* (2010b). mTOR-Dependent Synapse Formation Underlies the Rapid Antidepressant Effects of NMDA Antagonists. *Science (80-)* **329**: 959–964.

Liguz-Lecznar M, Urban-Ciecko J, Kossut M (2016). Somatostatin and Somatostatin-Containing Neurons in Shaping Neuronal Activity and Plasticity. *Front Neural Circuits* **10**: 48.

Lima AD De, Morrison JH (1989). Ultrastructural analysis of somatostatin-immunoreactive neurons and synapses in the temporal and occipital cortex of the macaque monkey. *J Comp Neurol* **283**: 212–227.

Lindsley CW (2012). The top prescription drugs of 2011 in the United States: antipsychotics and antidepressants once again lead CNS therapeutics. *ACS Chem Neurosci* **3**: 630–1.

Lipton JO, Sahin M (2014). The Neurology of mTOR. *Neuron* **84**: 275–291.

Liu C, Chan CB, Ye K (2016). 7,8-dihydroxyflavone, a small molecular TrkB agonist, is useful for treating various BDNF-implicated human disorders. *Transl Neurodegener* **5**: 2.

Liu R-J, Fuchikami M, Dwyer JM, Lepack AE, Duman RS, Aghajanian GK (2013). GSK-3 Inhibition Potentiates the Synaptogenic and Antidepressant-Like Effects of Subthreshold Doses of Ketamine. *Neuropsychopharmacology* **38**: 2268–2277.

Liu, Wong TP, Pozza MF, Lingenhoehl K, Wang Y, Sheng M, *et al* (2004). Role of NMDA receptor subtypes in governing the direction of hippocampal synaptic plasticity.

Science (80-) **304**: 1021–1024.

Lom B, Cohen-Cory S (1999). Brain-Derived Neurotrophic Factor Differentially Regulates Retinal Ganglion Cell Dendritic and Axonal Arborization In Vivo. *J Neurosci* **19**: 9928–9938.

Lovett-Barron M, Kaifosh P, Kheirbek MA, Danielson N, Zaremba JD, Reardon TR, *et al* (2014). Dendritic Inhibition in the Hippocampus Supports Fear Learning. *Science (80-)* **343**: 857–863.

Lu B, Nagappan G, Guan X, Nathan PJ, Wren P (2013). BDNF-based synaptic repair as a disease-modifying strategy for neurodegenerative diseases. *Nat Rev Neurosci* **14**: 401–416.

Luca C De, Papa M (2016). Looking Inside the Matrix: Perineuronal Nets in Plasticity, Maladaptive Plasticity and Neurological Disorders. *Neurochem Res* **41**: 1507–1515.

Luo D, Shi Y, Wang J, Lin Q, Sun Y, Ye K, *et al* (2016). 7,8-dihydroxyflavone protects 6-OHDA and MPTP induced dopaminergic neurons degeneration through activation of TrkB in rodents. *Neurosci Lett* **620**: 43–49.

Maher P, Akaishi T, Abe K (2006). Flavonoid fisetin promotes ERK-dependent long-term potentiation and enhances memory. *Proc Natl Acad Sci* **103**: 16568–16573.

Malcolm CP, Picchioni MM, Ellett L (2015). Intrusive prospective imagery, posttraumatic intrusions and anxiety in schizophrenia. *Psychiatry Res* **230**: 899–904.

Maren S, Phan KL, Liberzon I (2013). The contextual brain: implications for fear conditioning, extinction and psychopathology. *Nat Rev Neurosci* **14**: 417–428.

Mariga A, Zavadil J, Ginsberg SD, Chao M V (2015). Withdrawal of BDNF from hippocampal cultures leads to changes in genes involved in synaptic function. *Dev Neurobiol* **75**: 173–92.

Markram H, Toledo-Rodriguez M, Wang Y, Gupta A, Silberberg G, Wu C (2004). Interneurons of the neocortical inhibitory system. *Nat Rev Neurosci* **5**: 793–807.

Martínez A, Alcántara S, Borrell V, Río J a Del, Blasi J, Otal R, *et al* (1998). TrkB and TrkC signaling are required for maturation and synaptogenesis of hippocampal connections. *J Neurosci* **18**: 7336–50.

Matsuzaki M, Honkura N, Ellis-Davies GCR, Kasai H (2004). Structural basis of long-term potentiation in single dendritic spines. *Nature* **429**: 761–6.

Mauney S a, Athanas KM, Pantazopoulos H, Shaskan N, Passeri E, Berretta S, *et al* (2013). Developmental pattern of perineuronal nets in the human prefrontal cortex and their deficit in schizophrenia. *Biol Psychiatry* **74**: 427–35.

McAllister AK, Katz LC, Lo DC (1997). Opposing roles for endogenous BDNF and NT-3 in regulating cortical dendritic growth. *Neuron* **18**: 767–778.

McAllister AK, Lo DC, Katz LC, Carolina N (1995). Neurotrophins Regulate Dendritic Growth in Developing Visual Codex. *Neuron* **15**: 791–803.

McAuley EZ, Scimone A, Tiwari Y, Agahi G, Mowry BJ, Holliday EG, *et al* (2012). Identification of Sialyltransferase 8B as a Generalized Susceptibility Gene for Psychotic and Mood Disorders on Chromosome 15q25-26. *PLoS One* **7**: e38172.

McEwen B, Morrison J (2013). The Brain on Stress: Vulnerability and Plasticity of the Prefrontal Cortex over the Life Course. *Neuron* **79**: 16–29.

McEwen BS (1999). Stress and Hippocampal Plasticity. *Annu Rev Neurosci* **22**: 105–122.

McEwen BS, Nasca C, Gray JD (2016). Stress Effects on Neuronal Structure: Hippocampus, Amygdala, and Prefrontal Cortex. *Neuropsychopharmacology* **41**: 3–23.

McIntire SL, Reimer RJ, Schuske K, Edwards RH, Jorgensen EM (1997). Identification and characterization of the vesicular GABA transporter. *Nature* **389**: 870–6.

McKinney RA, Capogna M, Dürr R, Gähwiler BH, Thompson SM (1999a). Miniature synaptic events maintain dendritic spines via AMPA receptor activation. *Nat Neurosci* **2**: 44–49.

McKinney RA, Lüthi A, Bandtlow CE, Gähwiler BH, Thompson SM (1999b). Selective glutamate receptor antagonists can induce or prevent axonal sprouting in rat hippocampal slice cultures. *Proc Natl Acad Sci U S A* **96**: 11631–6.

McRae PA, Porter BE (2012). The perineuronal net component of the extracellular matrix in plasticity and epilepsy. *Neurochem Int* **61**: 963–972.

McRae PA, Rocco MM, Kelly G, Brumberg JC, Matthews RT (2007). Sensory Deprivation Alters Aggrecan and Perineuronal Net Expression in the Mouse Barrel Cortex. *J Neurosci* **27**: 5405–5413.

Meis S, Endres T, Lessmann V (2012). Postsynaptic BDNF signalling regulates long-term potentiation at thalamo-amygdala afferents. *J Physiol* **590**: 193–208.

Mendez P, Pazienti A, Szabo G, Bacci A (2012). Direct Alteration of a Specific Inhibitory Circuit of the Hippocampus by Antidepressants. *J Neurosci* **32**: 16616–16628.

Merlio JP, Ernfors P, Kokaia Z, Middlemas DS, Bengzon J, Kokaia M, *et al* (1993). Increased production of the TrkB protein tyrosine kinase receptor after brain insults. *Neuron* **10**: 151–164.

Miceli S, Negwer M, Eijs F van, Kalkhoven C, Lierop I van, Homberg J, *et al* (2013). High serotonin levels during brain development alter the structural input-output connectivity of neural networks in the rat somatosensory layer IV. *Front Cell Neurosci* **7**: 88.

Miller PD, Styren SD, Lagenaur CF, DeKosky ST (1994). Embryonic neural cell adhesion molecule (N-CAM) is elevated in the denervated rat dentate gyrus. *J Neurosci* **14**: 4217–25.

Minichiello L (2009). TrkB signalling pathways in LTP and learning. *Nat Rev Neurosci* **10**: 850–60.

Minichiello L, Calella AM, Medina DL, Bonhoeffer T, Klein R, Korte M (2002). Mechanism of TrkB-mediated hippocampal long-term potentiation. *Neuron* **36**: 121–137.

Mitchell AC, Jiang Y, Peter C, Akbarian S (2015). Transcriptional regulation of GAD1 GABA synthesis gene in the prefrontal cortex of subjects with schizophrenia. *Schizophr Res* **167**: 28–34.

Mody I, MacDonald JF (1995). NMDA receptor-dependent excitotoxicity: the role of intracellular Ca2+ release. *Trends Pharmacol Sci* **16**: 356–359.

Moreau AW, Kullmann DM (2013). NMDA receptor-dependent function and plasticity in inhibitory circuits. *Neuropharmacology* **74**: 23–31.

Morishita H, Kundakovic M, Bicks L, Mitchell A, Akbarian S (2015). Interneuron epigenomes during the critical period of cortical plasticity: Implications for schizophrenia. *Neurobiol Learn Mem* **124**: 104–10.

Morita M, Gravel S-P, Hulea L, Larsson O, Pollak M, St-Pierre J, *et al* (2015). mTOR coordinates protein synthesis, mitochondrial activity and proliferation. *Cell Cycle* **14**: 473–480.

Mostany R, Anstey JE, Crump KL, Maco B, Knott G, Portera-Cailliau C (2013). Altered synaptic dynamics during normal brain aging. *J Neurosci* **33**: 4094–104.

Mostany R, Portera-Cailliau C (2008). A craniotomy surgery procedure for chronic brain imaging. *J Vis Exp* e680doi:10.3791/680.

Müller C, Remy S (2014). Dendritic inhibition mediated by O-LM and bistratified interneurons in the hippocampus. *Front Synaptic Neurosci* **6**: 23.

Murphy D, Cole NB, Segal M (1998). Brain-derived neurotrophic factor mediates estradiol-induced dendritic spine formation in hippocampal neurons. *Proc Natl Acad Sci U S A* **95**: 11412–7.

Murray EA (2007). The amygdala, reward and emotion. *Trends Cogn Sci* **11**: 489–497.

Nacher J, Blasco-Ibáñez JM, McEwen BS (2002a). Non-granule PSA-NCAM immunoreactive neurons in the rat hippocampus. *Brain Res* **930**: 1–11.

Nacher J, Guirado R, Castillo-Gómez E (2013). Structural Plasticity of Interneurons in the Adult Brain: Role of PSA-NCAM and Implications for Psychiatric Disorders. *Neurochem Res* **38**: 1122–1133.

Nacher J, Guirado R, Varea E, Alonso-Llosa G, Röckle I, Hildebrandt H (2010). Divergent impact of the polysialyltransferases ST8SiaII and ST8SiaIV on polysialic acid expression in immature neurons and interneurons of the adult cerebral cortex. *Neuroscience* **167**: 825–837.

Nacher J, Lanuza E, McEwen B. (2002b). Distribution of PSA-NCAM expression in the amygdala of the adult rat. *Neuroscience* **113**: 479–484.

Nagahara AH, Tuszynski MH (2011). Potential therapeutic uses of BDNF in neurological and psychiatric disorders. *Nat Rev Drug Discov* **10**: 209–219.

Negrón-Oyarzo I, Lara-Vásquez A, Palacios-García I, Fuentealba P, Aboitiz F (2016). Schizophrenia and reelin: a model based on prenatal stress to study epigenetics, brain development and behavior. *Biol Res* **49**: 16.

Nestler EJ, Barrot M, DiLeone RJ, Eisch AJ, Gold SJ, Monteggia LM (2002). Neurobiology of depression. *Neuron* **34**: 13–25.

Nibuya M, Morinobu S, Duman RS (1995). Regulation of BDNF and trkB mRNA in rat brain by chronic electroconvulsive seizure and antidepressant drug treatments. *J Neurosci* **15**: 7539–7547.

Nibuya M, Nestler EJ, Duman RS (1996). Chronic antidepressant administration increases the expression of cAMP response element binding protein (CREB) in rat hippocampus. *J Neurosci* **16**: 2365–2372.

Nikonenko I, Jourdain P, Muller D (2003). Presynaptic Remodeling Contributes to Activity-Dependent Synaptogenesis. *J Neurosci* **23**: 8498–8505.

Nowicka D, Soulsby S, Skangiel-Kramska J, Glazewski S (2009). Parvalbumin-containing neurons, perineuronal nets and experience-dependent plasticity in murine barrel cortex. *Eur J Neurosci* **30**: 2053–2063.

Nozari M, Mansouri FA, Shabani M, Nozari H, Atapour N (2015). Postnatal MK-801 treatment of female rats impairs acquisition of working memory, but not reference memory in an eight-arm radial maze; no beneficial effects of enriched environment. *Psychopharmacology (Berl)* **232**: 2541–2550.

Nyíri G, Stephenson F. A, Freund T. F, Somogyi P (2003). Large variability in synaptic n-methyl-d-aspartate receptor density on interneurons and a comparison with pyramidal-cell spines in the rat hippocampus. *Neuroscience* **119**: 347–363.

Oldendorf WH (1971). Brain uptake of radiolabeled amino acids, amines, and hexoses after arterial injection. *Am J Physiol* **221**: 1629–39.

Oliva AA, Jiang M, Lam T, Smith KL, Swann JW (2000). Novel hippocampal interneuronal subtypes identified using transgenic mice that express green fluorescent protein in GABAergic interneurons. *J Neurosci* **20**: 3354–68.

Oren I, Nissen W, Kullmann DM, Somogyi P, Lamsa KP (2009). Role of Ionotropic Glutamate Receptors in Long-Term Potentiation in Rat Hippocampal CA1 Oriens-Lacunosum Moleculare Interneurons. *J Neurosci* **29**: 939–950.

Otte C, Gold SM, Penninx BW, Pariante CM, Etkin A, Fava M, *et al* (2016). Major depressive disorder. *Nat Rev Dis Prim* **2**: 16065.

Ottenweller JE (2007). Animal Models (Nonprimate) for Human Stress. *Encycl Stress* 190–195doi:10.1016/B978-012373947-6.00035-0.

Pallanti S, Cantisani A, Grassi G (2013). Anxiety as a core aspect of schizophrenia. *Curr Psychiatry Rep* **15**: 354.

Pallanti S, Salerno L (2015). Raising attention to attention deficit hyperactivity disorder in schizophrenia. *World J psychiatry* **5**: 47–55.

Pandya CD, Kutiyanawalla A, Pillai A (2013). BDNF-TrkB signaling and neuroprotection in schizophrenia. *Asian J Psychiatr* **6**: 22–28.

Paoletti P, Bellone C, Zhou Q (2013). NMDA receptor subunit diversity: impact on receptor properties, synaptic plasticity and disease. *Nat Rev Neurosci* **14**: 383–400.

Parajuli LK, Tanaka S, Okabe S (2017). Insights into age-old questions of new dendritic spines: From form to function. *Brain Res Bull* **129**: 3–11.

Paxinos G, Franklin KBJ (2013). *Paxinos and Franklin's the Mouse Brain in Stereotaxic Coordinates*. at <https://books.google.de/books?id=8RJZLwEACAAJ>.

Paylor JW, Lins BR, Greba Q, Moen N, Moraes RS de, Howland JG, *et al* (2016). Developmental disruption of perineuronal nets in the medial prefrontal cortex after maternal immune activation. *Sci Rep* **6**: 37580.

Pérez-Otaño I, Larsen RS, Wesseling JF (2016). Emerging roles of GluN3-containing NMDA receptors in the CNS. *Nat Rev Neurosci* **17**: 623–635.

Pfeffer CK, Xue M, He M, Huang ZJ, Scanziani M (2013). Inhibition of inhibition in visual cortex: the logic of connections between molecularly distinct interneurons. *Nat Neurosci* **16**: 1068–76.

Phoumthipphavong V, Barthas F, Hassett S, Kwan AC, Autry A, Adachi M, *et al* (2016). Longitudinal Effects of Ketamine on Dendritic Architecture In Vivo in the Mouse Medial Frontal Cortex. *Eneuro* **3**: 91–95.

Pi H-J, Hangya B, Kvitsiani D, Sanders JI, Huang ZJ, Kepecs A (2013). Cortical interneurons that specialize in disinhibitory control. *Nature* **503**: 521–4.

Pizzorusso T, Medini P, Berardi N, Sabrina C, Fawcett JW, Maffei L (2002). Reactivation of Ocular Dominance Plasticity in the Adult Visual Cortex. *Science (80-)* **298**: 1248–1251.

Pollak DD, Rey CE, Monje FJ (2010). Rodent models in depression research: Classical strategies and new directions. *Ann Med* **42**: 252–264.

Popoli M, Yan Z, McEwen BS, Sanacora G (2012). The stressed synapse: the impact of stress and glucocorticoids on glutamate transmission. *Nat Rev Neurosci* **13**: 22–37.

Porrero C, Rubio-Garrido P, Avendaño C, Clascá F (2010). Mapping of fluorescent protein-expressing neurons and axon pathways in adult and developing Thy1-eYFP-H transgenic mice. *Brain Res* **1345**: 59–72.

Preston AR, Eichenbaum H (2013). Interplay of hippocampus and prefrontal cortex in memory. *Curr Biol* **23**: R764–R773.

Qiao H, Li M-X, Xu C, Chen H-B, An S-C, Ma X-M, *et al* (2016a). Dendritic Spines in Depression: What We Learned from Animal Models. *Neural Plast* **2016**: 1–26.

Qiao Q, Ma L, Li W, Tsai JW, Yang G, Gan WB (2016b). Long-term stability of axonal boutons in the mouse barrel cortex. *Dev Neurobiol* **76**: 252–261.

Radley JJ, Sisti HM, Hao J, Rocher AB, McCall T, Hof PR, *et al* (2004). Chronic behavioral

stress induces apical dendritic reorganization in pyramidal neurons of the medial prefrontal cortex. *Neuroscience* **125**: 1–6.

Ramón y Cajal S (1909). *Histologie du système nerveux de l'homme et des Vertébrés*. at <http://cataleg.ub.edu/record=b1267770~S1*cat>.

Real MA, Heredia R, Labrador M del C, Dávila JC, Guirado S (2009). Expression of somatostatin and neuropeptide Y in the embryonic, postnatal, and adult mouse amygdalar complex. *J Comp Neurol* **513**: 335–348.

Rocamora N, Welker E, Pascual M, Soriano E (1996). Upregulation of BDNF mRNA expression in the barrel cortex of adult mice after sensory stimulation. *J Neurosci* **16**: 4411–9.

Romero AM, Renau-Piqueras J, Pilar Marin M, Timoneda J, Berciano MT, Lafarga M, *et al* (2013). Chronic alcohol alters dendritic spine development in neurons in primary culture. *Neurotox Res* **24**: 532–548.

Rompala GR, Zsiros V, Zhang S, Kolata SM, Nakazawa K (2013). Contribution of NMDA Receptor Hypofunction in Prefrontal and Cortical Excitatory Neurons to Schizophrenia-Like Phenotypes. *PLoS One* **8**: e61278.

Rosoklija G, Toomayan G, Ellis SP, Keilp J, Mann JJ, Latov N, *et al* (2000). Structural abnormalities of subicular dendrites in subjects with schizophrenia and mood disorders: preliminary findings. *Arch Gen Psychiatry* **57**: 349–356.

Rotaru DC, Lewis DA, Gonzalez-Burgos G (2012). The role of glutamatergic inputs onto parvalbumin-positive interneurons: relevance for schizophrenia. *Rev Neurosci* **23**: 97–109.

Rotaru DC, Yoshino H, Lewis DA, Ermentrout GB, Gonzalez-Burgos G (2011). Glutamate Receptor Subtypes Mediating Synaptic Activation of Prefrontal Cortex Neurons: Relevance for Schizophrenia. *J Neurosci* **31**: 142–156.

Roux L, Buzsáki G (2015). Tasks for inhibitory interneurons in intact brain circuits. *Neuropharmacology* **88**: 10–23.

Rubio FJ, Ampuero E, Sandoval R, Toledo J, Pancetti F, Wyneken U (2013). Long-term fluoxetine treatment induces input-specific LTP and LTD impairment and structural plasticity in the CA1 hippocampal subfield. *Front Cell Neurosci* **7**: 66.

Rung JP, Carlsson A, Rydén Markinhuhta K, Carlsson ML (2005). (+)-MK-801 induced social withdrawal in rats; a model for negative symptoms of schizophrenia. *Prog Neuropsychopharmacol Biol Psychiatry* **29**: 827–32.

Russo E, Ciriaco M, Ventrice P, Russo G, Scicchitano M, Mazzitello G, *et al* (2013). Corticosteroid-related central nervous system side effects. *J Pharmacol Pharmacother* **4**: 94.

Rutishauser U (1996). Polysialic acid and the regulation of cell interactions. *Curr Opin Cell Biol* **8**: 679–684.

Rutishauser U (2008). Polysialic acid in the plasticity of the developing and adult

vertebrate nervous system. *Nat Rev Neurosci* **9**: 26–35.

Saffari R, Teng Z, Zhang M, Kravchenko M, Hohoff C, Ambrée O, *et al* (2016). NPY(+)-, but not PV(+)-GABAergic neurons mediated long-range inhibition from infra- to prelimbic cortex. *Transl Psychiatry* **6**: e736.

Sah P, Faber ESL, Lopez de Armentia M, Power J (2003). The Amygdaloid Complex : Anatomy and Physiology. *Physiol Rev* **83**: 803–834.

Sakaguchi T, Okada M, Kuno M, Kawasaki K (1997). Dual mode of N-methyl-d-aspartate-induced neuronal death in hippocampal slice cultures in relation to N-methyl-d-aspartate receptor properties. *Neuroscience* **76**: 411–423.

Sánchez-Huertas C, Rico B (2011). CREB-dependent regulation of gad65 transcription by BDNF/TrκB in cortical interneurons. *Cereb Cortex* **21**: 777–788.

Sandi C (2004). Stress, cognitive impairment and cell adhesion molecules. *Nat Rev Neurosci* **5**: 917–30.

Sanz-Clemente A, Nicoll RA, Roche KW (2013). Diversity in NMDA Receptor Composition: Many Regulators, Many Consequences. *Neurosci* **19**: 62–75.

Scheuss V, Bonhoeffer T (2014). Function of Dendritic Spines on Hippocampal Inhibitory Neurons. *Cereb Cortex* **24**: 1–12.

Scheyltjens I, Arckens L, Scheyltjens I, Arckens L (2016). The Current Status of Somatostatin-Interneurons in Inhibitory Control of Brain Function and Plasticity. *Neural Plast* **2016**: 1–20.

Seamans JK, Lapish CC, Durstewitz D (2008). Comparing the prefrontal cortex of rats and primates: Insights from electrophysiology. *Neurotox Res* **14**: 249–262.

Seymour B, Dolan R (2008). Emotion, Decision Making, and the Amygdala. *Neuron* **58**: 662–671.

Shatz CJ (1990). Impulse activity and the patterning of connections during cns development. *Neuron* **5**: 745–756.

Shen K, Cowan CW (2010). Guidance Molecules in Synapse Formation and Plasticity. *Cold Spring Harb Perspect Biol* **2**: a001842–a001842.

Shimada A, Mason CA, Morrison ME (1998). TrkB signaling modulates spine density and morphology independent of dendrite structure in cultured neonatal Purkinje cells. *J Neurosci* **18**: 8559–70.

Shimizu E, Hashimoto K, Okamura N, Koike K, Komatsu N, Kumakiri C, *et al* (2003). Alterations of serum levels of brain-derived neurotrophic factor (BDNF) in depressed patients with or without antidepressants. *Biol Psychiatry* **54**: 70–75.

Shimizu H, Ishizuka Y, Yamazaki H, Shirao T (2015). Allopregnanolone increases mature excitatory synapses along dendrites via protein kinase A signaling. *Neuroscience* **305**: 139–145.

Shimono K, Baudry M, Panchenko V, Taketani M (2002). Chronic multichannel

recordings from organotypic hippocampal slice cultures: protection from excitotoxic effects of NMDA by non-competitive NMDA antagonists. *J Neurosci Methods* **120**: 193–202.

Shin LM, Liberzon I (2010). The Neurocircuitry of Fear, Stress, and Anxiety Disorders. *Neuropsychopharmacology* **35**: 169–191.

Shipp S (2007). Structure and function of the cerebral cortex. *Curr Biol* **17**: R443–R449.

Siksou L, Silm K, Biesemann C, Nehring RB, Wojcik SM, Triller A, *et al* (2013). A role for vesicular glutamate transporter 1 in synaptic vesicle clustering and mobility. *Eur J Neurosci* **37**: 1631–42.

Simons JS, Spiers HJ (2003). Prefrontal and medial temporal lobe interactions in long-term memory. *Nat Rev Neurosci* **4**: 637–648.

Singer W (1999). Neuronal synchrony: a versatile code for the definition of relations? *Neuron* **24**: 49–65, 111–25.

Slattery DA, Cryan JF (2017). Modelling depression in animals: at the interface of reward and stress pathways. *Psychopharmacology (Berl)* **234**: 1451–1465.

Smith QR (2000). Transport of glutamate and other amino acids at the blood-brain barrier. *J Nutr* **130**: 1016S–22S.

Smythies J (2002). *The dynamic neuron*. *MIT Press* .

Snellenberg JX Van, Girgis RR, Horga G, Giessen E van de, Slifstein M, Ojeil N, *et al* (2016). Mechanisms of Working Memory Impairment in Schizophrenia. *Biol Psychiatry* **80**: 617–626.

Sousa N, Lukoyanov NV V, Madeira MDD, Almeida OFXFX, Paula-Barbosa MMM (2000). Reorganization of the morphology of hippocampal neurites and synapses after stress-induced damage correlates with behavioral improvement. *Neuroscience* **97**: 253–266.

Spampanato J, Polepalli J, Sah P (2011). Interneurons in the basolateral amygdala. *Neuropharmacology* **60**: 765–773.

Spruston N (2008). Pyramidal neurons: dendritic structure and synaptic integration. *Nat Rev Neurosci* **9**: 206–221.

Starc M, Murray JD, Santamauro N, Savic A, Diehl C, Cho YT, *et al* (2017). Schizophrenia is associated with a pattern of spatial working memory deficits consistent with cortical disinhibition. *Schizophr Res* **181**: 107–116.

Stoppini L, Buchs PA, Muller D (1991). A simple method for organotypic cultures of nervous tissue. *J Neurosci Methods* **37**: 173–82.

Straub RE, Lipska BK, Egan MF, Goldberg TE, Callicott JH, Mayhew MB, *et al* (2007). Allelic variation in GAD1 (GAD67) is associated with schizophrenia and influences cortical function and gene expression. *Mol Psychiatry* **12**: 854–69.

Striedter GF (2016). Evolution of the hippocampus in reptiles and birds. *J Comp Neurol*

524: 496–517.

Sul JH, Kim H, Huh N, Lee D, Jung MW (2010). Distinct roles of rodent orbitofrontal and medial prefrontal cortex in decision making. *Neuron* **66**: 449–60.

Sun L, Castellanos N, Grützner C, Koethe D, Rivolta D, Wibral M, *et al* (2013). Evidence for dysregulated high-frequency oscillations during sensory processing in medication-naïve, first episode schizophrenia. *Schizophr Res* **150**: 519–25.

Takamori S (2006). VGLUTs: "Exciting" times for glutamatergic research? *Neurosci Res* **55**: 343–351.

Tandon R, Gaebel W, Barch DM, Bustillo J, Gur RE, Heckers S, *et al* (2013). Definition and description of schizophrenia in the DSM-5. *Schizophr Res* **150**: 3–10.

Tao R, Li C, Zheng Y, Qin W, Zhang J, Li X, *et al* (2007). Positive association between SIAT8B and schizophrenia in the Chinese Han population. *Schizophr Res* **90**: 108–14.

Tarsa L, Goda Y (2002). Synaptophysin regulates activity-dependent synapse formation in cultured hippocampal neurons. *Proc Natl Acad Sci U S A* **99**: 1012–6.

Thibault K, Lin WK, Rancillac a., Fan M, Snollaerts T, Sordoillet V, *et al* (2014). BDNF-Dependent Plasticity Induced by Peripheral Inflammation in the Primary Sensory and the Cingulate Cortex Triggers Cold Allodynia and Reveals a Major Role for Endogenous BDNF As a Tuner of the Affective Aspect of Pain. *J Neurosci* **34**: 14739–14751.

Thomases DR, Cass DK, Meyer JD, Caballero A, Tseng KY (2014). Early Adolescent MK-801 Exposure Impairs the Maturation of Ventral Hippocampal Control of Basolateral Amygdala Drive in the Adult Prefrontal Cortex. *J Neurosci* **34**: 9059–66.

Thomases DR, Cass DK, Tseng KY (2013). Periadolescent exposure to the NMDA receptor antagonist MK-801 impairs the functional maturation of local GABAergic circuits in the adult prefrontal cortex. *J Neurosci* **33**: 26–34.

Tian L, Stefanidakis M, Ning L, Lint P Van, Nyman-Huttunen H, Libert C, *et al* (2007). Activation of NMDA receptors promotes dendritic spine development through MMP-mediated ICAM-5 cleavage. *J Cell Biol* **178**: 687–700.

Tiraboschi E, Guirado R, Greco D, Auvinen P, Maya-Vetencourt JF, Maffei L, *et al* (2013). Gene Expression Patterns Underlying the Reinstatement of Plasticity in the Adult Visual System. *Neural Plast* **2013**: 1–8.

Tolwani RJ, Buckmaster PS, Varma S, Cosgaya JM, Wu Y, Suri C, *et al* (2002). BDNF overexpression increases dendrite complexity in hippocampal dentate gyrus. *Neuroscience* **114**: 795–805.

Torrey EF, Barci BM, Webster MJ, Bartko JJ, Meador-Woodruff JH, Knable MB (2005). Neurochemical markers for schizophrenia, bipolar disorder, and major depression in postmortem brains. *Biol Psychiatry* **57**: 252–260.

Tran P V, Bymaster FP, Mcnamara RK, Potter WZ (2003). Dual Monoamine Modulation

for Improved Treatment of Major Depressive Disorder Abstract : *J Clin Psychopharmacol* **23**: 78–86.

Tsien RY (2013). Very long-term memories may be stored in the pattern of holes in the perineuronal net. *Proc Natl Acad Sci U S A* **110**: 12456–61.

Tsoory M, Guterman A, Richter-Levin G (2008). Exposure to stressors during juvenility disrupts development-related alterations in the PSA-NCAM to NCAM expression ratio: potential relevance for mood and anxiety disorders. *Neuropsychopharmacology* **33**: 378–93.

Tuncdemir SN, Wamsley B, Stam FJ, Osakada F, Goulding M, Callaway EM, *et al* (2016). Early Somatostatin Interneuron Connectivity Mediates the Maturation of Deep Layer Cortical Circuits. *Neuron* **89**: 521–535.

Tyler WJ, Pozzo-Miller L (2003). Miniature synaptic transmission and BDNF modulate dendritic spine growth and form in rat CA1 neurones. *J Physiol* **553**: 497–509.

Ueno H, Suemitsu S, Okamoto M, Matsumoto Y, Ishihara T (2016). Parvalbumin neurons and perineuronal nets in the mouse prefrontal cortex. *Neuroscience* **343**: 115–127.

Ultanir SK, Kim J-E, Hall BJ, Deerinck T, Ellisman M, Ghosh A (2007). Regulation of spine morphology and spine density by NMDA receptor signaling in vivo. *Proc Natl Acad Sci* **104**: 19553–19558.

Uluc K, Kendigelen P, Fidan E, Zhang L, Chanana V, Kintner D, *et al* (2013). TrkB receptor agonist 7, 8 dihydroxyflavone triggers profound gender- dependent neuroprotection in mice after perinatal hypoxia and ischemia. *CNS Neurol Disord Drug Targets* **12**: 360–70.

Urban-Ciecko J, Barth AL (2016). Somatostatin-expressing neurons in cortical networks. *Nat Rev Neurosci* **17**: 401–9.

Uylings HBM, Groenewegen HJ, Kolb B (2003). Do rats have a prefrontal cortex? *Behav Brain Res* **146**: 3–17.

VanDongen AMJ (CRC Press/Taylor & Francis: 2009). *Biology of the NMDA Receptor*. *Front Neurosci* at <http://www.ncbi.nlm.nih.gov/pubmed/21204416>.

Varea E, Blasco-Ibáñez JM, Gómez-Climent MÁ, Castillo-Gómez E, Crespo C, Martínez-Guijarro FJ, *et al* (2007a). Chronic Fluoxetine Treatment Increases the Expression of PSA-NCAM in the Medial Prefrontal Cortex. *Neuropsychopharmacology* **32**: 803–812.

Varea E, Castillo-Gómez E, Gómez-Climent MA, Blasco-Ibáñez JM, Crespo C, Martínez-Guijarro FJ, *et al* (2007b). Chronic antidepressant treatment induces contrasting patterns of synaptophysin and PSA-NCAM expression in different regions of the adult rat telencephalon. *Eur Neuropsychopharmacol* **17**: 546–557.

Varea E, Castillo-Gómez E, Gómez-Climent MA, Blasco-Ibáñez JM, Crespo C, Martínez-Guijarro FJ, *et al* (2007c). PSA-NCAM expression in the human prefrontal cortex. *J Chem Neuroanat* **33**: 202–9.

Varea E, Guirado R, Gilabert-Juan J, Martí U, Castillo-Gomez E, Blasco-Ibáñez JM, *et al* (2012). Expression of PSA-NCAM and synaptic proteins in the amygdala of psychiatric disorder patients. *J Psychiatr Res* **46**: 189–97.

Varea E, Nácher J, Blasco-Ibáñez JM, Gómez-Climent MÁ, Castillo-Gómez E, Crespo C, *et al* (2005). PSA-NCAM expression in the rat medial prefrontal cortex. *Neuroscience* **136**: 435–443.

Vauzour D, Vafeiadou K, Rice-Evans C, Williams RJ, Spencer JPE (2007). Activation of pro-survival Akt and ERK1/2 signalling pathways underlie the anti-apoptotic effects of flavanones in cortical neurons. *J Neurochem* **103**: 1355–1367.

Velázquez-Zamora DA, González-Ramírez MM, Beas-Zárate C, González-Burgos I (2011). Egocentric working memory impairment and dendritic spine plastic changes in prefrontal neurons after NMDA receptor blockade in rats. *Brain Res* **1402**: 101–108.

Versendaal D van, Rajendran R, Saiepour MH, Klooster J, Smit-Rigter L, Sommeijer J-P, *et al* (2012). Elimination of inhibitory synapses is a major component of adult ocular dominance plasticity. *Neuron* **74**: 374–83.

Vetencourt JFM, Sale A, Viegi A, Baroncelli L, Pasquale R De, F. O'Leary O, *et al* (2008). The Antidepressant Fluoxetine Restores Plasticity in the Adult Visual Cortex. *Science (80-)* **320**: 385–388.

Vissavajjhala P, Janssen WG, Hu Y, Gazzaley a H, Moran T, Hof PR, *et al* (1996). Synaptic distribution of the AMPA-GluR2 subunit and its colocalization with calcium-binding proteins in rat cerebral cortex: an immunohistochemical study using a GluR2-specific monoclonal antibody. *Exp Neurol* **142**: 296–312.

Volk DW, Lewis DA (2010). Prefrontal cortical circuits in schizophrenia. *Curr Top Behav Neurosci* **4**: 485–508.

Volk DW, Lewis DA (2016). The Role of Endocannabinoid Signaling in Cortical Inhibitory Neuron Dysfunction in Schizophrenia. *Biol Psychiatry* **79**: 595–603.

Vutskits L, Gascon E, Potter G, Tassonyi E, Kiss JZ (2007). Low concentrations of ketamine initiate dendritic atrophy of differentiated GABAergic neurons in culture. *Toxicology* **234**: 216–226.

Vyas A, Bernal S, Chattarji S (2003). Effects of chronic stress on dendritic arborization in the central and extended amygdala. *Brain Res* **965**: 290–294.

Vyas A, Mitra R, Shankaranarayana Rao BS, Chattarji S (2002). Chronic stress induces contrasting patterns of dendritic remodeling in hippocampal and amygdaloid neurons. *J Neurosci* **22**: 6810–6818.

Wang D, Fawcett J (2012). The perineuronal net and the control of CNS plasticity. *Cell Tissue Res* **349**: 147–160.

Wang H-X, Gao W-J (2012). Prolonged exposure to NMDAR antagonist induces cell-type specific changes of glutamatergic receptors in rat prefrontal cortex. *Neuropharmacology* **62**: 1808–1822.

Wang Y-C, Ho U-C, Ko M-C, Liao C-C, Lee L-J (2012). Differential neuronal changes in medial prefrontal cortex, basolateral amygdala and nucleus accumbens after postweaning social isolation. *Brain Struct Funct* **217**: 337–51.

Wang Y, Toledo-Rodriguez M, Gupta A, Wu C, Silberberg G, Luo J, *et al* (2004). Anatomical, physiological and molecular properties of Martinotti cells in the somatosensory cortex of the juvenile rat. *J Physiol* **561**: 65–90.

Watanabe Y, Gould E, McEwen BS (1992). Stress induces atrophy of apical dendrites of hippocampal CA3 pyramidal neurons. *Brain Res* **588**: 341–345.

Weickert CS, Hyde TM, Lipska BK, Herman MM, Weinberger DR, Kleinman JE (2003). Reduced brain-derived neurotrophic factor in prefrontal cortex of patients with schizophrenia. *Mol Psychiatry* **8**: 592–610.

Weickert CS, Ligons DL, Romanczyk T, Ungaro G, Hyde TM, Herman MM, *et al* (2005). Reductions in neurotrophin receptor mRNAs in the prefrontal cortex of patients with schizophrenia. *Mol Psychiatry* **10**: 637–650.

Werd HJJM Van De, Rajkowska G, Evers P, Uylings HBM (2010). Cytoarchitectonic and chemoarchitectonic characterization of the prefrontal cortical areas in the mouse. *Brain Struct Funct* **214**: 339–53.

Wiltgen BJ, Brown RAM, Talton LE, Silva AJ (2004). New Circuits for Old Memories. *Neuron* **44**: 101–108.

Wondolowski J, Frerking M (2009). Subunit-dependent postsynaptic expression of kainate receptors on hippocampal interneurons in area CA1. *J Neurosci* **29**: 563–574.

Woodruff AR, Anderson S a, Yuste R (2010). The enigmatic function of chandelier cells. *Front Neurosci* **4**: 201.

Woodruff PWR, Ph D, Psych MRC, David AS, Psych FRC, Murray RM, *et al* (2000). Meta-Analysis of Regional Brain Volumes in Schizophrenia. *Am J Psychiatry* **157**: 16–25.

Woolley CS, McEwen BS (1994). Estradiol regulates hippocampal dendritic spine density via an N-methyl-D-aspartate receptor-dependent mechanism. *J Neurosci* **14**: 7680–7687.

Woolsey TA, Loos H Van der (1970). The structural organization of layer IV in the somatosensory region (S I) of mouse cerebral cortex. *Brain Res* **17**: 205–242.

Woolsey TA, Welker C, Schwartz RH (1975). Comparative anatomical studies of the Sml face cortex with special reference to the occurrence of “barrels” in layer IV. *J Comp Neurol* **164**: 79–94.

Wyllie DJAJA, Livesey MRR, Hardingham GEE (2013). Influence of GluN2 subunit identity on NMDA receptor function. *Neuropharmacology* **74**: 4–17.

Xu H-T, Pan F, Yang G, Gan W-B (2007). Choice of cranial window type for in vivo imaging affects dendritic spine turnover in the cortex. *Nat Neurosci* **10**: 549–551.

Yacoubian T a, Lo DC (2000). Truncated and full-length TrkB receptors regulate distinct

modes of dendritic growth. *Nat Neurosci* **3**: 342–9.

Yamada J, Jinno S (2013). Spatio-temporal differences in perineuronal net expression in the mouse hippocampus, with reference to parvalbumin. *Neuroscience* **253**: 368–379.

Yang C, Shirayama Y, Zhang J, Ren Q, Yao W, Ma M, *et al* (2015). R-ketamine: a rapid-onset and sustained antidepressant without psychotomimetic side effects. *Transl Psychiatry* **5**: e632.

Yavorska I, Wehr M (2016). Somatostatin-Expressing Inhibitory Interneurons in Cortical Circuits. *Front Neural Circuits* **10**: 76.

Yizhar O, Fenno LE, Prigge M, Schneider F, Davidson TJ, O'Shea DJ, *et al* (2011). Neocortical excitation/inhibition balance in information processing and social dysfunction. *Nature* **477**: 171–178.

Yoshii A, Constantine-Paton M (2010). Postsynaptic BDNF-TrkB signaling in synapse maturation, plasticity, and disease. *Dev Neurobiol* **70**: 304–22.

Yuwiler A, Oldendorf WH, Geller E, Braun L (1977). Effect of albumin binding and amino acid competition on tryptophan uptake into brain. *J Neurochem* **28**: 1015–23.

Zeng Y, Liu Y, Wu M, Liu J, Hu Q (2012a). Activation of TrkB by 7,8-dihydroxyflavone prevents fear memory defects and facilitates amygdalar synaptic plasticity in aging. *J Alzheimer's Dis* **31**: 765–778.

Zeng Y, Lv F, Li L, Yu H, Dong M, Fu Q (2012b). 7,8-Dihydroxyflavone Rescues Spatial Memory and Synaptic Plasticity in Cognitively Impaired Aged Rats. *J Neurochem* **122**: 800–811.

Zhang H, Miller RH, Rutishauser U (1992). Polysialic acid is required for optimal growth of axons on a neuronal substrate. *J Neurosci* **12**: 3107–14.

Zhang J, Wu J, Fujita Y, Yao W, Ren Q, Yang C, *et al* (2015). Antidepressant effects of TrkB ligands on depression-like behavior and dendritic changes in mice after inflammation. *Int J Neuropsychopharmacol* **18**: 1–12.

Zhang Z, Liu X, Schroeder JP, Chan C-B, Song M, Yu SP, *et al* (2014). 7,8-Dihydroxyflavone Prevents Synaptic Loss and Memory Deficits in a Mouse Model of Alzheimer's Disease. *Neuropsychopharmacology* **39**: 638–650.

Zhao J, Bao AM, Qi XR, Kamphuis W, Luchetti S, Lou JS, *et al* (2012). Gene expression of GABA and glutamate pathway markers in the prefrontal cortex of non-suicidal elderly depressed patients. *J Affect Disord* **138**: 494–502.

Zuccato C, Cattaneo E (2009). Brain-derived neurotrophic factor in neurodegenerative diseases. *Nat Rev Neurol* **5**: 311–322.

Zuo D-Y, Zhang Y-H, Cao Y, Wu C-F, Tanaka M, Wu Y-L (2006). Effect of acute and chronic MK-801 administration on extracellular glutamate and ascorbic acid release in the prefrontal cortex of freely moving mice on line with open-field behavior. *Life Sci* **78**: 2172–2178.